Investigating acute N-methyl-D-aspartate (NMDA) receptor hypofunction and novel therapeutic targets with an aim to understanding the cognitive deficits associated with schizophrenia

Bethany Helen Dennis

Thesis submitted for the degree of Doctor of Philosophy at Newcastle University, Biosciences Institute

December 2024

Supervisors:

Dr Fiona LeBeau

Dr Gavin Clowry

Abstract

Schizophrenia is a neuropsychiatric disorder characterized by significant cognitive deficits, including impairments in working memory, selective attention, and executive function. The anterior cingulate cortex (ACC) and hippocampus are critical regions involved in these cognitive processes. N-methyl-D-aspartate (NMDA) receptor hypofunction has been proposed as a key mechanism underlying the cognitive impairments observed in schizophrenia. This hypofunction is associated with aberrant beta (20-30 Hz) and gamma (30-80 Hz) oscillations, as well as impaired working memory in patients. Additionally, increased neuroinflammation and a loss of fast-spiking parvalbumin (PV)+ interneurons have been documented in post-mortem brain tissue from patients with schizophrenia. However, the relationship between cognitive dysfunction and neuroinflammation in schizophrenia remains poorly understood.

This study aimed to explore the effects of NMDA receptor hypofunction on beta and gamma oscillations in the ACC and hippocampus of rat brain slices, utilizing phencyclidine (PCP) as an NMDA receptor antagonist to model schizophrenia-related cognitive deficits. *In vitro* electrophysiological recordings demonstrated that PCP had no significant impact on gamma oscillations in the CA3 region of the hippocampus. However, in the ACC, PCP significantly increased beta oscillations and induced a shift from gamma to beta frequencies. These aberrant beta oscillations were normalized by activating metabotropic glutamate 2 (mGlu2) receptors and could be blocked by the sigma-1 (σ1) receptor antagonist, NE-100. Immunofluorescence microscopy was used to assess changes in interneuron populations (PV+ and somatostatin; SST+), perineuronal net (PNN) expression, and neuroinflammatory markers (microglia and astrocytes) in the ACC. A trend toward an increased SST to PV expression ratio was observed in KA-exposed slices, although no significant effects of KA or PCP on glial or PNN expression were detected.

These findings suggest that targeting mGlu2 and σ1 receptors may mitigate PCP-induced network disruptions in the ACC, offering potential therapeutic strategies for addressing cognitive dysfunction in schizophrenia.

Acknowledgements and Dedication

First and foremost, I would like to thank my PhD supervisors Dr Fiona LeBeau and Dr Gavin Clowry for all your guidance and support throughout my PhD. I would like to particularly thank Fiona for being so patient, supportive, and encouraging throughout the 7 years of my studies.

I would also like to thank Dr Stuart Neale and Professor Tom Salt of Neurexpert Ltd for funding my tuition and experiments, and also for sharing their expertise and knowledge. I am a much better electrophysiologist for it, thank you!

I would also like to acknowledge and thank my progress panel, Dr Sasha Gartside and Professor Richard McQuade, for their guidance and contributions throughout my project. Thank you for challenging me to defend my work and offering valuable insight along the way. I wish you both the best for your retirement!

All the work presented in this thesis is my own, with the exception of assistance from undergraduate and masters students that I have supervised and worked with over the years. Firstly, Kourosh Parvizi for his contribution to the σ1 electrophysiology experiments, Oliver Baddeley and Olivia Burton for their work on the slice incubations, immunohistochemistry staining and analysis, and Rowan Paxman for all his recording in the CA3, where nothing happened! I am grateful to all of you for your contributions and wish you all lots of luck for the future.

I would also like to make a special mention and acknowledge the guidance and support I have received from Dr Felix Chan, Dr Tamara Modebadze and Dr Faye McLeod throughout my project. You have all been incredible mentors during our time together in the lab and have all taught me so much, thank you.

Having spent nearly 7 years completing my PhD, I also have lots of friends to thank who have come and gone in that time. Firstly, the original lunch club, thank you Myrto, Jean, Clare, Anderson, Mark and Ashan for being so welcoming and providing *interesting* lunch time debates! To my friends from Trev lab, thank you Laura, Rob and Darren for your immaculately timed pub trips. Thank you to Lucy Gee and Emma Robson for being the best company, in and out of the lab! Thank you to everyone who has been part of the LeBeau lab in more recent years; Dave, Ibtisam, Connie, Liza, Laura and Daipayan. And lastly, a huge thank you to Anastasia and Lauren for getting

me through the last year; for offering help, knowledge, laughter and wine, you are the best!

I am incredibly lucky to have such loving family and friends and would like to thank all of them for their support over the last 10 years. To Mum and Phil, thank you so much for all your support (both emotional and financial!) throughout all my years at university. Your belief in me has been unwavering and I am so grateful to you both. Thank you to the rest of the Hendendrews for putting up with me being the eternal student, you're all amazing, and I can't wait to have more time to spend with you all. Thank you to my grandparents, Gran and Grandad Dennis and Grandma and Grandad Hughes, for all their love and support. Unfortunately, my Grandads are not here to see me get my PhD, but I know they would have been so proud.

I cannot thank my friends enough for standing by me throughout my PhD journey. Nina, Sophie, and Ellie, you have always been my greatest cheerleaders—celebrating the highs and supporting me through the lows. A special thanks to Chob for always being funny, rational, and optimistic; for always offering solutions and making a mountain feel more like a walk across the moors.

And finally, the biggest thank you goes to Jon. Thank you for always supporting, encouraging, and loving me throughout my PhD, I couldn't have done it without you.

This thesis is dedicated to Bobbie Dennis, loved always.

Conference Presentations

Work from this thesis was presented at the following conferences:

Federation of European Neuroscience Societies Forum (June 2024), Vienna, AT.

Poster presentation: "*The role of sigma-1 receptors in neuroinflammation using an acute slice model of NMDA receptor hypofunction.*"

Federation of European Neuroscience Societies - Hertie Winter School (December 2023), Obergurgl, AT.

Poster presentation: "*The role of sigma-1 receptors in neuroinflammation in an acute slice model of schizophrenia.*"

British Neuroscience Association Festival of Neuroscience (April 2023), Brighton, UK.

Poster presentation: "*NMDA and sigma-1 receptor modulation of network oscillations and neuroinflammation in the rodent hippocampus and anterior cingulate cortex.*"

Poster presentation: "*Modulation of beta and gamma frequency oscillations in the rat anterior cingulate cortex (ACC) in vitro by the mGlu2 metabotropic glutamate receptor.*"

Society for Neuroscience, Neuroscience (November 2022), San Diego, CA, USA.

Poster presentation: "*NMDA and sigma-1 receptor modulation of network oscillations and neuroinflammation in the rodent hippocampus and anterior cingulate cortex.*"

Poster presentation: "*Modulation of beta and gamma frequency oscillations in the rat anterior cingulate cortex (ACC) in vitro by the mGlu2 metabotropic glutamate receptor.*"

Federation of European Neuroscience Societies Forum (July 2022), Paris, FR.

Poster presentation: "*NMDA and sigma-1 receptor modulation of rodent network oscillations and neuroinflammation*."

Publications

Work in chapters 3 and 4 has been published with first authorship:

Dennis, B. H., Neale, S. A., LeBeau, F. E. N., & Salt, T. E. (2023). Modulation of circuit oscillations in the rat anterior cingulate cortex (ACC) *in vitro* by mGlu2 metabotropic glutamate receptors and alleviation of the effects of phencyclidine-induced NMDA-receptor hypofunction. *Pharmacology, biochemistry, and behavior*, *223*, 173532. https://doi.org/10.1016/j.pbb.2023.173532

Work was also contributed to the following publications:

Al-Musawi, I., **Dennis, B. H.,** Clowry, G. J., & LeBeau, F. E. N. (2024). Evidence for prodromal changes in neuronal excitability and neuroinflammation in the hippocampus in young alpha-synuclein (A30P) transgenic mice. *Frontiers in dementia*, 3, 1404841. https://doi.org/10.3389/frdem.2024.1404841

(Review) Olkhova, E. A., Smith, L. A., **Dennis, B. H.,** Ng, Y. S., LeBeau, F. E. N., & Gorman, G. S. (2024). Delineating mechanisms underlying parvalbumin neuron impairment in different neurological and neurodegenerative disorders: the emerging role of mitochondrial dysfunction. *Biochemical Society transactions*, 52(2), 553–565. https://doi.org/10.1042/BST20230191.

Table of Contents

List of Figures

List of Tables

List of Abbreviations

^{1}HS-MRS	Proton magnetic resonance spectroscopy
5-HT	Serotonin
ACC	Anterior cingulate cortex
ACSF	Artificial cerebral spinal fluid
AD	Alzheimer's disease
AMPA	α-amino-3-hydroxy-5-methyl-4-isoxazolepropionic acid
ATP	Adenosine triphosphate
BA	Brodmann's area
BDNF	Brain derived neurotrophic factor
BGT	Betaine/GABA transporter-1
BiP	Binding immunoglobulin protein
BLA	Basolateral amygdala
CA	*Cornu ammonis*
Ca^{2+}	Calcium ion
Cg	Cingulate area
CMA	Cingulate motor area
CNS	Central nervous system
CO_2	Carbon dioxide
COX1	Cyclooxygenase 1
CS-GAG	Chondroitin sulfate glycosaminoglycan
CSPG	Chondroitin sulfate proteoglycans
D	Dopamine
dACC	Dorsal anterior cingulate cortex
DAP5	D-(-)-2-Amino-5-phosphonopentanoic acid
DAPI	4′,6-diamidino-2-phenylindole
DG	Dentate gyrus
dlPFC	Dorsolateral prefrontal cortex
dmPFC	Dorsomedial prefrontal cortex
DMSO	Dimethyl sulfoxide
DV	Dorsal-ventral

E	Embryonic day
EAAT	Excitatory amino acid transporters
EC	Entorhinal cortex
ECM	Extracellular matrix
EEG	Electroencephalogram
EPSC	Excitatory postsynaptic currents
EPSP	Excitatory postsynaptic potential
ER	Endoplasmic reticulum
ErbB4	Epidermal growth factor receptor 4
fEPSP	Field excitatory postsynaptic potential
FGA	First generation antipsychotic
GABA	Gamma-aminobutyric acid
GAD	Glutamic acid decarboxylase
GAG	Glycosaminoglycan
GAT	Gamma-aminobutyric acid transporter
GFAP	Glial fibrillary acidic protein
GWAS	Genome wide association study
HAPLN	Hyaluronan and proteoglycan link protein
HFS	High frequency stimulation
Hz	Hertz
Iba1	Ionized calcium binding adaptor molecule 1
IGF1	Insulin-like growth factor 1
iGlu	Ionotropic glutamate
IL	Interleukin
iNOS	Inducible nitric oxide synthase
IP_3	Inositol triphosphate
IPSC	Inhibitory postsynaptic current
IPSP	Inhibitory postsynaptic potential
IQR	Interquartile range
K^+	Potassium ion
KA	Kainic acid / kainate
L	Layer

LFP	Local field potential
LTP	Long-term potentiation
MAM	Methylazoxymethanol acetate
MCC	Midcingulate cortex
MDD	Major depressive disorder
MEG	Magnetoencephalography
Mg^{2+}	Magnesium ion
mGlu	Metabotropic glutamate
MK-801	Dizocilpine
mPFC	Medial prefrontal cortex
mRNA	Messenger ribonucleic acid
Na^{+}	Sodium ion
NMDA	N-methyl-D-aspartate
NOR	Novel object recognition
NRG1	Neuregulin 1
O_2	Oxygen
OFC	Orbitofrontal cortex
OTX2	Orthodenticle homeobox 2
P	Postnatal day
pACC	Perigenual anterior cingulate cortex
PAM	Positive allosteric modulator
PCP	Phencyclidine (1 ,1-phenylcyclohexylpiperidine)
PET	Positron emission tomography
PFA	Paraformaldehyde
PFC	Prefrontal cortex
PNN	Perineuronal net
PV	Parvalbumin
PV+	Parvalbumin-positive
PVBC	Parvalbumin basket cell
PVCC	Parvalbumin chandelier cell
QOL	Quality of life
RM	Repeated measures

RNA	Ribonucleic acid
RNS	Reactive nitrogen species
ROS	Reactive oxygen species
RSC	Retrosplenial cortex
sACC	Subgenual anterior cingulate cortex
SEM	Standard error of the mean
SGA	Second generation antipsychotic
SNP	Single-nucleotide polymorphism
SST	Somatostatin
SST+	Somatostatin-positive
TGA	Third generation antipsychotic
TNF-α	Tumour necrosis factor alpha
vACC	Ventral anterior cingulate cortex
VGAT	Vesicular GABA transporter
vHPC	Ventral hippocampus
vlPFC	Ventrolateral prefrontal cortex
vmPFC	Ventromedial prefrontal cortex
σ1	Sigma-1

Chapter 1. Introduction

1.1 Schizophrenia

Schizophrenia is a neuropsychiatric disorder affecting around 24 million people, in 2021, worldwide (IHME, 2024). The term schizophrenia, ‘schizo’ (splitting) and ‘phren’ (mind), is derived from Greek and was first used in 1908 by the Swiss Professor of Psychiatry, Eugen Bleuler. “Schizophrenia” described the symptoms Bleuler was observing in his psychiatric patients (Bleuler, 1911), it is not a split personality as it is often misdescribed. Specifically, ‘schizophrenia’ referred to the disconnection between a person’s personality, thinking, memory and perception, the key hallmarks of the disorder (Gaebel and Kerst, 2019). Patients with schizophrenia present with a diverse range of symptoms, classified as either positive, negative, or cognitive (Liddle, 1987, Tandon et al., 2013). The positive symptoms, also characterised as psychosis, include delusions, auditory and visual hallucinations, and hyperactivity (Tandon et al., 2013). The negative symptoms include inability to experience joy or pleasure (anhedonia), poverty of speech (alogia), reduced or absent expression of emotion (affective flattening) and social withdrawal (Correll and Schooler, 2020, Tandon et al., 2013). The cognitive symptoms affect learning and memory, specifically impairments in working memory, executive function, and selective attention (Nuechterlein et al., 2004). Although the severity of cognitive decline varies between different cognitive functions, overall cognitive deficits can be exacerbated during episodes of psychosis (Zanelli et al., 2019).

The positive symptoms of schizophrenia can be relatively well managed by antipsychotic medication, although some of these medications can cause various unpleasant side effects that impact compliance (Kane et al., 2001). Initial first generation antipsychotic (FGA; typical) medications (e.g. haloperidol) are primarily dopamine 2 (D2) receptor antagonists, whereas second generation antipsychotic (SGA; atypical) medications (e.g. risperidone, olanzapine and clozapine) target D2, as well as other receptor sites including D1, D3 and D4, serotonin (5-HT2A and 5-HT2C), adrenergic, histamine and muscarinic receptors (Maric et al., 2016). In more recent years, third generation antipsychotic (TGA) medications (e.g. cariprazine, brexpiprazole and aripiprazole), that act as either functionally selective or partial D2 receptor agonists, have been developed (Mailman and Murthy, 2010, Maric et al., 2016). However, there is currently no specific or targeted treatment for the negative or cognitive symptoms of schizophrenia, even though they affect 40% and 80% of

patients, respectively (Carbon and Correll, 2014, Maroney, 2022). The mechanisms underlying these symptoms are still unclear and a lack of treatments for negative and cognitive symptoms contribute significantly to the long-term burden of the disorder (Provencher and Mueser, 1997). Specifically, the cognitive symptoms of schizophrenia can significantly impact an individual's functional independence, causing social and/or occupational disability (Carbon and Correll, 2014).

Clinically, schizophrenia first presents in late adolescence to early adulthood, although premorbid and prodromal cognitive deficits have been reported in teenagers, younger than 16 years old, and young adolescents (Cullen et al., 2020, Giuliano et al., 2012). Although the prevalence of schizophrenia is similar between genders, presentation is earlier in males than females (Häfner et al., 1994, Loranger, 1984). Typically, males have a single peak-presentation between 21 and 25 years, whereas females have an early peak at 25 – 30 years and a second, later-life peak between 45 and 49 years (Li et al., 2016). Sex differences in symptoms have also been reported, with males showing an increased risk of negative symptoms whilst females are more likely to experience affective symptoms, such as depression, impulsivity, and emotional instability (Leger and Neill, 2016). Males showed poorer performance on measures of executive function, verbal memory, and information processing speed, compared to females, whereas females showed greater deficits in visual memory and attention (Mendrek and Mancini-Marïe, 2016).

Individuals with schizophrenia are reported to have a lower quality of life (QOL), compared to the general population (Bobes et al., 2007). QOL is affected by disease pathology, pharmacotherapy, and physiological and clinical factors, such as obesity and hypertension, which can be caused by medication. Unhealthy lifestyle habits, such as tobacco smoking, also contribute to poor QOL. Amongst patients affected by mental illness, tobacco smoking is most prevalent in those diagnosed with schizophrenia (70 – 80%), with anecdotal and clinical evidence suggesting that tobacco smoking helps to alleviate the negative and cognitive symptoms of the disorder, as well as the side effects of antipsychotic medication (Winterer, 2010). These QOL factors are likely a result of the various symptoms of the disorder and can also be adverse effects of antipsychotic medication.

Adverse effects of antipsychotics include sedation, weight gain, and decreased motivation which can lead to reduced physical activity and self-neglect behaviours (Dong et al., 2019, Tsirigotis, 2018). Cognitive impairment is likely to affect socioeconomic factors, which can also have significant effects on an individuals' physical and mental health. As a result, individuals with schizophrenia are predicted to have a 15 – 20 year shorter life expectancy and a 2 – 4 times greater increase in sudden cardiac death than the general population (Buckley and Sanders, 2000). In addition, people with schizophrenia have a 5 – 10% lifetime risk of death by suicide (Hjorthøj et al., 2017). By understanding the mechanisms underlying the symptoms of schizophrenia, particularly those causing the cognitive deficits, new treatments can be developed to target these symptoms and patient outcomes could therefore be significantly improved.

1.2 The NMDA receptor hypofunction theory

Several neurotransmitters and neurochemical pathways are involved in regulating normal brain function and cognitive activity. Due to the wide array of symptoms, abnormal functioning of various neurotransmitter receptors has been associated with schizophrenia pathology. Historically, dopamine dysregulation was the first neurotransmitter to be associated with symptoms of schizophrenia, and it was proposed that hyperactive dopamine transmission results in schizophrenic symptoms (Seeman, 2021, van Rossum, 1966). However, this original hypothesis has since been revised and better resolution positron emission tomography (PET) imaging has shown that dopamine function is increased in the associative striatum of patients with schizophrenia (Egerton et al., 2013). Furthermore, increased dopamine function in the associative striatum is associated with psychosis severity (Laruelle, 2013). These aberrant changes in dopamine transmission underlie the positive symptoms of schizophrenia, and by targeting D2 receptors, antipsychotics can decrease excess dopamine transmission, reducing positive symptoms. However, as previously mentioned, there is currently no treatment for the cognitive and negative symptoms, and typical antipsychotics do not alleviate either the negative or cognitive symptoms of schizophrenia, suggesting negative and cognitive symptoms are caused by changes or disruptions to a different mechanism, or mechanisms.

1.2.1 Glutamate

Glutamate has also been implicated in the symptoms and pathology of schizophrenia (Halberstadt, 1995). Glutamate is an essential excitatory neurotransmitter in the brain that binds to two major classes of glutamate receptors: ionotropic glutamate (iGlu) receptors and metabotropic glutamate (mGlu) receptors (Figure 1.1). The iGlu receptors are ligand-gated ion channels, crucial for synaptic plasticity and include N-methyl-D-aspartate (NMDA), α-amino-3-hydroxy-5-methyl-4-isoxazolepropionic acid (AMPA) and kainate (KA) receptors. mGlu receptors modulate synaptic transmission via secondary messenger signalling pathways and are subdivided into Group I (mGlu1 and mGlu5), Group II (mGlu2 and mGlu3) and Group III (mGlu4, mGlu6, mGlu7 and mGlu8) receptors. iGlu receptors and mGlu receptors

are composed of individual subunits, each of which is encoded by a single gene (Traynelis et al., 2010).

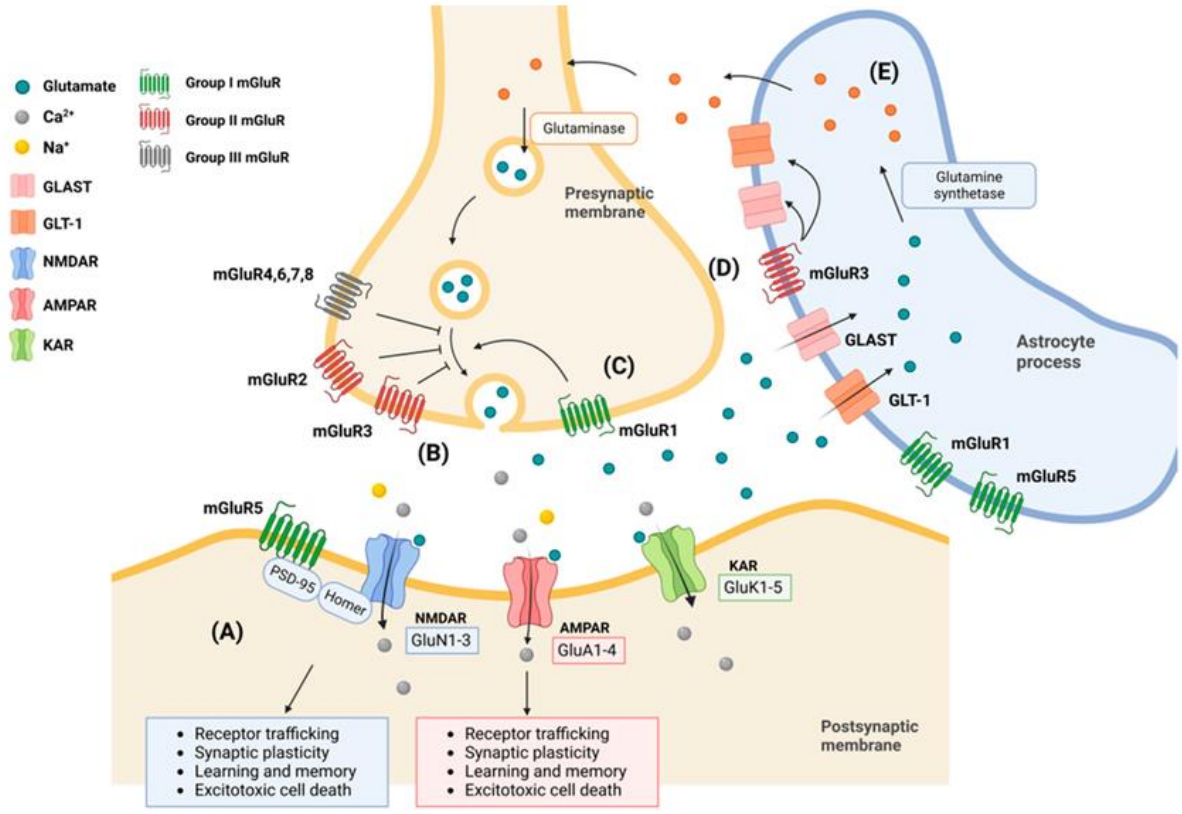

Figure 1.1 Types of ionotropic and metabotropic glutamate receptors, and their associated mechanisms, including glutamate cycling. Ionotropic receptors and their subunits include NMDA (GluN1-3), AMPA (GluA1-4) and KA (GluK1-5). Metabotropic glutamate receptors include Group I (mGlu1 and 5), Group II (mGlu2 and 3) and Group III (mGlu4, 6, 7, and 8). Glutamate is released into the synaptic cleft, interacts with receptors and is taken up by neighbouring astrocytes, where glutamate is recycled into glutamine by gluatamine synthetase, transported back to the presynaptic terminal and converted back to glutamate by glutaminase. Figure adapted from Chen et al. (2023).

Glutamate plays a fundamental role in synaptic plasticity (the activity-dependent strengthening and weakening of synapses over time) and neuronal network formation and function (Dingledine et al., 1999, Platt, 2007). However excess

glutamate levels can cause excitotoxicity, oxidative stress, and neurodegeneration (Lau and Tymianski, 2010). To prevent toxicity, cells perform a process called glutamate-glutamine cycling (Andersen et al., 2021) (Figure 1.1). Glutamate is released into the synaptic cleft from the presynaptic terminal where it binds to pre- and post-synaptic receptors. Following activation of the post-synaptic neuron, glutamate is then removed from the cleft by excitatory amino acid transporters (EAAT) into astrocytes, a type of glial cell. In the astrocytes, most of the glutamate is converted to glutamine by glutamine synthetase, which is then transferred back to the presynaptic terminal and converted back to glutamate by the catalytic enzyme, glutaminase (Kruse and Bustillo, 2022). Dysfunctional glutamate cycling has been found in patients with schizophrenia and this is primary evidence for disturbed glutamate function in the disorder (Burbaeva et al., 2003, Gluck et al., 2002).

Initially, the glutamate hypothesis of schizophrenia developed following clinical observations of the psychoactive, non-competitive NMDA receptor antagonists, phencyclidine (PCP) and ketamine (Coyle, 1996, Javitt, 1987, Javitt and Zukin, 1991). When administered at a sub-anaesthetic dose, PCP transiently mimics many symptoms of schizophrenia, including psychosis and also the cognitive deficits (Javitt and Zukin, 1991). Furthermore, both PCP and ketamine exacerbate cognitive symptoms and psychosis when administered in individuals with schizophrenia (Lahti et al., 1995, Luby et al., 1959, Malhotra et al., 1997). The glutamate hypothesis of schizophrenia suggests that cognitive impairment and the positive symptoms of schizophrenia are due to NMDA receptor hypofunction, leading to disturbances in glutamate-mediated neurotransmission (Coyle, 1996), especially in the PFC and hippocampus (Moghaddam and Javitt, 2012).

Evidence for glutamate dysregulation in schizophrenia has been found across genetic and human imaging studies. In a 2014 genome-wide association study (GWAS) of nearly 40,000 schizophrenia patients, several mutated genes involved in glutamatergic neurotransmission, including mGlu3 (*GRM3)*, GluN2A (*GRIN2A*) and AMPA receptor 1 (*GRIA1)*, were identified as being associated with schizophrenia-risk (Ripke et al., 2014). A meta-analysis of recent proton magnetic resonance spectroscopy (^{1}H-MRS) studies have shown significant increases in glutamatergic transmission in the limbic system of schizophrenia patients (Merritt et al., 2016), whilst a ^{1}H-MRS study looking at the hippocampus specifically, found a positive correlation

between increased glutamate and glutamine levels and poor executive functioning of schizophrenia patients (Poels et al., 2014). A PET imaging study of schizophrenia patients found greater blood flow to the anterior cingulate cortex (ACC) following a ketamine challenge, compared to controls, suggesting the glutamatergic system is more sensitive to NMDA receptor antagonism in patients with schizophrenia (Holcomb et al., 2005).

1.2.2 Gamma-aminobutyric acid (GABA)

Gamma-aminobutyric acid (GABA) is the primary inhibitory neurotransmitter in the adult mammalian brain and balances excitatory glutamate activity. GABA binds to GABA receptors of which there are two types: the ionotropic $GABA_A$ receptor and the muscarinic $GABA_B$ receptor (Fischer et al., 2022, Marques et al., 2021) (Figure 1.2). In humans, the $GABA_A$ receptor has 19 subunit isoforms encoded by distinct genes (α1-α6, β1-β3, γ1-γ3, δ, ∈, θ, π and ρ1-ρ3) (Goetz et al., 2007), where $GABA_B$ has just two: $GABA_{B1}$ and $GABA_{B2}$ (Calver et al., 2000). Diverse sub-unit composition allows $GABA_A$ receptors to have distinct and varied functional and physiological roles throughout the brain (Mody and Pearce, 2004). $GABA_B$ inhibits neuronal activity by reducing exocytosis, hyperpolarizing post-synaptic membranes, and inhibiting neuronal activity.

GABA is synthesised from glutamate by glutamic acid decarboxylase (GAD). GAD exists as two distinct enzymes, GAD65 and GAD67, each encoded by its own gene, *GAD2* and *GAD1*, respectively (Erlander et al., 1991). GAD67 is a cytosolic enzyme found in the cell bodies, dendrites, and axonal processes of GABAergic interneurons. When GAD67 expression is decreased, there is deficient extracellular GABA and, in turn, GABA-mediated inhibition on pyramidal cells is reduced (Kalkman and Loetscher, 2003, Zeng et al., 2024). GAD65 is located in the presynaptic terminals and is closely associated with the membrane of synaptic vesicles (Kanaani et al., 2010). This allows GAD65 to rapidly synthesise GABA for release, modulating synaptic inhibition, affecting neuronal plasticity, learning, and memory formation (Lange et al., 2014, Walls et al., 2010).

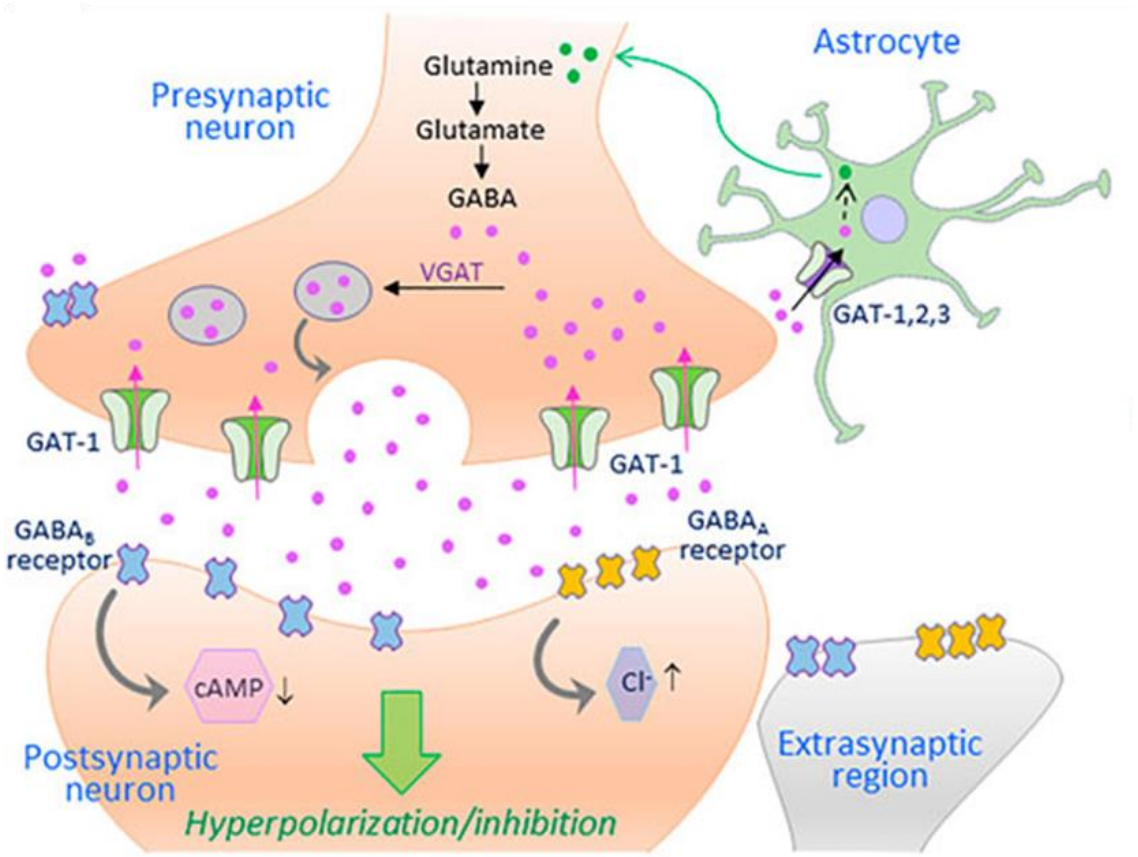

Figure 1.2 A simplified schematic of a GABAergic synapse. GABA (pink) is released into the synaptic cleft, activating $GABA_A$ and $GABA_B$ type receptors. GABA transporter 1 (GAT1), on the presynaptic neuron, transports GABA back into the neuron. GAT1 – 3 on astrocytes transports GABA into the astrocyte, and release glutamine, to be taken up into the presynaptic neuron. Glutamine is converted to glutamate by glutaminase, and glutamate to GABA by glutamate decarboxylase (GAD). GABA is taken up into synaptic vesicles by vesicular GABA transporter (VGAT), where it is then ready to be released into the synaptic cleft. Adapted from Fischer et al. (2022).

GABA transporters (GATs), of which there are four distinct proteins (GAT-1, GAT-2, GAT-3, and betaine/GABA transporter-1; BGT-1), mediate GABA uptake (Borden et al., 1992) (Figure 1.2). GAT-1 is the most highly expressed GAT in the CNS, localised predominantly on neuronal presynaptic axon terminals, but is also found on astrocytic processes (Cherubini and Conti, 2001). GAT-3 is expressed on astrocytic processes, almost exclusively, except for some retinal neurons (Cherubini

and Conti, 2001, Johnson et al., 1996). GAT-2 is also expressed in neurons and astrocytes but is mostly extraparenchymal and is most highly expressed in the choroid plexus and ependyma (Conti et al., 1999). The GABA is then taken up into synaptic vesicles via the vesicular GABA transporter (VGAT), where it is then ready to be released into the synaptic cleft.

Abnormalities in GABA have been one of the most consistent findings in schizophrenia research, as post-mortem PFC studies find lower density of GABAergic interneurons (Kaar et al., 2019), reduced levels of GAD67 messenger ribonucleic acid (mRNA) and GAD67 protein (Dienel and Lewis, 2019), and reduced GAT1 in some interneurons (Volk et al., 2001), in schizophrenia patients compared to controls. *In vivo*, radiotracers show no difference in overall GABA receptor levels between patients with schizophrenia and controls, however a reduction in the α5 subunit of the GABA (α5-$GABA_A$) receptor was found in the hippocampus of schizophrenia patients (Marques et al., 2021), compared to healthy controls. Reductions in α5-$GABA_A$ mRNA and protein levels have also been found in the dorsolateral PFC (dlPFC) of schizophrenia patients (Beneyto et al., 2011, Duncan et al., 2010). The α5-$GABA_A$ receptor is more highly expressed in the hippocampus, than other areas of the brain, and genetic and pharmacological studies have shown it plays an important role in learning and memory (Jacob, 2019). Taken together, this data implicates changes in GABA and inhibitory neurons in schizophrenia pathology and indicates a specific vulnerability of the α5 subunit of the $GABA_A$ receptor.

Changes in GABA can disrupt the balance between excitatory and inhibitory neurotransmission. The healthy development and function of GABAergic interneurons is dependent on glutamatergic NMDA receptors (Cohen et al., 2015), the function of which is also reported to be dysfunctional, or hypofunctional, in schizophrenia (Nakazawa and Sapkota, 2020).

1.2.3 NMDA receptor hypofunction

NMDA receptors are heterotetrameric iGlu channels, permeable to Ca^{2+}. NMDA receptors are heterogenous and composed of a mixture of subunits; GluN1, GluN2 (GluN2A-D) and GluN3 (GluN3A-B) (Hollmann, 1999, Moriyoshi et al., 1991) (Figure 1.3). Typically, NMDA receptors are composed of two glycine-binding GluN1 and two

glutamate-binding GluN2 subunits (Mayer et al., 1984). Once released into the synaptic cleft, glutamate binds to postsynaptic NMDA receptors causing excitatory postsynaptic currents (EPSCs). To activate NMDA receptors, both glutamate and glycine must bind to their respective binding sites on the receptor, removing the channel's voltage-dependent Mg^{2+} block, allowing the channel to open and an influx of Ca^{2+} into the neuron (Hansen et al., 2018). NMDA receptor-gated Ca^{2+} influx is crucial for regulating synaptic plasticity and underlies learning and memory mechanisms (Lau et al., 2009).

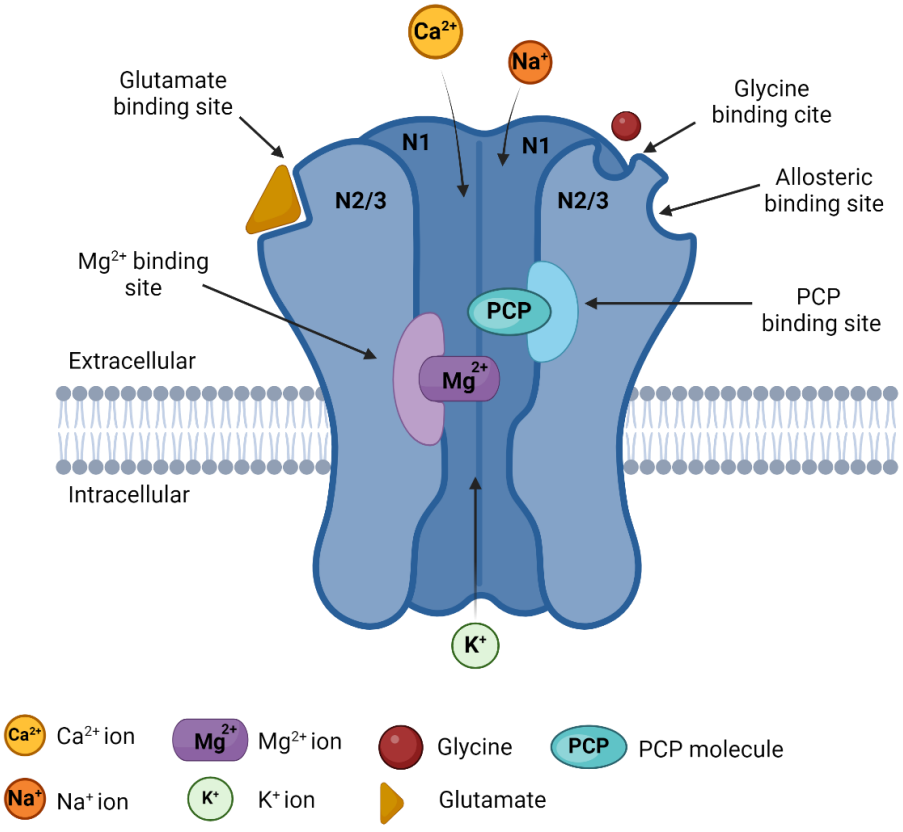

Figure 1.3 A schematic diagram of the ionotropic NMDA receptor. NMDA receptors are comprised of four subunits; two N1 subunits and a combination of N2 and N3 subunits. co-agonist binding site to activate the NMDA receptor. The NMDA receptor is blocked by voltage-dependent Mg^{2+}. Once activated, extracellular Na^{+} and Ca^{2+} can flow into the cell and intracellular K^{+} can flow out of the cell. PCP, and other NMDA receptor antagonists, bind to the PCP receptor on the inside of the NMDA receptor. Created with BioRender.com.

Proposed hypofunction of NMDA receptors on GABAergic parvalbumin (PV)-positive (PV+) inhibitory interneurons causes inactivation of these interneurons and a subsequent disinhibition of the interacting excitatory pyramidal cells (Homayoun and Moghaddam, 2007). Overall, there is a resulting increase of cortical excitation, typical of that seen after NMDA receptor antagonism in human and animal studies (Breier et al., 1997, Jackson et al., 2004). Prolonged NMDA hypofunction leads to excitotoxicity in postsynaptic neurons and it has been proposed that neurodegeneration may be caused by this excessive release of glutamate (Rothman and Olney, 1987). There is also evidence that neuroinflammation is higher in patients with schizophrenia (Goldsmith et al., 2016, Wang and Miller, 2018), likely because of excitotoxicity. The exact mechanisms underlying NMDA receptor hypofunction, and the downstream consequences, are not fully understood, but studying brain regions sensitive to, or affected by, NMDA receptor hypofunction could be beneficial in understanding it's associated pathology.

1.2.4 Animal models of schizophrenia and NMDA hypofunction

To model NMDA receptor hypofunction in rodents, pharmacological, genetic, and neurodevelopmental techniques can be used to target the NMDA receptor or other components that effect NMDA receptor function.

Pharmacological techniques use NMDA receptor antagonists, including PCP, dizocilpine (MK-801) and ketamine, to block the NMDA receptor and inhibit cell firing. *In vivo* rodent studies typically model NMDA receptor hypofunction by administering PCP using one of three paradigms, defined by the duration and frequency of exposure: acute, subchronic, and chronic (Noli et al., 2017). Acute treatment is typically a single dose of PCP but can also be multiple doses over a short time, from hours to a couple of days. Subchronic treatment usually consists of daily, or twice daily, dosing for multiple days, up to two weeks, followed by a withdrawal or washout period. Finally, chronic treatment refers to prolonged and continuous administration that initially follows a similar regimen to subchronic treatment but, following daily dosing, intermittent dosing is maintained for a further few weeks or months.

Using the appropriate pharmacological treatment protocol is crucial for recapitulating different aspects of disease (see Neill et al. (2010) for comprehensive

review of acute, subchronic and chronic PCP effects). To study first-episode psychosis, acute PCP treatment is used as it induces hyperactivity and social deficits in rodents (Mitchell et al., 2020), as well as short-lasting cognitive deficits (Savolainen et al., 2021). Subchronic and chronic treatment are used to model the persistent behavioural symptoms, including cognitive deficits and negative symptoms, but also some of the cellular and molecular changes (Janhunen et al., 2015, Li et al., 2024a). For example, PCP alters animal behaviour, mimicking aspects of schizophrenia including presentation of cognitive deficits, as well as reduced PV expression in the prelimbic cortex when administered subchronically (McKibben et al., 2010), and the cingulate cortex and hippocampus when administered acutely (Abdul-Monim et al., 2007).

Neurodevelopmental animal models of schizophrenia are also often used as evidence suggests the pathology arises from abnormalities in neurodevelopment of the PFC and hippocampus during pre- and perinatal stages, which result in long term pathological changes in behaviour and brain structure and function (Białoń and Wąsik, 2022). Neurodevelopmental rodent models include the methylazoxymethanol acetate (MAM) model. MAM is a neurotoxin which reduces DNA synthesis. The MAM model involves prenatal administration of MAM on embryonic day (E) 17, which causes disruption of embryonic brain development (Białoń and Wąsik, 2022), resulting in a reduction in cortical thickness and simultaneous elevation in neuronal density in the medial PFC (mPFC) and hippocampus, of the adult brain. The MAM model also showed decreased PV expression in the mPFC and hippocampus, and deficits in mPFC gamma oscillatory activity (Gill and Grace, 2014, Maćkowiak et al., 2014). The E17 MAM model also causes several behavioural disturbances observed in adult offspring, such as cognitive dysfunction (Kállai et al., 2020), social impairment (Flagstad et al., 2004), and sensorimotor gating deficits (Le Pen et al., 2006) in rats.

Genetic rodent models are also used to model schizophrenia, and multiple GWAS have reported various schizophrenia-risk associated genes. A popular model includes knockdown and point mutations in the Disrupted-in-Schizophrenia 1 (*DISC1*) gene, which leads to a number of cognitive deficits in mice, as well as reduced expression of GAD67 and GluN1, and decreased GABAergic neuron density (Białoń and Wąsik, 2022). Although abnormalities in *DISC1* have been found and linked with developing schizophrenia (Liu et al., 2019a), the link between *DISC1* and

schizophrenia is unclear, and considered somewhat controversial (Sullivan, 2013). Other popular schizophrenia-risk associated gene targets include the dysbindin-1 *(DTNBP1)* model and the neurotrophic factor neuregulin-1 (*NRG1*) model. The dysbinin-1 model sees changes in the dysbindin-1 protein, linked to synaptic function and plasticity (Mullin et al., 2015, Trantham-Davidson and Lavin, 2019) as well as working memory (Wolf et al., 2011). The neuregulin-1 model, which effects both the NRG1 protein and its receptor, epidermal growth factor receptor 4 (ErbB4), displays behavioural deficits and impacted GABAergic transmission in mice (Wang et al., 2018). Overall, the genetic component underlying the development of schizophrenia is complex, and it is likely that more than one gene is implicated. Currently, there are no genetic models that completely recapitulate all aspects of the disease, but those available can help understand disease pathology, and be useful for pharmaceutical screening.

1.3 Cognition and working memory

The term limbic was first used by Paul Broca in 1878 to refer to the brain structures around the edge, or border, of the two hemispheres (Broca, 1878). The ‘limbic lobe’ as it was first described, now known as the limbic system, comprises of the limbic cortex, including the cingulate gyrus and parahippocampal gyrus, the hippocampal formation, the amygdala, the septal area and the hypothalamus (Rajmohan and Mohandas, 2007) (Figure 1.4). The structures of the limbic system have many different connections and functions, each playing key roles in learning, memory, and emotion (Rolls, 2019).

While regions such as the amygdala are strongly associated with emotion and reward processing (Seymour and Dolan, 2008), the ACC and hippocampus are crucial for learning and memory (Goto, 2022). It is well established that patients with schizophrenia display aberrant emotional processing, and this is strongly associated with abnormalities in the amygdala (see Aleman and Kahn (2005) for review), however this thesis focuses on the learning and memory impairments of schizophrenia and the role of the ACC and hippocampus.

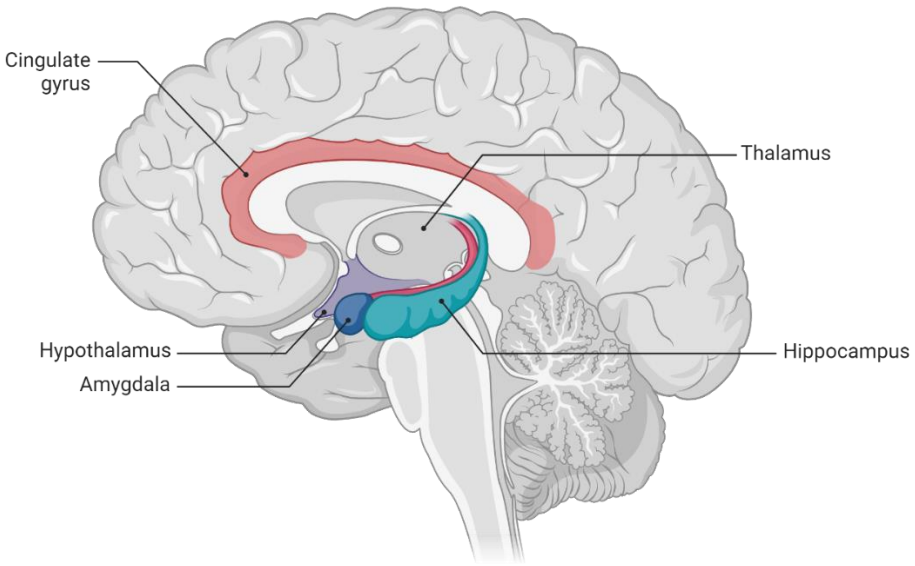

Figure 1.4 A schematic diagram of the human limbic system. The limbic system consists of several interconnected structures, including the cingulate gyrus, hippocampus, amygdala, thalamus and hypothalamus. Created with BioRender.com.

1.3.1 The human anterior cingulate cortex (ACC)

The human ACC is a bilateral structure located in the medial frontal lobes. The ACC is often included as a part of the prefrontal cortex (PFC; Figure 1.5a-b), however, cytoarchitecturally it does not meet the same criteria as the PFC as it lacks a clear granular layer (Haber et al., 2022). The ACC encompasses Brodmann's area (BA) 24, 25, 32 and 33 and can be further divided into the perigenual ACC (pACC; BA24 and 32), the subgenual ACC (sACC; BA24, 25 and 32) and the cingulate motor area (CMA; BA33) (Jumah and Dossani, 2019) (Figure 1.5b). The ACC can also be divided into dorsal (dACC) and ventral (vACC), corresponding to BA32 and BA24, respectively.

Although the function of the ACC is strongly debated, it is evident that the ACC sits in a unique and important position in the brain, forming connections to both the 'emotional' and 'cognitive' systems (Bush et al., 2000, Rolls, 2019). The sACC and pACC both play a crucial role in the cognitive regulation of emotion (Palomero-Gallagher et al., 2019), but the sACC does play a more general role in cognitive control (Scharnowski et al., 2020). Located next to the primary motor cortex, the CMA is involved in higher-order motor processing (Jumah and Dossani, 2019).

The vACC receives inputs from the amygdala and orbitofrontal cortex and is more associated with emotional processing. The dACC forms connections to the hippocampus via the parahippocampal gyrus and entorhinal cortex (EC), and is central for complex cognitive processes (Bush et al., 2000), such as response selection, error detection and reward-based decision-making (Bush et al., 2002, Vogt, 2016), as well as sensorimotor processing (Ou et al., 2024). It is these connections to the amygdala and hippocampus that allows the ACC to act as an important interface between cognition and emotion and play an important role in executive function.

In schizophrenia, structural and functional studies suggest abnormalities in the ACC may underlie pathology. Imaging studies mostly find that schizophrenia patients show reduced grey matter volume in the ACC, compared to controls (Fornito et al., 2009). Post-mortem studies are consistent with these results, finding a reduction in ACC laminar thickness in tissue taken from patients with schizophrenia, compared to controls (Bouras et al., 2001), a feature indicative of neuronal loss. Although a key study found a decrease in pyramidal neuron and interneuron density (Benes et al., 1986), loss of pyramidal cells is not consistent with the literature and does not

necessarily correlate with grey matter changes (Fornito et al., 2009). Neuroimaging studies have found abnormal ACC activity in patients with schizophrenia. Although results are mixed, overall ACC hypofunction, or hypoactivation, was found in patients with schizophrenia, across a variety of cognitive tasks (Adams and David, 2007). However, findings in patients with schizophrenia may be confounded by antipsychotic medication and may underlie some of the variation in results.

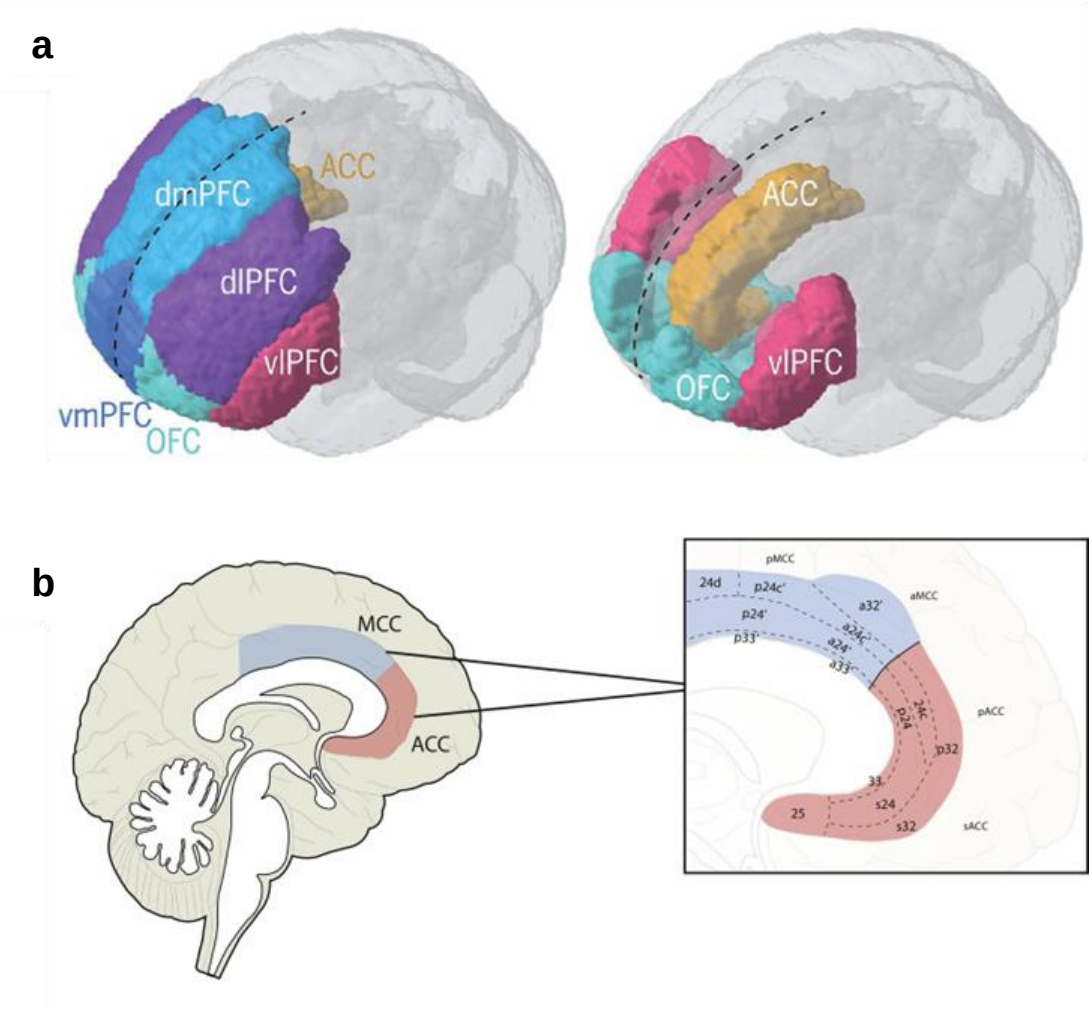

Figure 1.5 The human PFC, highlighting the functional and structural divisions of the cingulate cortex, including ACC and MCC. (a) Illustration of the common functional areas of the human PFC, including dorsolateral PFC (dlPFC), dorsomedial PFC (dmPFC), ventrolateral PFC (vlPFC), ventromedial PFC (vmPFC), orbitofrontal cortex (OFC) and anterior cingulate cortex (ACC). (b) Subdivisions of the cingulate cortex, including ACC (red) and MCC (blue), defined by Brodmann's area (BA) 24, 25, 32 and 33. The ACC includes the perigenual ACC (pACC) and subgenual ACC

(sACC), and CMA (not shown), indicated by BA33. Adapted from (a) Carlén (2017) and (b) van Heukelum et al. (2020).

1.3.2 The rat anterior cingulate cortex (ACC)

In both humans and rodents, the ACC is considered as a key brain region controlling cognition and emotion, or affection (Rolls, 2019), and rodent studies have played a crucial role in understanding the role of the ACC in human studies. The rodent ACC forms part of the mPFC, which also includes the infralimbic and the prelimbic cortices (Xu et al., 2019). The mPFC is considered a higher cortical area and exerts top-down control over other brain regions, and is therefore crucial for higher order cognitive processing (Anastasiades and Carter, 2021). The mPFC receives long-range excitatory inputs from the ventral hippocampus (vHPC), whilst sending outputs to the dorsomedial striatum, and has reciprocal connections with the cortex, basolateral amygdala, ventral tegmental area and thalamus amongst others (Anastasiades and Carter, 2021). The connection between vHPC and mPFC is important for working memory and the connections between the amygdala and striatum form the circuit underlying decision-making (Jobson et al., 2021).

The classical nomenclature that defines the structure and function of the rodent (mouse and rat) cingulate cortex comprises cingulate area 1 (Cg1) and cingulate area 2 (Cg2) which runs perpendicular through both the ACC and midcingulate cortex (MCC) (Figure 1.6a). In a review by van Heukelum et al. (2020), a definition using Brodmann areas has been suggested which better aligns rodent ACC functional and anatomical research with other mammals, including humans and non-human primates (Figure 1.6b). In most mammals, including humans, the border between the MCC and ACC is drawn along the rostro-caudal axis (Figure 1.5b), clearly defining ACC and MCC. This review better links cognitive functions such as reward-based decision making, attention and social behaviour with the ACC and not MCC, rather than attributing the function to Cg1 and/or Cg2. This discrepancy in definition must therefore be considered when reviewing literature describing the rodent ACC.

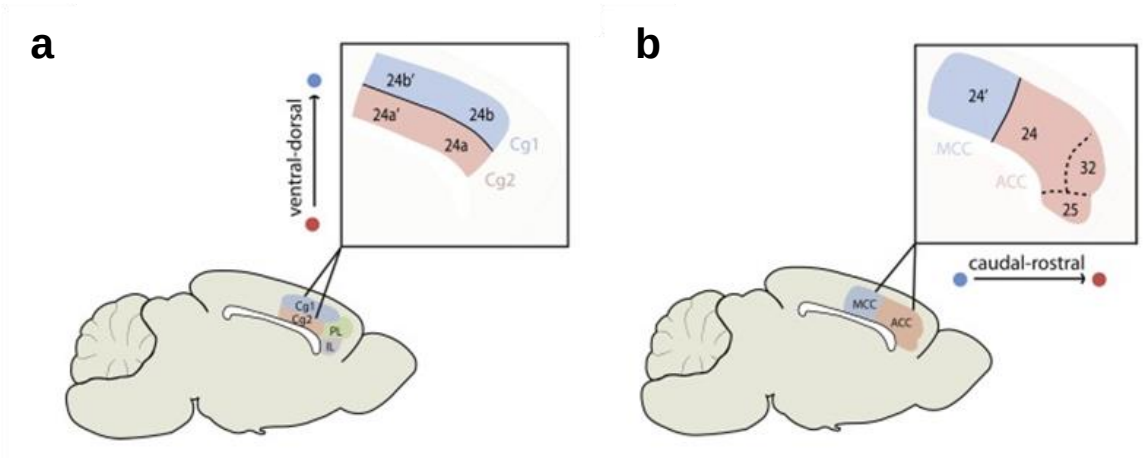

Figure 1.6 Schematic of the rat mPFC, highlighting differences in ACC nomenclature. (a) The classic definiton of the rodent mPFC divides the region into the prelimbic (green) and infralimbic (purple) cortices, and the cingulate cortex along the ventral-dorsal axis into Cg1 (blue) and Cg2 (red); Brodmann's Area (BA) 24 in the ACC, and 24' in the MCC. (b) A homologous definition of the mPFC defining the ACC (red) as BA24, 25 and 32, and MCC (blue) as BA24', dividing the two regions by the caudal-rostral axis. Taken from van Heukelum et al. (2020).

Overall, nomenclature does not change the evidence for the function of the rodent ACC which, as in humans, is associated with cognitive and emotional control. The ACC has been implicated in working memory in rodents (Teixeira et al., 2006) as it has in humans (Kaneda and Osaka, 2008). A chronic PCP mouse model used to assess working memory found c-Fos expression, a molecular marker for cellular activity, increased in the dorsomedial striatum following a T-maze task. (Arime and Akiyama, 2017). The dorsomedial striatum is a direct output of the ACC, and although no changes were seen in the ACC, this highlighted the importance of the ACC in working memory (Arime and Akiyama, 2017). Using an acute MK-801 treatment, Huang et al. (2022) induced schizophrenia-like social and working memory deficits, specifically in the novel object recognition (NOR) task, in mice. Interestingly, by activating the basolateral amygdala (BLA) – ACC pathway using chemogenic and optogenetic methods, the group were able to alleviate these social and cognitive deficits. The role of the ACC and the brain regions it is connected to is, therefore, very important for understanding underlying working memory deficits of schizophrenia.

1.3.3 The human hippocampus

The hippocampus is one of the most extensively studied brain regions and was first implicated in learning and memory when patient Henry Gustav Molaison (commonly known in the literature as patient H.M) underwent surgery for refractory epilepsy. H.M suffered anterograde amnesia following the removal of the hippocampus (Scoville and Milner, 1957). Following the discovery of long-term potentiation (LTP) by Bliss and Lomo (1973), experimental evidence proved that synapses were plastic and that high-frequency stimulation at excitatory synapses in the hippocampus resulted in rapid and long-lasting strengthening of synapses (Bliss and Gardner-Medwin, 1973). LTP quickly became the favoured theory for the mechanisms underlying learning and memory with NMDA receptor-mediated LTP becoming the main research focus for most (Nicoll, 2017).

The hippocampus is a complex bilateral brain structure and takes its name from its distinct ‘seahorse’, or ‘S’, -shape. As part of the limbic system, the hippocampus is formed by a densely packed, highly organised laminar structure of neurons, embedded deep into the temporal lobe. Structurally, the hippocampus is divided into the dentate gyrus (DG), *cornu ammonis* (CA) regions (1 - 4) and the subiculum (de Nó, 1934). The major input to the hippocampus comes from the EC via two different pathways (Van Strien et al., 2009). The perforant pathway projects to the DG and CA3, and the temporo-ammonic pathway projects to the CA1 and subiculum (Marks et al., 2022). The subiculum then inputs back to the EC. Although the human hippocampus is anatomically symmetrical, it is functionally lateralized. The hippocampus is essential for a range of cognitive functions, where the left hippocampus specialises in episodic, contextual and long-term autobiographical memory, whereas the right hippocampus is more specific for spatial information processing and navigation (Jordan, 2019).

As the hippocampus plays a crucial role in learning and memory, it is unsurprising that there is considerable evidence for hippocampal pathology in patients with schizophrenia. Most consistently, hippocampal volume is reduced in patients with schizophrenia, by around 5% (McCarley et al., 1999, Nelson et al., 1998). Loss of volume is associated with loss of neurons. Zhang and Reynolds (2001) reported a significant reduction in PV-immunoreactive neuron density, across all regions of the hippocampus, suggesting a reduction in the expression of PV. Furthermore, Gao et al.

(2000) found changes in the NMDA receptor subunits in the hippocampus of patients with schizophrenia, showing an increase in N2B mRNA and a decrease in N1 mRNA. When studying hippocampal activity, patients with schizophrenia showed decreased or abnormal hippocampal activation during memory tasks (Weiss et al., 2003, Weiss et al., 2004), indicative of abnormal cellular network activity.

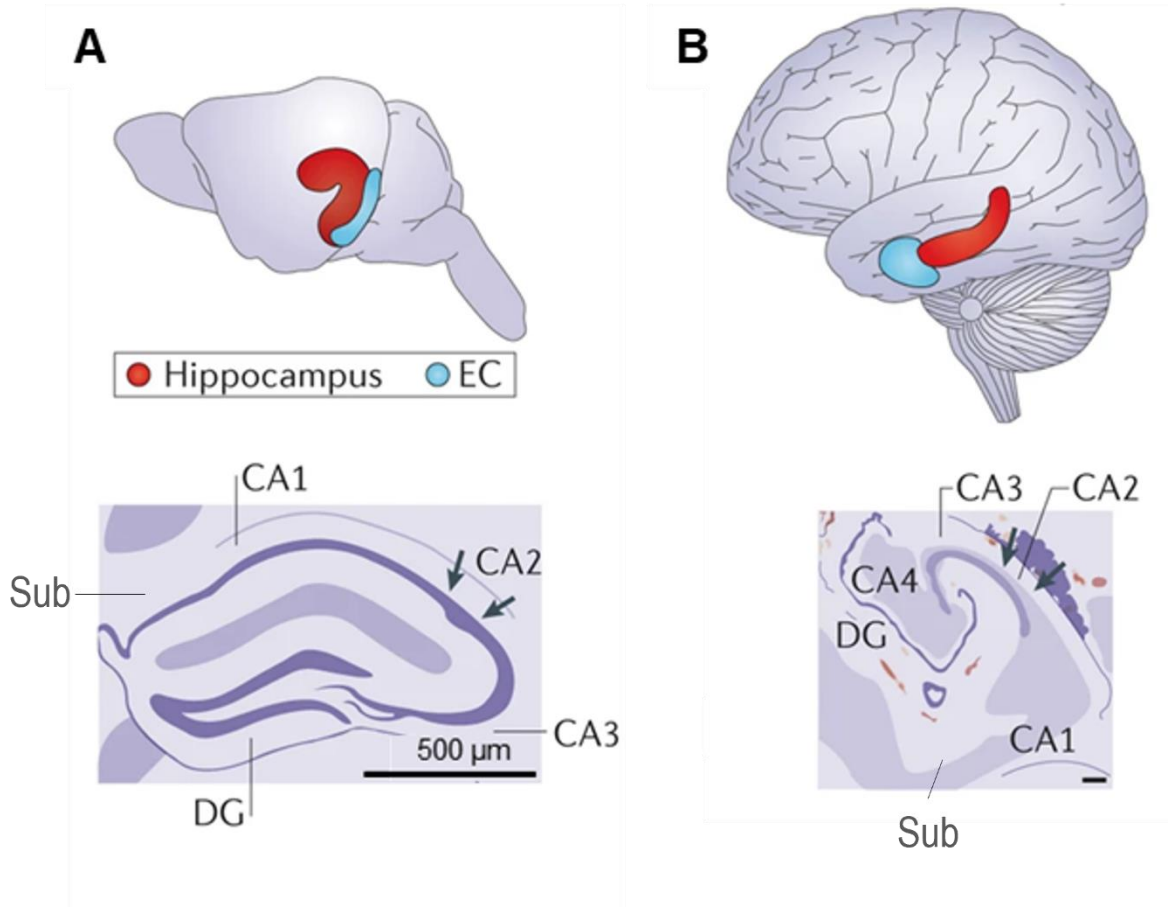

Figure 1.7 A comparison between the rat and human brain, highlighting the location and structure of the hippocampus in each species. The location of the hippocampus (red) and associated EC (blue) in both (a) rat and (b) human brain. The cross-sectional schematic of the structure of the hippocampus in both species indicates the organised morphology of CA1, CA2 and CA3, dentage gyrus (DG) and subiculum (Sub). The CA4 is also indicated in human. Adapted from Strange et al. (2014).

1.3.4 The rat hippocampus

The hippocampus has been studied in rodents since the 1950s as an incredibly useful tool for understanding circuits underlying learning and memory (Eichenbaum, 1999, Kandel and Spencer, 1968), as well as spatial navigation (Buzsáki and Moser, 2013, Dostrovsky and O'Keefe, 1971, Zemla and Basu, 2017). The function and neuroanatomical organisation of the rodent, and specifically rat, hippocampus is similar to the human hippocampus (Figure 1.7), as both share the same clear laminar structure and neuronal pathways within the hippocampus (Kesner and Hopkins, 2006). The rat brain also shows clear lateralization of spatial memory (Klur et al., 2009), akin to the human hippocampus (Spiers et al., 2001). The vHPC plays a crucial role in social and emotional memory, through direct connections with the mPFC, particularly the ACC, and amygdala. Furthermore, although the dorsal CA1 is considered the hub for spatial memory, optogenetic studies have shown the vHPC also plays a functional role in spatial working memory encoding, along the vHPC - mPFC pathway (Spellman et al., 2015).

The prenatal MAM model (described above 1.2.4) is a rodent developmental model of schizophrenia. Studies have shown that the rat MAM model leads to reduced hippocampal volume and schizophrenia-related behavioural abnormalities in offspring (Featherstone et al., 2007, Moore et al., 2006). Specifically, MAM treatment at E17 in rats affected the hippocampus, impairing glutamatergic neurotransmission and reducing AMPA-receptor-mediated synaptic transmission (Hradetzky et al., 2012). This results in hyperactivity in the vHPC, leading to reduced gamma frequency oscillations (Lodge et al., 2009). In mice, MAM treatment on gestational days 16 and 17 also reduced hippocampal volume, impaired contextual fear memory, and decreased LTP in the CA1 (Chalkiadaki et al., 2019). Furthermore, male offspring showed deficits in cognitive tasks but female offspring did not, highlighting an interesting sex difference (Chalkiadaki et al., 2019).

The rodent hippocampus is therefore incredibly useful for studying cognitive deficits in schizophrenia due to its structural and functional similarities to the human hippocampus. It is crucial for understanding learning, memory, and spatial navigation, all areas impacted in schizophrenia.

1.4 Neuronal network activity underlying cognition, learning and memory

1.4.1 High frequency oscillations

When referring to brain or neuronal oscillations, the term describes the rhythmic electrical activity generated spontaneously, or in response to stimuli, by neuronal tissue in the CNS (Başar, 2013). In this thesis, such brain oscillations will be referred to simply as oscillations, or oscillatory activity. Oscillations control the local microscale timing of action potentials as well as the macroscale coordination of cortical activity across brain regions, allowing temporal and spatial brain connectivity (Guan et al., 2022, Zhang et al., 2018). Oscillations were first observed by Hans Berger in 1929 using an electroencephalogram (EEG), a non-invasive method of recording electrical activity over the skull. An example of a raw EEG signal, comprised of multiple brain rhythms, can be seen in Figure 1.8a. This raw signal can be filtered and separated to reveal the distinct, underlying oscillations that each occupy different frequency bands (Figure 1.8b).

Following on from EEG recordings, oscillations have since been recorded *in vivo* from animals (Beker et al., 2016, Colgin et al., 2009, Furth et al., 2017, Gretenkord et al., 2016, Tavares and Tort, 2022), and *in vitro* (or *ex vivo*) from prepared brain slices, both animal (Buhl et al., 1998, Cunningham et al., 2003, Fisahn et al., 1998, Glykos et al., 2015, LeBeau et al., 2002, Pietersen et al., 2009, Whittington et al., 1995) and human (de la Prida and Huberfeld, 2019, Florez et al., 2015). Further studies, determined that different oscillation frequencies correlated with different brain states, including sleep and rest, and cognitive or motor activity (Başar et al., 2001, Bonanni et al., 2012, Buzsáki, 2005, Grosmark et al., 2012, Niedermeyer, 1997, Schmidt et al., 2019, Zhang et al., 2008). *In vitro* oscillations can be spontaneous, and gamma frequency oscillations have been recorded from the CA3 of the vHPC (Pietersen et al., 2009). However, studies usually evoke oscillations pharmacologically, using the glutamate receptor agonist kainate (KA) or the cholinergic agonist carbachol (Buhl et al., 1998, Cunningham et al., 2003, Fisahn et al., 1998, Pietersen et al., 2009, Whittington et al., 1995), or in response to electrical stimuli (Traub et al., 1996, Whittington et al., 1997).

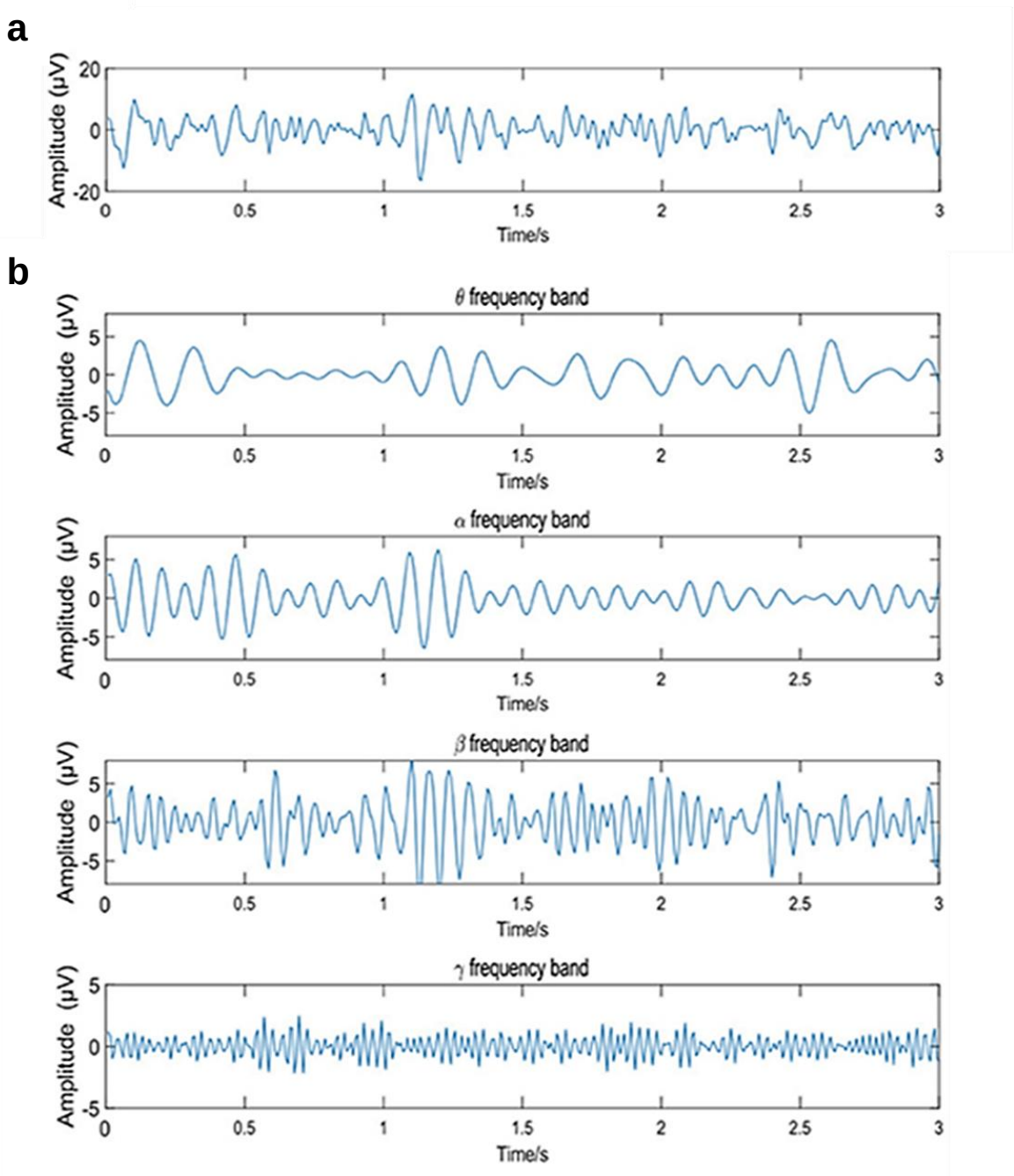

Figure 1.8 EEG oscillations frequency bands. (A) An example raw EEG. (C) The EEG signals of delta (θ), alpha (α), beta (β) and gamma (γ) frequency bands. Adapted from Zhang et al. (2022).

The frequencies of these oscillations are determined by intrinsic neuronal properties, synaptic currents and precisely timed spiking activity of neuronal populations, allowing information processing and cellular communication within and

between brain regions (Uhlhaas, 2011). As different frequency bands correlate with different types of activity, oscillations are often used as biomarkers of behaviour or brain state (Guerra et al., 2019). Gamma (30 - 80 Hz) frequency oscillations, for example, are associated with working memory and executive function (Howard et al., 2003, Lisman, 2010, Thompson et al., 2021, van Vugt et al., 2010, Yamamoto et al., 2014), and changes in gamma frequency oscillations are observed in several neuropsychiatric disorders and neurodegenerative diseases, particularly in patients with cognitive impairment, including schizophrenia (Dienel and Lewis, 2019, Palmisano et al., 2024), major depressive disorder (MDD) (Fitzgerald and Watson, 2018, Palmisano et al., 2024), and Alzheimer's disease (AD) (Jafari et al., 2020) patients (Guan et al., 2022). Figure 1.9 demonstrates how spontaneous activity in each frequency band topographically differs across the brain in schizophrenia patients compared to healthy controls, showing aberrantly larger oscillatory power in theta (4 – 8 Hz), alpha (8 – 15 Hz), beta (15 – 30 Hz) and gamma (30 – 80 Hz) bands (Tanaka-Koshiyama et al., 2020). This thesis primarily focuses on beta and gamma frequency oscillations, as their association with the cognitive impairments in schizophrenia are well documented, but still not fully understood.

High frequency oscillations can be subdivided into different rhythms, or frequency bands, namely beta (15 - 30), low-gamma (30 – 80 Hz) and high-gamma (80 – 150 Hz) oscillations, although the exact divisions vary between research group. Beta and gamma oscillations are generated and maintained by different interneuron populations (discussed in detail below 1.6). Low- and high-gamma are also mechanistically distinct types of activity and, as this thesis focuses on the mechanisms underlying low-gamma oscillations, from this point forwards low-gamma will simply be referred to as gamma, or gamma frequency, and any mention of high-gamma will reference it as such.

Beta and gamma frequency oscillations are biomarkers of cognitive function, specifically working memory (Lundqvist et al., 2016, Miller et al., 2018), and are modulated by inhibitory interneuron populations (Fuchs et al., 2007, Tamás et al., 2000, Whittington et al., 1995). Normal cognitive function depends on the excitatory-inhibitory balance generated by precisely timed firing of interneurons and a favoured hypothesis suggests that interneuron dysfunction, via NMDA hypofunction (Figure

1.10), may cause disinhibition in excitatory-inhibitory neuronal circuits and may underlie abnormal oscillations and the cognitive deficits of schizophrenia.

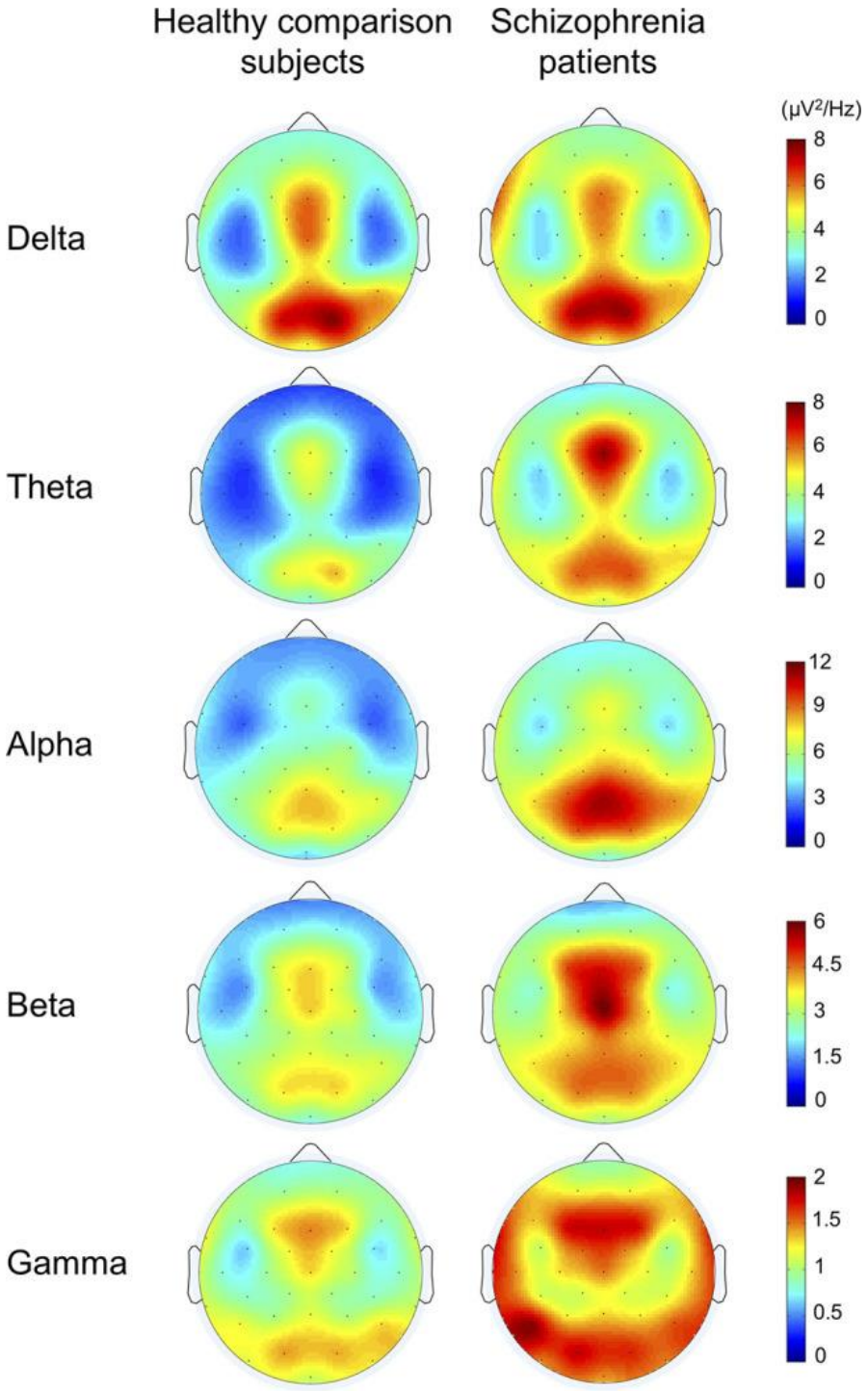

Figure 1.9 Topographical representation of the average resting spectral power across different oscillation frequency bands, of healthy controls in comparison to patients with schizophrenia. Theta, alpha, beta and gamma power is visibly greater in patients with schziophrenia, compared to healthy control subjects. Adapted from Tanaka-Koshiyama et al. (2020).

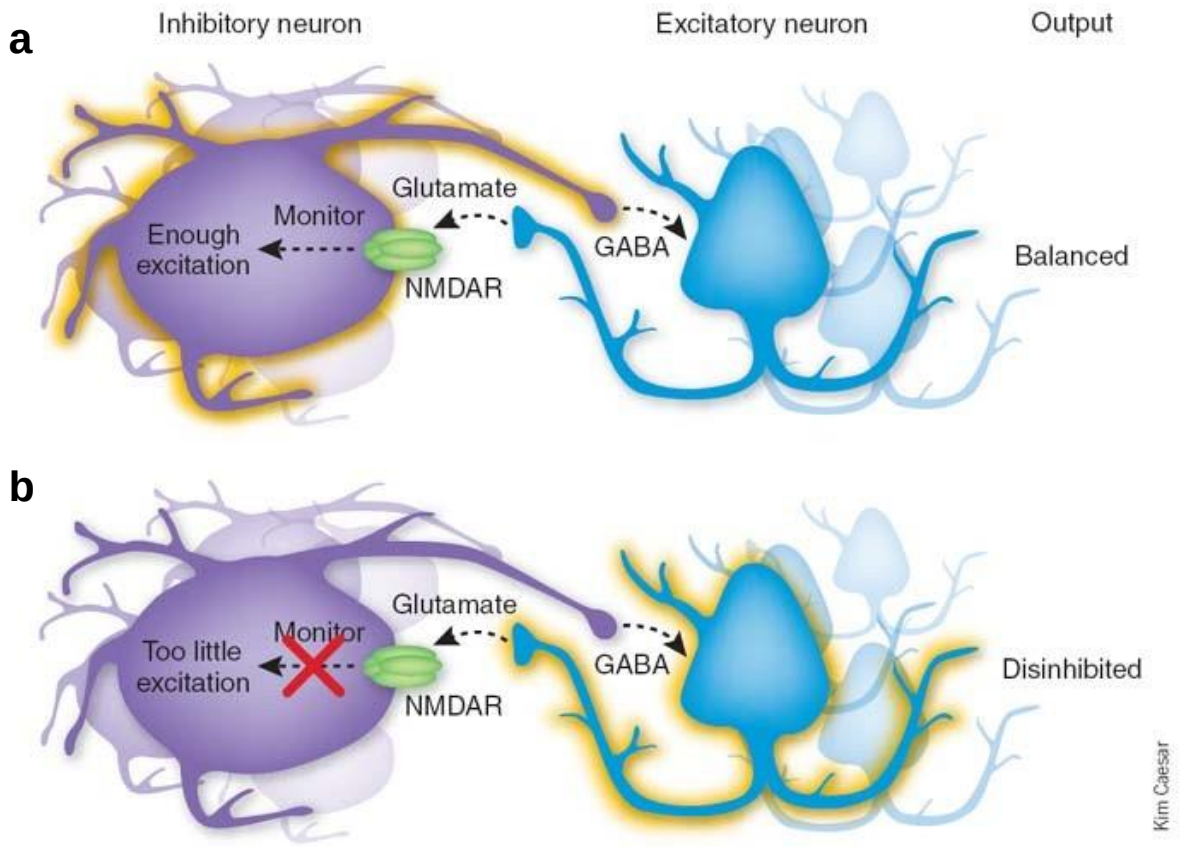

Figure 1.10 NMDA redceptor hypofunction causes disinhibition of excitatory pyramidal cells. (a) Inhibitory interneurons monitor excitatory glutamatergic levels via NMDA receptors, and release inhibitory GABA to maintain excitatory-inhibitory balance with excitatory neurons. (b) NMDA receptor hypofunction disrupts glutamatergic singalling and interneuron firing, causing reduced GABAergic output, disinhibition of excitatory neurons, and increased glutamatergic tone. Taken from Gordon (2010).

Gamma oscillations are important in synchronising activity across and between brain regions, as well as modulating the activity evoked when performing a broad spectrum of cognitive tasks (Guan et al., 2022). Resting, or steady state gamma, is present during a relaxed or baseline state, without specific task demands or sensory input. Resting state EEG gamma power studies have repeatedly found increased gamma power in patients with schizophrenia, compared to healthy controls. Tanaka-Koshiyama et al. (2020) found increased gamma power in the frontal and occipital-temporal regions (Figure 1.9). Baradits et al. (2019) and Tikka et al. (2014) also found increased gamma power in chronic and first episode schizophrenia patients, respectively. Conversely, in a magnetoencephalography (MEG) study, Grent-'t-Jong et al. (2018) found reduced gamma power in the PFC of first episode schizophrenia patients, and the frontal, spatial and temporal areas of chronic schizophrenia patients. Differences may be due to the spatiotemporal resolution EEG / MEG recording techniques, however factors such as patient medication, recording session length and session condition (eyes open vs eyes closed), could also affect results. Taken together, this evidence indicates that gamma oscillations in patients with schizophrenia are abnormal and differ across different stages of the disorder.

Deficits in gamma oscillations have also been reported during cognitive tasks. When performing working memory tasks specifically, patients with schizophrenia showed reduced gamma activity during the memory retrieval phase of tasks (Haenschel et al., 2009). Furthermore, where healthy controls demonstrated an increase in gamma activity in response to tasks that required increased executive control (Cho et al., 2006) and working memory load (Basar-Eroglu et al., 2007), patients with schizophrenia did not.

The relationship between beta frequency oscillations and cognitive impairment is more varied. In patients with schizophrenia, resting-state beta power is also reported to be abnormally increased in comparison to healthy controls (Newson and Thiagarajan, 2018, Tanaka-Koshiyama et al., 2020). When comparing findings of auditory stimulation experiments to healthy controls, there was no difference in beta power (Kwon et al., 1999), whereas a visual-perception task found a reduction (Spencer et al., 2004) and memory tasks showed increased beta activity (Meconi et al., 2016), in patients with schizophrenia. Beta oscillations are highly correlated with

sensorimotor function (Kilavik et al., 2013), thus changes in beta frequency oscillations are highly dependent on the task being performed.

Gamma oscillations can be generated locally and projected across large distances across different brain regions. These oscillations are generated by a network of fast-spiking PV+ inhibitory interneurons, which can fire up upwards of 400 Hz (Wang et al., 2016), and excitatory pyramidal cells, which only fire up to 3 Hz (Gray et al., 1989, Whittington et al., 1995, Womelsdorf et al., 2007) (Figure 1.11). The pyramidal cells are driven by the precise spike timing of the PV+ interneurons, where excitatory postsynaptic potentials (EPSPs) generated in the interneurons drive an inhibitory feedback mechanism in the pyramidal cells, causing rhythmic, synchronous firing, which is terminated by the train of inhibitory postsynaptic potentials (IPSPs) in the excitatory cells.

Evidence suggests that beta frequency oscillations are orchestrated by somatostatin (SST)-positive (SST+) interneurons (Chen et al., 2017, Kuki et al., 2015) and the basic inhibition-based mechanism that generates and drives gamma frequency oscillations, described above, is also believed to underpin beta frequency oscillations (Roopun et al., 2008). *In vivo* studies in mice demonstrate that optogenetically driving PV+ interneurons enhanced gamma oscillations (Sohal et al., 2009, Cardin et al., 2009) and inhibiting PV+ and SST+ interneurons suppressed gamma and beta oscillations, respectively (Chen et al., 2017, Sohal et al., 2009). Interestingly, beta oscillations recorded from the sensory association neocortex *in vitro* do not depend on $GABA_A$ receptor-mediated IPSPs, and when both gamma and beta rhythms are in co-existence, $GABA_A$ block diminishes gamma frequency oscillations, whilst potentiating beta frequency oscillations (Roopun et al., 2008). This suggests that even though gamma and beta frequency oscillations are generated and maintained by different interneuron populations, the two mechanisms are inextricably linked.

Disruption to this synchronous activity, by NMDA receptor hypofunction, has been proposed to be the cause of impaired cognitive function in schizophrenia (Lesh et al., 2011). Using beta and gamma oscillations as biomarkers, this thesis aims to explore how the underlying mechanisms may cause these deficits.

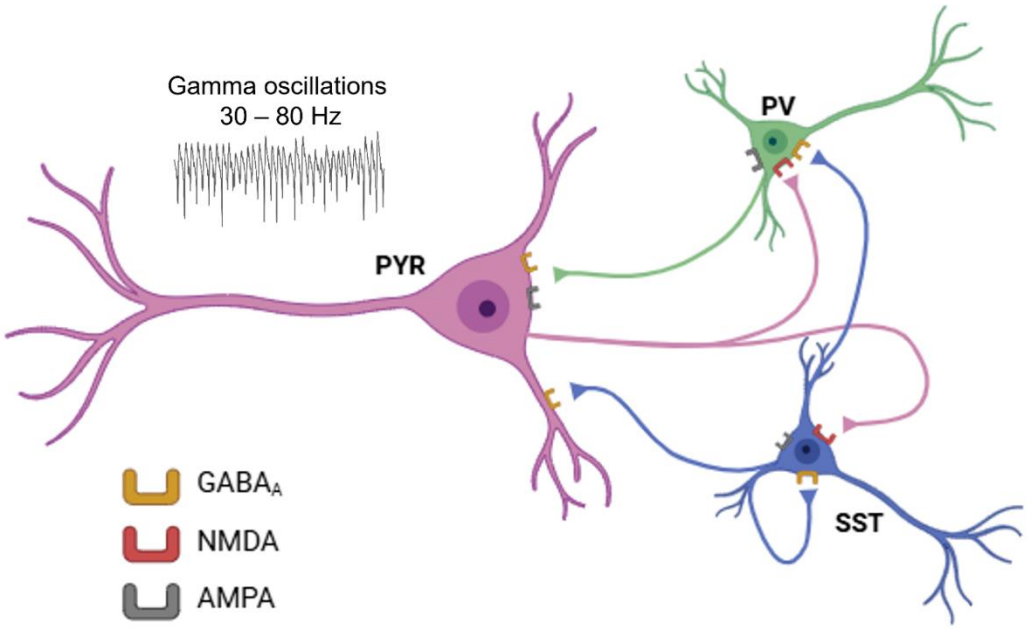

Figure 1.11 The excitatory–inhibitory network mechanism of gamma oscillations. Schematic showing the connectivity between pyramidal cells and PV+ and SST+ interneurons, generating gamma frequency oscillations through pyramidal-interneuron network gamma (PING) or interneuron network gamma (ING) mechanisms. Adapted from Guan et al. (2022) and created with BioRender.com.

1.4.2 Long-term potentiation (LTP)

While oscillations are known to be critical for learning and memory the cellular correlate of learning has been proposed to be LTP. Early LTP research was pivotal for understanding memory and synaptic plasticity (Bliss and Collingridge, 2019). The discovery of LTP began with T.V.P. Bliss's 1968 experiments which shifted focus from complex cortical pathways to the simpler hippocampus, inspired by Donald Hebb's theories (Hebb, 1949). LTP is a model of neuronal plasticity, first observed in hippocampal recordings, where tetanic stimulation along the Schaffer collateral pathway induced a persistent increase in the amplitude of EPSPs in CA1 neurons (Abraham and Bear, 1996, Bliss and Lomo, 1973). LTP can be triggered by tetanic high-frequency stimulation (HFS) of 100 Hz for 1 second, or with a theta burst stimulation that consists of repeated short bursts (four or five stimuli at 100 Hz) . LTP

has two phases: an early-phase LTP, lasting up to 2 hours, which requires modification of pre-existing proteins, and late-LTP, which is critically dependent on new protein synthesis at the time of LTP induction and sustains the enhancement of synaptic efficacy for long periods of time (Vickers et al., 2005).

LTP is caused by changes in the number and biophysical properties of AMPA receptors (Andrásfalvy and Magee, 2004). LTP induction also requires postsynaptic events, such as activation of NMDA receptors and an increase in postsynaptic Ca^{2+} (Collingridge et al., 1983, Lynch et al., 1983). Given the necessary need to activate NMDA receptors, it is unsurprising that animal experiments that use the NMDA receptor antagonists PCP and MK-801 cannot induce LTP *in vitro* (Coan et al., 1987, Stringer et al., 1983) or *in vivo* (Abraham and Mason, 1988, Stringer et al., 1983). Interestingly, an acute model of psychosis found a single injection of the NMDA receptor antagonist MK-801 can impair LTP, along the perforant path-DG synapse of the hippocampus in rats, for weeks following injection (Wiescholleck and Manahan-Vaughan, 2013). The same treatment also causes long lasting impairments in spatial (Manahan-Vaughan et al., 2008a) and object recognition memory (Manahan-Vaughan et al., 2008b).

The role of LTP in learning and memory has led researchers to explore various approaches to mitigate LTP deficits in schizophrenia, particularly focusing on the glutamatergic system, NMDA receptor function, and the effects of antipsychotic medications. Studies have shown that augmenting NMDA receptor function with co-agonists like glycine or D-serine can reduce LTP deficits in animal models of schizophrenia (Pei et al., 2021). Alternatively, some SGAs, such as clozapine and risperidone, have been found to partially restore LTP deficits in animal models of schizophrenia (Price et al., 2014).

Brain derived neurotrophic factor (BDNF) is an important neurotrophin that is involved in neurodevelopment and neuroprotection, synapse regulation and synaptic plasticity. BDNF is necessary for LTP, and schizophrenia is associated with low BDNF levels in the hippocampus (Ray et al., 2011, Takahashi et al., 2000), PFC (Weickert et al., 2003), and ACC (Takahashi et al., 2000). Tanqueiro et al. (2021) showed that PCP-induced NMDA receptor hypofunction induced dysfunctional BDNF signalling in the PFC, but not in the hippocampus, which may contribute to the PFC-dependent

cognitive deficits seen in the subchronic PCP model. This suggests that targeting BDNF signalling may improve cognitive dysfunction in schizophrenia.

Overall, studying LTP in schizophrenia is vital for understanding the deficits in learning and memory associated with the disorder. LTP, a key mechanism of synaptic plasticity, underlies memory formation and cognitive function, and examining LTP deficits provides insight into the neuronal basis of cognitive dysfunction. Research focusing on restoring LTP through pharmacological interventions may offer potential strategies to alleviate learning and memory impairments in schizophrenia, contributing to better management of the disorder.

1.5 The GABAergic inhibitory network

There are many millions of interneurons in the mammalian brain, and therefore classifying different types of interneurons is helpful, providing a logistical and conceptual system for understanding cellular and network function. GABAergic interneurons are commonly categorised depending on their anatomical, molecular, and physiological properties (Ascoli et al., 2008, DeFelipe et al., 2013). However, due to the heterogeneity of these cells a more comprehensive system that accounts for electrophysiological, biochemical, immunohistochemical and genetic properties would better define and categorise different interneuron populations (Cembrowski and Spruston, 2019, Huang and Paul, 2019, Tremblay et al., 2016, Zeng and Sanes, 2017).

PV+ interneurons and SST+ interneurons are key in driving gamma and beta frequency oscillations, respectively, and this thesis therefore focuses on these two interneuron types. Genetic studies have shown that patients with schizophrenia that have a single-nucleotide polymorphism (SNP), and a subsequent missing allele, at *GAD1*, are correlated with decreased PV, SST receptors, and GAD ribonucleic acid (RNA) (Năstase et al., 2022). Understanding interneurons and changes in interneuron populations is crucial to understanding NMDA hypofunction and schizophrenia pathology.

1.5.1 Parvalbumin-positive interneurons

PV is a small, mostly cytosolic Ca^{2+}-binding protein found in different classes of cortical interneurons and in some mammalian neocortical pyramidal cells (Hof et al., 1999, Jinno and Kosaka, 2004). Physiologically, PV acts as a buffer to sequester and transport Ca^{2+} in the cytoplasm of inhibitory cells (Lee et al., 2000). PV also regulates various enzymatic activity and protects neurons from calcium overload (Heizmann, 1993). Interneurons containing PV are characterised as PV-positive or PV-containing (PV+) interneurons. PV allows PV+ interneurons to cope with the high frequency firing rate and subsequently balances glutamatergic tone. Genetic ablation of PV causes changes in GABAergic synaptic transmission, an impairment found in patients with schizophrenia (Frankle et al., 2015).

PV+ interneurons can be further categorised into two distinct types, PV basket cells (PVBCs) and chandelier cells (PVCCs; sometimes known as axo-axonic cells), based on their morphology, firing properties and projection targets. Around 50% of cortical basket and chandelier interneurons that innervate pyramidal cells are PV+ (Hu et al., 2014). The axon terminals of PVBCs primarily target the perisomatic region of pyramidal cells, whereas the axon terminals of chandelier cells target the axon initial segment of pyramidal cells, giving them their chandelier-like structure (Somogyi, 1977). The axon terminals of PVBCs and PVCCs also differ in the GABA synthesizing enzymes contained within: PVBCs' contain both GAD65 and GAD67, whereas PVCCs' contain GAD67 only (Fish et al., 2011).

PVBCs comprise the majority of PV+ interneurons and their activity is clearly closely coupled to gamma oscillatory activity (Freund, 2003, Klausberger and Somogyi, 2008). The role of PVCCs in the generation of gamma oscillations is less clear, however, animal models of schizophrenia suggest that pyramidal cell innervation by PVCCs is reduced causing reduced inhibition at the axon initial segment, contributing to aberrant oscillatory activity (Vivien et al., 2023).

PV interneurons also differ in the principal type of $GABA_A$ receptors at their synaptic targets. The PVBC synapse onto pyramidal cells and predominantly express $GABA_A$ receptors containing the α1 subunit, which mediate fast decay of the inhibitory postsynaptic current (IPSC). The $GABA_A$ receptors on PVCC inputs to pyramidal cells, however, contain the α2 subunit, and exhibit a slower IPSC decay (Mody and Pearce, 2004). Gamma oscillations require fast decay IPSCs, indicating PVBCs critical role in gamma oscillation generation (Bartos et al., 2007). Thus, the available data strongly implicate the PVBC-pyramidal cell microcircuit as the neuronal substrate of gamma oscillations.

Across human studies, differences in PV+ interneurons have been reported in multiple brain regions of schizophrenia patients (Marín, 2024). Although results vary, most studies suggest that patients with schizophrenia present with lower PV protein expression and *PVALB* mRNA, in comparison to controls, in the PFC (Beasley and Reynolds, 1997, Chung et al., 2016, Hashimoto et al., 2003, Sakai et al., 2008), hippocampus (Konradi et al., 2011) and EC (Wang et al., 2011). Conversely, other studies found no significant change in PV expression in the PFC (Beasley et al., 2002,

Tooney and Chahl, 2004) whilst elevated PV expression was found in the ACC (Kalus et al., 1997), of patients with schizophrenia. However, decreased expression of GAD67 has been found in PV+ interneurons in the PFC of patients with schizophrenia and specifically, a reduction in NR2A expressing GAD67+ cells has been found in the ACC (Woo et al., 2004). Furthermore, the density of excitatory synapses onto PFC PV+ interneurons is lower in schizophrenia patients than controls (Chung et al., 2016).

In rodent models, loss of PV+ or PV+ dysfunction is reported across pharmacological and developmental models of schizophrenia. PCP alters animal behaviour, inducing a schizophrenia-like phenotype including presentation of cognitive deficits, alongside reduced PV expression in the prelimbic cortex when administered subchronically (McKibben et al., 2010), and the cingulate cortex and hippocampus when administered acutely (Abdul-Monim et al., 2007)**.** The MAM model shows PV+ density is reduced in the rat DG (Du and Grace, 2016), mPFC, ACC and ventral subiculum (Lodge et al., 2009)

1.5.2 Somatostatin-positive interneurons

SST is a neuropeptide produced by neurons and endocrine cells in the brain and other parts of the body. In the nervous system, SST acts as a neurotransmitter and neuromodulator, modulating synaptic transmission and regulating neuronal functions (Pittaluga et al., 2021). SST+ cells are the second largest population of interneurons (Riedemann, 2019), comprising 30 – 50% of GABAergic inhibitory cells in the hippocampus and neocortex (Rudy et al., 2011). In these interneurons, SST is produced by the endoplasmic reticulum (ER) and stored in dense-core vesicles and is mainly released in a Ca^{2+}-dependent manner (Iversen et al., 1978).

Broadly, there are three distinct subtypes of SST+ interneurons; two are types of Martinotti cells and a non-Martinotti cell type. Martinotti cells are small, multipolar neurons, with short branching dendrites, distributed throughout the layers of the cortex, defined by an axonal plexus in layer (L) 1. Martinotti cell axons either ramify in a fan-shape in L2/3 and L1, or simply in L1 in a T-shape. Non-Martinotti cells target L4, instead of L1. However, in order to better define and understand the functional diversity of SST+, more recent work by Wu et al. (2023) used single-cell transcriptomics to form precise and possibly reciprocal microcircuits with excitatory

neurons that are laminar, cell-type, and subcellular specific. For example, SST-Membrane metalloendopeptidase (*Mme*), SST-Calbindin 2 (*Calb2*) are mainly found L2/3 whereas SST-Heparanase (*Hpse)* reside in L4 and L5a, for further details see Wu et al. (2023).

Within cortical circuits, SST+ cells are densely connected to most neighbouring pyramidal cells (Fino and Yuste, 2011). A key characteristic of SST+ interneurons is their high level of spontaneous activity which persists even without synaptic input (Urban-Ciecko and Barth, 2016). GABA released from SST+ interneuron synapses target the apical dendrites of pyramidal cells and other interneurons, including PV+ interneurons, but SST+ interneurons do not target other SST+ cells. This GABA release directly modulates excitatory inputs via $GABA_A$ and $GABA_B$ receptor-mediated inhibition (Kanigowski et al., 2023, Pfeffer et al., 2013).

Although most studies focus on PV+ interneuron changes in schizophrenia, there is evidence for changes in SST+ interneurons too. Human studies have shown there is a reduction in the number of hippocampal SST+ interneurons (Konradi et al., 2011), and a decreased level of SST mRNA in the hippocampus, ACC and dlPFC, of patients with schizophrenia (Fung et al., 2010, Hashimoto et al., 2008, Konradi et al., 2011). Interestingly, there is a greater reduction in the level of SST in patients with schizophrenia in comparison to any other measured biomarker, including PV (Alherz et al., 2017). As neuronal SST expression is activity dependent (Hou and Yu, 2013), reduced expression in post-mortem tissue does suggest either a loss of SST or SST dysfunction, however the associated pathology is still unclear. Reduced SST has also been found in AD, where the reduced levels of SST has been directly associated with the memory impairment and poor cognitive functioning of the disease (Grouselle et al., 1998), suggesting it could play a similar role in schizophrenia.

Chronic administration of NMDA receptor antagonists during neurodevelopment is a well-established rodent model used to recapitulate some aspects of schizophrenia pathology, including cognitive and behaviour disturbances. Using rat pups at postnatal day (P)10 – 20, Murueta-Goyena et al. (2020) showed subchronic MK-801 treatment resulted in a loss of SST+ in the adult (P73) hippocampus, mPFC and ACC, but did not examine behaviour. Perez et al. (2019) used an SST+ region-specific knock-down model and did find that loss of SST in the

mPFC caused cognitive deficits, but knockdown in the vHPC did not. Similar results were obtained with knock down of PV in the PFC and vHPC (Perez et al., 2019), suggesting that NMDA receptor hypofunction affected both populations of interneurons.

1.5.3 Perineuronal nets (PNNs)

Plasticity in the brain is highly important for healthy learning and memory function. An important structure in these mechanisms is the extracellular matrix (ECM), a non-cellular component composed of proteins, proteoglycans and hyaluronan, that surrounds both neurons and glial cells. The ECM not only provides structural and functional support but also significantly contributes to the communication between neurons and glia. There are 3 major types of ECM: (1) the 'loose' ECM, a diffuse structure present throughout the brain and spinal cord; (2) the membrane-bound molecules on cells; and, importantly for this thesis, (3) the lattice-like perineuronal nets (PNNs) (Sorg et al., 2016).

PNNs were first observed by Camillo Golgi in 1898 and were described as a "delicate covering" that surrounded certain cell bodies and extensions of neurons (Fawcett et al., 2019, Shen, 2018). Since then, studies have demonstrated that PNNs are more complex, net-like structures that primarily envelop GABAergic interneurons, surrounding the cell soma and proximal dendrites, with the majority of PNNs found to co-localise with fast-spiking PV+ interneurons (Härtig et al., 1992), where they act to buffer Ca^{2+} and K^{+} (Brückner et al., 1993), aiding PV+ interneurons fast-spiking behaviour (Balmer, 2016). PNNs are found throughout several brain regions, including the forebrain, midbrain and cerebullum (Li et al., 2024b).

Although PNNs vary in composition within and between brain regions, all PNNs have a similar stucture; chondroitin sulfate proteoglycans (CSPGs), linked together by glycoprotein tenascin-R (Yamaguchi, 2000), bound to a hyaluronan backbone (Figure 1.12). Hyaluronan is a glycosaminoglycan (GAG) produced by hyaluronan synthase, a cell surface enzyme produced by neurons. PNNs consist of four types of CSPGs, of which aggrecan is the most fundamental. Link proteins (hyaluronan and proteoglycan link protein 1 (HAPLN1); hyaluronan and proteoglycan link protein 4 (HAPLN4)) are needed to stabilise CSPG-hyaluronan binding, and are crucial to the PNNs structure

(Carulli et al., 2010). As well as link proteins, chondroitin sulfate glycosaminoglycan (CS-GAG) chains attach to CSPG proteins. The ability of PNNs to control plasticity is dependent on these CS-GAGs, and the structure and function of GAG chains are determined by their number and chain length, as well as their sulfation patterns (eg. CS-4, CS-6) and the position of the sulfated residues. Other ECM molecules, homeoprotein orthodenticle homeobox 2 (OTX2) and semaphorin 3A, are also components of PNNs, and are associated with regulating critical periods in development.

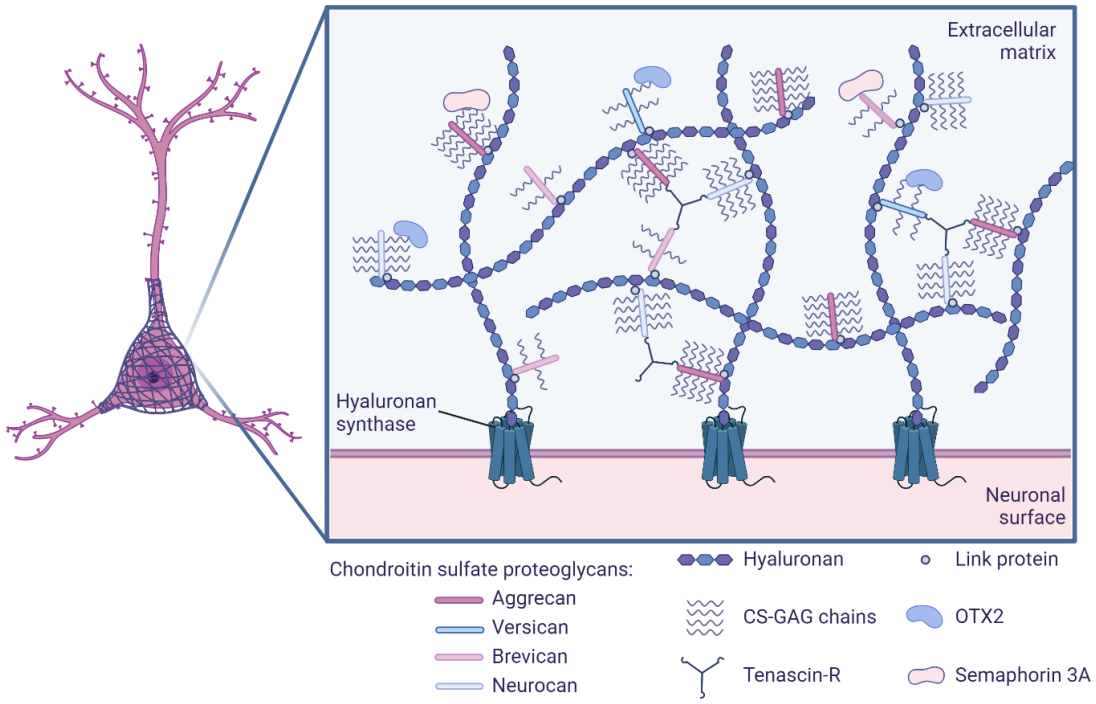

Figure 1.12 The structural components of perineuronal nets surrounding neuronal cells. PNNs are composed of a hyaluronan backbone, secreted by hyaluronan synthase, bound by chondroitin sulfate proteoglycans (CSPGs); aggrecan, versican, brevican and neurocan. Link proteins support CSPG-hyaluronan binding and tenascin-R links CSPGs. Chondroitin sulfate glycosaminoglycan (CS-GAG) chains attach to CSPG proteins. Other extracellular matrix molecules such as OTX2 and semaphorin 3A bind to the CS-GAG chains and form part of the nets. Created with BioRender.com.

Functionally, PNNs are involved in different forms of memory, including object recognition, fear and spatial memory and have been identified as being crucial for neuronal plasticity, and aiding in the consolidation and maintenance of memories over time (Li et al., 2024b). Interestingly, mouse studies found that PNN formation was increased in the hippocampus during memory formation, and memory consolidation within both the hippocampus and ACC is dependent on PNN formation (Shi et al., 2019). Furthermore, studies that degraded PNNs in the hippocampus, mPFC and ACC impaired fear conditioning learning in mice (Hylin et al., 2013, Shi et al., 2019).

In the developing brain PNNs promote interneuron maturation and maintain synaptic stability in the adult CNS (Kwok et al., 2011). In the adult brain, PNNs have been shown to control interneuron excitability as PV+ interneurons recorded from hippocampal slices, taken from brevican (another type of CSPG found in PNNs) knockout mice, were found to have a decreased firing threshold (Favuzzi et al., 2017), making PV+ interneurons more excitable (Wingert and Sorg, 2021). Furthermore, a pharmacological mouse model of sepsis-associated encephalopathy, often used to model brain dysfunction and abnormal inflammation, showed that decreased PNN+ and PV+ density in the CA1 was associated with cognitive impairments and decreased beta and gamma oscillatory power (Zhang et al., 2023). Due to their relationship with synaptic plasticity and PV+ interneurons, it is unsurprising that, in post-mortem studies, PNN's are decreased in the PFC (Alcaide et al., 2019, Mauney et al., 2013), vHPC (Shah and Lodge, 2013), and amygdala (Pantazopoulos et al., 2015) of patients with schizophrenia.

A key role of PNNs is to protect neurons from oxidative stress. Increased levels of oxidative stress are associated with schziophrenia (Murray et al., 2021) and is a known pathological mechanism causing PV+ interneuron impairment. In the hippocampus, PV+ interneurons lacking PNNs express less PV than those surrounded by PNNs, suggesting PV expression is directly affected by the presence or absence of PNNs (Yamada and Jinno, 2014). Experiments by Carceller et al. (2020) support this demonstrating that PFC PV+ cells surrounded by PNNs show higher PV expression when compared with PV+ cells not surrounded by a PNN, as well as higher density of perisomatic excitatory and inhibitory puncta, and longer axonal initial segments. However, evidence sugests that PNNs are themselves susceptible to oxidative stress when oxidative burden is high, causing both PV+ interneuron and PNN

impairment (Steullet et al., 2017). Therefore, understanding dysfunctional oxidative stress mechanisms in PV+ interneuron-PNN circuits could identiify a pathway through which PNNs, and the subsequent neuronal circuit, could be protected.

1.6 Neuroinflammation and oxidative stress

Neuroinflammation is the normal and innate immune response of cells in the CNS, and functions to stop infection and eliminate pathogens, as well as clear cell debris and misfolded proteins (Olajide and Sarker, 2020). Neuroinflammation relies on the interaction between neurons and glial cells, particularly astrocytes and microglia. Generally, the neuroinflammatory response is beneficial to the CNS, by restoring and maintaining homeostasis through activation of glial cells, release of inflammatory mediators, such as cytokines and chemokines, and generation of reactive oxygen species (ROS) and reactive nitrogen species (RNS) (Sochocka et al., 2017). However, neuroinflammation can be detrimental to the CNS if it becomes severely acute or chronic (Minogue, 2017), and schizophrenia pathology has been associated with chronic neuroinflammation (Anderson et al., 2013). Astrocytes and microglia both mediate neuroinflammation and changes in glial marker expression are associated with cognitive deficits of schizophrenia (de Oliveira Figueiredo et al., 2022, Zhuo et al., 2023).

Until recently, studies suggested that both astrocytes and microglia exist in either a “resting” state or a “reactive” or “activated” state, and that the “reactive” or “activated” state is either proinflammatory or anti-inflammatory. However, this simple dichotomy of both astrocytic and microglial states has become controversial, and experts in the field have called for a re-evaluation and expansion of how to define and study the dynamic states of both astrocytes and microglia (Bennett and Viaene, 2021, Gao et al., 2023, Paolicelli et al., 2022). It is therefore necessary to re-evaluate outdated studies in the light of contemporary insights when considering the role of glia in schizophrenia pathology.

1.6.1 Astrocytes

Like neurons, astrocytes are derived from neuroepithelium-derived radial glial cells (Kriegstein and Alvarez-Buylla, 2009), and are very heterogeneous (Verkhratsky and Nedergaard, 2018). As mentioned, astrocytes were previously characterised as either “resting” or “reactive” and reactive astrocytes were characterised as either anti-inflammatory or pro-inflammatory. A recent review by Sofroniew (2020) summarises heterogeneity of astrocytes in a range of states, categorising astrocytes as “non-

reactive", rather than resting, or "reactive". In healthy tissue, astrocytes show varying gene expression and functions based on their regional context (Sofroniew, 2020). Their responses to damage can be influenced by initial conditions and different external signals. When tissue is damaged (e.g., from trauma, ischemia, or infection), astrocytes proliferate to form barriers that isolate damaged areas from healthy tissue (Sofroniew and Vinters, 2010). Astrocytes can also react without proliferating, adjusting their interactions and gene expression depending on the specific context and triggers (Burda and Sofroniew, 2014, Sofroniew, 2015). This reaction can resolve if the initial triggers are removed, however persistent triggers can lead to chronic reactivity, which may worsen tissue damage and disease pathology (Sofroniew, 2015). Mutations or genetic variations can cause astrocyte dysfunction independently of external triggers, leading to nonreactive states that contribute to ongoing tissue dysfunction and further astrocyte reactivity (Sofroniew, 2020). Overall, astrocyte responses are complex and can influence, or be influenced by, ongoing tissue damage and disease. A summary of the heterogeneity of both healthy and pathological astrocytes is summarised in Figure 1.13.

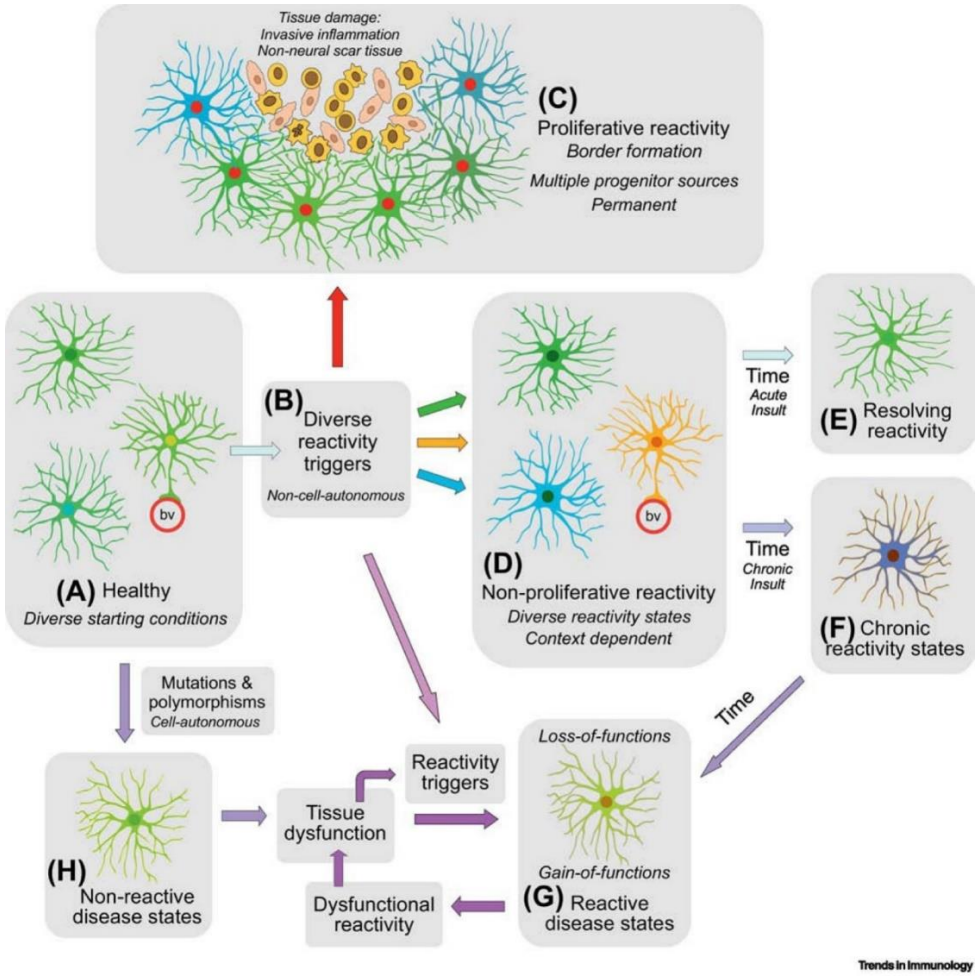

Figure 1.13 Diversity of astrocyte response in CNS. (A) Astrocytes in healthy tissue display regional and local heterogeneity in gene expression and function, influencing their reactivity responses. (B) Diverse CNS insults trigger different forms of astrocyte reactivity via non-cell-autonomous signals. (C) Proliferative astrocyte reactivity occurs in response to tissue damage, forming borders around damaged areas to separate them from viable neuronal tissue. (D) Nonproliferative astrocyte reactivity is context-dependent, with varied gene expression and modified interactions within preserved tissue architecture. (E) Nonproliferative reactivity may resolve if triggers recede. (F) Persistent triggers can cause chronic astrocyte reactivity. (G) Chronic reactivity may lead to dysfunctional states that exacerbate tissue pathology. (H) Genetic mutations may cause nonreactive disease states, leading to further tissue dysfunction and perpetuating a cycle of dysfunctional reactivity. Taken from Sofroniew (2020).

Astrocytes are the most numerous glial cells in the brain (Pelvig et al., 2008) and are integrated into neuronal networks, structurally aiding in homeostasis maintenance through ion transportation (Lia et al., 2023), neurotransmitter uptake and release of neurotransmitter precursors (Sofroniew, 2020) and ROS degradation (Chen et al., 2020). Due to their close structural association with neuronal synapses, astrocytes, as mentioned previously, also regulate GABA, playing an important role in the glutamate/GABA-glutamine cycle (Figure 1.2) (Andersen et al., 2022, Fischer et al., 2022). GABA released from astrocytes reduces neuronal excitability, in part through activation of a tonic inhibitory conductance generated by extrasynaptic $GABA_A$ receptors (Koh et al., 2023, Yoon and Lee, 2014), regulating synaptic plasticity and brain function (Wang et al., 2024). Furthermore, astrocytes contribute to regulation of synaptic transmission and play a role in learning and memory, particularly LTP, through the release of glutamate, adenosine triphosphate (ATP) and cytokines (Ota et al., 2013). Increases in pro-inflammatory cytokines lead to chronic neuroinflammation, which is also linked to increased oxidative stress and results in the stimulation of astrocyte activity.

Increased levels of ROS and oxidative stress damage are present in schizophrenia and several post-mortem studies have identified significant changes in the density and morphology of astrocytes in patients with schizophrenia (Tarasov et al., 2020). However, evidence for changes in the levels of astrocytic marker expression in patients with schizophrenia is conflicting. In a comprehensive review of glial fibrillary protein (GFAP) expression, a common marker for reactive astrocytes, Trépanier et al. (2016) found that GFAP expression was largely unchanged across brain regions of patients with schizophrenia (studies finding no change = 21, increased = 6, decreased = 6). Most importantly for this thesis, no change in GFAP expression was found in the hippocampus (Arnold et al., 1996, Radewicz et al., 2000) or the ACC (Radewicz et al., 2000), but GFAP mRNA levels are increased in the ACC (Webster et al., 2005) of schizophrenia patients.

Animal studies, however, show an increase in GFAP in the hippocampus of rats treated subchronically with the NMDA antagonist MK-801 (Yu et al., 2015), as well as primary hippocampal astrocyte cultures incubated with MK-801 (Yu et al., 2015). Alternatively, subchronic PCP treatment also increases GFAP expression in the CA1 and retrosplenial cortex (RSC; an interconnected brain region involved in cognitive

tasks) of mice, a finding which also corresponded with poorer performance in short-term memory tasks (Zhu et al., 2014).

1.6.2 Microglia

Microglia are a non-neuronal population of macrophage-like cells in the CNS. Like astrocytes, microglia modulate neuroinflammation, homeostasis, synaptic transmission, and synaptic plasticity. Additionally, microglia directly mediate synaptic pruning during development, significantly shaping synaptic plasticity (Paolicelli et al., 2011, Schafer et al., 2012). More recent data suggests that microglia act as dynamic regulators of neuronal networks through bidirectional communication with neurons (Whitelaw et al., 2023). Recent studies have uncovered a multitude of signalling pathways that enable microglia to interact closely with synapses, neurons, glia and other CNS components (Pósfai et al., 2019). Microglial processes exhibit both spontaneous and directed motility (Izquierdo et al., 2019), allowing them to survey their environment and dynamically interact with specific neuronal structures, such as dendrites, neuronal cell bodies, and axons (Whitelaw et al., 2023). This motility is modulated by neuronal activity, with reductions in activity enhancing microglial surveillance and increased microglial process extension (Liu et al., 2019b).

Microglia are also sensitive to traditional brain signals, including neurotransmitters and neuromodulators (Umpierre and Wu, 2021). Under conditions of heightened neuronal activity, microglial motility increases, facilitating interactions with active neurons, astrocytes, and the vasculature (Davalos et al., 2005, Nimmerjahn et al., 2005, Umpierre and Wu, 2021). These interactions often serve to maintain homeostasis by reducing neuronal firing (Badimon et al., 2020) and dampening hyperactivity, such as during seizures (Eyo et al., 2014, Eyo et al., 2016). Notably, microglia can respond to the activity of an individual neuron, as shown in acute brain slices, where Kato et al. (2016) found microglial processes were specifically recruited to the neuronal axon following trains of action potentials. These findings underscore the role of microglia as active participants in neuronal network modulation, responding to both hyperactivity and hypoactivity within the brain.

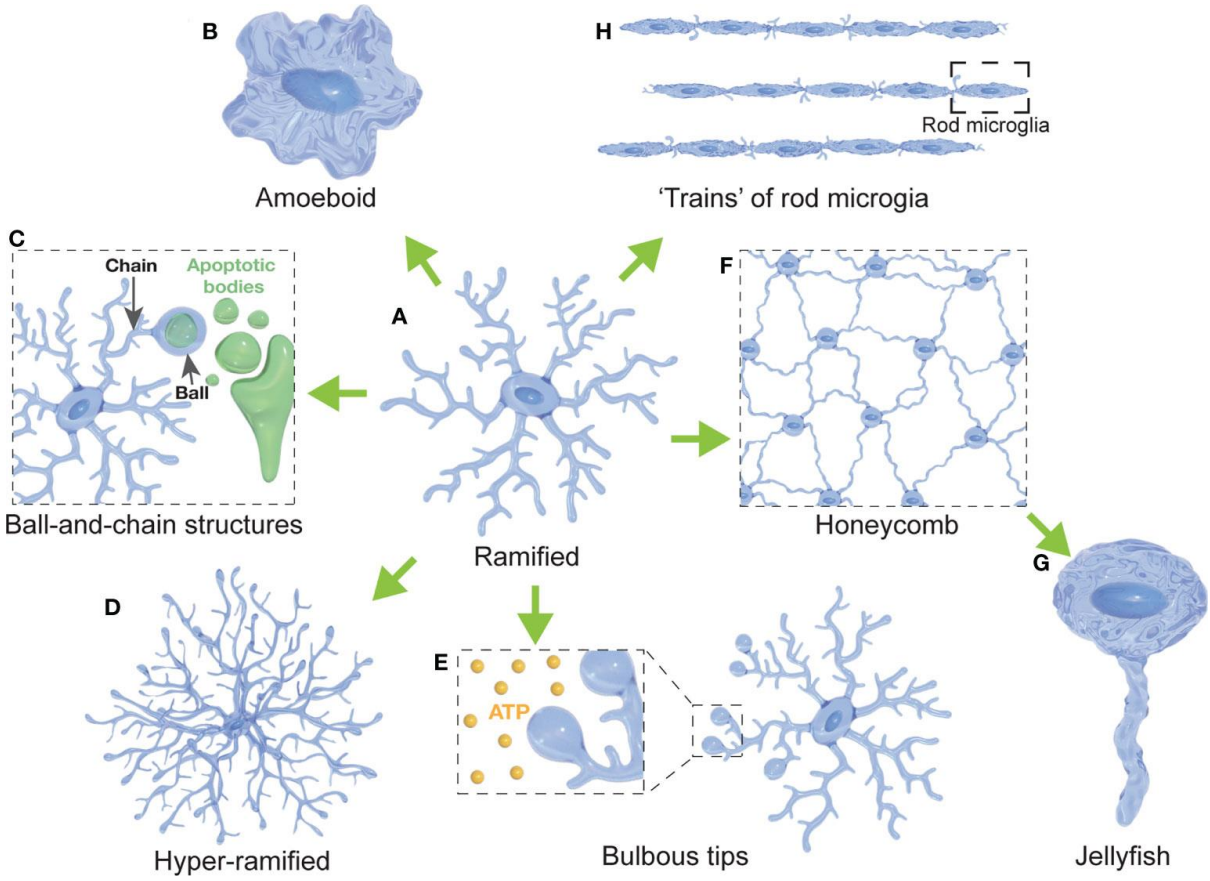

Figure 1.14 Diversity of microglial morphologies. (A) Ramified microglia are highly branched with multiple processes, often considered surveillant. (B) Amoeboid microglia have a rounded morphology, associated with high phagocytic and migratory capacity. (C) Ball-and-chain structures form at process tips to phagocytose small materials like synapses or apoptotic bodies. (D) Hyper-ramified microglia have increased branching. (E) Bulbous budding occurs at process ends, important for ATP sensing. (F) Honeycomb network is formed by several microglia in response to blood-brain barrier leakage. (G) Jellyfish morphology is seen after astrocytic death, transitioning from honeycomb microglia in response to traumatic brain injury. (H) Rod microglia have elongated, narrowed soma, often forming cell trains in response to injury. Taken from Vidal-Itriago et al. (2022).

Activated microglia mediate the neuroinflammatory response, responding to neuronal damage, removing damaged cells and debris by phagocytosis (Gehrmann et al., 1995, Neumann et al., 2009). When activated, microglia adapt their morphology by increasing their soma size and retracting their processes (Figure 1.14) (Szalay et al., 2016), whilst also releasing an array of cytokines, including interleukins (IL) and tumour necrosis factor alpha (TNF-α). Activated microglia adopt pro-inflammatory and anti-inflammatory inflammatory properties. Pro-inflammatory microglia release TNF-α, IL-6, IL-1β, ROS and glutamate molecules, whereas anti-inflammatory express IL-4, IL-13, IL-25, IL-1ra, insulin-like growth factor 1 (IGF1), BDNF and cyclooxygenase 1 (COX1) (Réus et al., 2015).

When exploring microglia in human post-mortem studies, increases in aberrant microglial activation have been found in the hippocampus, midcingulate cortex and PFC of patients with schizophrenia (Doorduin et al., 2009, Hill et al., 2021, Petrasch-Parwez et al., 2020, Trépanier et al., 2016). Significantly higher cytokine levels have also been measured in serum taken from schizophrenia patients with first-episode psychosis, including increased IL-6, IL-1β and TNF-α, suggesting abnormal pro-inflammatory microglial phenotype.

In the same PCP mouse study mentioned previously (Chapter 1.6.1), Zhu et al. (2014) found that as well as increased GFAP expression, indicating an increase in reactive astrocytes, there was also increased ionized calcium binding adaptor molecule 1 (Iba1) expression, a common microglia marker, indicating increased numbers of microglia in the mouse CA1 and RSC. Furthermore, the increase in Iba1 expression corresponded with an increase in the pro-inflammatory factor IL-1β (Zhu et al., 2014), further highlighting a potential pro-inflammatory pathology.

In conclusion, microglial activation increases cytokine release, which can cause increased ROS and oxidative stress, which in turn can lead to increased astrocyte activation, high ATP production and further microglial activation. Pinpointing the primary step in the neuroinflammatory cycle in schizophrenia, and intervening before the cycle escalates, could help reduce chronic neuroinflammation and prevent long-term neuronal damage, and cognitive impairment.

1.7 Modelling acute NMDA receptor hypofunction with PCP

Classically, PCP is a non-competitive NMDA receptor antagonist, that binds at the PCP- binding site in the NMDA receptor complex (Figure 1.3). As previously mentioned, PCP can induce schizophrenia-like psychosis and cognitive deficits in healthy individuals and exacerbate symptoms in schizophrenia patients (Javitt and Zukin, 1991). Therefore, PCP is now widely used as a preclinical animal model of schizophrenia as it induces behaviours associated with the disorder, including hyperactivity, impaired sensorimotor-gating and cognitive deficits in rodents (Lee and Zhou, 2019).

Previous rodent studies have shown that subchronic treatment with PCP disrupted learning and memory (Kesner and Dakis, 1993), increased extracellular PFC glutamate levels (Amitai et al., 2012), reduced PV and GAD67 expression (Amitai et al., 2012, Kaalund et al., 2013), altered unit firing (Kargieman et al., 2007) and increased gamma oscillatory activity *in vivo* (Hakami et al., 2009, Lee et al., 2017) and *in vitro* (Lemercier et al., 2017, Rebollo et al., 2018) in the PFC. Subchronic PCP administration also increased neuroinflammation, inducing astrocyte and microglia activation in the mouse cortex and hippocampus (Zhu et al., 2014)

Given PCP's ability to recapitulate multiple pathologies of NMDA receptor hypofunction, this thesis aimed to use PCP to establish an acute rodent brain slice model to explore the effect of NMDA receptor hypofunction in neuronal circuits in the ACC, and CA3 of the hippocampus. To assess the model, this study will examine PCPs effects on KA-induced beta and gamma frequency oscillations, and its subsequent effects on PV+ and SST+ interneurons, as well as PNNs. Furthermore, to understand any interneuron changes, PCP-induced neuroinflammation will also be assessed by studying astrocyte and microglia responses.

1.8 Potential therapeutic mechanisms for NMDA receptor hypofunction

As previously mentioned, there are currently no successful treatments for the cognitive symptoms associated with NMDA receptor hypofunction in schizophrenia. Using PCP as an acute model of NMDA receptor hypofunction, this thesis highlights two receptor targets through which NMDA receptor hypofunction could be alleviated: the group II metabotropic glutamate receptors (mGlu2 and mGlu3) and the intracellular sigma-1 (σ1) receptor.

1.8.1 Group II metabotropic glutamate (mGlu) receptors

The mGlu receptors represent a family of 8 receptors divided into 3 groups on the basis of sequence homology, pharmacology and signal transduction mechanism: Group I includes receptors mGlu1 and mGlu5; Group II includes receptors mGlu2 and mGlu3, and Group III comprises mGlu4, mGlu6, mGlu7 and mGlu8. In general, mGlu receptors have been identified as possible treatments for neurological and psychiatric diseases (Niswender and Conn, 2010). More specifically, mGlu receptors have been shown to modulate glutamatergic activity associated with schizophrenia pathology and are popular receptor targets for schizophrenia treatment (Coyle, 2006).

Group II mGlu receptors, mGlu2 and mGlu3, are expressed throughout the CNS and higher mGlu2 and mGlu3 receptor expression has been found in regions of the brain associated with schizophrenia pathology, including the ACC, PFC and hippocampus (Ghose et al., 2008, Gonzalez-Maeso et al., 2008, Gu et al., 2008). NMDA hypofunction involves both glutamatergic and GABAergic dysregulation in limbic circuits (Coyle, 2006, Lisman et al., 2008, Marino and Conn, 2002).

mGlu2/3 receptors are often expressed presynaptically, located on the periphery of the synapse, acting as a negative feedback mechanism to reduce the release of glutamate, and therefore inhibit excessive glutamate release (Cartmell and Schoepp, 2000, Schoepp, 2001). mGlu2/3 receptor activation could be a potential mechanism through which excess glutamatergic tone in schizophrenia patients could be reduced (Marek et al., 2000, Schoepp et al., 1999). mGlu2/3 receptors are also expressed on the postsynaptic terminal and are closely associated with pre-synaptic neurotransmitter release sites, modulating signal transduction. Interestingly both

mGlu2 and mGlu3 receptors are found on astrocytes, whilst mGlu3 receptors are also found on microglia, where they interact with glutamate transporters. As well as glutamate, mGlu2/3 receptors can also negatively modulate other neurotransmitters, including GABA (Cartmell and Schoepp, 2000).

Human (Krystal et al., 1994) and animal (Engel et al., 2016, Tyszkiewicz et al., 2004) studies show mGlu2/3 receptors modulate NMDA receptor activity, and activating mGlu2/3 receptors reverses PCP-induced (Moghaddam and Adams, 1998) and neurodevelopmental (Xing et al., 2018) working memory deficits in rodent models of schizophrenia. More recently, specific mGlu2 receptor agonists, and mGlu2 receptor positive allosteric modulators (PAMs) have become available. Modulating the mGlu2 receptor subtype specifically is effective in models of schizophrenia where glutamatergic signalling is disrupted (Morrow et al., 2012, Vinson and Conn, 2012), and suggests it is the mGlu2 receptor that modulates cognition. Phase II clinical studies with an oral prodrug of the orthosteric mGlu2/3 receptor agonist LY404039 suggested statistically significant improvements in positive and negative symptoms of schizophrenia (Patil et al., 2007). By targeting metabotropic receptors, it is thought that glutamatergic tone and phasic release may be modulated more subtly, than by ionotropic glutamate signalling (Fell et al., 2012), and may normalise hyperactive glutamate activity caused by NMDA receptor hypofunction. Therefore, restoration of normal glutamatergic signalling via activation of mGlu receptors may be a possible mechanism through which the symptoms of schizophrenia could be treated.

Preclinically, an mGlu2 receptor PAM, SAR218645, improved cognitive deficits in an MK-801 model of schizophrenia, and reversed working memory impairments in an NMDA - GluN1 knockout mouse model of the disease (Griebel et al., 2016). LY395756, an mGlu2 receptor agonist and mGlu3 receptor antagonist (Dominguez et al., 2005), also effectively reversed NMDA receptor impairments and cognitive deficits in a rat MAM model of schizophrenia (Li et al., 2017). LY541850 is another orthosteric selective mGlu2 receptor agonist and mGlu3 receptor antagonist, shown to be effective in reducing PCP-induced locomotor activity (Hanna et al., 2013), a measure of positive-like symptoms.

The mGlu2 receptor thus appears to be a promising target for modulating glutamate, and clinical trials have provided some evidence that this approach may be

of use in patients (Witkin et al., 2022). Therefore, this thesis aims to explore the effects of a selective, novel mGlu2 receptor agonist / mGlu3 receptor antagonist, LY541850, on KA-induced beta and gamma frequency oscillations in the ACC. Furthermore, I wanted to explore whether selective activation of mGlu2 receptors modulated an acute PCP slice model of NMDA receptor hypofunction.

1.8.2 Sigma-1 (σ1) receptors

σ1 receptors are 223-amino-acid-long, single-pass, intracellular membrane-associated chaperone proteins (Hayashi, 2019, Ryskamp et al., 2019), that are highly expressed in the CNS (Weissman et al., 1988). Initial identification of the σ1 receptors was via the psychomimetic effects produced by N-allylnormetazocine (SKF-10047), a σ1 receptor agonist (Freeman and Bunney, 1984). Following their discovery, σ1 receptors were wrongly characterised as a type of opioid receptor (Su, 1982) however, σ receptors form an individual class of receptor, including σ1 and σ2 receptors (Hellewell et al., 1994). Interestingly, the psychomimetic effects of SKF-10047 mimicked those induced by PCP (Ishikawa and Hashimoto, 2009), leading to the belief that the σ1 binding site and PCP binding site are the same (Itzhak et al., 1985, Mendelsohn et al., 1985, Zukin and Zukin, 1981). However, further investigation identified the σ1 receptor to be distinct from the NMDA receptor PCP-binding site, whilst also identifying both PCP and SKF-10047 as NMDA receptor antagonists and also σ1 receptor agonists (Stafford et al., 1983).

Since their initial discovery, genetic studies have found σ1 receptors are associated with schizophrenia risk. The σ1 receptor gene (*SIGMAR1*) is located on chromosome 9p13, a region associated with schizophrenia (Chodirker et al., 1987, Prasad et al., 1998), and *SIGMAR1* polymorphism increases the risk of schizophrenia (Ohi et al., 2011, Ohmori et al., 2000). Initial post-mortem studies suggested that σ1 receptor expression in schizophrenia patients is reduced in the temporal, frontal and occipital cortices, and increased in the cingulate cortex (Weissman et al., 1991). However, this assay used haloperidol, a D2 receptor antagonist, to assess σ1 receptor binding and not a selective σ1 receptor compound. There have been no more recent studies assessing changes in σ1 receptor expression in schizophrenia patients, therefore post-mortem findings remain uncertain.

Located on the ER mitochondria-associated membranes of neurons and glial cells, σ1 receptors modulate Ca^{2+} signalling via the inositol triphosphate (IP_3) receptor, a membrane glycoprotein which acts as a Ca^{2+} release channel. Ca^{2+} modulation activates σ1 receptors causing them to dissociate from binding immunoglobulin protein (BiP) and translocate to the plasma membrane, where they interact with other receptors. Due to their location and role in Ca^{2+} modulation, σ1 receptors regulate many neurotransmitter systems including glutamatergic, dopaminergic, serotonergic, noradrenergic and cholinergic systems, as well as modulating ion channels, including NMDA receptors (Rousseaux and Greene, 2016).

By interacting with other proteins and receptors, σ1 receptors modulate cellular responses, including ER stress and calcium homeostasis (Mori et al., 2013). σ1 receptors also play a role in cellular plasticity by directly modulating signalling pathways, including NMDA-dependant mechanisms, and reportedly enhancing LTP (Martina et al., 2007, Pabba et al., 2014). σ1 receptors are also implicated in the mechanisms involved in neuroinflammation and degeneration, and activation of σ1 receptors can be neuroprotective (Maurice et al., 2019, Mavlyutov et al., 2013, Mavlyutov et al., 2015). In addition to neurons, σ1 receptors are also expressed in microglia and astrocytes and can modulate anti-inflammatory responses in the CNS (Gekker et al., 2006, Jia et al., 2018). Activating σ1 receptors triggers neuroprotective effects and promotes neuronal survival via multiple mechanisms, including decreasing oxidative stress and regulating neuroinflammation (Jia et al., 2018).

Furthermore, σ1 receptor agonists fluvoxamine and donepezil both rescue cognitive impairments induced, *in vivo,* by subchronic PCP treatment in rodents (Hashimoto et al., 2007, Kunitachi et al., 2009). σ1 receptors, therefore, present an interesting route of study, as they could represent a pathway through which PCP-induced impaired learning and memory mechanisms could be rescued (Rothman and Olney, 1987).

σ1 receptors play a role in many of the identified pathological mechanisms of schizophrenia, including cognitive impairment, NMDA receptor modulation, neuroinflammation and oxidative stress. Considering the complex interplay between NMDA receptors and σ1 receptors, as well as the overlapping effects on other neurotransmitter systems, it is unsurprising that the potentially significant role of σ1

receptors in cognition, schizophrenia, and PCP mechanism, is difficult to elucidate. This project aimed to further characterise PCP effects and the role of σ1 receptors by investigating network oscillations, in the ACC and CA3. This thesis also aimed to explore how activation of σ1 receptors may alleviate the subsequent effects of NMDA receptor hypofunction, including PV+ and PNN dysfunction, and whether activating σ1 receptors has any neuroprotective effects by studying microglial and astrocytic changes.

1.9 Aims of thesis

The aim of this thesis is to advance our understanding of key neuronal mechanisms and their potential therapeutic targets in models of NMDA receptor hypofunction. Specifically, this thesis aims to:

- Identify novel biomarkers of NMDA receptor hypofunction: Utilizing PCP to induce acute NMDA receptor hypofunction in rodent ACC and hippocampus slices, this study will explore the dynamics of KA-evoked beta and gamma frequency oscillations as a biomarker for disrupted cognition.
- Examine mGlu2 receptor's role in glutamate modulation: By assessing the activation of mGlu2 receptors, this work aims to uncover the receptor's role in modulating rodent ACC beta and gamma frequency oscillations and whether mGlu2 receptors could be targeted to rescue oscillatory changes characterised using an acute PCP model of schizophrenia.
- Explore the potential of σ1 receptor activation: This thesis will assess the acute neuromodulatory and neuroprotective effects of activating σ1 receptors, both independently and within the PCP model. It will investigate their impact on key neuronal processes, including beta and gamma oscillations, LTP, and the expression of interneuron markers, PNNs, and glial cells, potentially revealing innovative avenues for neuroprotection and therapeutic intervention.

Chapter 2. General Materials and Methods

2.1 Animals

All animals used were male Lister Hooded rats, aged between 6 and 10 weeks. All animals were supplied by Charles River (Tranent, UK). Animals were housed in the Comparative Biology Centre (CBC) facility at Newcastle University. Animals were maintained on a 12-hour dark/light cycle with lights on at 7.00 am, with food and water supplied ad libitum. The housing unit was maintained at 20 – 24°C and 45 – 65% humidity.

This project has ethical approval from Newcastle University's ethics committee. All procedures were carried out in accordance with The United Kingdom Animals Scientific Procedures Act (1986) and the European Union Directive 2010/63/EU, under the provision of appropriate personal and project licenses.

2.2 Acute rodent brain slice preparation

Animals used for high frequency oscillation recordings and immunohistochemistry were anaesthetised with inhaled isoflurane (AErrane, Baxter Healthcare Ltd, UK) followed by a terminal, intramuscular (i.m.) lethal injection with a ketamine (100 mg/kg; Ketabel 100 mg/ml, Duggan Veterinary, IE) and xylazine (10 mg/kg; Xylacare2%, Animalcare, UK) solution. Once anaesthetised, and all pedal and eye-blink reflexes had ceased, rats were intracardially perfused with 60 ml modified sucrose artificial cerebrospinal fluid (ACSF) (Table 2.1 - 2.2). The brain was then removed and submerged in ice-cold, oxygenated (95% O_2 / 5% CO_2) sucrose ACSF. To prepare brain tissue slices, tissue was sliced in ice-cold, oxygenated sucrose ACSF using an Integraslice 7550 MM vibrating microtome (Campden Instruments, UK). Slices were cut at 450 µm using stainless steel microtome blades (Campden Instruments).

Animals used for LTP recordings were anaesthetised with inhaled isoflurane and quickly euthanised by cervical dislocation under Schedule 1. The head was removed to confirm death of the animal. The brain was then removed and submerged in ice-cold oxygenated hippocampal ACSF (Table 2.1 – 2.2). To prepare brain tissue slices, tissue was sliced in ice-cold, oxygenated hippocampal ACSF using an Integraslice 7550 MM vibrating microtome (Campden Instruments). Slices were cut at 400 µm using stainless steel microtome blades (Campden Instruments).

The slices were trimmed by hand using a scalpel blade (Swann Morton, UK) to isolate the region of interest. For oscillation recordings, the brain was sliced coronally (Figure 2.1a) and the ACC isolated (Figure 2.1b) or the brain was sliced horizontally (Figure 2.2a) and the hippocampus (HPC) isolated (Figure 2.2b), depending on the region of interest. To avoid dorsal-ventral (DV) variation in CA3 recordings, hippocampal sections were taken between DV Bregma -4.6 and -6.1 mm. For LTP recordings, the brain was hemi-sected along the midline and sliced parasagittally (Figure 2.3a), to elongate the CA1 region in the hippocampal slice (Figure 2.3b).

Slices were transferred to a recovery holding chamber kept at room temperature, containing oxygenated ACSF solution (Table 2.2). ACC and hippocampus slices were maintained and perfused with region specific ACSF (Table 2.2). Both $MgSO_4$ and $CaCl_2$ were reduced in the ACC specific ACSF solution to

increase cellular excitability, as networks in slices from the PFC have been found to be more quiescent than hippocampal slices. Slices were allowed to recover from slicing in the holding chamber for at least 1 hour, but could remain in the holding chamber for up to 12 hours before slice viability was compromised (Buskila et al., 2014). Slices were then transferred to an interface electrophysiology recording chamber for subsequent experiments.

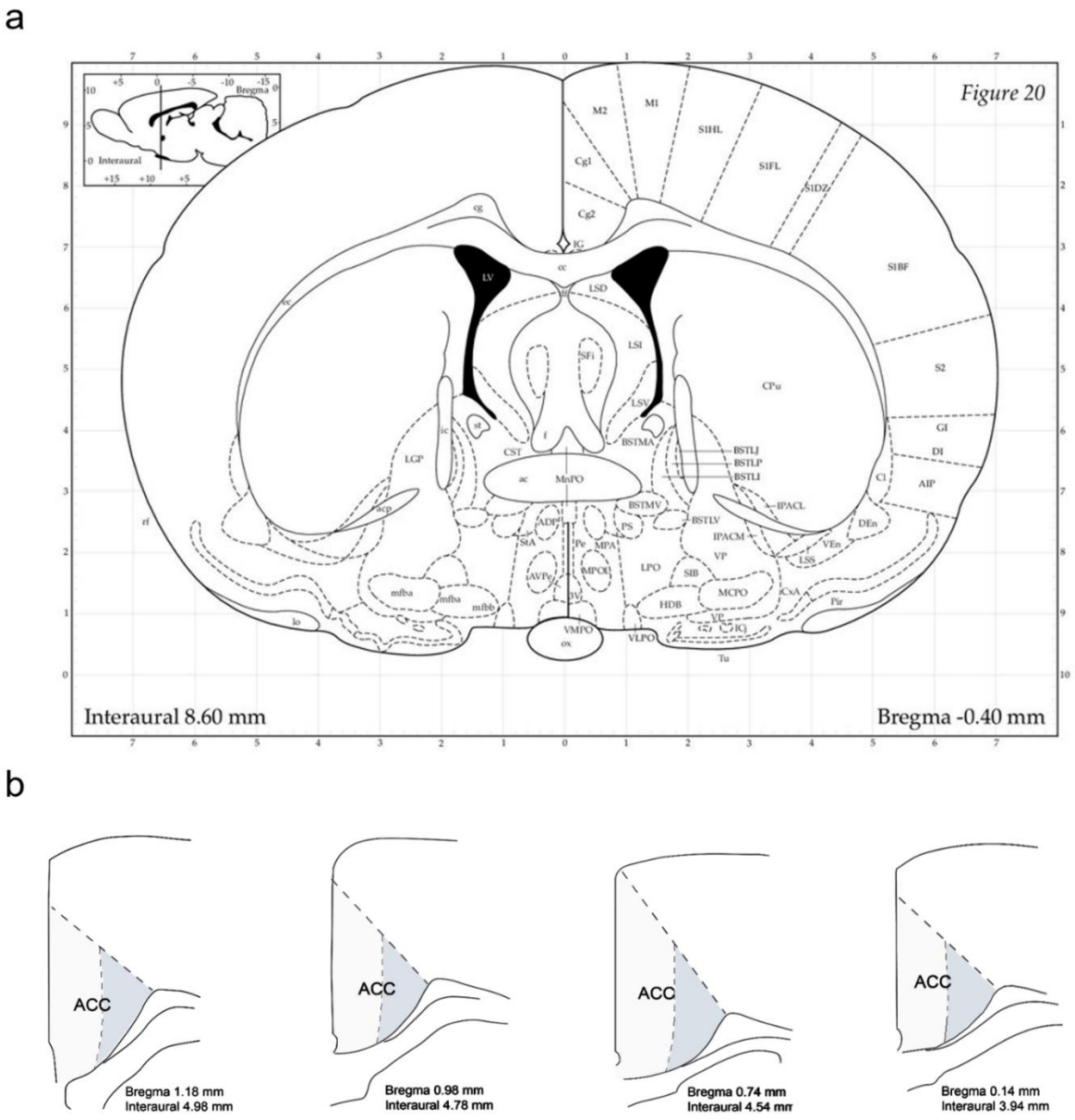

Figure 2.1 Rat brain atlas demonstrating whole and isolated coronal slices taken for ACC sections. a) From Paxinos, George, and Charles Watson. The rat brain in stereotaxic coordinates: hard cover edition. Access Online via Elsevier, 2006. b) Schematics representing the isolated ACC slices, detailing the whole ACC region divided into the superficial (light grey) and deep (dark grey) layers, and stereotaxic coordinates of each section.

a

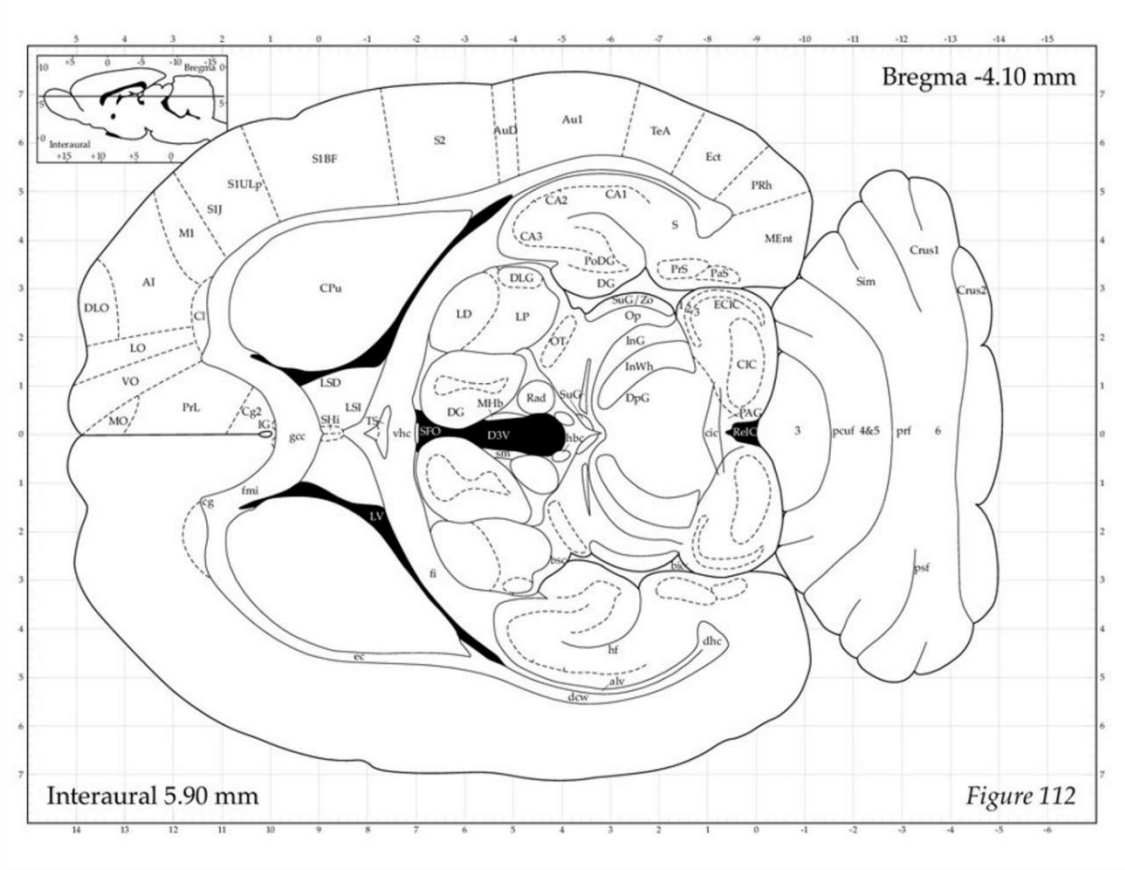

b

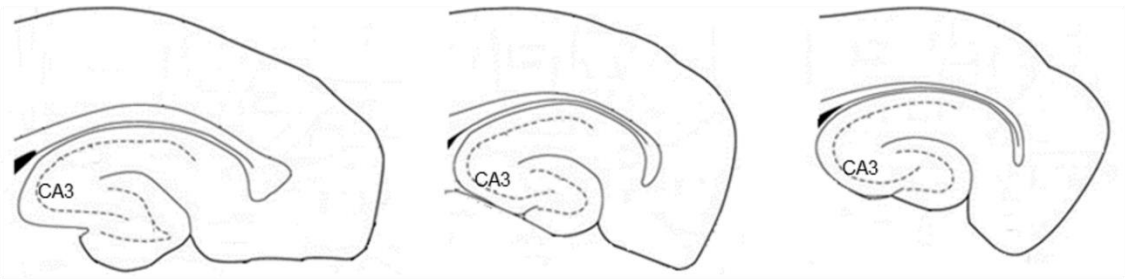

Figure 2.2 Rat brain atlas demonstrating whole and isolated horizontal slices taken for hippocampus sections. a) From Paxinos, George, and Charles Watson. The rat brain in stereotaxic coordinates: hard cover edition. Access Online via Elsevier, 2006. b) Schematics representing the isolated hippocampus slices, detailing the CA3 region and stereotaxic coordinates of each section.

a

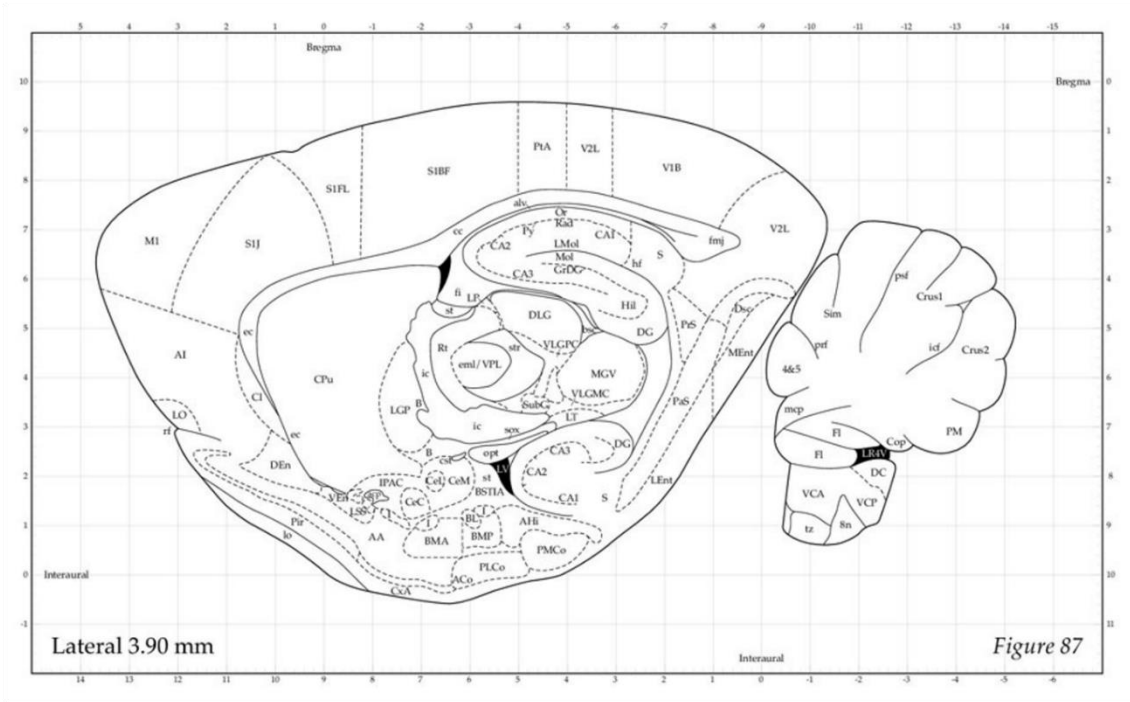

b

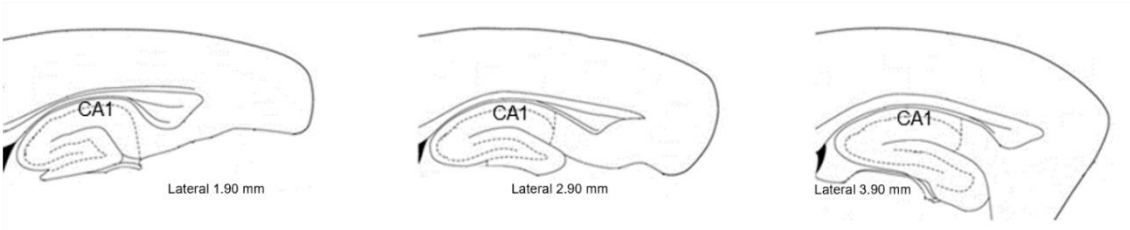

Figure 2.3 Rat brain atlas demonstrating whole and isolated parasagital slices taken for hippocampus sections. a) From Paxinos, George, and Charles Watson. The rat brain in stereotaxic coordinates: hard cover edition. Access Online via Elsevier, 2006. b) Schematics representing the isolated hippocampus slices, detailing the CA1 region and stereotaxic coordinates of each section.

Table 2.1 Chemicals used in ACSF solutions. Name, formula and vendor of chemicals used for ACC, hippocampus, and sucrose ACSF solutions for acute rodent brain slice experiments and preparation.

Chemical name	Chemical formula	Manufacturer (Product code)
Sodium chloride	NaCl	Sigma-Aldrich (S7653)
Potassium chloride	KCl	Sigma-Aldrich (P9333)
Sodium phosphate monobasic	NaH_2PO_4	Sigma-Aldrich (71496)
Magnesium sulphate	$MgSO_4$	Sigma-Aldrich (M7506)
Calcium chloride	$CaCl_2$	Sigma (C7902)
Sodium hydrogen carbonate	$NaHCO_3$	VWR Chemicals BDH (102477B)
D(+)-Glucose anhydrous	$C_6H_{12}O_6$	VWR Chemicals (10117HV)
Sucrose	$C_{12}H_{22}O_{11}$	Sigma-Aldrich (16104)

Table 2.2 The chemicals and concentrations (mM) used in ACSF solutions. Subdivided into final volume concentrations for sucrose, ACC, and hippocampus ACSF solutions.

Chemical	Sucrose ACSF	ACC ACSF	HPC ACSF
Sodium chloride (NaCl)	-	126	126
Potassium chloride (KCl)	3	3	3
Sodium phosphate monobasic (NaH_2PO_4)	1.25	1.25	1.25
Magnesium sulfate ($MgSO_4$)	2	1	2
Calcium chloride ($CaCl_2$)	2	1.2	2
Sodium hydrogen carbonate ($NaHCO_3$)	24	24	24
D(+)-Glucose anhydrous ($C_6H_{12}O_6$)	10	10	10
Sucrose ($C_{12}H_{22}O_{11}$)	252	-	-

2.3 Human cortical tissue slice preparation

Human tissue slices were prepared from overlying cortical tissue obtained from patients undergoing surgical resection for a deep brain tumour at Newcastle RVI. Tissue from 1 patient has been included in this study.

Ethical approval (IRAS Project ID 173990) was given by Newcastle University's Ethics Committee and written informed consent was obtained from all patients prior to undergoing resective surgery. Cortex was carefully dissected by the neurosurgeons using a scalpel blade and directly transferred into ice-cold, oxygenated filter sterilised sucrose ACSF, adjusted to 300 – 310 mOsM and pH 7.4, adapted for human tissue (Table 2.3), for transportation from surgical theatres to the laboratory.

Prior to cutting, tissue was inspected for tissue quality, assessing factors including presence or absence of tumour, and microdissection injury and removal of any meninges. Tissue was mounted and cut in the orientation that included all cortical grey and white matter layers. Tissue was sliced in ice-cold, oxygenated, filter sterilised sucrose ACSF (Table 2.3) using a Campden Instruments 51000mZ vibrating microtome (Campden Instruments). Slices were cut at 400 µm using stainless steel microtome blades (Campden Instruments) and trimmed by hand using a scalpel blade (Swann Morton). Slices were transferred to a recovery holding chamber kept at room temperature, containing oxygenated human ACSF solution (Table 2.3). Slices were allowed to recover from slicing in the holding chamber for at least 1 hour, before being transferred to an interface electrophysiology recording chamber for subsequent electrophysiological recordings.

Table 2.3 The chemicals and concentrations (mM) used in human tissue adapted ACSF solutions. Components subdivided into concentrations for sucrose transport and slicing ACSF and human recording ACSF solutions.

Chemical	Manufacturer (Product code)	Sucrose ACSF	Human ACSF
Sodium chloride (NaCl)	Sigma-Aldrich (S7653)	-	126
Potassium chloride (KCl)	Sigma-Aldrich (P9333)	2.5	3
Sodium phosphate monobasic (NaH_2PO_4)	Sigma-Aldrich (71496)	1.25	1.25
Magnesium sulphate ($MgSO_4$)	Sigma-Aldrich (M7506)	10	1
Calcium chloride ($CaCl_2$)	Sigma (C7902)	0.5	1.2
Sodium hydrogen carbonate ($NaHCO_3$)	VWR Chemicals BDH (102477B)	25	24
D(+)-Glucose anhydrous ($C_6H_{12}O_6$)	VWR Chemicals (10117HV)	10	10
Sucrose ($C_{12}H_{22}O_{11}$)	Sigma-Aldrich (16104)	180	-
N-acetylcysteine (NAC)	Sigma-Aldrich (A7250)	2	-
Taurine	Sigma-Aldrich (T0625)	1	-
Ascorbic acid	Sigma-Aldrich (A92902)	1	-
Amino guanidine hydrochloride	Aldrich (396494)	0.1	-
Indomethacin	Sigma Life Science (I7378)	0.044	-
Ethyl pyruvate	Sigma-Aldrich (E47808)	0.044	-

2.4 Pharmacological compounds

All pharmacological compounds were prepared according to the manufacturer's instructions (Table 2.4). Water soluble compounds were dissolved in deionised water and non-water-soluble compounds were dissolved in dimethyl sulfoxide (DMSO; Sigma Life Science, UK). All pharmacological compounds were bath applied to the slices via the circulating ACSF. Compound solutions were stored as stock solutions at either +4°C or -20°C, according to manufacturer's information, compound stability in solution and frequency of use.

Where compounds were dissolved in DMSO, the final ACSF solution contained ≤0.1% DMSO to avoid adverse effects on cell viability (Zhang et al., 2017). To control for any effect of DMSO, DMSO was added to ACSF at the beginning of all experiments and maintained at 0.1% throughout the experiment.

To evoke and maintain high frequency beta and gamma frequency oscillations, KA, an agonist of the iGlu kainate receptor, was applied in electrophysiological experiments. PCP, MK-801 and DAP5, are NMDA receptor antagonists, applied to model NMDA receptor hypofunction. SKF-10047 and PRE-084 are σ-1 receptor agonists applied to activate σ-1 receptors, and NE-100 is a selective σ-1 receptor antagonist. LY341495, LY354740 and LY541850 are group 2 mGlu receptor compounds, used in chapter 4 to explore the role of glutamatergic transmission in high frequency oscillations.

Table 2.4 The pharmacological compounds used in experiments throughout this thesis. All names, formulas, biological targets, and manufacturers (and product code) of compounds used in electrophysiology and immunohistochemistry experiments.

Compound name	Compound formula	Action	Manufacturer (product code)
(+)-MK-801 maleate (MK-801)	(5S,10R)-(+)-5-Methyl-10,11-dihydro-5H-dibenzo[a,d]cyclohepten-5,10-imine maleate	Selective, non-competitive NMDA receptor antagonist	Tocris (0924)
(+)-SKF-10047 (SKF-10047)	(2S,6S,11S)-1,2,3,4,5,6-Hexahydro-6,11-dimethyl-3-(2-propenyl)-2,6-methano-3-benzazocin-8-ol hydrochloride	σ-1 receptor agonist; NMDA receptor antagonist	Tocris (1079)
DAP5	D-(-)-2-Amino-5-phosphonopentanoic acid	Selective, competitive NMDA receptor antagonist	Tocris (0106); Hello Bio (HB0225)
Kainic acid (kainate; KA)	(2S,3S,4S)-Carboxy-4-(1-methylethenyl)-3-pyrrolidineacetic acid	Kainate receptor agonist	Tocris (0222)
LY341495	(2S)-2-Amino-2-[(1S,2S)-2-carboxycycloprop-1-yl]-3-(xanth-9-yl) propanoic acid	Selective group II mGlu antagonist	Tocris (1209)
LY354740	(1S,2S,5R,6S)-2-Aminobicyclo[3.1.0]hexane-2,6-dicarboxylic acid	Selective group II mGlu agonist	Tocris (3246)
LY541850	(1S,2S,4R,5R,6S)-2-Amino-4-methylbicyclo[3.1.0]hexane2,6-dicarboxylic acid	Selective orthosteric mGlu2 agonist; mGlu3 antagonist	Eli-Lilly (gifted)

NE-100 hydrochloride (NE-100)	4-Methoxy-3-(2-phenylethoxy)-N,N-dipropylbenzeneethanamine hydrochloride	Selective σ-1 receptor antagonist	Tocris (3133)
Phencyclidine hydrochloride (PCP)	1-(1-Phenylcyclohexyl)piperidine hydrochloride	Non-competitive NMDA receptor antagonist; sigma-1 receptor agonist	Tocris (2557)
PRE-084 hydrochloride	2-(4-Morpholinethyl) 1-phenylcyclohexanecarboxylate hydrochloride	Selective σ-1 receptor agonist	Tocris (0589)

2.5 Electrophysiological recordings

2.5.1 High frequency beta and gamma oscillation recordings

To record high frequency beta and gamma frequency oscillations, the same electrophysiological recording rigs, equipment, and technique were used for both animal and human tissue recordings.

Following at least 1 hour of recovery, individual slices were transferred to an interface recording chamber where they were perfused with oxygenated ACSF solution (Table 2.2), at a rate of 1.5 ml/min using a MINIPULS 3 peristaltic pump (Gilson, WI, US). and maintained at 30 - 34°C, using an Optima TC120 heated circulating bath (Grant Instruments, UK). Slices were allowed to equilibrate for 30 minutes in the recording chamber before inserting electrodes or applying pharmacological compounds.

Extracellular field recordings were made with microelectrodes pulled from borosilicate glass (1.2 OD x 0.94 ID x 100 L mm; Harvard Apparatus, UK), with a resistance of 3 – 7 MΩ, using a P97 Flaming/Brown micropipette puller (Sutter Instrument Company, US) and filled with ACSF. The electrode was positioned in the region of interest before applying any pharmacological compounds.

The signal was recorded and amplified using an Axoclamp-2B amplifier (Axon Instruments, UK) and further amplified and filtered at 0.001 - 0.4 kHz using a NeuroLog System (Cambridge Electronic Design Ltd, UK). Mains noise was removed from the signal with a Humbug (Digitimer, Welwyn Garden City, Herts, UK). Data were digitised at 10 kHz using a CED1401 interface (Cambridge Electronic Design Ltd, Cambridge, UK) or an ITC-18 interface (Digitimer, UK). Data were collected online using the electrophysiology acquisition and analysis computer software Spike2 (version 7.2; Cambridge Electronic Design Ltd, UK) or Axograph (version 1.7.6; Axon Instruments Inc., Union City, CA, US). Oscillation recording experiments were analysed offline using Spike2 or Axograph software.

To analyse oscillation recording, power spectral density analysis was performed on recorded data using Axograph and Spike2's Fast Fourier Transform algorithms. Using power spectra analysis of 60 second epochs, the peak frequency (Hz) and the area under the curve, described in this thesis as area power, (μV^2/Hz)

were measured (Figure 2.4). To analyse ACC beta frequency oscillations, peak frequency and area power were measured between 15 – 32.9. To analyse ACC gamma frequency oscillations, peak frequency and area power were measured between 33 – 80 Hz. KA-evoked network oscillations were considered stable when peak frequency and area power measurements varied no more than +/-10% over a 20 minute 'control' period, where 60 second epochs were measured at 10 minute intervals. Once oscillations were stable, other pharmacological compounds were applied.

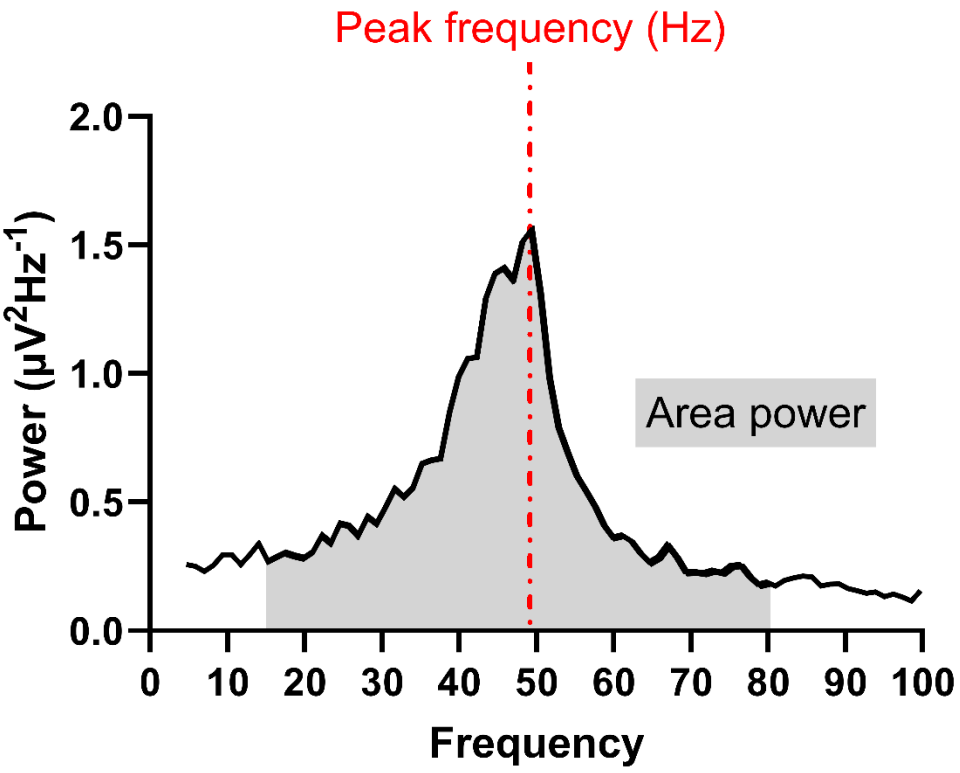

Figure 2.4 Analysis of peak frequency and area power. An example power spectrum showing a gamma frequency oscillation. Peak frequency (Hz) was measured where power was greatest between 15 and 80 Hz, indicated by the red dashed line. Area power (μV^2/Hz) was measured as the area under the curve between 15 and 80 Hz, indicated by the greyed region.

2.5.2 Long-term potentiation (LTP) recordings

Following at least 1 hour of recovery, individual hippocampus slices (Figure 2.3b) were transferred to an interface recording chamber where slices were perfused with hippocampus ACSF solution, oxygenated and maintained at 32°C, at a rate of 1.5 ml/min (Table 2.2). Slices were allowed to equilibrate for 30 minutes in the recording chamber before inserting electrodes, starting stimulation protocols, or applying pharmacological compounds. Pharmacological compounds were bath applied 30 minutes after slices were placed in the recording chamber. Control experiments were performed in circulating ACSF only. Compounds were applied alone at a single concentration and once applied, were present throughout the experiment: DAP5 (100 µM), PCP (10 µM) and PRE-084 (10 µM).

The recording microelectrode and metal stimulating electrode were positioned in the CA1 of the hippocampus, along the Schaffer-collateral pathway (Figure 2.5), 30 minutes after slices were placed in the recording chamber. Activity was recorded using microelectrodes pulled from borosilicate glass (1.2 OD x 0.94 ID x 100 L mm; Harvard Apparatus) using a Sutter P97 micropipette puller and filled with ACSF, with a resistance of 3 – 7 MΩ. Stimulating pulses were delivered using a metal stimulating electrode (made in house), triggered by an 8-channel programmable pulse stimulator (Master8, A.M.P.I., IL), in conjunction with a DS2A Isolated Stimulator (Digitimer Ltd., UK).

As outlined above for the oscillation recordings, the signals were recorded and amplified using an Axoclamp-2B amplifier (Axon Instruments, UK) and further amplified and filtered at 0.001 - 0.3 kHz using a NeuroLog System (Cambridge Electronic Design Ltd., UK). Mains noise was removed from the signal with a Humbug (Digitimer Ltd.). Data were digitised at 10 kHz using a CED1401 interface (Cambridge Electronic Design Ltd, UK). Data were collected online using the electrophysiology acquisition and analysis computer package Signal (version 6.05a; Cambridge Electronic Design Ltd.). LTP recording experiments were analysed offline using Signal software (CED).

The pathway was stimulated at approximately 20% maximal response. A single 0.02ms pulse was delivered every 20s and the amplitude of the fEPSP was measured (Figure 2.6). Following a 20 minute stable baseline, tetanic HFS (100 Hz, 1 sec) was

delivered to induce LTP and the peak amplitude (mV) of the response was measured for a further 20 or 40 minutes (see Chapter 5 for specific experimental detail). Baseline amplitude (mV) was calculated by averaging 20 ms of data in the region before the stimulation response. The maximum amplitude (mV) was measured where the trough of the response was lowest. Peak amplitude was calculated by subtracting the mean baseline amplitude from the maximum amplitude. For statistical analysis, an epoch (5 minutes) of peak amplitude before HFS stimulation was averaged (baseline). Following HFS stimulation, an epoch at the end of the recording was averaged and normalised to baseline.

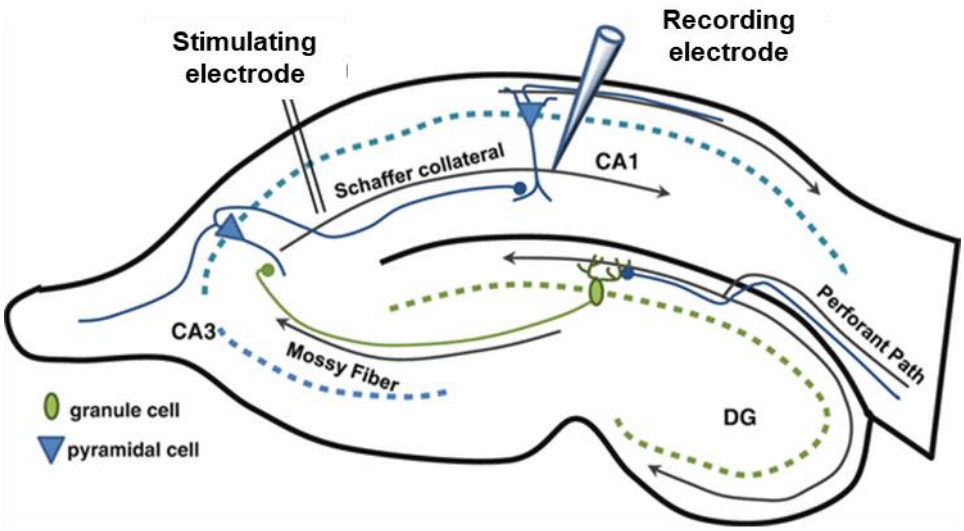

Figure 2.5 Schematic of a rat parasagittal hippocampus brain slice. The schematic indicates the position of the glass recording microelectrode and the metal stimulating electrode in the CA1, along the Schaffer-collateral pathway, in relation to the pyramidal cell layer, during LTP recordings.

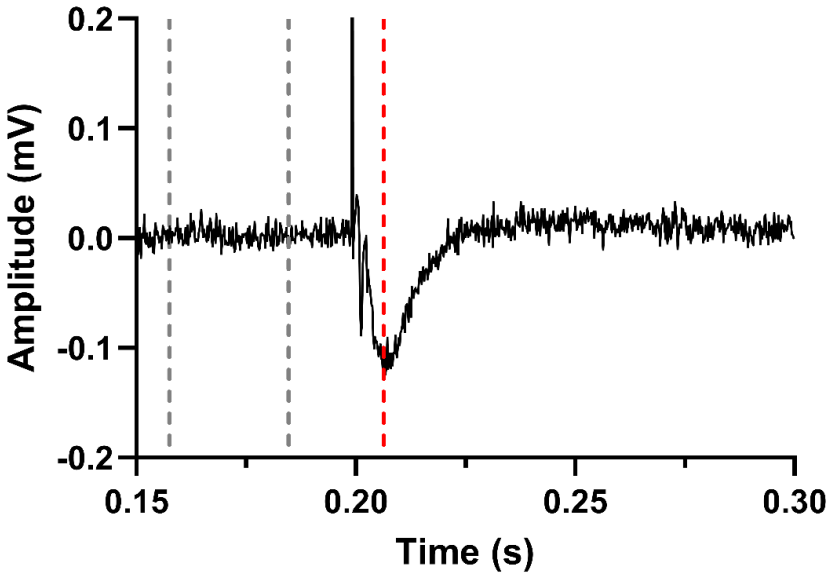

Figure 2.6 Analysis for peak amplidude analysis for LTP experiment analysis. An example trace showing a fEPSP evoked by electrical stimulation. Baseline amplitude (mV) was calculated by averaging the region between the two grey dashed lines (20 ms). The maximum amplitude (mV) was measured where the trough of the response was lowest, indicated by the red dashed line. Peak amplitude = maximum amplitude – mean baseline amplitude.

2.6 Free-floating immunohistochemistry – immunofluorescence

2.6.1 Slice preparation

Tissue for immunohistochemical experiments was prepared from animals as described in sections 2.1 and 2.2. Slices used in this thesis for IHC were first used for electrophysiological recordings. After slicing, ACC and hippocampus slices were transferred to a recovery holding chamber kept at room temperature, containing oxygenated ACC or hippocampus ACSF solution. Following 1 hour of recovery, individual slices were transferred to an interface recording chamber where slices were perfused with ACC or hippocampus ACSF solution at a rate of 1.5 ml/min, and maintained at 32 - 34°C.

Slices prepared from each individual animal were divided between multiple interface rigs and allowed to equilibrate for 30 minutes in the bath at 32 - 34°C, followed by a four different 4-hour drug incubation periods. Condition 1: Slices incubated in ACSF only were used as the control group. Condition 2: Slices were incubated in ACSF containing KA, to generate 'normal' oscillatory conditions. Condition 3: Slices were incubated in ACSF containing KA and PCP, to model 'pathological' oscillations. Condition 4: Finally, to explore the effects of activating σ-1Rs, slices were incubated in PRE-084 for an initial 30 minutes, whilst equilibrating in the bath, and then a further 4 hours after application of KA and PCP.

Following the four different incubation periods, all slices were fixed in 4% paraformaldehyde (PFA; Thermo Scientific, UK) phosphate buffered saline (PBS; PBS tablets, Oxoid, UK) for at least 12 hours. Once fixed, slices were transferred to cryoprotectant solution (Table 2.5) and stored at -20°C until required for immunofluorescence staining. In preparation of staining, slices were transferred to a sucrose (30%) PBS solution, 24 hours before re-sectioning. Sections (40 µm) were cut at -20°C, using a Solid State Freezer freeze-stage microtome (Bright Instruments, UK), and stored in PBS in 24-well plates (CytoOne, non-treated; StarLab, UK) until staining.

Table 2.5 Chemicals used in cryoprotectant solution. Name, final volume as a percentage (%) and manufacturer (and product code) of chemicals used to prepare cryoprotectant solution, used for preserving tissue slices and sections.

Chemical name	Final volume (%)	Manufacturer (Product code)
Glycerol	30	Sigma-Aldrich (49781)
Ethylene glycol	30	Sigma-Aldrich (1.09621)
Phosphate buffered saline (0.3M)	20	Oxoid (BR0014G)
Deionised water (dH_2O)	20	-

2.6.2 Free-floating immunohistochemistry

For immunofluorescence staining, sections were stained using the free-floating method, where solution was added and removed to the sections in the wells of 24-well plates. In some experiments, an initial antigen retrieval step was performed using citrate buffer solution (pH 6.0), heated to 80°C. Sections were washed using PBS and incubated with primary antibodies (Table 2.6), diluted in a solution of PBS, Triton X-100 (0.3%) and normal donkey serum (5%), overnight (18 – 20 hours) at 4°C. Sections were incubated in secondary antibodies (Table 2.7), diluted in a solution of PBS and Triton X-100 (0.3%), for 2 hours at room temperature. Sections were mounted on glass Menzel-Gläser Superfrost Plus microscope slides (Thermo Scientific) and cover-slipped (type 1.5; Fisherbrand™, Fisher Scientific, UK) using Fluoromount-G™ Mounting Medium, with DAPI (4′,6-diamidino-2-phenylindole; Thermo Fisher Scientific, UK). See figure 2.7 for an outline of the full staining protocol.

2.6.3 Confocal imaging and FIJI image analysis

Imaging was performed using an SP8 DLS (Leica, DE) confocal microscope. Tile scans were taken at taken at 2x 20x (equal to 40x) magnification of the whole region of interest (ACC or hippocampus) to get an overview image of the section. Z-

stacks (20 µm thickness) were taken at taken at 2x 20x (equal to 40x) magnification, to sample across the region of interest (ACC), capturing images from the superficial (layers II / III) and deep (layer V) layers (Figure 2.8).

All image analysis was performed using the image analysis software Fiji (version 2.15.1; ImageJ). Initially, all tile scan images were stitched together and the ACC region hand-drawn around and isolated. Z-stack images were collapsed into 2D images. Images were then transformed into 8-bit. For all analysis, brightness and contrast, and image threshold values were optimised and averaged across all images, for each channel. Average brightness and contrast values for each channel were applied across all images. Background noise was removed by subtracting background noise and applying the ‘median’ (GFAP and Iba1) or ‘unsharp mask’ (PV, SST and WFA) filters were applied. Average threshold values were applied across all images and further noise was cleaned using the ‘remove outliers’ (PV, SST) and ‘despeckle’ (GFAP, Iba1, PV, SST and WFA) function.

Particle analysis was performed by adjusting the size and circularity according to the ‘particles’ (cells) of interest, for each channel. For statistical analysis, percentage area (%Area) and integrated density (ID) of GFAP, Iba1, PV, SST and WFA were calculated. At least two sections from each slice were imaged per condition, per animal. Slices from at least 4 animals were included in each condition. Section %Area and IDs were averaged for each animal and compared across the different conditions (Table 5.1).

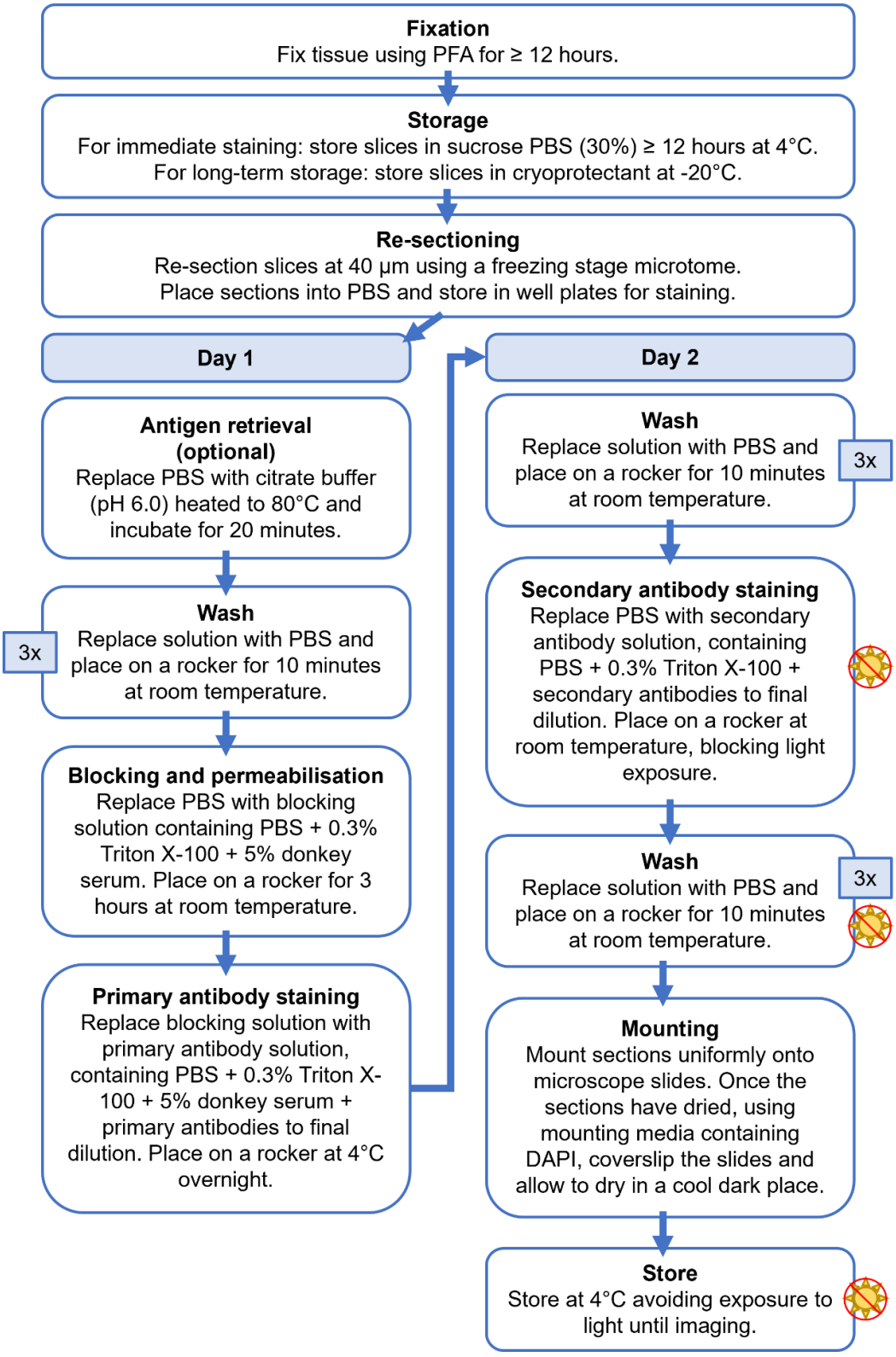

Figure 2.7 Schematic of immunofluorescence staining protocol. Outline of fixation, storage, and primary and secondary antibody steps for free-floating immunofluoresence staining used in this thesis. symbol represents steps performed avoiding exposure to light.

Table 2.6 List of primary antibodies and lectin used. Primary antibody target, host species (if applicable), manufacturer, dilution, and serum (depending on secondary antibody) used for immunofluorescence staining.

Primary antibody	Host species	Manufacturer brand (RRID)	Dilution	Serum used
Anti-GFAP (astrocytes)	Chicken	Abcam (ab4674)	1:1000	Donkey
Anti-Iba1 (microglia)	Goat	Abcam (ab5076)	1:500	Donkey
Anti-parvalbumin (PV)	Rabbit	Swant (PV-27)	1:1000	Donkey
Anti-somatostatin (SST)	Mouse	Santa Cruz (sc-55565)	1:1000	Donkey
Biotinylated *Wisteria Floribunda* Lectin (WFA; PNNs)	-	Vector Laboratories (B-1355-2)	1:500	Donkey

Table 2.7 List of secondary antibodies used. Secondary antibody target, fluorophore (if applicable), manufacturer and dilution use for immunofluorescence staining.

Secondary antibody	Fluorophore	Manufacturer brand (product code)	Dilution
Donkey anti-goat IgG	Alexafluor488	Abcam (ab150129)	1:500
Donkey anti-mouse IgG	Alexafluor568	Invitrogen (A10037)	1:500
Donkey anti-rabbit IgG	Alexafluor647	Abcam (ab150075)	1:500
Donkey anti-chicken IgG	Alexafluor647	Jackson ImmunoResearch Laboratories Inc. (703-605-155)	1:500
Streptavidin, fluorescein		Vector Laboratories (SA-5001-1)	1:100

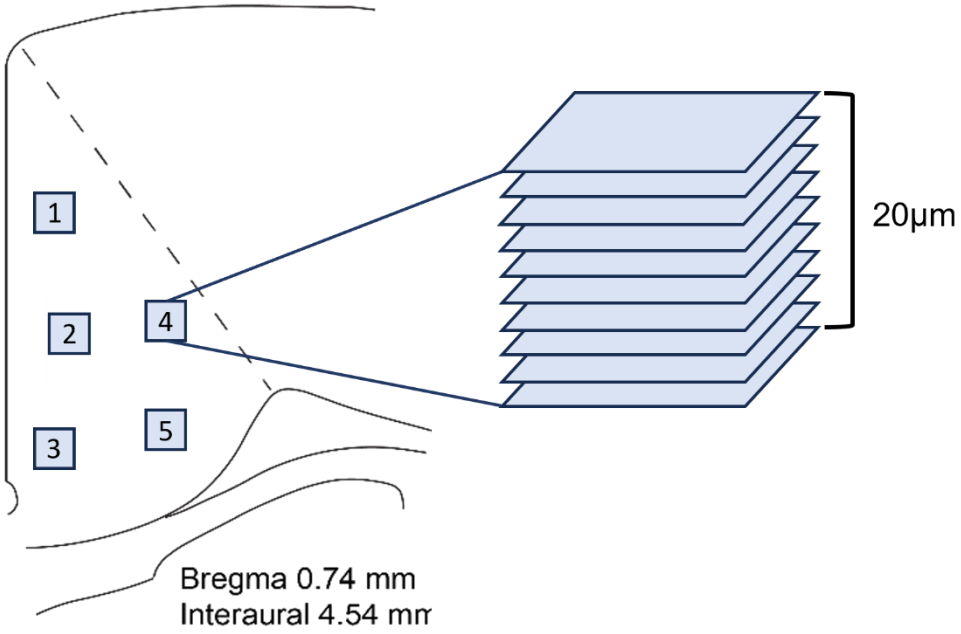

Figure 2.8 Schematic of the locations of the 40x magnification, sampled Z-Stack microscope images from ACC. Boxes 1 - 3 were positioned in the superficial layers and boxes 4 - 5 positioned in the deep chapter s. Z-stacks were 20 µm total thickness and 2 µm between individual images.

2.7 Statistical analysis

All statistical analysis were performed using Excel (Microsoft, USA) and Prism 10 (version 10.2.3; GraphPad Software, USA). Graphs were produced using Prism 8. A significant result was defined as $p < 0.05$. Graphically, significance values (*p*) are represented in figures as 'ns' not significant, * ≤ 0.05, ** ≤ 0.01 and *** ≤ 0.001. All sample sizes (*n* / *N*) are presented in figure legends, where *n* describes the number of tissue slices and *N* describes the number of animals / human cases.

Data were tested for normality using Shapiro-Wilk ($n \leq 50$) and Kolmogorov–Smirnov ($n > 50$) tests. If data were found to follow a normal (Gaussian) distribution, parametric tests were used. Parametric data were presented as mean ± standard error of the mean (SEM) and represented as bar charts or line graphs, where the error bars represent the SEM. If data were not normally distributed, non-parametric tests were used. Non-parametric data were presented as median and interquartile ranges (IQR, Q1 – Q3) and represented as box plots, where the whiskers represent the minimum and maximum values. Within this thesis, if plots presented in the same figure included both parametric and non-parametric data, all data were analysed using the non-parametric test and presented as box plots.

To compare two independent samples, an unpaired *t* test was used if data were parametric and a Mann-Whitney rank sum test was used if data were non-parametric. To compare two dependent samples, a paired *t* test was used if data were parametric, and a Wilcoxon matched-pairs test was used if data were non-parametric. A one-way analysis of variance (ANOVA) was used to compare the means of more than two groups when there was one independent variable and one dependent variable. A 2-way ANOVA was used to compare the effect of two independent variables, in combination, on a dependent variable. If comparisons were made over the same set of slices, the test also incorporated repeated measures (RM), with Greenhouse-Geisser correction if lack of sphericity was found. If an overall effect was found, multiple comparisons were performed post-hoc using Dunnett's or Tukey's tests.

Chapter 3. Modelling acute NMDA receptor hypofunction *in vitro* using PCP in rat ACC and hippocampus

3.1 Introduction

The cognitive deficits of schizophrenia (Liddle, 1987, Nuechterlein et al., 2004, Tandon et al., 2013) are associated with dysfunction in specific brain regions, particularly the ACC (Adams and David, 2007) and the hippocampus (Goto, 2022, Weiss et al., 2003, Weiss et al., 2004). Both structures play crucial roles in cognitive processes such as memory, attention, and executive function, which are often impaired in individuals with schizophrenia (Bowie and Harvey, 2006). Understanding the relationship between schizophrenia, cognitive symptoms, and the roles of the ACC and hippocampus can provide insights into the underlying mechanisms of the disorder.

One proposed mechanism contributing to schizophrenia is the hypofunction of NMDA receptors on GABAergic PV+ inhibitory interneurons (Gonzalez-Burgos and Lewis, 2008, Lesh et al., 2011, Marín, 2024). This leads to the inactivation of these interneurons and subsequent disinhibition of excitatory pyramidal cells, resulting in increased cortical excitation (Homayoun and Moghaddam, 2007). This is supported by studies using NMDA receptor antagonists, such as PCP and ketamine, which induce schizophrenia-like symptoms in humans (Coyle, 1996, Javitt, 1987, Javitt and Zukin, 1991) and animal models (Neill et al., 2010).

In the ACC, structural and functional abnormalities are consistently observed in patients with schizophrenia. Reduced grey matter volume in the ACC (Fornito et al., 2009), as well as decreased laminar thickness (Bouras et al., 2001), has been reported in post-mortem studies. Functionally, neuroimaging studies have shown abnormal ACC activity in schizophrenia, with hypofunction observed across various cognitive tasks (Adams and David, 2007). The ACC's role in cognitive control (Rolls, 2019), and its connections with the hippocampus and other brain regions (Anastasiades and Carter, 2021), highlights its importance in the cognitive deficits seen in schizophrenia. The hippocampus, a structure crucial for learning and memory (Biderman et al., 2020, Scoville and Milner, 1957), also shows significant pathology in schizophrenia. Studies have consistently found reduced hippocampal volume in schizophrenia patients (McCarley et al., 1999, Nelson et al., 1998), often linked to interneuron loss, particularly PV+ interneurons (Zhang and Reynolds, 2001). Abnormal hippocampal

activation during memory tasks further supports hippocampal dysfunction in schizophrenia (Guo et al., 2019, Weiss et al., 2003, Weiss et al., 2004).

PV+ and SST+ interneurons play critical roles in generating gamma (30-80 Hz) and beta (15-30 Hz) frequency oscillations (Chen et al., 2017, Fuchs et al., 2007, Kuki et al., 2015, Tamás et al., 2000, Whittington et al., 1995), respectively, which are crucial for cognitive processes. In schizophrenia, NMDA receptor hypofunction disrupts the excitatory-inhibitory balance mediated by these interneurons, contributing to the cognitive deficits observed in the disorder. Gamma and beta oscillations are associated with specific cognitive functions (Lundqvist et al., 2016, Miller et al., 2018). Gamma oscillations, for example, are linked to working memory and executive function, while beta oscillations are involved in sensorimotor processes and more general cognitive control (Guan et al., 2022, Lundqvist et al., 2016, Miller et al., 2018).

PV+ interneurons are fast-spiking inhibitory neurons and the precise timing of PV+ interneuron firing synchronises the activity of excitatory pyramidal cells, generating gamma oscillations (Whittington et al., 1995, Womelsdorf et al., 2007). Gamma oscillations are essential for synchronizing neuronal activity across brain regions, particularly during cognitive tasks that require memory and attention (Howard et al., 2003, Lisman, 2010). SST+ interneurons, on the other hand, are primarily involved in generating beta oscillations. These interneurons orchestrate inhibitory feedback mechanisms that produce beta rhythms, particularly in cortical regions associated with sensorimotor function and cognitive control (Chen et al., 2017, Kuki et al., 2015). Although beta and gamma oscillations are generated by different interneuron populations, the mechanisms driving these rhythms are interconnected.

In schizophrenia, NMDA receptor hypofunction on PV+ interneurons disrupts the generation of gamma oscillations, leading to impaired cognitive function. The hypofunction of NMDA receptors reduces the excitatory input necessary for PV+ interneurons to maintain their fast-spiking activity, resulting in decreased synchronization of pyramidal cells and abnormal gamma oscillations (Lesh et al., 2011). This disruption in gamma rhythms is linked to cognitive deficits, such as impaired working memory and executive function, which are hallmarks of schizophrenia (Haenschel et al., 2009).

Similarly, beta oscillations are also affected by NMDA hypofunction. Although the relationship between beta rhythms and cognitive symptoms in schizophrenia is less well understood, studies have shown that abnormal beta oscillations are associated with sensorimotor and cognitive impairments in the disorder (Meconi et al., 2016, Spencer et al., 2004). SST+ interneurons, which are responsible for generating beta oscillations, may also be impacted by NMDA receptor dysfunction, further contributing to the cognitive deficits observed in schizophrenia (Chen et al., 2017).

Animal models, particularly rodent models, have been instrumental in studying the roles of the ACC and hippocampus in schizophrenia. These models have demonstrated the involvement of the ACC in working memory (Teixeira et al., 2006) and its connections with the hippocampus in cognitive tasks (Jobson et al., 2021). The prenatal MAM model, a developmental rodent model of schizophrenia, has shown that hippocampal dysfunction, including reduced volume (Featherstone et al., 2007) and impaired neurotransmission (Hradetzky et al., 2012), leads to cognitive deficits akin to those seen in schizophrenia patients (Moore et al., 2006).

Furthermore, beta and gamma oscillations can be generated in ACC and hippocampus slices *in vitro* using the glutamate agonist KA (Adams et al., 2017, Fisahn et al., 2004, Shinozaki et al., 2016, Steullet et al., 2014). This approach allows for the study of oscillatory activity in a controlled environment, providing insights into the underlying mechanisms of oscillation generation and maintenance. PCP, an NMDA receptor antagonist, is widely used in preclinical animal models of schizophrenia because it induces behaviours associated with the disorder, such as hyperactivity, impaired sensorimotor gating, and cognitive deficits (Lee and Zhou, 2019). PCP disrupts PFC function, increasing glutamate efflux (Amitai et al., 2012, Moghaddam et al., 1997), altering unit firing (Kargieman et al., 2007), and increasing gamma oscillatory activity both *in vivo* (Hakami et al., 2009, Lee et al., 2017) and *in vitro* (Lemercier et al., 2017, Rebollo et al., 2018).

Given PCP's ability to replicate multiple pathologies of NMDA receptor hypofunction, this thesis aims to use PCP to establish an acute rodent brain slice model to explore the effects of NMDA receptor hypofunction in neuronal circuits in the ACC and CA3 region of the hippocampus. By examining the effects of PCP on KA-induced beta and gamma frequency oscillations, this study seeks to provide further

insights into the mechanisms underlying cognitive deficits in schizophrenia. Understanding these mechanisms may contribute to the development of targeted interventions to alleviate cognitive symptoms in schizophrenia.

3.2 Aims

- Characterise KA-evoked high frequency oscillations in rat ACC and hippocampus, *in vitro*.

- Explore the effect of PCP, and other NMDA receptor antagonists MK-801 and DAP5, on KA-evoked oscillations in rat ACC and hippocampus, *in vitro*.

- Determine whether KA can evoke high frequency oscillations in human tissue and compare PCP effects to findings in rat cortex.

3.3 Methods

3.3.1 Animals

Acute rodent brain tissue slices were prepared from wild-type, male Lister Hooded rats (7 – 10 weeks) as described in Chapter 2.2. Animals were anaesthetised with inhaled isoflurane prior to injection (i.m.) of ketamine (100 mg/kg) and xylazine (10 mg/kg). Animals were intracardially perfused with 60 ml of sucrose-modified ACSF, and the brain was removed and placed in ice-cold sucrose-modified ACSF.

3.3.2 ACC slice recordings

Following removal of the brain, the whole brain was cut in half coronally to isolate the front half of the brain and mounted on a vibrating microtome stage. Coronal tissue slices (450 µm) were cut, and ACC slices were trimmed and transferred to a holding chamber at room temperature for approximately 60 minutes before being placed in the recording interface chamber where they were perfused with oxygenated ACC ACSF and maintained at 30 – 32°C. After 30 minutes, glass field electrodes were inserted into the layer 5 of the ACC, and KA (800 nM) was bath applied via the circulating ACSF.

3.3.3 HPC slice recordings

Following removal of the brain, the whole brain was inverted and mounted on a vibrating microtome stage. Horizontal tissue slices (450 µm) were cut, and hippocampus slices were trimmed and transferred to a holding chamber at room temperature for approximately 60 minutes before being placed in the recording interface chamber where they were perfused with oxygenated hippocampus ACSF and maintained at 32 – 34°C. After 30 minutes, glass field electrodes were inserted into *stratum radiatum* of the CA3 of the hippocampus, and KA (100 nM) was bath applied via the circulating ACSF.

3.3.4 Human cortical slice recordings

Human tissue slices were prepared from overlying cortical tissue obtained from patients undergoing surgical resection for a deep brain tumour. Details of the patient tissue included in this study can be found in table 3.1.

Following microdissection, the tissue was mounted on a vibrating microtome stage. Tissue slices (400 µm) were cut, trimmed, and transferred to a holding chamber at room temperature for approximately 60 minutes before being placed in the recording interface chamber where they were perfused with oxygenated human ACSF and maintained at 30 – 32°C. After 30 minutes, glass field electrodes were inserted into superficial and/or deep layers across the slice, and KA (800 nM) was bath applied via the circulating ACSF.

Table 3.1 Human tissue sample included in this study

Age at surgery	Gender	Resected brain area
56	M	Temporal, right

3.3.5 Data analysis of beta and gamma frequency activity

Oscillations were evoked using the glutamatergic agonist KA and field oscillations were recorded. Using Fast Fourier Transform algorithms, power spectral density analysis was performed on recorded data using Axograph and Spike2. Using power spectra analysis of 60 second epochs, the peak frequency (Hz) and the area under the curve (area power; $\mu V^2/Hz$) were measured between 15 and 80 Hz. To analyse ACC beta frequency oscillations, peak frequency and area power were measured between 15 – 32.9. To analyse ACC gamma frequency oscillations, peak frequency and area power were measured between 33 – 80 Hz. KA-evoked network oscillations were considered stable when peak frequency and area power measurements varied no more than 10% over a 20 minute 'control' period, where 60 second epochs were measured at 10 minute intervals. Once oscillations were stable, other pharmacological compounds were applied. As multiple tissue slices could be obtained from each animal or patient, two values *(n / N)* are presented below to represent slice (*n*) and animal / patient (*N*) numbers, respectively. For statistical

analysis, 60 second epochs were analysed at 10 minute intervals. Due to large variance in baseline area power measurements, percentage change from the control mean (% control) was calculated and analysed.

3.3.6 Pharmacological compounds

All pharmacological compounds were bath-applied to circulating ACSF. KA was applied 30 minutes after slices were placed in the recording chamber, to induce and maintain oscillations, and was present throughout the experiment (3 – 5 hours). The NMDA receptor antagonists, PCP (10 µM), DAP5 (100 µM), and MK-801 (10 µM), were applied for 60 minutes once oscillations had stabilised.

3.4 Results

3.4.1 KA application induced stable beta and gamma frequency oscillations in rat ACC slices

The cognitive deficits associated with schizophrenia have been strongly linked to changes in network oscillations (Senkowski and Gallinat, 2015). Beta and gamma frequency oscillations can be evoked and recorded from rodent ACC brain slices, *in vitro* (Adams and David, 2007, Adams et al., 2017). Firstly, to establish and characterise the network activity that could be evoked in ACC slices, KA (800 nM) was bath applied to generate high frequency oscillations. Extracellular field recordings were made from layer V of the ACC and baseline activity was recorded before KA was applied. After KA application, oscillations started to emerge after 15 – 20 minutes and continued to increase in magnitude and stabilise in frequency, over 2 - 3 hours. Peak frequency (Hz) and area power (μV^2/Hz) measurements were taken throughout recording and oscillations were considered stable when peak frequency and area power stabilised (see Methods).

Previous studies have shown that ACC slices *in vitro* generate either beta or gamma or a mixed beta/gamma oscillatory activity (Adams et al., 2017), and similar findings were made here (Figure. 3.1 – 3.2). Example power spectra and local field potential (LFP) traces demonstrate that KA induced ACC oscillations consisted of a single beta frequency peak (Figure. 3.1a), or a single gamma frequency peak (Figure. 3.1b), that builds up and stabilises over 2 – 3 hours. The frequency of KA-evoked oscillations varied from 19 to 61 Hz (*n* / *N* = 165 slices / 62 animals, Figure. 3.1c) and resulted in a bimodal distribution which I used to determine the beta (18 – 32.9 Hz) and gamma (33 - 80 Hz) frequency bands. Stable beta and gamma frequency oscillations had a mean peak frequency of 26.3 ± 0.26 Hz and 45.7 ± 0.23 Hz, respectively (Figure. 3.1d). Of 165 ACC slices, prepared from 62 animals, 65% had a peak frequency within the beta frequency band (n = 107/165 slices) and 35% had a peak frequency within the gamma frequency band (n = 58/165; Figure. 3.1e).

Once stable, other compounds were applied to beta and gamma frequency oscillations to modulate and record changes in oscillatory activity. In this thesis, only oscillations with a clear single beta or gamma frequency peak were used for experiments, unless stated otherwise.

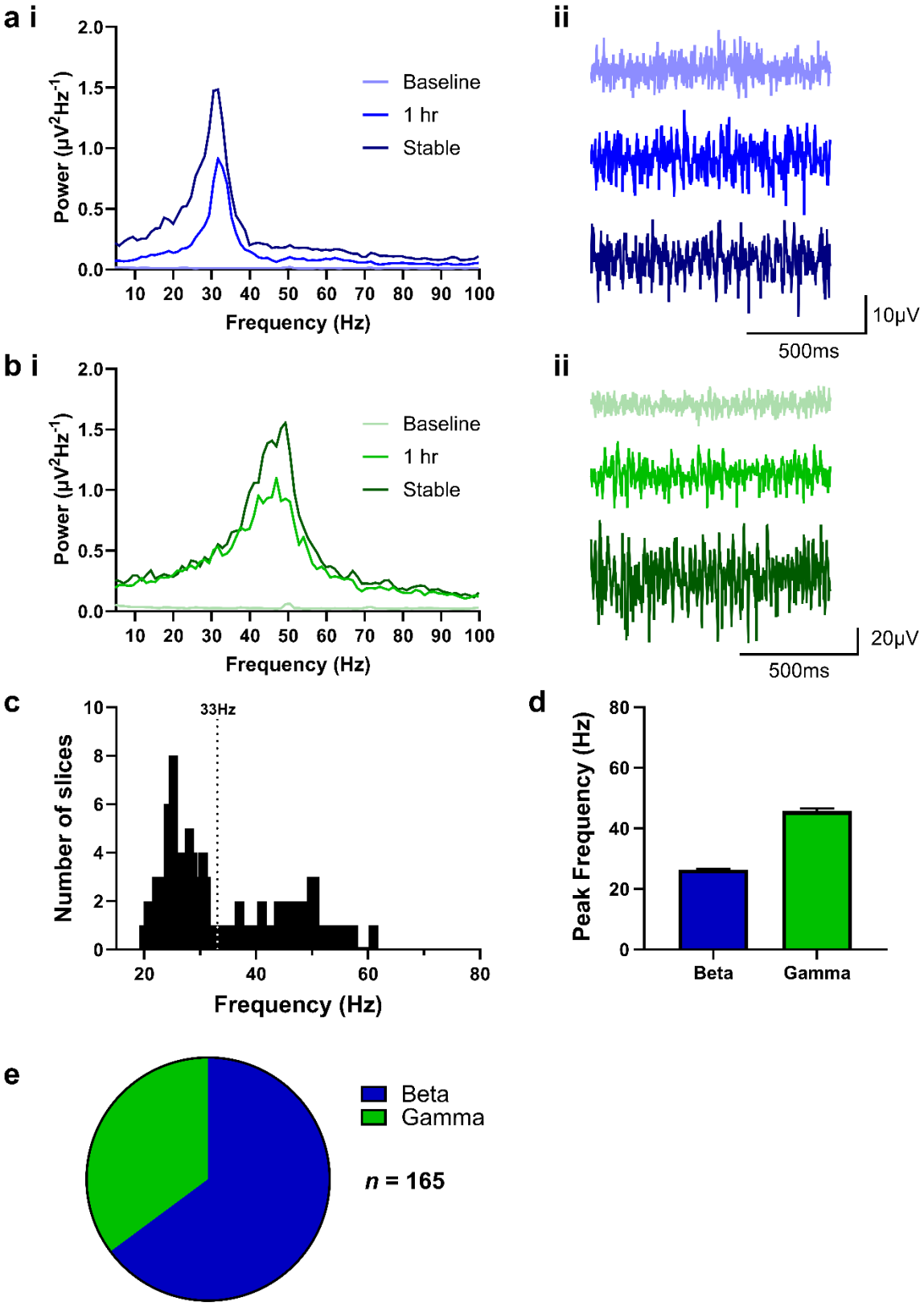
a i
ii
Power (μV²Hz⁻¹)
Frequency (Hz)
Baseline
1 hr
Stable
10μV
500ms
b i
ii
20μV
c
33Hz
Number of slices
d
Peak Frequency (Hz)
Beta
Gamma
e
n = 165

Figure 3.1 KA-evoked (800 nM) beta (18 – 32 Hz; blue) and gamma (33 – 80 Hz; green) frequency oscillations recorded from layer V of ACC slices prepared from young, male adult rats. Representative power spectra (i) and LFP traces (ii) of ACC (a) beta frequency and (b) gamma frequency oscillation baseline prior to KA application (without KA; Baseline / top trace), after 1 hour KA application (1 hr / middle trace) and stable oscillations, 2 – 3 hours after KA application (Stable / bottom trace). (c) Distribution histogram of stable KA-induced oscillation frequency defining beta frequency and gamma frequency. Oscillations were either single-peak beta (18 – 32 Hz) frequency or gamma (33 – 80 Hz) frequency oscillations. (d) Mean (± SEM) peak beta and gamma frequencies (Hz). (e) Proportion of KA-evoked, stable beta frquency (n = 107) and gamma frequency (n = 58) oscillations recorded from ACC slices. Total slices / animals (*n* / *N*) = 165 / 62.

As mentioned previously, KA can also generate mixed beta/gamma frequency oscillations in ACC slices *in vitro*. In this thesis, mixed beta/gamma oscillations were also recorded from layer V of the ACC. Examples of this can be seen in figure 3.2. In all so-called mixed oscillations, a clear peak was visible in both the beta and the gamma frequency bands (Figure 3.1).

Mixed beta/gamma oscillations were highly variable and dynamic throughout recordings. Depending on the slice, either the beta or the gamma rhythm could be dominant, with one peak noticeably larger than the second peak (Figure. 3.2). Alternatively, the beta and gamma peaks could be of similar size, with neither being the dominant rhythm. In some instances, these dynamics were maintained throughout the recording and the dominant rhythm would be larger than the secondary rhythm throughout. However, in some slices the dominant rhythm would gradually change from beta to gamma, or vice versa. As the dynamics of these mixed beta/gamma oscillations were highly variable, and they were a small proportion of the total number of ACC oscillation recordings, the data from these recordings have not been quantified in this thesis. Examples are shown in figure 3.2 to demonstrate the different types of mixed oscillations that were observed throughout recordings and highlight that these are two distinct rhythms.

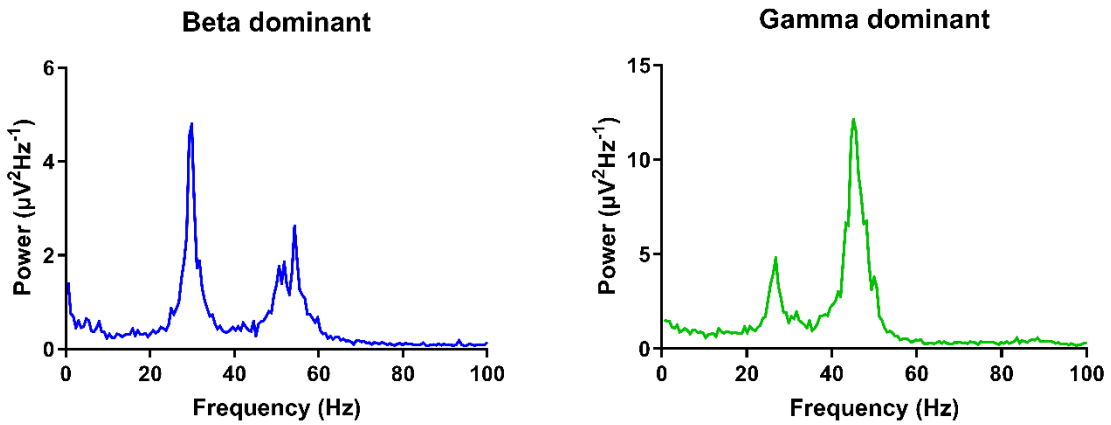

Figure 3.2 Examples of KA-evoked mixed beta/gamma frequency oscillations, recorded from layer V of ACC slices prepared from young, male adult rats. Representitive power spectra of a mixed beta dominant (left) and gamma dominant (right) KA-evoked (800 nM) oscillation, showing peaks within the beta (20 – 32 Hz) and gamma (33 – 80 Hz) frequency bands.

3.4.2 Acute PCP application increased beta oscillatory power in ACC slices

PCP is a well-established NMDA receptor antagonist and has frequently been used to model NMDA receptor hypofunction *in vivo* and *in vitro*. *In vivo*, PCP disrupts cortical oscillations recorded from the PFC in the beta/gamma frequency range (Hakami et al., 2009, Lee et al., 2017). Little is known about the effects of PCP in the ACC specifically, as most studies to date have focused on other regions of the mPFC such as prelimbic cortex (Kargieman et al., 2007), an area also associated with the cognitive deficits of schizophrenia (Sakurai et al., 2015). Furthermore, the effect of NMDA receptor hypofunction on beta frequency oscillations is also less well understood than the effects in gamma frequency oscillations. Therefore, to establish a model of NMDA receptor hypofunction that assessed changes in power and frequency of distinct beta and gamma frequency oscillations, PCP was applied to 'normal', stable beta and gamma KA-evoked ACC oscillations.

Firstly, PCP was applied to slices exhibiting stable beta oscillations. PCP application resulted in a rapid, large increase in the magnitude of beta oscillations over 60 minutes (Figure. 3.3a). Peak frequency analysis (Figure. 3.3b) comparing control to PCP (60 minutes) application found PCP significantly decreased the peak frequency of beta oscillations from 27.0 (IQR 24.7 – 28.6) Hz to 23.5 (IQR 22.3 – 25.8) Hz ($p < 0.0001$; Wilcoxon matched-pairs test), indicating a slowing of the oscillation. Area power analysis (Figure. 3.3c) clearly demonstrated that PCP induced a significantly large increase in beta power from control 101.6 (IQR 98.0 – 105.7)% to 311.8 (IQR 191.9 – 390.7)% ($p < 0.0001$; Wilcoxon matched-pairs test), indicating a very large increase in the size of the oscillation.

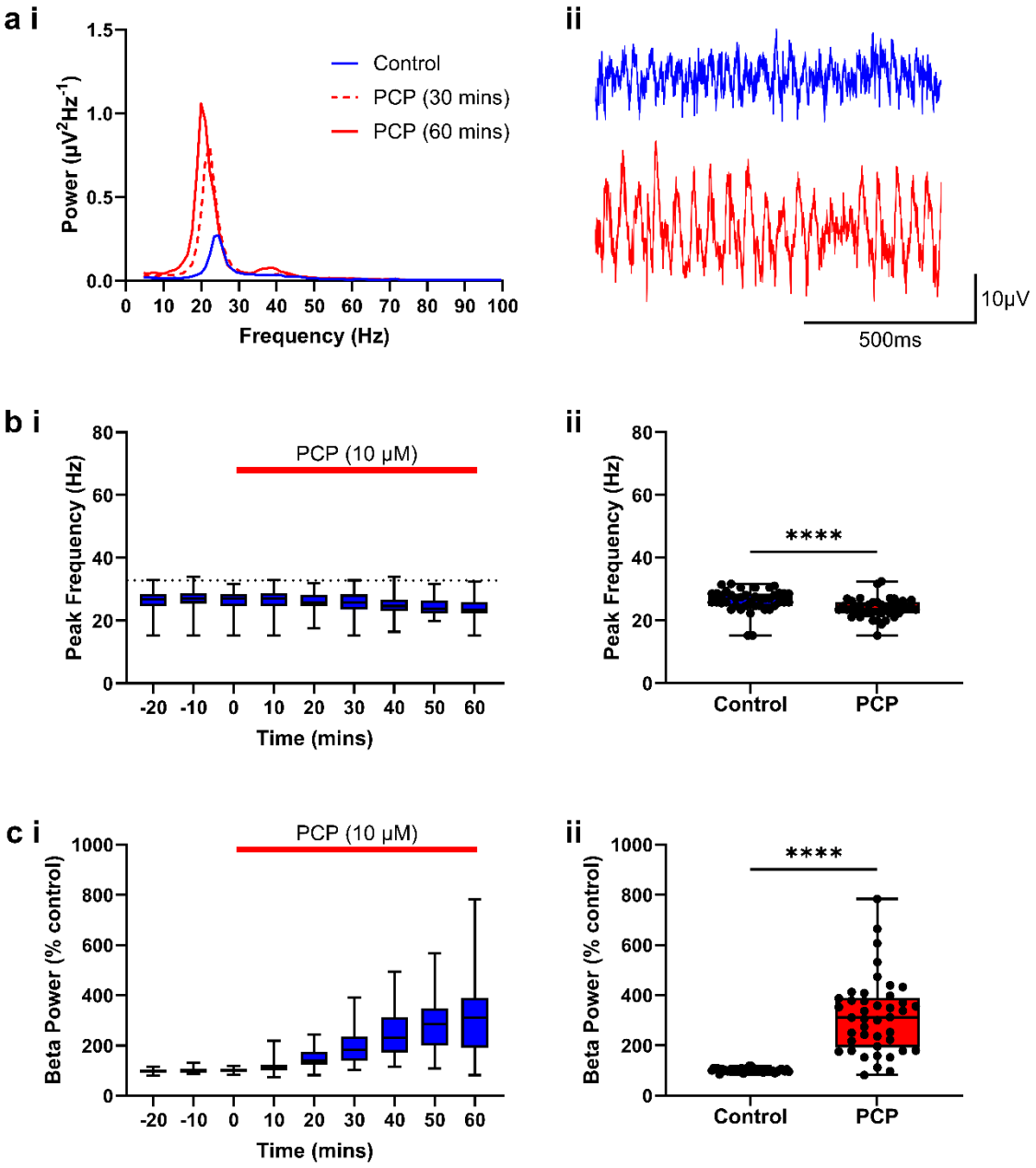

Figure 3.3 PCP induces a large increase in KA-evoked beta area power in rat ACC slices. (a) Example (i) power spectra and (ii) LFP traces from one experiment: control (blue solid line), after 30 minutes PCP (red dashed line) and 60 minutes PCP (red solid line). (b) Effect of 60 minutes PCP application on beta oscillation peak frequency (Hz), shown as (i) time-course plot medians (IQR) where PCP was applied for duration of red bar and (ii) compared to control median (IQR). (c) Effect of 60 minutes PCP application on beta power (% control), shown as (i) time-course plot medians (IQR) where PCP was applied for duration of red bar and (ii) compared to control median (IQR). Total slices / animals (*n* / *N*) = 43 / 22.

3.4.3 Acute PCP application increased beta power but not gamma power in ACC slices

The effect of PCP on gamma oscillations has been widely studied but not specifically in the ACC. PCP was therefore applied to slices exhibiting a stable gamma frequency oscillation for 60 minutes (Figure. 3.4). Interestingly, when PCP was applied to gamma frequency oscillations, there was a clear change in the frequency and size of the oscillation (Figure. 3.4a). Over the 60 minutes PCP application, the frequency of the oscillation significantly decreased (Figure. 3.4b), showing a shift from a gamma frequency oscillation of 40.5 (IQR 37.8 – 46.0) Hz to a beta frequency oscillation of 27.6 (IQR 23.2 – 32.0) Hz. This frequency band shift was observed in 12 of 14 slices (85.7%; Figure. 3.4e). To understand the effect on the control gamma oscillation, gamma band area power was measured between 33 and 80 Hz, but there was no significant change in gamma power from control (Figure. 3.4c). As the peak frequency shifted to the beta band, area power was also measured within the beta frequency band (15 – 32.9 Hz). The area power of the oscillation increased greatly in the beta band (Figure. 3.4d) from 103.2 (IQR 96.1 – 107.4)% in control to 321.0 (IQR 205.7 – 404.5)% in PCP ($p < 0.0001$; Wilcoxon matched-pairs test).

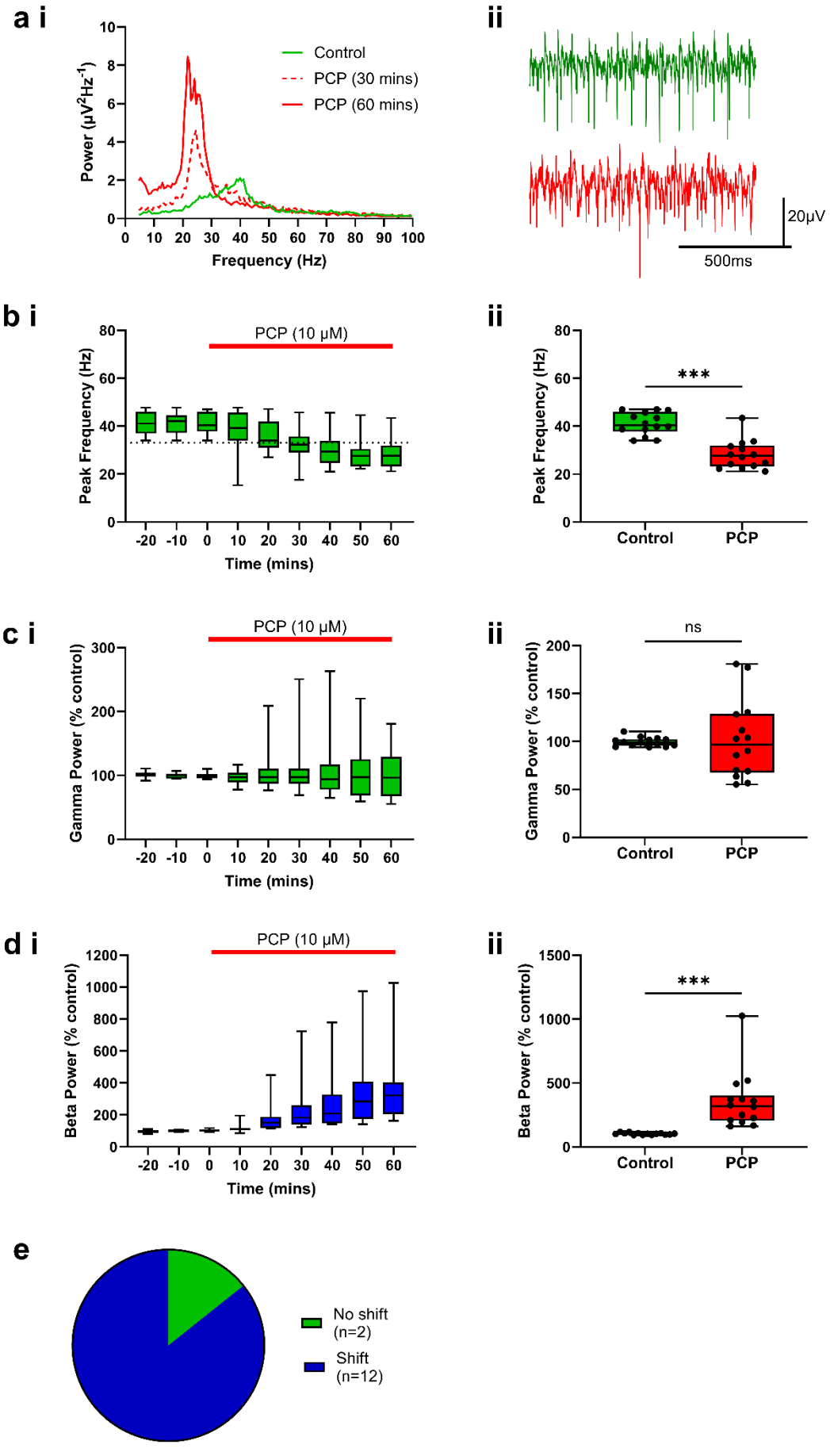
a i
Power (μV²Hz⁻¹)
Frequency (Hz)
Control
PCP (30 mins)
PCP (60 mins)
ii
20μV
500ms
b i
PCP (10 μM)
Peak Frequency (Hz)
Time (mins)
ii
***
Control
PCP
c i
PCP (10 μM)
Gamma Power (% control)
Time (mins)
ii
ns
d i
PCP (10 μM)
Beta Power (% control)
Time (mins)
ii
***
e
No shift (n=2)
Shift (n=12)

Figure 3.4 Application of PCP to stable gamma oscillation caused the emergence of a a large beta oscillation in rat ACC slices. (a) Example (i) power spectra and (ii) traces from one experiment: control prior to PCP (green solid line), a growing beta oscillation after 30 minutes (red dashed line) and 60 minutes PCP (red solid line). (b) Effect of 60 minutes PCP application on gamma oscillation peak frequency (Hz), shown as (i) time-course plot medians (IQR) where PCP was applied for duration of red bar and (ii) compared to control median (IQR). (c) Effect of 60 minutes PCP application on gamma power (% control), shown as (i) time-course plot medians (IQR) where PCP was applied for duration of red bar and (ii) compared to control median (IQR). (d) Effect of 60 minutes PCP application on beta power (% control) of stable gamma frequency oscillations, shown as (i) time-course plot medians (IQR) where PCP was applied for duration of red bar and (ii) compared to control median (IQR). (e) Pie chart deomonstrating proportion of gamma frequency oscillations to shift to a beta-dominant frequency following 60 minutes PCP application. Total slices / animals (*n* / *N*) = 14 / 13.

3.4.4 Acute MK801 and DAP5 application does not alter beta oscillations in ACC slices

Like PCP, MK-801 is a non-competitive NMDA receptor antagonist often used to model NMDA receptor hypofunction. In contrast, DAP5 is an NMDA receptor competitive antagonist that blocks the glutamate binding site. Both MK-801 and DAP5 are selective NMDA receptor antagonists, whereas PCP also interacts with other pharmacological targets (Johnson and Jones, 1990). To explore whether the effects of PCP on the beta oscillations is due to its blockade of NMDA receptors, MK-801 and DAP5 were also applied to KA-evoked ACC beta oscillations for 60 minutes.

When applying MK-801 (10 µM) for 60 minutes, there was no significant change in beta power from control (p = 0.465; Wilcoxon matched-pairs test; Figure 3.5ai). However, there was a significant slowing in the peak frequency from control 28.7 (± 0.79) Hz to 27.4 (± 0.65) Hz with MK-801 (p = 0.002; paired t test; Figure 3.5aii). When applying DAP5 (100 µM) for 60 minutes, there was no significant change from control in beta power (p = 0.313; Wilcoxon matched-pairs test; Figure 3.5bi), or in the peak frequency (p = 0.224; paired t test; Figure 3.5bii). However, the effect of both NMDA receptor antagonists is variable and a large effect of MK-801 and DAP5 can be seen in some slices, similar to the effect seen with PCP.

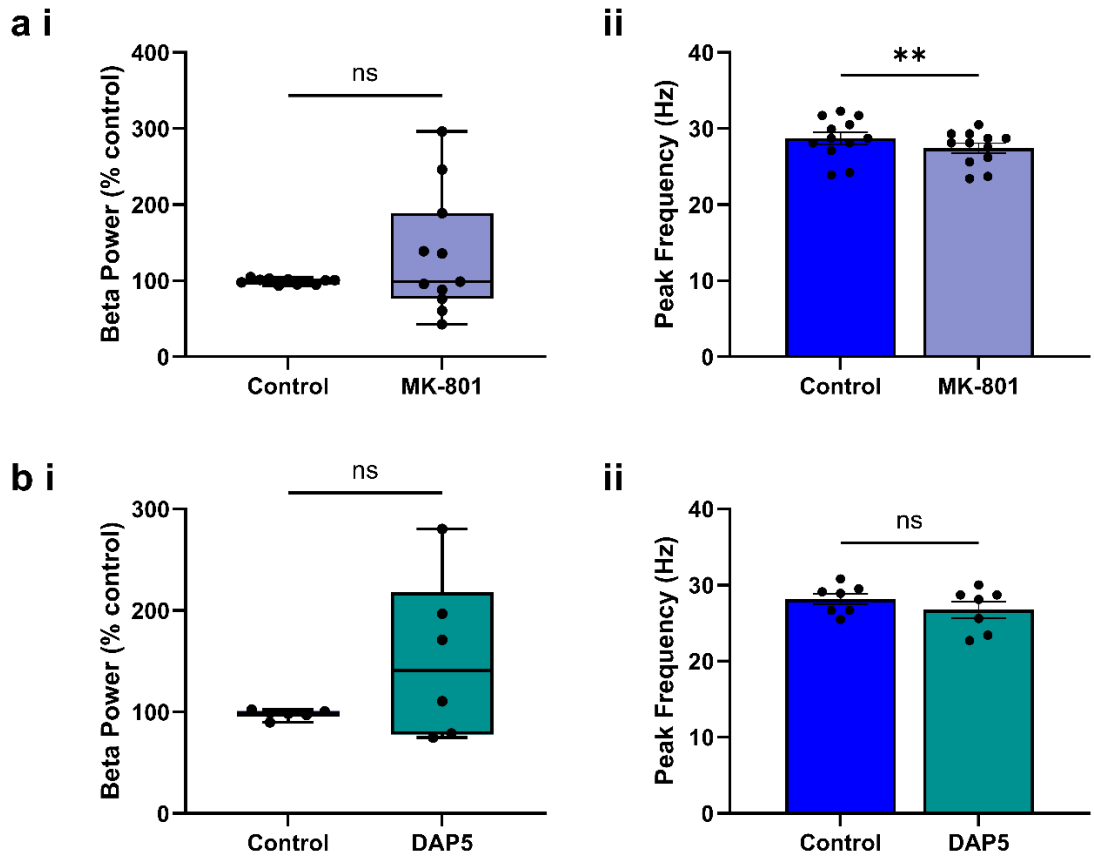

Figure 3.5 Effects of NMDA receptor antagonists MK-801 and DAP5 on beta oscillations in ACC slices. (a) Effect of 60 minutes MK-801 (10 µM) application on (i) median (IQR) beta area power (% control) and mean (± SEM) peak frequency (Hz), compared to control. (b) Effect of 60 minutes DAP5 (100 µM) application on (i) median (IQR) beta area power (% control) and mean (± SEM) peak frequency (Hz), compared to control. Total slices / animals (*n* / *N*) = 7-12 / 3-4

To assess the contribution of NMDA receptor antagonism to the beta power effect, PCP application was compared against the effect of MK-801 and DAP5 (Figure 3.6). There was a significant effect of NMDA receptor antagonist on beta power ($p < 0.001$; Kruskal-Wallis). When comparing changes in beta power (% control) between PCP and MK-801, the effect of PCP 311.5 (IQR 192 – 391)% was significantly greater than that of MK-801 99.0 (IQR 76.3 – 189)% ($p < 0.001$; Dunn's multiple comparisons). When comparing changes in beta power (% control) between PCP and DAP5, the effect of PCP was significantly greater than that of DAP5 140.9 (IQR 77.9 – 218)% ($p = 0.020$; Dunn's multiple comparisons).

This data suggests that the significantly large beta power increase that PCP induces is likely due to other pharmacological interactions of PCP, beyond the NMDA receptor. Variability in the data suggests that there is an NMDA receptor component involved in this effect, but that other receptor targets are likely involved.

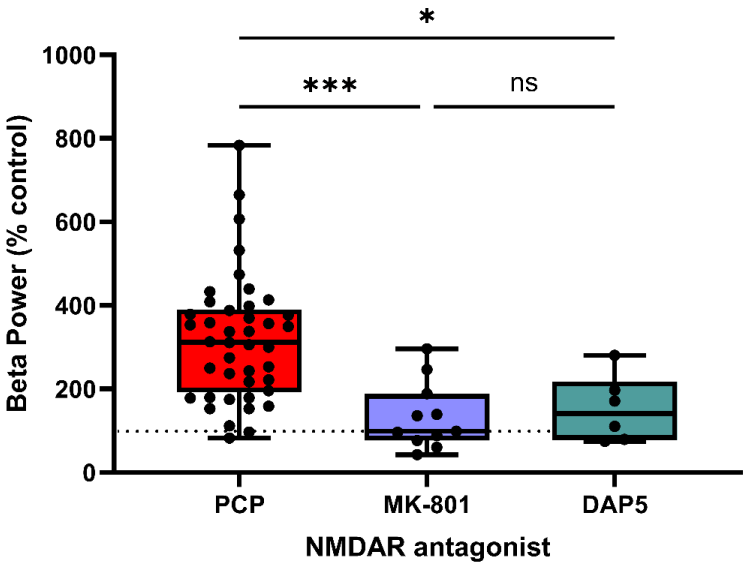

Figure 3.6 PCP has a greater effect on KA-evoked beta oscillations than other NMDA antagonists, MK-801 and DAP5, in ACC slices. Effect of 60 minutes PCP (10 µM), MK-801 (10 µM) or DAP5 (100 µM) application on beta oscillation power (% control) from control. Total slices / animals (*n* / *N*) = 7-43 / 3-22.

3.4.5 Acute KA application induces stable gamma frequency oscillations in CA3 of rat hippocampal slices.

The hippocampus is a key region involved learning and memory (Biderman et al., 2020, Scoville and Milner, 1957). High frequency oscillations can also be evoked and recorded from rodent hippocampal brain slices, *in vitro*. Numerous studies have reported KA evoked oscillation *in vitro* in the CA3 region (Cunningham et al., 2003, Fisahn et al., 2004). CA3 oscillations were evoked using KA (100 nM). Extracellular field recordings were made from *stratum radiatum* of the CA3 and baseline activity was recorded before KA was applied. After KA application, oscillations started to emerge after 15 – 20 minutes and continued to increase in magnitude and stabilise in frequency, over 2 - 3 hours. Peak frequency (Hz) and area power (μV^2/Hz) measurements were taken throughout recording and oscillations were considered stable when peak frequency and area power stabilised.

Example power spectra and LFP traces demonstrated that KA induced CA3 oscillations consisting of a single gamma frequency peak (Figure. 3.7a), that built up and stabilised over 2 – 3 hours. Unlike oscillations recorded from the ACC, CA3 oscillations show a unimodal distribution where peak frequency of KA-evoked oscillations varied from 24.2 to 39.2 Hz (*n* / *N* = 93 slices / 23 animals; Figure. 3.7b). The mean peak frequency was 29.9 ± 0.27 Hz (Figure. 3.7c).

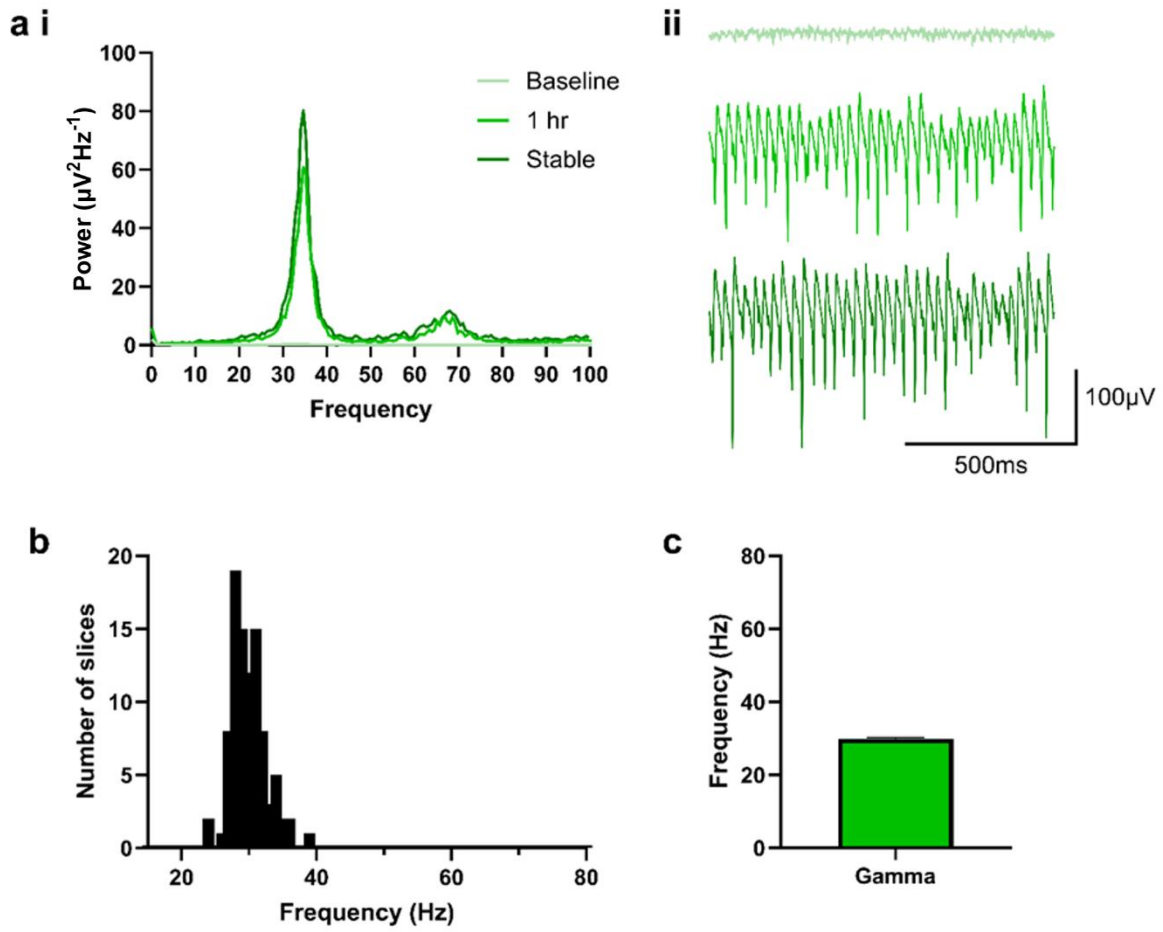

Figure 3.7 KA-evoked gamma frequency oscillations recorded from rat CA3 of the hippocamus. (a) Example (i) power spectra and (ii) LFP traces of gamma frequency oscillation recorded from *stratum radiatum* of CA3. (b) Frequency distribution histogram of stable KA-evoked oscillation frequencies recorded from the CA3. (c) Mean peak frequency of stable gamma oscillaions recorded from CA3. Total slices / animals (*n* / *N*) = 93 / 23.

PCP was then applied to stable gamma frequency oscillation for 60 minutes (Figure. 3.8a). Peak frequency and area power were measured between 15 and 80 Hz. Over the 60 minutes PCP application, there was a small but significant decrease in the peak frequency of the oscillation from a median of 30.5 (IQR 28.7 – 31.7) Hz in control to 27.5 (IQR 25.5 – 30.1) Hz ($p < 0.0001$; Wilcoxon matched-pairs test; Figure 3.8b). However, gamma power was not significantly different following 60 minutes PCP application 103.2 (IQR 84.6 – 122.7)% vs control 99.8 (IQR 97.9 – 103.1)% ($p = 0.672$; Wilcoxon matched-pairs test; Figure 3.8c).

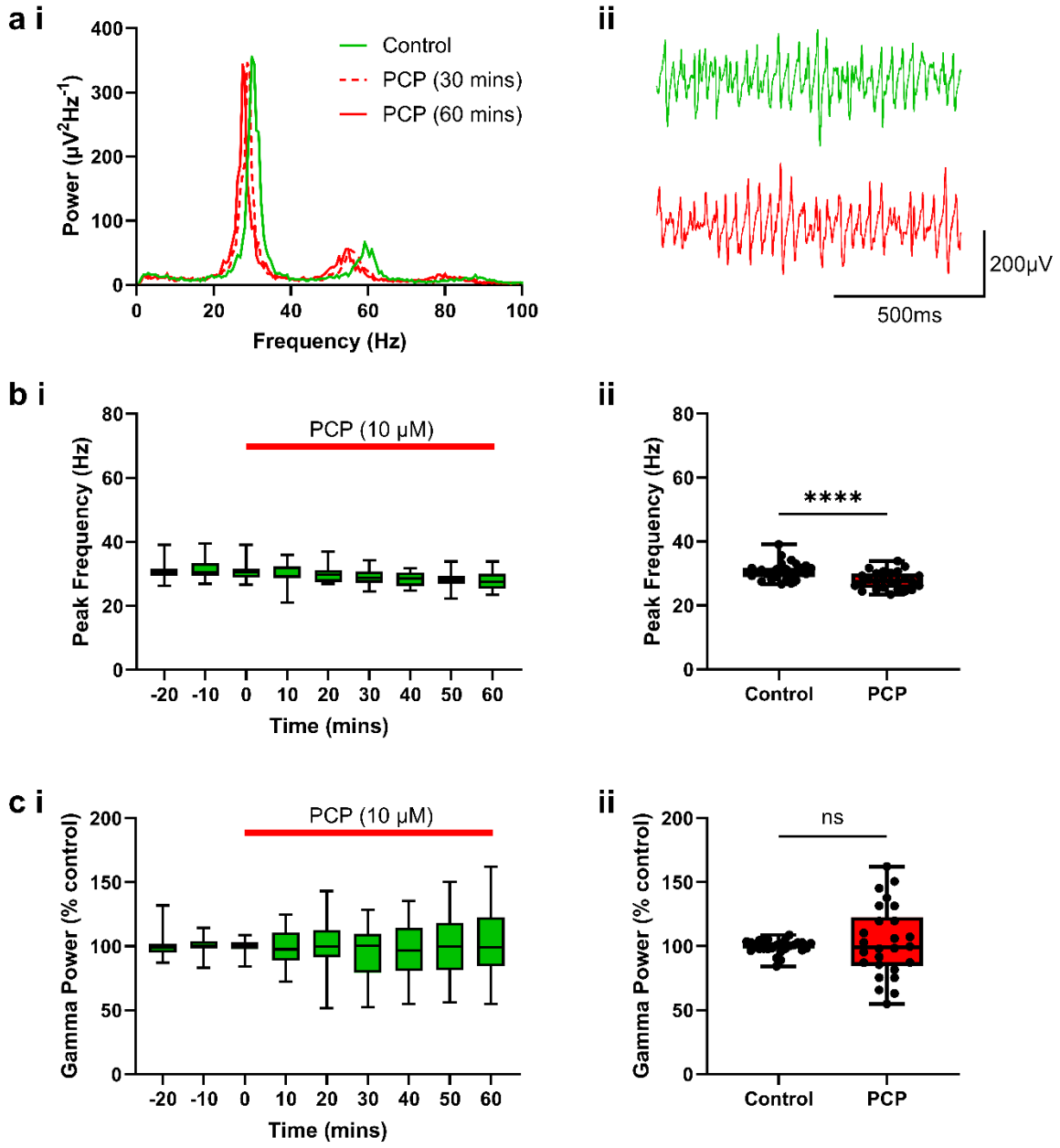

Figure 3.8 When applied to a stable gamma frequency oscillation, PCP did not effect the power of gamma oscillations recorded from rat hippocampal slices. (a) Example (i) power spectra and (ii) LFP traces from one experiment: control (green solid line), after 30 minutes PCP (red dashed line) and 60 minutes PCP (red solid line). (b) Effect of 60 minutes PCP application on gamma oscillation peak frequency (Hz), shown as (i) time-course plot medians (IQR) where PCP was applied for duration of red bar and (ii) compared to control median (IQR). (c) Effect of 60 minutes PCP application on gamma power (% control), shown as (i) time-course plot medians (IQR) where PCP was applied for duration of red bar and (ii) compared to control median (IQR). Total slices / animals (*n* / *N*) = 27 / 18.

3.4.6 Acute application of MK801 and DAP5 had no effect on CA3 gamma power

Mouse studies have shown that the power of CA3 gamma oscillations evoked with carbachol, a commonly used cholinergic agonist, increased with MK-801 (Wang et al., 2020), but DAP5 had no effect (Mann and Mody, 2010). Here I applied MK-801 and DAP5 to KA-evoked CA3 gamma oscillations for 60 minutes and compared against PCP application.

When applying MK-801 (10 µM) for 60 minutes, there was no significant change in gamma power from control (p = 0.219; Wilcoxon matched-pairs test; Figure 3.9ai). However, there was a significant slowing in the peak frequency from control 29.7 (± 0.81) Hz to 27.7 (± 0.86) Hz with MK-801 (p = 0.037; paired t test; Figure 3.9aii). When applying DAP5 (100 µM) for 60 minutes, there was no significant change from control in gamma power (p = 0.297; Wilcoxon matched-pairs test; Figure 3.9bi), or in the peak frequency (p = 0.587; paired t test; Figure 3.9bii).

Next, PCP application was compared against the effect of MK-801 and DAP5 (Figure 3.10). There was no effect of NMDA receptor antagonist on gamma power (p = 0.141; Kruskal-Wallis), finding no significant differences on gamma power between any NMDA receptor antagonists.

Overall, these data showed that neither PCP, MK-801 or DAP5 had any significant effect on the power of the gamma oscillations in the hippocampus. Although there is a small decrease in frequency with PCP and MK-801, this was not a clear switch to beta activity as seen in the ACC.

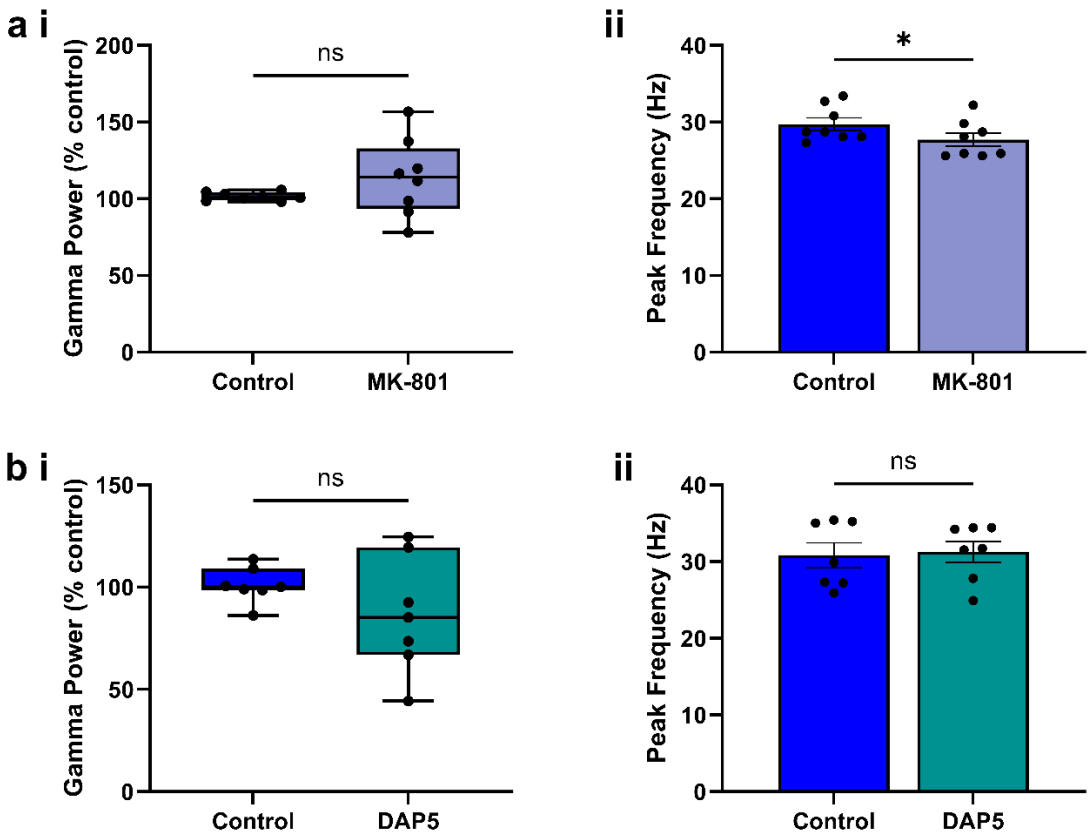

Figure 3.9 The NMDA receptor antagonists PCP, MK-801 and DAP5 do not affect KA-evoked gamma power in CA3 of hippocampal slices. Effect of 60 minutes PCP (10 µM), MK-801 (10 µM) or DAP5 (100 µM) application on gamma oscillation power (% control) from control. Total slices / animals (*n* / *N*) = 7-8 / 3-4.

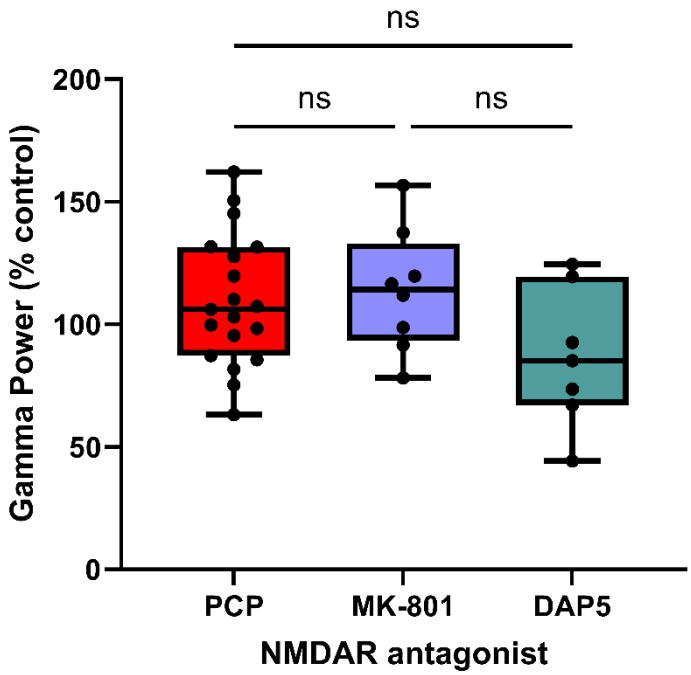

Figure 3.10 The NMDA receptor antagonists PCP, MK-801 and DAP5 do not affect CA3 gamma power. Effect of 60 minutes PCP (10 µM), MK-801 (10 µM) or DAP5 (100 µM) application on gamma oscillation power (% control) from control. Total slices / animals (*n* / *N*) = 7-19 / 3-12).

3.4.7 Acute KA application induces stable beta/gamma frequency oscillations in human tissue cortical slices

In vitro high frequency oscillations can also be evoked and recorded from re-sectioned, human cortical tissue slices. Rodent tissue is used as a translational model to explore the pathology of a human condition. Being able to use human cortical tissue to model NMDA receptor hypofunction, and compare data to rodent tissue findings, is an incredibly useful resource. Human cortical tissue was re-sectioned and, once transferred to the laboratory, maintained in the same conditions as ACC rodent tissue.

Here, the aim was to evoke and characterise high frequency oscillations from human cortical tissue, using KA. Baseline activity was recorded from the deep layer (layer V) for 20 minutes before applying KA. Following previous work from the lab, 800nM KA was used to induce oscillations, and the build-up of oscillation power and frequency was recorded. As n / N = 1 / 1, the data presented in Chapter 3.4.7 and 3.4.8 has not been statistically analysed but does serve as an example of preliminary data which could be expanded upon in future.

Figure 3.11 demonstrates an example recording from one human tissue slice, re-sectioned from the right temporal cortex, following KA application. Although small, a clear oscillation can be seen in the power spectra and representative LFP trace (Figure 3.11a). Following baseline, where there was no oscillatory activity (Figure 3.11a; baseline), the oscillation began to build (Figure 3.11a; KA) into a synchronous, single-peak oscillation. The oscillation peak frequency measured 23.2 (± 0.40) Hz after 60 minutes KA application. Area power increased over the 60 minute KA application, from 0.838 $\mu V^2/Hz$ at baseline, to 2.063 $\mu V^2/Hz$ (Figure 3.11b).

Collecting human tissue samples of good enough quality to induce oscillations was difficult, hence the single example presented here in this thesis. To induce oscillations, it seems a clear laminar structure and definition between the white and grey matter correlated with the quality of oscillations.

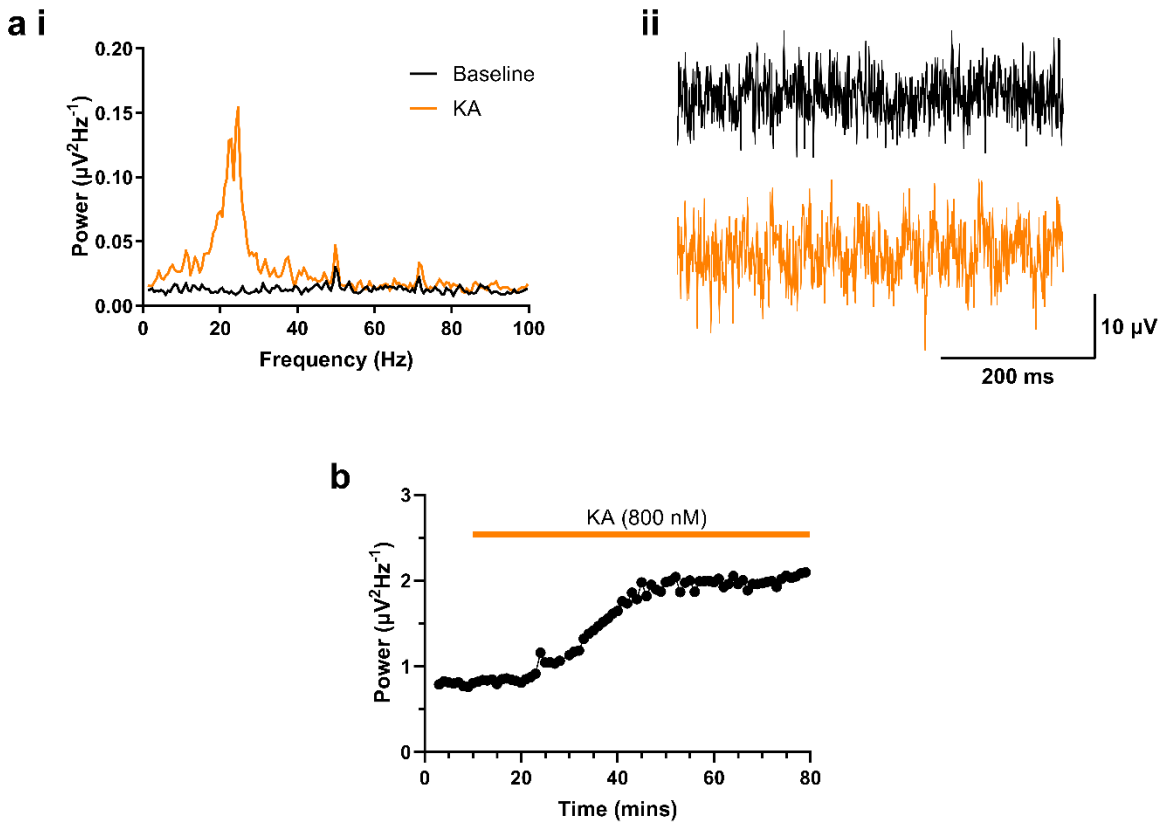

Figure 3.11 KA (800 nM) evokes a high frequency oscillation between 15 and 80 Hz oscillations in human cortical tissue. a) Example (i) power spectra and (ii) LFP traces from first 80 minutes of experiment: baseline prior to KA (black solid line), and a beta oscillation after 60 minutes KA (orange solid line). Time-course plot shows KA (applied for duration of orange bar) modulated increased (b) area power over 60 minutes. Total slices / cases (*n* / *N*) = 1 / 1.

3.4.8 Acute application of PCP to human brain tissue slices mimics ACC oscillation effects

Beta oscillations recorded from the rat ACC were a similar peak frequency to the oscillation recorded from the human cortical tissue. Therefore, I applied PCP (10 μM) to the stable KA-evoked beta oscillation recorded from the human tissue to compare to my rodent data. The following data is recorded from the same slice presented in figure 3.11.

Remarkably, following KA application the oscillation stabilised after 60 minutes, compared to 2 – 3 hours in rat ACC slices. Once stable, PCP was applied for 60 minutes (Figure 3.12). Example LFP traces (Figure 3.12a) and representative power spectra (Figure 3.12b) show a clear dramatic increase in the oscillation power and a minor slowing of oscillation frequency, following 60 minutes PCP application. Peak frequency analysis shows the frequency decreased slightly from 23.7 (± 0.40) Hz to 22.2 (± 0.22) Hz (Figure 3.12b). Oscillation power increased greatly following PCP application, from 2.07 (± 0.012) $\mu V^2/Hz$ to 4.83 (± 0.070) $\mu V^2/Hz$ (Figure 3.12c), an increase of 233%. The increase in oscillation power and slight slowing of frequency reproduces the effect seen in rat ACC beta oscillations. Although the data presented in 3.4.7 and 3.4.8 is from one individual slice, it does suggest that human cortical beta oscillations are greatly enhanced by PCP as seen in rat ACC.

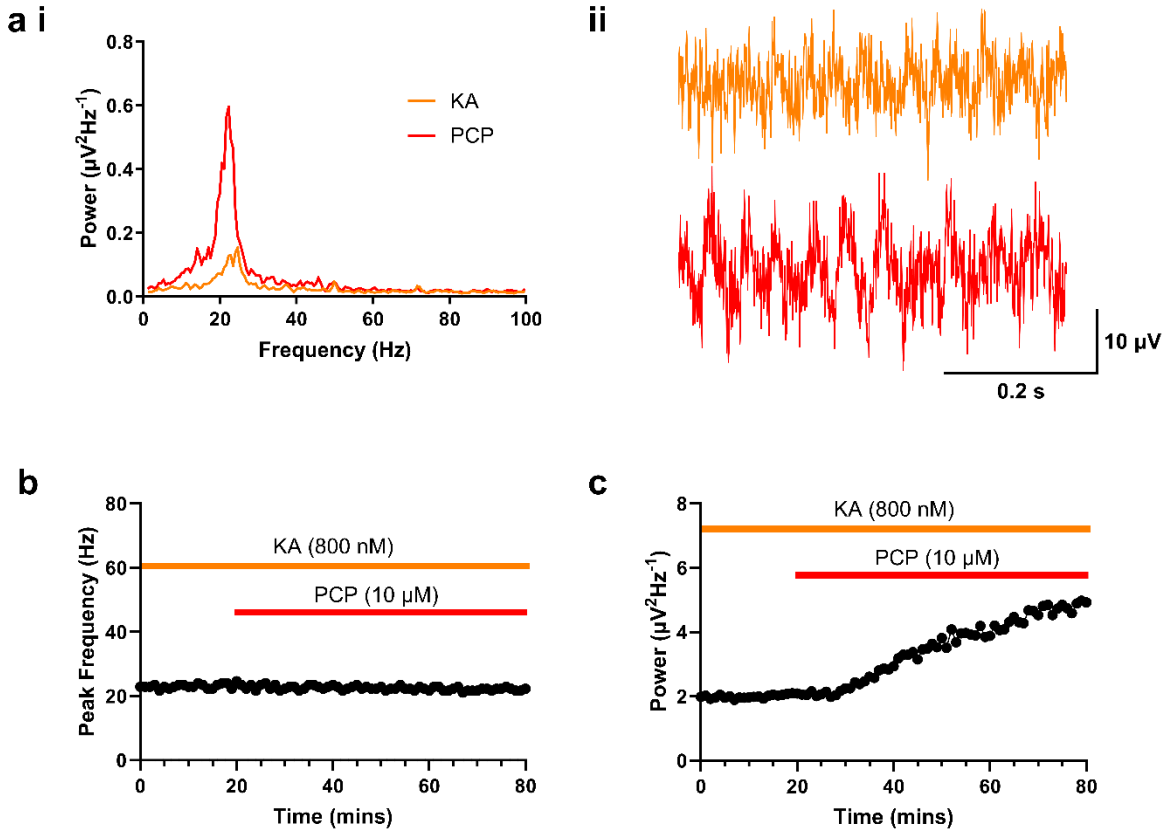

Figure 3.12 PCP effects on KA-evoked oscillations in human tissue cortex. When applied to an acute human cortical tissue slice, PCP (10 μM) increases the power of a high frequency (15 and 80 Hz) KA-evoked oscillation. (a) Example (i) LFP trace and (ii) power spectra prior to PCP (orange solid line), and after 60 minutes PCP (red solid line). Time-course plots show (b) peak frequency and (c) area power, over 60 minutes PCP application (applied for duration of red bar). Total slices / cases (*n* / *N*) = 1 / 1.

3.5 Discussion

Summary of the main findings in Chapter 3:

- In rat ACC, KA evoked beta frequency (20 – 33 Hz) and gamma frequency (33 – 80 Hz) oscillations as single-peak oscillations, or as mixed beta-gamma oscillations.
- KA-evoked beta oscillations significantly increased in power when PCP was applied, in the ACC. KA-evoked gamma oscillations shifted from gamma frequency to a beta frequency oscillation when PCP was applied. The power of the subsequent oscillation also significantly increased. Other NMDA receptor antagonists, MK-801 and DAP5, did not significantly increase oscillation power.
- In rat CA3 of the hippocampus, KA evoked gamma oscillations only, with a mean frequency of 30 Hz. PCP did not significantly affect KA-evoked gamma oscillation power in rat CA3, and neither MK-801 or DAP5 had any effect on gamma oscillations.
- In human cortical tissue, KA evoked a high frequency oscillation that built up and stabilised. PCP application significantly increased oscillation power, in a manner similar to rat ACC beta oscillations.

This thesis found that distinct beta (20 – 32 Hz) and gamma (33 – 80 Hz) frequency oscillations can be evoked by bath application of KA in the rat ACC *in vitro*, as previously reported (Adams et al., 2017). I have also shown that KA-evoked oscillations in ACC can consist of a mixed beta–gamma frequency oscillation, also previously reported (Adams et al., 2017). However, the underlying mechanisms of beta and gamma oscillations are still uncertain. By evoking beta and gamma oscillations independently and simultaneously, my data supports the theory that the two rhythms must be controlled by distinct mechanisms.

In contrast, I found that only oscillations of gamma (20 - 80 Hz) frequency were evoked by bath application of KA in the CA3 of the hippocampus, as previously reported (Cunningham et al., 2003, Fisahn et al., 2004). The differences in the types of oscillatory activity evoked in ACC and hippocampus, therefore, suggest there must be important differences in the underlying neuronal networks between the two regions.

Gamma frequency oscillations have been evoked in numerous studies in both the hippocampus (Fisahn et al., 2004) and neocortex using KA (Adams et al., 2017, Middleton et al., 2008, Roopun et al., 2008). In addition, KA-evoked beta frequency activity has been reported in different cortical regions, including the sensorimotor cortex, and the basal ganglia (Adams et al., 2017, Roopun et al., 2008). In the current study I defined beta frequency activity as 20 – 32.9 Hz based on the frequency distribution histogram, however, in some studies this frequency range has been referred to as low gamma activity. As shown previously in ACC (Adams et al., 2017), I found that that either beta, gamma, or a mixture of both oscillations, can occur *in vitro* following application of KA. In the current study, the majority of ACC slices exhibited clear beta frequency activity (65%) compared to gamma (35%) upon KA application, a higher gamma to beta ratio than previously reported (Adams et al., 2017).

Activity in different interneuron populations has been proposed to contribute to the generation of these two different rhythms. Numerous studies have highlighted the critical role for soma-targeting PV+ interneurons in the generation of gamma frequency activity (Cardin et al., 2009, Sohal et al., 2009). More recently the activity of dendrite-targeting SST+ interneurons has been suggested to contribute to the slower beta band activity (Chen et al., 2017, Kuki et al., 2015, Ter Wal and Tiesinga, 2021). Both PV+ and SST+ interneurons show an area-specific distribution across the ACC (van Heukelum et al., 2019). PV+ interneurons increase in density along the anterior-posterior axis, whereas SST+ interneurons find the opposite; BA25 is densely populated with SST+ interneurons whereas BA32 contains few SST+ interneurons (van Heukelum et al., 2019). The varied distribution and proportion of interneurons throughout ACC slices could underlie the heterogeneity of oscillations I observed. For example, a slice taken from the posterior ACC, where PV+ interneuron density is greater, may be more likely to generate a gamma frequency oscillation *in vitro* than a more anterior slice. Details of the slices' anterior-posterior location were not noted in this study, but recording this in future studies would be very interesting to explore.

When studying oscillations in the CA3 of the hippocampus, gamma frequency activity was defined as 20 – 80 Hz, and stable oscillation frequencies were recorded between 24 and 40 Hz. Unlike in the ACC, only single-peak oscillations were recorded in the CA3, represented by a unimodal distribution of stable peak frequencies around 30 Hz suggested the CA3 generates a low-gamma oscillation, opposed to separate

beta and gamma frequency oscillations (Fisahn et al., 2004). *In vitro* CA3 KA-evoked beta oscillations have not been reported in the literature, and are notably absent when gamma oscillations are present (Roopun et al., 2008). Gamma frequency oscillations are dependent on GABAergic development (Luhmann and Khazipov, 2018), because at postnatal day (P) 5 KA-evoked oscillations are of beta frequency, developing into gamma frequency oscillations at around P15 (Tsintsadze et al., 2015). This correlates with *in vivo* data that shows gamma oscillations do not emerge in rats until the end of the second postnatal week (Doischer et al., 2008, Lahtinen et al., 2002, Mohns and Blumberg, 2008). This is also consistent with immunohistochemical studies that find PV-immunoreactive neurons appear in rat cingulate cortex between P8 and P13 (Frassoni et al., 1991).

The two major GABAergic inhibitory interneuron populations in the hippocampus are also PV+ and SST+ interneurons (Jinno and Kosaka, 2002, Jinno and Kosaka, 2003). In the CA3 specifically, gamma oscillations are formed by precisely timed feedback loops between local pyramidal cells and inhibitory interneurons (Atallah and Scanziani, 2009, Dugladze et al., 2012, Mann et al., 2005). Studies have linked recruitment of fast-spiking PV+ interneurons to the generation and synchrony of gamma frequency oscillations in the hippocampus (Fuchs et al., 2007, Wulff et al., 2009). SST+ interneurons synchronise gamma oscillations in the visual cortex (Veit et al., 2017, Veit et al., 2023), but they have only recently been implicated in CA3 gamma oscillations (Aery Jones et al., 2021, Antonoudiou et al., 2020). Interestingly, in optogenetic studies, the power of *in vitro* carbachol-evoked CA3 gamma oscillations is suppressed by inhibition of PV+ interneurons and inhibition of SST+ interneurons (Antonoudiou et al., 2020). Optogenetic inhibition of SST+ interneurons also increased *in vitro* CA3 gamma frequency (Antonoudiou et al., 2020). Conversely, photoexcitation of hippocampus SST+ interneurons evoked a high gamma (> 60 Hz) frequency oscillation (Antonoudiou et al., 2020). The CA3 is strongly coupled with the CA1 and suppression of PV+ and SST+ interneurons differentially affect downstream CA1 activity. *In vivo,* PV+ interneuron suppression increased power of CA3-CA1 coupling, increased CA1 gamma power and decreased CA1 fast-gamma power (> 60 Hz) (Aery Jones et al., 2021). Inversely, suppression of SST+ interneurons reduced CA3-CA1 coupling, increased EC-CA1 coupling, decreased CA1 gamma power, and increased CA1 fast-gamma power (Aery Jones et al., 2021).

The rodent CA3 is a specially developed network of strong recurrent connectivity (Ishizuka et al., 1990, Laurberg and Sørensen, 1981, Sammons et al., 2024, Swanson et al., 1978), highly specialised for encoding and recalling memories (Kesner and Rolls, 2015, Le Duigou et al., 2014, Papp et al., 2007). The ACC forms part of the wider mPFC, and forms connections with the cortex, amygdala, ventral tegmental area and thalamus (Anastasiades and Carter, 2021). Compared to the CA3, the ACC is involved in a more diverse range of cognitive functions (Bush et al., 2000) such as attention, working memory, decision-making, emotional cognition and sensorimotor function. Together, this suggests the ACC needs to be more dynamic and flexible than the hippocampus, which may be reflected in the different oscillatory rhythms recorded from both regions in this study.

PCP is an NMDA receptor antagonist commonly used to model schizophrenia in rodents, *in vivo* and *in vitro* (Białoń and Wąsik, 2022). I used acute bath application of PCP to on-going, stable ACC oscillations to explore the effects of acute NMDA receptor blockade. In the ACC, PCP was applied to stable KA-evoked (800 nM) beta and gamma frequency oscillations. In the ACC, I showed that NMDA receptor hypofunction, induced by bath application of PCP, resulted in the emergence of a very large beta frequency oscillation. If beta activity was present prior to PCP application the power of this activity increased dramatically up to 312%. However, if gamma oscillations were initially evoked with KA, then blockade of NMDA receptors with PCP led to a clear shift in frequency from gamma to a large beta oscillation.

Numerous studies both *in vitro* and *in vivo* in different cortical regions have shown that NMDA receptor blockade increases gamma oscillation power (Hakami et al., 2009, Hiyoshi et al., 2014b, Lee et al., 2017, Lemercier et al., 2017, Rebollo et al., 2018). The literature regarding frequency changes is less clear because, while several studies show NMDA receptor blockade slows the gamma frequency activity, it remained within the gamma band in most cases (Anver et al., 2011, McNally et al., 2011). The gamma-to-beta frequency shift I have seen in ACC is, however, similar to a study which showed ketamine in the EC *in vitro* exposed a second slow 25 - 35 Hz oscillation (Middleton et al., 2008). In another study, discrete but co-existing beta and gamma oscillations recorded *in vitro* from the somatosensory cortex showed NMDA receptor antagonist DAP5 suppressed gamma power and significantly increased beta power, driving a mixed frequency oscillation to a large beta oscillation (Roopun et al.,

2006). Beta oscillations are associated with memory consolidation, whereas gamma oscillations are associated with memory retrieval. Aberrant beta that is not modulated appropriately by memory formation has been seen in patients with schizophrenia (Meconi et al., 2016), thus the large beta oscillation that emerges in ACC in the presence of PCP in this study could be a suitable model for pathological network activity.

The NMDA receptor hypofunction hypothesis of schizophrenia (Dienel and Lewis, 2019, Gonzalez-Burgos and Lewis, 2008) proposes that the function of NMDA receptors on PV+ interneurons are preferentially reduced, resulting in a loss of PV+ cell-mediated inhibition and a subsequent disinhibition of pyramidal cell firing (Dienel and Lewis, 2019, Gonzalez-Burgos and Lewis, 2008, Homayoun and Moghaddam, 2007). My data showing the PCP-mediated shift from single-peak gamma to beta-dominant activity could suggest SST+ interneurons are more susceptible to NMDA receptor antagonism, than PV+ interneurons. In cortical regions, SST+ interneurons contribute to low-frequency beta oscillations, which are abnormal in schizophrenia (Moran and Hong, 2011). In adult rodents, the contribution of NMDA receptor mediated excitatory transmission onto PV+ interneurons is relatively weak compared to SST+ interneurons (McGarry and Carter, 2016, Rotaru et al., 2011). *In vivo,* acute ketamine treatment reduced SST+ interneuron activity and increased pyramidal cell activity in the mouse cingulate cortex (Ali et al., 2020). This may therefore suggest that PCP application had little effect on PV+ interneuron activity, as gamma power was not significantly changed, and instead caused hypofunction of NMDA receptors on SST+ interneurons.

Other NMDA receptor antagonists that are typically used in schizophrenia models include MK-801, ketamine and DAP5. Given the considerable effect of PCP on beta and gamma oscillations in the ACC, I then acutely applied MK-801 and DAP5 to KA-evoked ACC beta oscillations. When MK-801 and DAP5 were bath applied to ACC beta oscillations, neither antagonist caused a significant change in power or frequency. PCP's effect on beta power was also significantly greater than that of MK-801. MK-801 is a high affinity analogue of PCP that interacts with the same open channel site on the NMDA ion channel as PCP, it is therefore surprising that MK-801 did not have a similar effect on beta oscillations as PCP. This differential effect of PCP in the ACC may occur as PCP has lower NMDA receptor specificity than MK-801 and

interacts with other receptors, including the serotonergic (5-HT2A), dopaminergic (D2), cholinergic receptors and also intracellular σ-1 receptors (Kapur and Seeman, 2002, Oswald et al., 1984).

In comparison to my findings in the ACC, there was no dramatic emergence of a large beta frequency oscillation or any change in the power of CA3 gamma oscillations when bath applying PCP. CA3 gamma power remained remarkably stable in the presence of PCP. The frequency of the oscillation did slow significantly by 3 Hz, but this was arguably still within my defined gamma frequency range.

The effect of acute PCP application on CA3 gamma oscillations *in vitro* has not been previously reported. In this thesis, neither DAP5 nor MK-801 changed CA3 gamma power *in vitro,* reproducing my PCP result. An alternative and popular protocol involves treating animals with NMDA receptor antagonists, acutely or subchronically, *in vivo*. Slices are then prepared from the treated animals and spontaneous or evoked oscillations are recorded *in vitro*. Lemercier et al. (2017) found no difference in spontaneous CA3 gamma power in slices taken from rats treated acutely with MK-801, compared to vehicle treated. Additionally, the same study found gamma oscillations evoked using a combination of cholinergic agonists (acetylcholine (ACh; 10 μM) and physostigmine (Physo; 2 μM)) were dramatically reduced in slices taken from the MK-801-treated animals, compared to control (Lemercier et al., 2017). A similar study that treated rats subchronically with MK-801 found peak power of KA-evoked and Ach + Physo-evoked hippocampal gamma oscillations increased, but only in female rats (Neuhäusel and Gerevich, 2024). The latter study suggests that the effects of NMDA antagonists may be sex dependent. A review by Gogos and van den Buuse (2023) showed that an acute subcutaneous (s.c.) injection with MK-801 (0.05 mg/kg) increased locomotor activity in female rats, compared to males. However, there was no difference between the locomotor activity of female and male rats when treated with an acute PCP injection (2.5 and 5.0 mg/kg; s.c.) (Gogos et al., 2017). In this study, I have used only male rats so it would be important in future to see if similar or different results were seen with female animals.

In vivo, subchronic PCP treatment does not affect basal gamma frequency oscillations recorded from rat vHPC (Aguilar et al., 2016), corresponding with my acute PCP *in vitro* findings. This is in contrast with *in vivo* data that showed acute application

of MK-801, and with ketamine (which was not studied in this thesis), increased ongoing hippocampal gamma oscillations in rats (Hakami et al., 2009).

The data presented in this thesis, to my knowledge, is the first study to compare the effects of several NMDA receptor antagonists on *in vitro* CA3 KA-evoked oscillations. While this thesis consistently demonstrated a lack of effect of NMDA receptor blockade on CA3 gamma oscillations, discrepancies in findings from other studies complicate drawing conclusions about the relevance of CA3 gamma oscillations as a pathological model for NMDA receptor hypofunction.

Schizophrenia is disorder specific to humans, and the higher cognitive functions implicated in schizophrenia, such as delusions and disorganised thought, are also specific to the human experience. Surgical treatment of brain tumours, and refractory epilepsies, offers a unique opportunity to collect a sample of non-pathological tissue and study the human brain *in vitro*. Therefore, to compare my rodent slice model, I evoked oscillations in human cortical tissue using KA. Human tissue was of limited availability and variable quality therefore only one sample, resected from the temporal cortex, is included in this thesis. Developmental dysfunction of inhibitory cortical circuits is a key factor in the cognitive deficits seen in schizophrenia (Lewis, 2014). In the human temporal cortex, PV+ and SST+ are the two main classes of inhibitory interneurons, with PV+ cell counts exceeding SST+ by over 10-fold in control tissue (Waller et al., 2020).

Various brain oscillations can be replicated *in vitro* by altering the composition of ACSF and using different reagents (see de la Prida and Huberfeld (2019) for review). Previously, beta frequency and theta-coupled gamma frequency bursts have been evoked using KA and KA + carbachol, in human neocortical tissue (Florez et al., 2015). In comparison, this thesis showed that KA alone evoked a stable persistent beta frequency oscillation, with a peak frequency of 23.5 Hz. The peak frequency recorded in the human cortical tissue was slower than the mean peak frequency of the KA-evoked ACC beta oscillations of 26.3 Hz. The area power was also lower than the average area power recorded from the rat ACC but, as this was just one slice from one case, no solid conclusions can be drawn about the size and frequency of human cortical oscillations compared to rat tissue. However, the oscillation was very stable,

allowing the recording of a stable baseline period and subsequent pharmacological manipulation.

Once stable, PCP induced a large increase in oscillation power, comparable to the effect seen in the rat ACC. To my knowledge, this is a novel finding and NMDA receptor antagonists have not been applied to human cortical tissue oscillations previously. The similarity of the human cortical tissue to my findings in the rat ACC is an interesting finding and needs to be explored further.

3.5 Conclusions

This chapter demonstrated distinct differences in the oscillatory behaviour of the ACC and CA3 regions of the rat brain, consistent with previous studies. In the ACC, PCP application resulted in a dramatic increase in beta oscillation power, accompanied by a shift from gamma frequency oscillations to beta, an effect not observed with other NMDA receptor antagonists such as MK-801 and DAP5. These findings highlight unique receptor target effects of PCP, opening potential avenues to explore its underlying mechanisms of action. In contrast, the CA3 region displayed robust KA-induced gamma oscillations that remained unaffected by PCP or NMDA receptor blockade, further emphasising the functional distinctions between these regions. Additionally, KA-evoked beta oscillations in human cortical tissue mirrored findings in the rat ACC, suggesting it may serve as a promising acute model system, though challenges with tissue availability and reproducibility need to be addressed in future studies.

Chapter 4. Alleviating the effects of phencyclidine-induced NMDA-receptor hypofunction by metabotropic glutamate 2 receptor modulation

4.1 Introduction

mGlu receptors, particularly of Group II, have long been to the focus of potential therapeutic targets for schizophrenia. Group II mGlu receptors include mGlu2 and mGlu3. In general, mGlu receptors have been identified as possible treatments for neurological and psychiatric diseases (Niswender and Conn, 2010). More specifically, Group II mGlu receptors are heavily expressed in the PFC and levels are reported to be altered in patients with schizophrenia (Ghose et al., 2008, Gonzalez-Maeso et al., 2008). Additionally, a number of studies have provided evidence that activation of mGlu2/3 receptors, and in particular the mGlu2 subtype, is effective in models of schizophrenia where glutamatergic signalling is disrupted (Morrow et al., 2012, Vinson and Conn, 2012). Phase II clinical studies with an oral prodrug of the orthosteric agonist LY404039 suggested statistically significant improvements in positive and negative symptoms of schizophrenia (Patil et al., 2007). Therefore, restoration of normal glutamatergic signalling via activation of mGlu receptors may be a possible mechanism through which the symptoms of schizophrenia could be treated.

The group II mGlu receptors, mGlu2 and mGlu3, are present throughout the brain, and are highly expressed in the rat ACC and hippocampus (Gu et al., 2008). Group II mGlu receptors are often expressed presynaptically and mGlu2/3 receptor activation can inhibit glutamate release, a potential mechanism through which excess glutamatergic tone in schizophrenia patients could be reduced (Marek et al., 2000, Schoepp et al., 1999). Human (Krystal et al., 2005) and animal (Engel et al., 2016, Tyszkiewicz et al., 2004) studies demonstrate that mGlu2/3 receptor activation modulates NMDA receptor activity. mGlu2/3 receptor agonists reduce working memory deficits in PCP (Moghaddam and Adams, 1998) and neurodevelopmental (Xing et al., 2018) rodent models of schizophrenia. Specifically, a novel mGlu2 receptor agonist / mGlu3 receptor antagonist, LY395756, rescues NMDA receptor expression and reverses working memory deficits in a neurodevelopmental rodent model of schizophrenia (Li et al., 2017). This therefore makes Group II mGlu receptors, and specifically mGlu2 receptors, a promising target for new drug development. Indeed, clinical trials have provided some evidence that this approach may be of use (Witkin et al., 2022).

In the last decade, several selective mGlu2 agonists and PAMs have become available, and studies using these compounds suggest it is the mGlu2 receptor that modulates cognition. Preclinically, an mGlu2 receptor PAM, SAR218645, improves cognitive deficits in an MK-801 model of schizophrenia, as well as reversing working memory impairments in an NMDA - GluN1 knockout mouse model of the disease (Griebel et al., 2016). LY395756, an mGlu2 receptor agonist and mGlu3 receptor antagonist (Dominguez et al., 2005), also effectively reverses NMDA receptor impairments and cognitive deficits in a MAM rat model of schizophrenia (Li et al., 2017). LY541850 is another orthosteric selective mGlu2 receptor agonist and mGlu3 receptor antagonist, shown to be effective in reducing PCP-induced locomotor activity (Hanna et al., 2013).

Given that mGlu2 receptors appear to modulate both cognitive, positive, and negative symptoms in a range of models of schizophrenia, I used brain slice electrophysiology to investigate the role of mGlu2/3 receptor modulation in rodent ACC beta and gamma frequency oscillations. To understand the role of mGlu2/3 receptors, the Group II mGlu receptor ligands LY354740, an orthosteric agonist of receptors mGlu2 and mGlu3, and a novel mGlu2 receptor agonist / mGlu3 receptor antagonist, LY541850 were used. This study also investigated whether mGlu2/3 receptors could be used to rescue oscillatory changes evoked by acute PCP application, as outlined above in chapter 3.

4.2 Aims

- Assess whether group II mGlu receptors can modulate ACC beta and gamma frequency oscillations.
- Target mGlu2 specifically to explore the differential effects of the group II mGlu receptor subtypes on NMDA receptor modulation.
- Evaluate the acute PCP slice model described in chapter 3 using a clinically significant receptor target, mGlu2.

4.3 Methods

4.3.1 Animals

Acute rodent brain tissue slices were prepared from wild-type, male Lister Hooded rats (7 – 10 weeks) as described in Chapter 2.2. Animals were anaesthetised with inhaled isoflurane prior to injection (i.m.) of ketamine (100 mg/kg) and xylazine (10 mg/kg). Animals were intracardially perfused with 60 ml of sucrose-modified ACSF, and the brain was removed and placed in ice-cold sucrose-modified ACSF.

4.3.2 ACC slice recordings

Following removal of the brain, the whole brain was cut in half coronally to isolate the anterior half of the brain and mounted on a vibrating microtome stage. Coronal tissue slices (450 µm) were cut, and ACC slices were trimmed and transferred to a holding chamber at room temperature for approximately 1 hour before being placed in the recording interface chamber where they were perfused with oxygenated ACC ACSF and maintained at 30 – 32°C. After 30 minutes, glass field electrodes were inserted into the layer 5 of the ACC, and KA (800 nM) was bath applied via the circulating ACSF.

4.3.3 Data analysis of beta and gamma frequency activity

Oscillations were evoked using the glutamatergic agonist KA and field oscillations were recorded. Power spectral density analysis was performed on recorded data using Axograph and Spike2's Fast Fourier Transform algorithms. Using power spectra analysis of 60 second epochs, the peak frequency (Hz) and the area under the curve (area power; $\mu V^2/Hz$) were measured. To analyse ACC beta frequency oscillations, peak frequency and area power were measured between 15 – 32.9. To analyse ACC gamma frequency oscillations, peak frequency and area power were measured between 33 – 80 Hz.

KA-evoked network oscillations were considered stable when peak frequency and area power measurements varied no more than 10 % over a 20 minute 'control' period, where 60 second epochs were measured at 10 minute intervals. Once

oscillations were stable, other pharmacological compounds were applied. As multiple tissue slices could be obtained from each animal, two values (n / N) are presented below to represent slice (n) and animal (N) numbers, respectively. For statistical analysis, 60 second epochs were analysed at 10 minute intervals. Due to large variance in baseline area power measurements, percentage change from the control mean (% control) was calculated and analysed.

4.3.4 Pharmacological compounds

All pharmacological compounds were bath-applied to circulating ACSF. KA was applied 30 minutes after slices were placed in the recording chamber, to induce and maintain oscillations, and was present throughout the experiment (3 – 5 hours). Details of group II mGlu receptor compounds are below (Table 4.1), and compound applications are described in the results. When applicable, PCP (10 µM) was applied for 2 hours once oscillations had stabilised.

Table 4.1 The group II mGlu receptor compounds used. All names, biological actions, manufacturers (and product code), and final concentrations used, of compounds used in electrophysiology experiments.

Compound name	Action	Manufacturer (product code)	Final concentration
LY341495	Selective group II mGlu antagonist	Tocris (1209)	300 nM
LY354740	Selective group II mGlu agonist	Tocris (3246)	100 nM / 3 µM
LY541850	Selective orthosteric mGlu2 agonist; mGlu3 antagonist	Eli-Lilly (gifted)	1 µM

4.4 Results

4.4.1 ACC beta and gamma frequency oscillations are modulated by the mGlu2/3 receptor agonist LY354740 in a concentration-dependant manner

The group II mGlu receptor orthosteric agonist LY354740 has been used both *in vivo* (Copeland et al., 2017, Copeland et al., 2022, Zheng et al., 2020) and *in vitro* (Copeland et al., 2017, Copeland et al., 2022, Menezes et al., 2013) to study mGlu2/3 receptor function in the CNS. LY354740 was bath-applied to stable KA-evoked oscillations for 1 hour at either low (100 nM) or high (3 µM) concentration, followed by a 1 hour wash period (Figure 4.1).

Firstly, the effects of LY354740 on beta frequency (15 – 32.9 Hz) oscillations were assessed. When applied at a low concentration for 1 hour, LY354740 (100 nM) caused a small but non-significant decrease in mean beta area power in the first 20 - 30 minutes of application, beta area power then stabilised from 30 - 60 minutes (Figure 4.1ai). After 60 minutes of LY354740 (100 nM) application, there was no significant change in beta area power from control (100.6 ± 1.32 % to 83.5 ± 8.33 %; paired *t* test $p = 0.055$; Figure 4.1aii). Peak frequency of the beta oscillation also was not affected (25.8 ± 0.8 Hz to 24.1 ± 1.1 Hz; paired *t* test; $p = 0.068$; Figure 4.1c). When applied at a high concentration, LY354740 (3 µM) rapidly reduced beta frequency oscillation power after 10 minutes application (Figure 4.1bi). Mean beta area power significantly decreased from 102.8 ± 1.56 % to 50.6 ± 4.56 % after 60 minutes of LY354740 (3 µM) (paired *t* test; $p = 0.0001$; Figure 4.1bii). However, mean peak beta frequency was not affected by LY354740 (3 µM) application (paired *t* test; $p = 0.403$; Figure 4.1d).

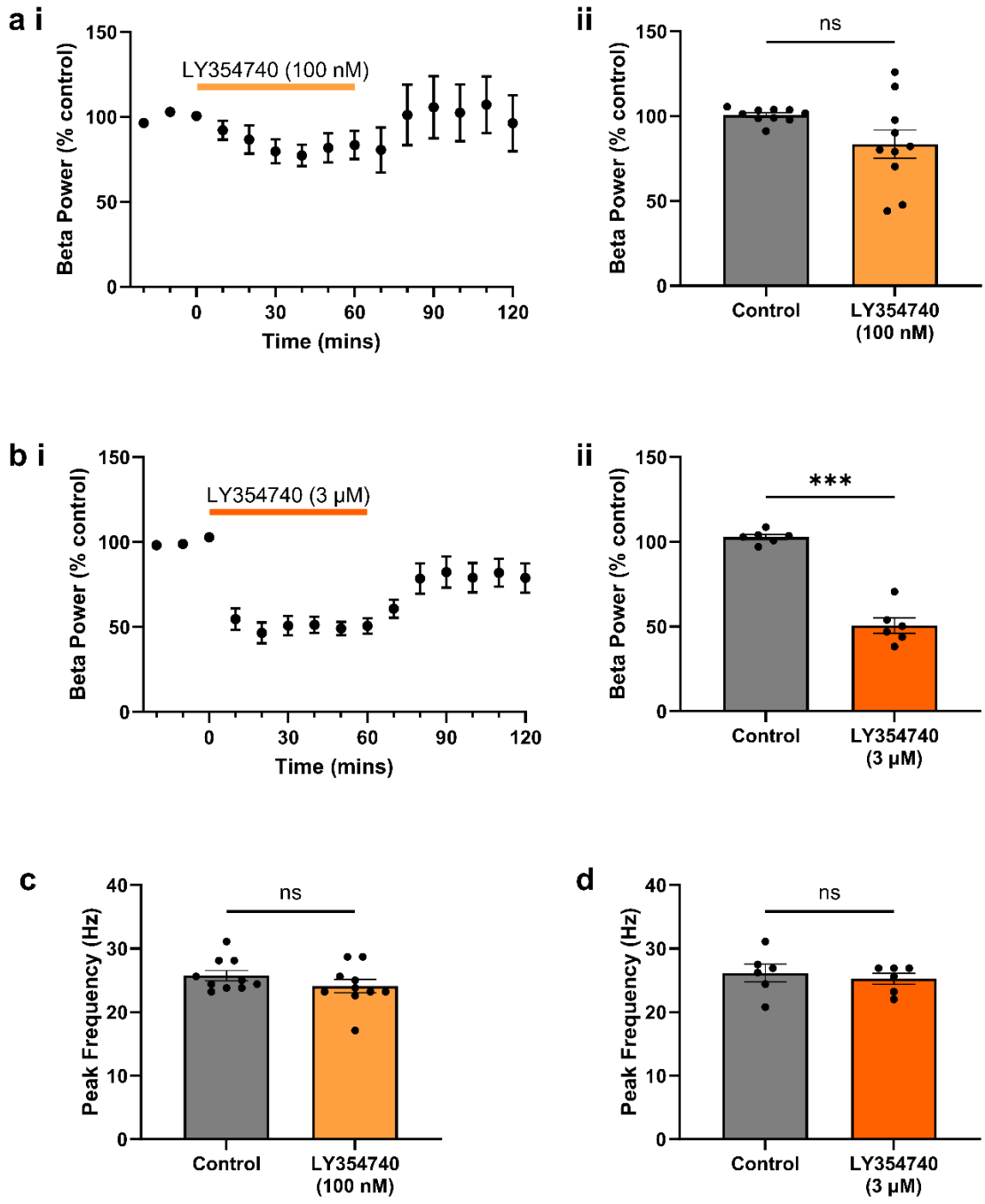

Figure 4.1 Effects of the Group II agonist LY354740 on beta frequency oscillations. (a) Effects of 60 minutes LY35740 (100 nM) on beta frequency oscillations. (i) Time-course of mean (± SEM) beta power (% control); horizontal orange bar represents duration of LY354740 application. (ii) Mean (± SEM) beta power (% control) after 60 minutes LY354740 application compared to control. (b) Effects of 60 minutes LY35740 (3 µM) on beta frequency oscillations. (i) Time-course of mean (± SEM) beta power (% control); horizontal orange bar represents duration of

LY354740 application. (ii) Mean (± SEM) beta power (% control) after 60 minutes LY354740 application compared to control. Mean ± SEM peak beta frequency (18 - 33 Hz) after 60 minutes LY354740 application at (c) 100nM and (d) 3 µM, compared to control. Total slices / animals (n / N) = 6-10 / 4-7.

In contrast when low concentration LY354740 (100 nM) was applied to gamma frequency (33 – 80 Hz) oscillations, the area power was significantly decreased in magnitude and stabilised over 60 minutes (Figure 4.2ai), from 101.8 ± 0.86 % to 74.9 ± 5.32 % (paired *t* test; *p* = 0.009; Figure 4.2aii). Peak gamma frequency was not affected (paired *t* test; *p* = 0.054; Figure 4.2c). When applied at a high concentration, LY354740 (3 µM) rapidly reduced gamma frequency oscillation power after 10 minutes application (Figure 4.2bi). Interestingly, mean gamma area power greatly decreased from 100.8 ± 2.32 % at control to 36.0 ± 11.1% by the high concentration of LY354740 (3 µM) (paired *t* test; *p* = 0.001; Figure 4.2bii). As the oscillation was severely disrupted, there was a large decrease in area power, so it was not possible to detect a true frequency peak in the power spectra which was therefore not quantified (Figure 4.2d).

These data therefore show that activating mGlu2/3 receptors, using LY354740 reduces beta and gamma frequency power in a concentration-dependent manner. Furthermore, there is a greater effect of LY354740 on ACC gamma power than beta power.

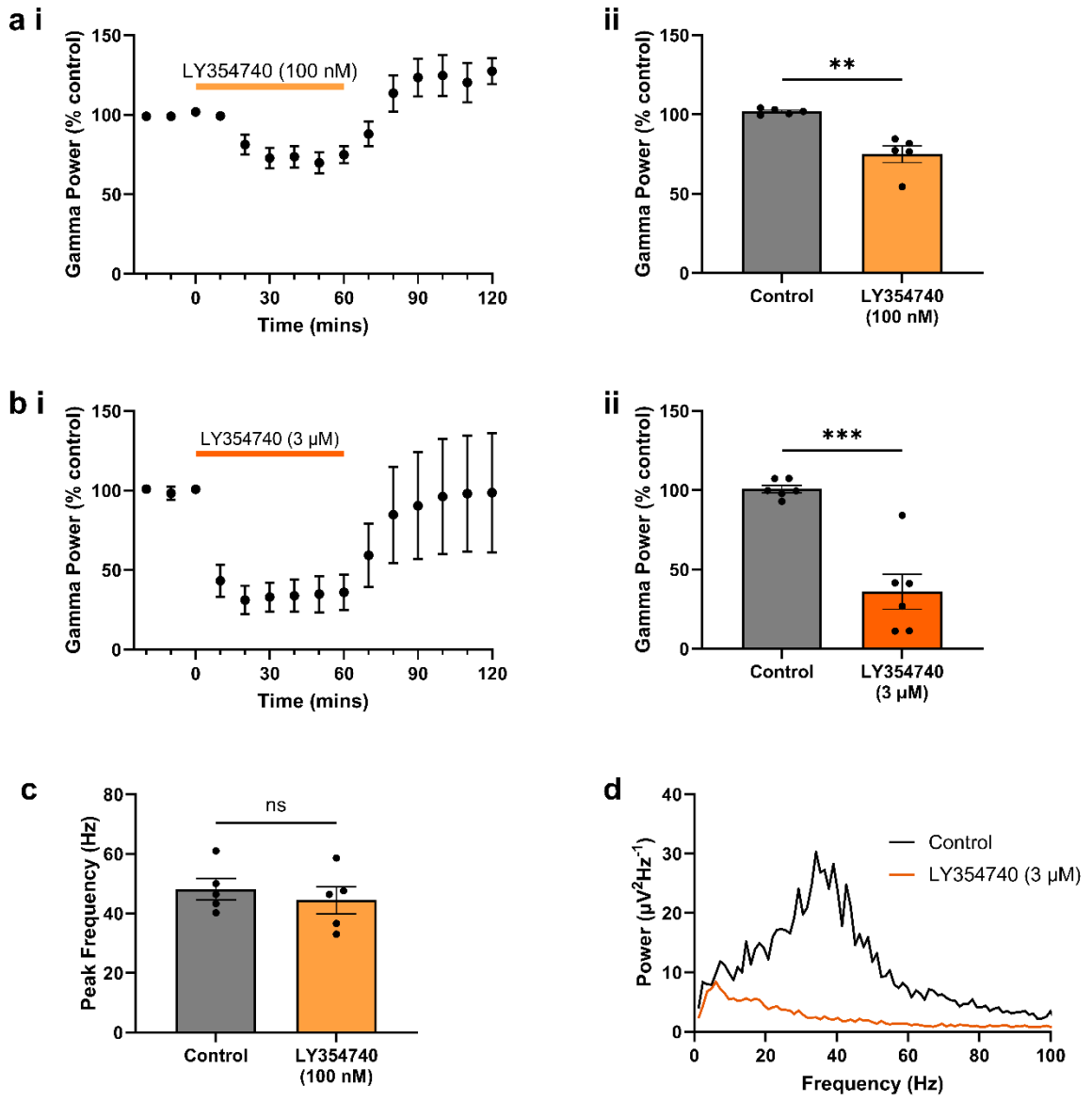

Figure 4.2 Effects of the Group II agonist LY354740 on gamma frequency oscillations. (a) Effects of 60 minutes LY35740 (100 nM) on gamma frequency oscillations. (i) Time-course of mean (± SEM) gamma power (% control); horizontal orange bar represents duration of LY354740 application. (ii) Mean (± SEM) gamma power (% control) after 60 minutes LY354740 application compared to control. (b) Effects of 60 minutes LY35740 (3 µM) on gamma frequency oscillations. (i) Time-course of mean (± SEM) gamma power (% control); horizontal orange bar represents duration of LY354740 application. (ii) Mean (± SEM) gamma power (% control) after 60 minutes LY354740 application compared to control. (c) Mean ± SEM peak gamma frequency (18 - 33 Hz) after 60 minutes LY354740 (100 nM) application compared to control. (d) Representative power spectra from a single experiment showing gamma

frequency oscillations before and following 60 minutes application of high concentration LY354740 (3 µM): LY354740 disrupted oscillations so that no peak-frequency could be measured. Total slices / animals (*n* / *N*) = 5-6 / 4-5.

4.4.2 The Group II mGlu receptor antagonist LY341495 occludes mGlu2/3 receptor activation in the rat ACC

The group II mGlu receptor orthosteric antagonist LY341495 is selective for mGlu2/3 receptors, exerting its effects at nanomolar concentrations (Kingston et al., 1998, Turner and Salt, 2003). To confirm that the effects of LY354740 outlined above (section 4.4.1) were indeed mediated by mGlu2/3 receptors, LY341495 (300 nM) was applied to slices exhibiting stable beta and gamma oscillations for 20 minutes, before co-application of LY354740 (100 nM) for a further 60 minutes in the continued presence of LY341495 (Figure 4.3a).

A RM One-way ANOVA test was performed to compare the effect of LY341495 on LY354740 application on beta power (% control) and peak frequency (Hz). There was no significant effect of compound application on beta power ($F(1.384, 13.84) = 0.1146$, $p = 0.819$; Figure 4.3bi). There was also no significant effect of compound application on beta oscillation peak frequency ($F(1.401, 14.01) = 0.077$, $p = 0.863$; Figure 4.3bii).

A RM One-way ANOVA test was performed to compare the effect of LY341495 on LY354740 application on gamma power (% control) and peak frequency (Hz). There was no significant effect of compound application on gamma power ($F(1.198, 10.78) = 0.1219$, $p = 0.778$; Figure 4.3ci). There was also no significant effect of compound application on gamma oscillation peak frequency $F(1.059, 9.530) = 2.136$, $p = 0.176$; Figure 4.3cii).

These data show that LY341495 robustly blocks the effect of LY354740 on both beta and gamma oscillation power, and the effect LY354740 is via mGlu2/3 receptors.

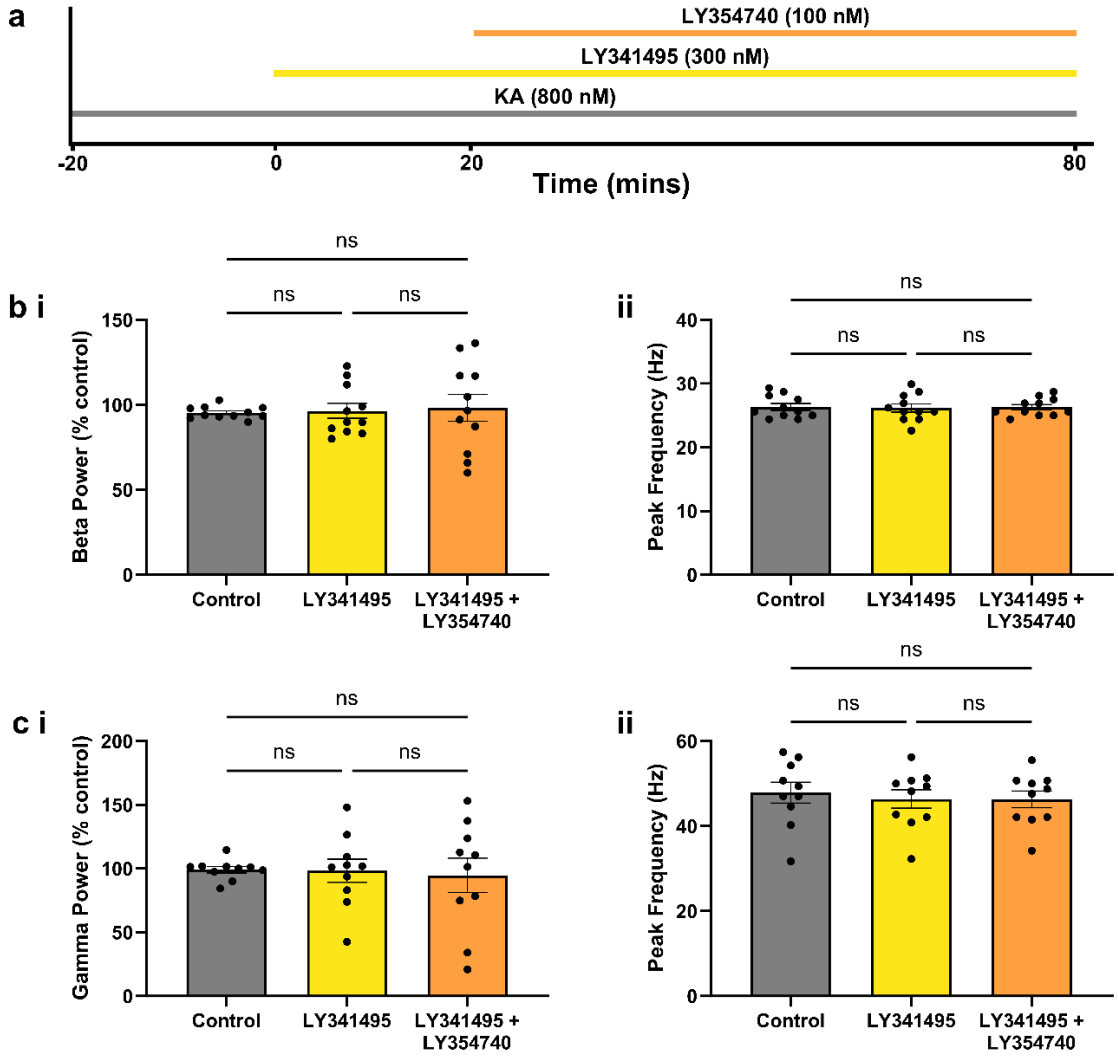

Figure 4.3 The mGlu2/3 receptor antagonist LY341495 blocks the mGlu2/3 receptor agonist LY354740-induced reduction in KA-evoked beta and gamma oscillations in rat ACC slices. (a) Schematic of experimental protocol: LY341495 (300 nM) was applied to stable KA-evoked beta / gamma oscillations for 20 minutes, and LY354740 (100 nM) was co-applied for a futher 60 minutes. (b) Effect of LY341495 and LY354740 application on ACC beta oscillation mean (±SEM) (i) beta power (% control) and (ii) peak frequency (Hz). (c) Effect of LY341495 and LY354740 application on ACC gamma oscillation mean (±SEM) (i) gamma power (% control) and (ii) peak frequency (Hz). Total slices / animals (*n* / *N*) = 10-11 / 5.

4.4.3 Selectively activating the mGlu2 receptor modulates beta and gamma oscillatory power without disrupting oscillation frequency

To explore mGlu2 receptor effects more specifically, LY541850 (1 μM), an orthosteric selective mGlu2 receptor agonist and mGlu3 receptor antagonist, was bath applied to slices exhibiting stable beta and gamma oscillations for 1 hour, followed by a 1 hour wash. LY541850 significantly reduced median beta area power from 101.0 (IQR 95.7 – 104.7) % to 58.1 (IQR 42.1 – 71.2) % (Wilcoxon matched-pairs; test p = 0.003; Figure 4.4ai) without significantly changing oscillation mean peak frequency (paired t test; p = 0.463; Figure 4.4aii).

LY541850 had an even greater effect on gamma frequency oscillations, reducing median area power from 97.5 (IQR 95.6 – 102.2) % at control to 33.2 (IQR 26.1 – 44.5) % (Wilcoxon matched-pairs test; p = 0.016; Figure 4.4bi), whilst still having no significant impact on oscillatory frequency (paired t test; p = 0.742; Figure 4.4bii). These data showed that selectively activating mGlu2 receptors, using LY541850, effectively reduced beta and gamma power, without affecting oscillation frequency.

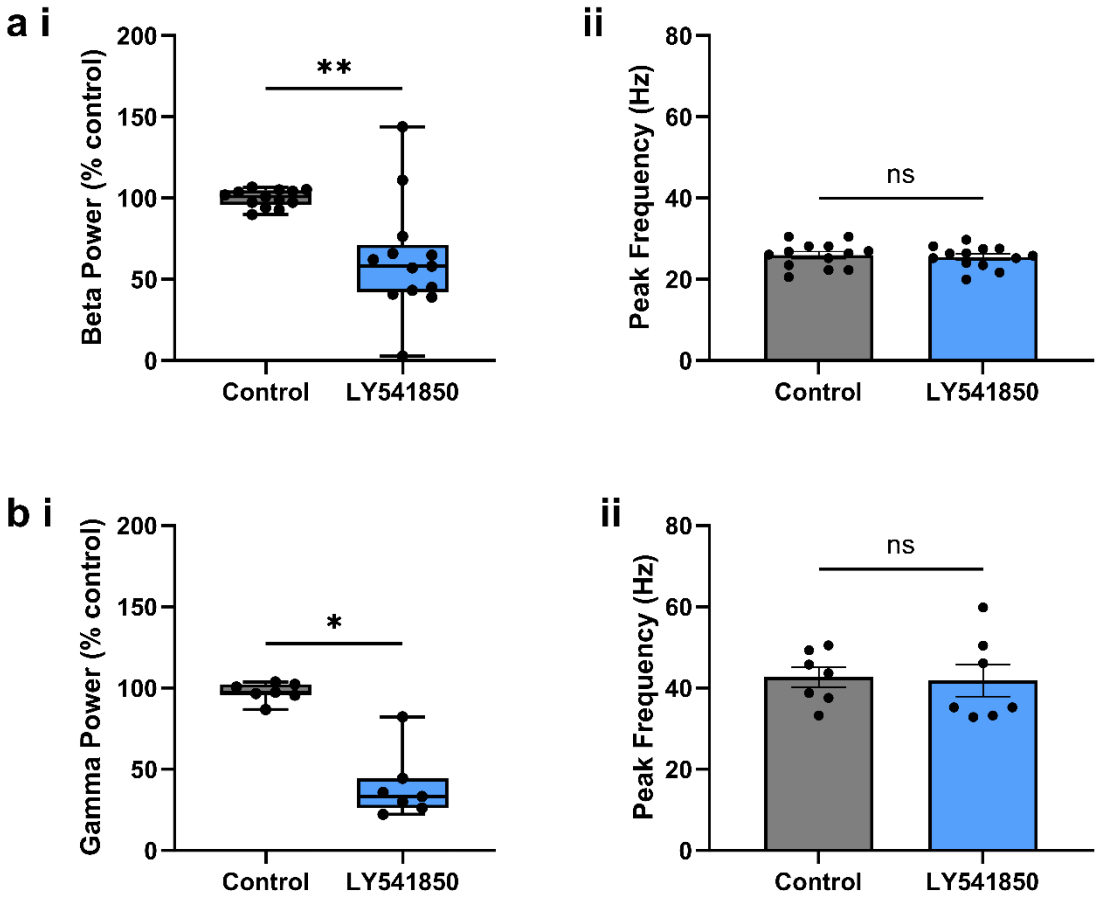

Figure 4.4 The mGlu2 receptor agonist / mGlu3 receptor antagonist LY541850 reduces KA-evoked beta and gamma power in rat ACC slices. (a) Effect of LY541850 (1 µM) on beta oscillation (i) beta power (% control) and (ii) peak frequency (Hz), following 60 minutes application. (b) Effect of LY541850 (1 µM) on gamma oscillation (i) gamma power (% control) and (ii) peak frequency (Hz), following 60 minutes application. Total slices / animals (*n* / *N*) = 7 / 6.

4.4.4 Selectively activating mGlu2 receptors reverses large beta oscillations induced by PCP

As seen in chapter 3, PCP induced an aberrantly large increase in beta frequency oscillations in ACC slices over a 60 minute application (Figure 3.3). To characterise how PCP modulates beta oscillations over a longer application period, PCP was continuously applied for 120 minutes to slices oscillating at a stable beta frequency (Figure 4.5).

A Friedman test was performed to compare the effect of 60- and 120-minutes PCP application on median beta power (% control). There was a significant effect of PCP application on beta power ($X^2 = 14.0$, $p < 0.001$; Figure 5.4aii). Median beta area power significantly increased after 60 minutes application from 99.3 (IQR 97.4 – 103.7) % to 353.2 (IQR 281.9 – 456.5) % ($p = 0.0012$; Dunn's multiple comparisons test). Median beta area power stabilised from 60 to 120 minutes, at 346.8 (IQR 227.3 – 489.9) % and was not significantly different from 60 minutes PCP application ($p > 0.999$; Dunn's multiple comparisons test).

A RM One-way ANOVA test was performed to compare the effect of 60- and 120-minutes PCP application on peak frequency. There was a significant effect of PCP application on peak frequency ($F (1.274, 10.20) = 18.64$, $p < 0.001$; Figure 4.5b). Mean beta frequency was significantly reduced from 26.3 (± 0.957) Hz to 24.1 (± 1.49) Hz after 60 minutes PCP application ($p = 0.036$; Tukey's multiple comparisons test), and further reduced to 23.0 (± 1.23) Hz after 120 minutes PCP application ($p = 0.029$; Tukey's multiple comparisons test).

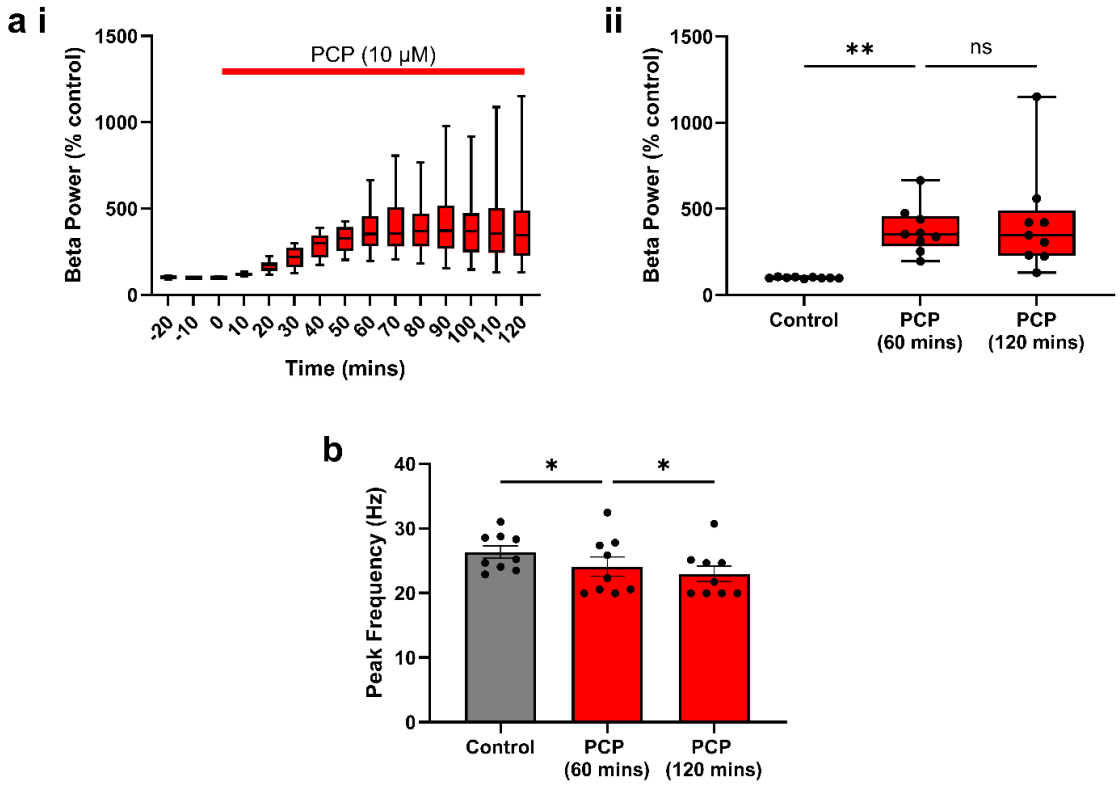

Figure 4.5 KA-evoked beta oscillations stabilise following acute PCP application, in rat ACC slices. (a) Effect of 120 minutes PCP application on beta power (% control), shown as (i) time-course plot medians (IQR) where PCP was applied for duration of red bar and (ii) compared to control median (IQR) at 60 and 120 minutes. (b) Effect of 60 and 120 minutes PCP application on beta oscillation peak frequency (Hz), compared to control. Total slices / animals (*n* / *N*) = 9 / 5.

Using the PCP 120 minute application as an NMDA receptor hypofunction model of the aberrant oscillations associated with schizophrenia, the mGlu2/3 agonist LY354740 and mGlu2 agonist / mGlu3 antagonist LY541850 were applied after 60 minutes. Area power and peak frequency were measured to assess whether these compounds were able to reverse the PCP-induced increase in beta oscillations.

A Friedman test was performed to compare the effect of low (100 nM) concentration LY354740 on PCP application on median beta power (% control; Figure 4.6). There was a significant effect of compound application on beta power ($X^2 = 7.143$, $p = 0.027$; Figure 4.6aii). Bath-application of LY354740 at 100 nM did not have a significant effect on the PCP-induced increase in median beta area power, as median area power decreased slightly from 300.0 (IQR 178.4 – 349.8) % in PCP to 278.6 (IQR 93.6 – 341.4) % with the low concentration LY354740 application ($p = 0.544$; Dunn's multiple comparisons test).

A RM One-way ANOVA test was performed to compare the effect of LY354740 at 100 nM on PCP application on peak frequency. There was a significant effect of compound application on peak frequency ($F (1.143, 6.861) = 14.23$, $p = 0.006$; Figure 4.6b). Peak frequency significantly decreased from control 26.5 (± 1.3) Hz to PCP 23.9 (± 0.57) Hz ($p = 0.023$; Tukey's multiple comparisons test). Low concentration of LY354740 had no significant effect on the mean beta frequency when applied with PCP ($p = 0.073$; Tukey's multiple comparisons test).

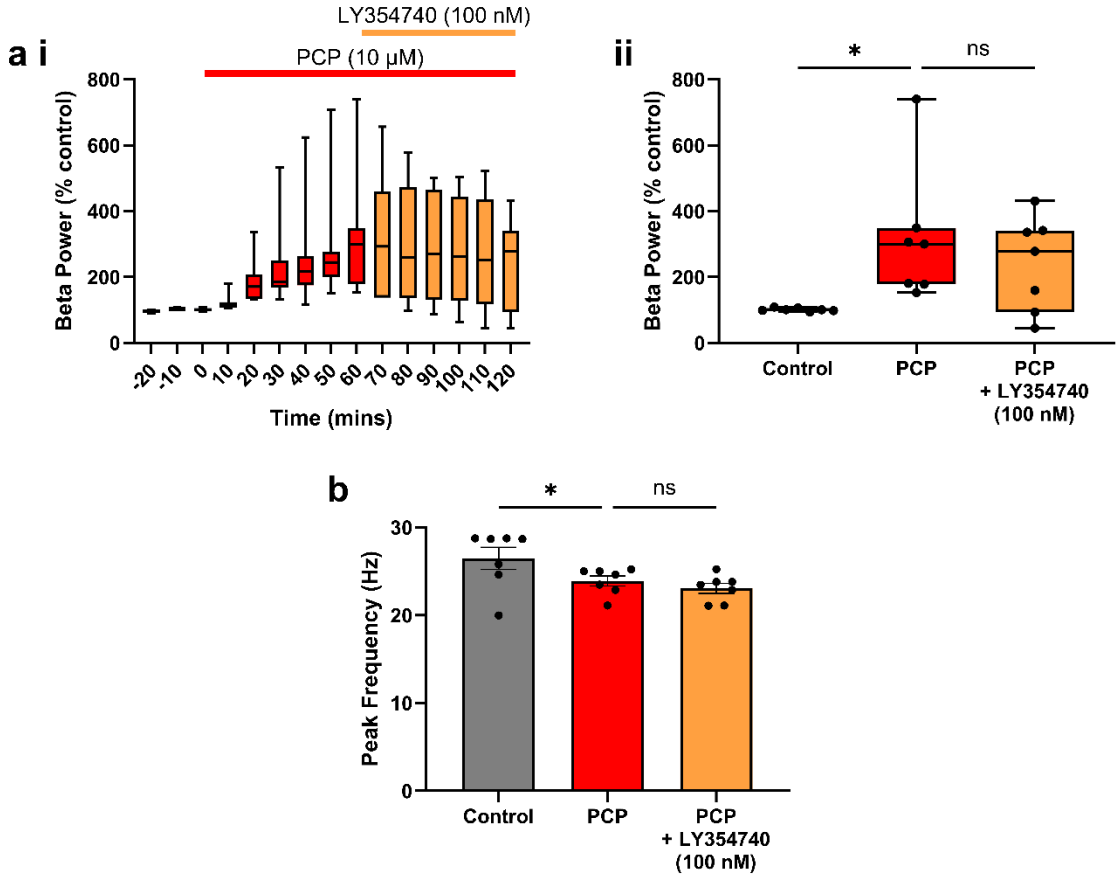

Figure 4.6 mGlu2/3 receptor agonist LY354740 at low concentration has no effect on PCP-induced increase in KA-evoked beta oscillations, in rat ACC slices. (a) Effect of PCP (10 µM) and LY354740 (100 nM) application on beta power (% control), shown as (i) time-course plot medians (IQR) where PCP and LY354740 were applied for duration of red and yellow bar, respectively, and (ii) compared to control median (IQR) at 60 and 120 minutes. (b) Effect of PCP (10 µM) and LY354740 (100 nM) application on beta oscillation peak frequency (Hz), compared to control. Total slices / animals (*n* / *N*) = 7 / 3.

A Friedman test was performed to compare the effect of high (3 µM) concentration LY354740 on PCP application on median beta power (% control; Figure 4.7). There was a significant effect of compound application on beta power ($X^2 = 11.14$, $p = 0.0012$; Figure 4.7bii). Applying LY354740 at the higher concentration of 3 µM significantly reduced median beta oscillation area power from 413.2 (IQR 221.8 – 531.9) % in PCP to 176.7 (IQR 77.8 – 267.7) % ($p = 0.049$; Dunn's multiple comparisons test).

A RM One-way ANOVA test was performed to compare the effect of LY354740 at 3 µM on PCP application on peak frequency. There was no significant effect of compound application on peak frequency ($F (1.062, 6.370) = 1.548$, $p = 0.260$; Figure 4.7c).

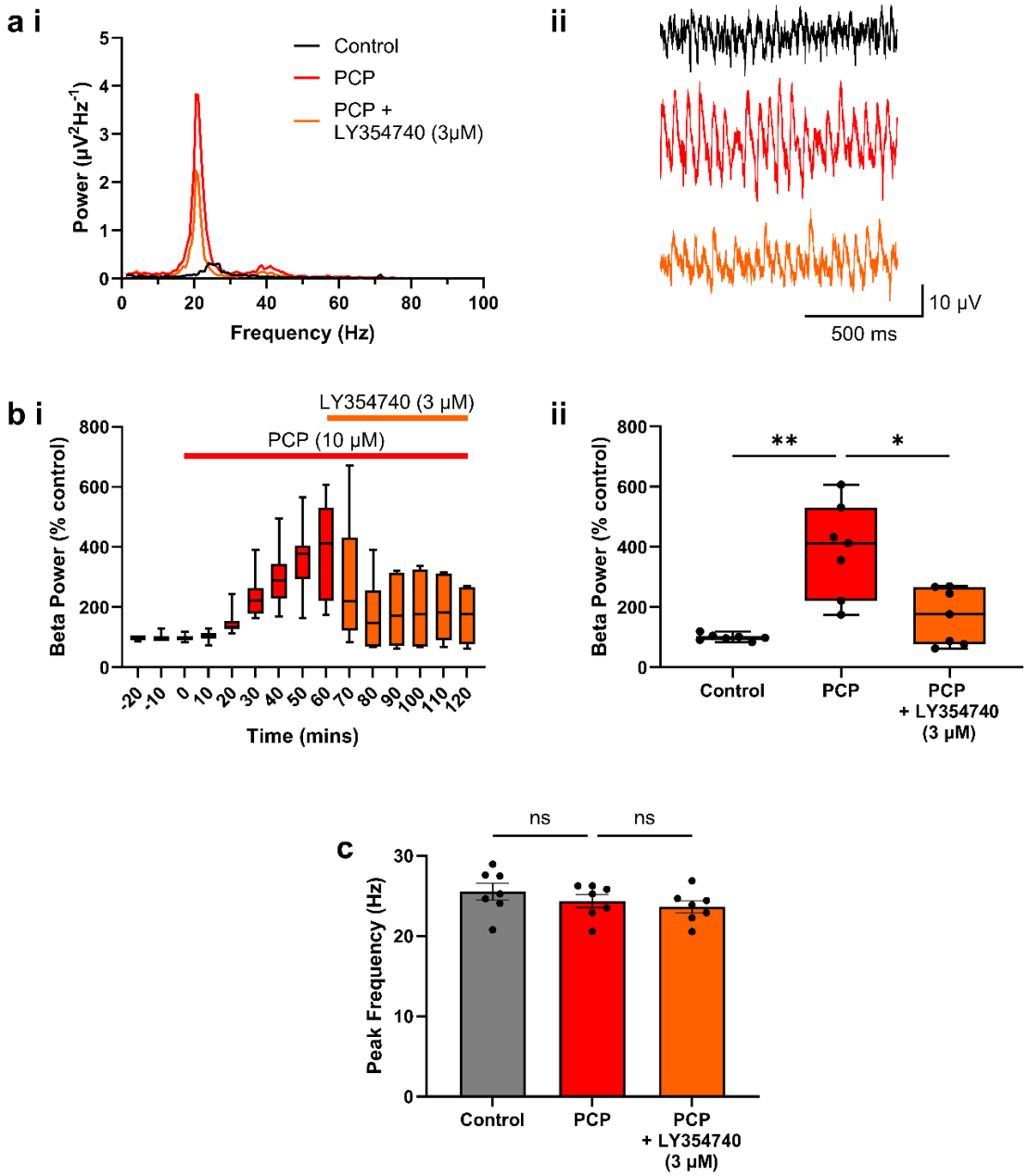

Figure 4.7 mGlu2/3 receptor agonist LY354740 reduces PCP-induced increase in KA-evoked beta oscillations, at high concentrations, in rat ACC slices. (a) Representative power spectra (i) and LFP traces (ii) of ACC beta frequency oscillation in control (black), after 60 minutes PCP (10 μM) application (red), and further 60 minutes LY354740 (3 μM) co-application (orange). (b) Effect of PCP (10 μM) and LY354740 (3 μM) application on beta power (% control), shown as (i) time-course plot medians (IQR) where PCP and LY354740 were applied for duration of red and yellow bar, respectively, and (ii) compared to control median (IQR) at 60 and 120 minutes. (c) Effect of PCP (10 μM) and LY354740 (3 μM) application on beta oscillation peak frequency (Hz), compared to control. Total slices / animals (*n* / *N*) = 7 / 3.

LY541850 (1 µM), the mGlu2 receptor agonist and mGlu3 receptor antagonist, was also applied to slices exhibiting PCP-enhanced beta oscillations to investigate whether activation of mGlu2 receptors alone is enough to counter the large increase in beta power caused by PCP (Figure 4.8).

A Friedman test was performed to compare the effect of LY541850 on PCP application on median beta power (% control; Figure 4.8b). There was a significant effect of compound application on beta power ($X^2 = 22.17$, $p < 0.0001$; Figure 4.8bii). After 60 minutes of PCP application, there was a large increase in median beta area power from 100.6 (IQR 95.1 – 107.1) % to 277.2 (IQR 225.0 – 395.7) % (Dunn's multiple comparisons test $p < 0.0001$). LY541850 application for 60 minutes resulted in a significant decrease in median area power to 201.0 (IQR 151.1 – 235.7) % from PCP at 60 minutes (Dunn's multiple comparisons test; $p = 0.024$).

A RM One-way ANOVA test was performed to compare the effect of LY541850 on PCP application on peak frequency. There was a significant effect of compound application on peak frequency ($F (1.754, 19.29) = 33.89$, $p < 0.0001$; Figure 4.8c). Mean peak frequency significantly decreased from control 27.0 (± 0.45) Hz following PCP application to 24.3 (± 2.71) Hz (Tukey's multiple comparisons test; $p = 0.001$). Mean peak frequency significantly decreased further from PCP application after 60 minutes LY541850 application, to 22.6 (± 0.68) Hz (Tukey's multiple comparisons test; $p = 0.008$).

These data suggest that the large increase in beta area power in ACC slices induced by PCP can be modulated and reduced through activation of the mGlu2 receptor, independent of the mGlu3 receptor.

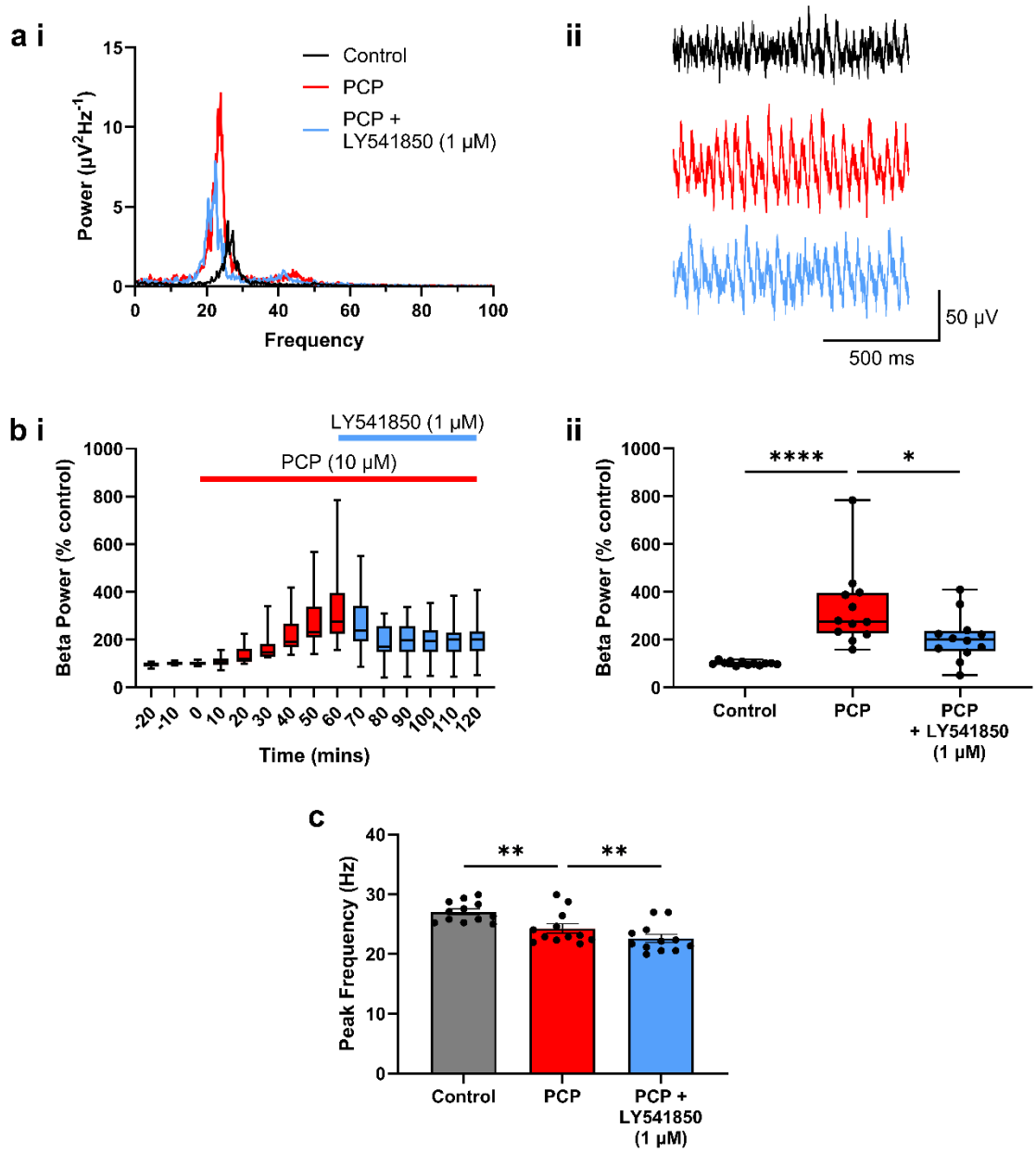

Figure 4.8 mGlu2 receptor agonist, LY541850, reduces PCP-induced increase in beta frequency oscillations. (a) Representative power spectra (i) and LFP traces (ii) of ACC beta frequency oscillation in control (black), after 60 minutes PCP (10 µM) application (red), and further 60 minutes LY541540 (1 µM) co-application (blue). (b) Effect of PCP (10 µM) and LY541540 (1 µM) application on beta power (% control), shown as (i) time-course plot medians (IQR) where PCP and LY541540 were applied for duration of red and yellow bar, respectively, and (ii) compared to control median (IQR) at 60 and 120 minutes. (c) Effect of PCP (10 µM) and LY541540 (1 µM) application on beta oscillation peak frequency (Hz), compared to control. Total slices / animals (*n* / *N*) = 12 / 7.

4.5 Discussion

Summary of the main findings in Chapter 4:

- ACC beta and gamma frequency oscillations can be modulated by activating group II mGlu receptors, specifically mGlu2.
- Aberrantly large beta oscillations, induced by PCP, can be normalised by activating mGlu2 receptors.
- We can target clinically significant receptors and study their effects using the acute PCP-NMDA receptor hypofunction model.

In chapter 3, we found that distinct beta (20 - 32Hz) and gamma (33 - 80 Hz) frequency oscillations can be evoked by bath application of KA (800 nM) in the rat ACC *in vitro*, as previously reported (Adams et al., 2017). In this chapter, we showed that both beta and gamma frequency oscillations are reduced by activation of Group II mGlu receptors using the mGlu2/3 receptor agonist LY354740 in a concentration-dependent manner. When investigating the effects of mGlu2 receptor activation specifically, using the novel mGlu2 agonist / mGlu3 antagonist LY541850 (1 µM), we found that both beta- and gamma frequency oscillations significantly reduced in power, again without disrupting oscillation frequency. These data demonstrate that both beta and gamma frequency oscillations in ACC can be modulated via mGlu2 activation alone.

In additional experiments we used acute application of PCP to an on-going, stable oscillation to model NMDA receptor hypofunction and assess the effects of Group II mGlu receptor modulation in this acute NMDA antagonist model. Subsequent assessment of the effects of mGlu receptor modulation on this large beta oscillation showed that the specific mGlu2 agonist / mGlu3 antagonist LY541850, significantly reduced the power of the beta frequency activity. Our data suggest that mGlu2 receptor activation could be a possible mechanism by which to modulate abnormal oscillatory activity caused by NMDA receptor hypofunction.

Here we showed that mGlu receptor modulation with the specific mGlu2 receptor agonist LY541850 was able to significantly reduce the power of the aberrant beta activity caused by PCP. LY354740 (10 $mgkg^{-1}$ intraperitoneal; i.p.) has been

shown to abolish PCP-induced efflux of glutamate in the prefrontal cortex and attenuated the effects of PCP on working memory and locomotor activity (Moghaddam and Adams, 1998), and a number of other studies have demonstrated efficacy of Group II mGlu receptor activation in models of schizophrenia (Morrow et al., 2012). In addition, there is evidence that aberrant oscillatory activity could be related to symptoms of schizophrenia, such as hallucinations, thought disorder and negative symptoms. Several studies have found that positive symptoms of schizophrenia are correlated with enhanced amplitude and phase-synchronization of evoked and induced beta- and gamma-band activity in circumscribed brain regions (Uhlhaas and Singer, 2010) and *in vivo* in rodents Group II mGlu receptor activation modulates NMDA receptor-induced changes in network activity (Hiyoshi et al., 2014a, Hiyoshi et al., 2014c). The data presented here suggest that Group II mGlu receptors may alleviate symptoms of schizophrenia by stabilising abnormal network activity.

4.6 Conclusions

Our results show that Group II mGlu receptors modulate network oscillations and point to a specific involvement of mGlu2 receptors. In addition, attenuation of the effect of PCP points to a mechanism by which mGlu2 receptors may stabilise aberrant network activity. These results underline the importance of Group II mGlu receptors, and particularly mGlu2, as targets for the treatment of neuropsychiatric and neurodegenerative diseases.

Chapter 5. The impact of σ1 receptor activation on interneuron dysfunction and neuroinflammation, in rat ACC and CA3, *in vitro*

5.1 Introduction

Rodent models have provided significant insight into the effects of PCP (Neill et al., 2010), particularly in relation to the ACC (Arime and Akiyama, 2017). The ACC is involved in higher cognitive processes (Kaneda and Osaka, 2008, Rolls, 2019, Teixeira et al., 2006) and is a key site of dysfunction in schizophrenia (Adams and David, 2007). Previous studies have demonstrated that subchronic PCP treatment disrupts learning and memory processes in rodents (Cadinu et al., 2018). One significant effect of subchronic PCP treatment in rodents is a reduction of PV expression (Abdul-Monim et al., 2007, McKibben et al., 2010, Reynolds and Neill, 2016). PV+ GABAergic interneurons are critical for regulating cortical network excitability and generating synchronous gamma oscillatory activity (Whittington et al., 1995, Womelsdorf et al., 2007). These interneurons are thought to be essential for cognitive functions such as attention and working memory (Lesh et al., 2011), processes that are often disrupted in schizophrenia (Ferguson and Gao, 2018, Hughes et al., 2024, Nuechterlein et al., 2004).

PV+ interneuron dysfunction has been consistently reported across multiple models of schizophrenia, including pharmacological and developmental models (Santos-Silva et al., 2023). Subchronic PCP administration reduces PV and GAD67 expression in the PFC (Amitai et al., 2012, Kaalund et al., 2013), as well as altering cortical oscillations and firing patterns (Kargieman et al., 2007). The reduction in PV+ expression suggests that NMDA receptor hypofunction induced by PCP disrupts the inhibitory control exerted by these interneurons, contributing to the cognitive deficits observed in animal models.

PCP has been shown to increase gamma oscillatory activity in both *in vivo* and *in vitro* studies (Hakami et al., 2009, Lemercier et al., 2017, Rebollo et al., 2018), and this thesis has shown that PCP disrupts both gamma and beta oscillations in the ACC, *in vitro* (Chapter 3.4.2 and 3.4.3). Together, this further supports the idea that NMDA receptor hypofunction impacts neuronal network dynamics.

While much research on schizophrenia focuses on PV+ interneurons, there is also evidence of changes in SST+ interneurons. Human studies show a reduction in hippocampal SST+ interneurons and decreased SST mRNA levels in the hippocampus, ACC, and dlPFC in schizophrenia patients (Fung et al., 2010,

Hashimoto et al., 2008, Konradi et al., 2011). Notably, SST reduction is more pronounced than other biomarkers, including PV (Alherz et al., 2017). Given that SST expression is activity-dependent (Hou and Yu, 2013), its reduction suggests potential loss of SST, or dysfunction of SST+ interneurons, though the pathology remains unclear. Rodent models using NMDA receptor antagonists replicate some schizophrenia-like pathologies, with subchronic MK-801 treatment leading to a decreased number of SST+ interneurons (Murueta-Goyena et al., 2020). SST knockdown in the rat mPFC causes cognitive deficits, mirroring similar effects seen with PV knockdown (Perez et al., 2019).

PNNs are extracellular matrix structures that surround specific neurons, including PV+ interneurons, playing a key role in maintaining their excitability (Wingert and Sorg, 2021) and supporting neuronal plasticity by regulating synaptic stability and excitability (Sorg et al., 2016). In both the hippocampus and ACC, PNNs are essential for memory consolidation and are involved in various forms of memory, including fear conditioning and spatial memory (Li et al., 2024b). The degradation of PNNs in the PFC and ACC impairs these memory processes (Shi et al., 2019), further contributing to the cognitive deficits observed in schizophrenia and in PCP-treated animals.

Beyond its effects on interneurons, PCP treatment also induces neuroinflammation in animal models (Li et al., 2024a), another key feature of schizophrenia pathology (Anderson et al., 2013). Subchronic PCP treatment has been shown to activate both astrocytes and microglia in the mouse cortex and hippocampus (Zhu et al., 2014), as indicated by increased expression of GFAP and Iba1, markers for reactive astrocytes and microglia, respectively. Glial activation is accompanied by elevated levels of pro-inflammatory cytokines which contribute to oxidative stress and neuronal damage. Oxidative stress can exacerbate the dysfunction of PV+ interneurons, specifically (Steullet et al., 2017).

σ1 receptors, located on the mitochondria-associated membrane of the ER, play a crucial role in modulating intracellular Ca^{2+} signalling and are involved in various neurotransmitter systems, including glutamatergic and dopaminergic pathways. Activation of σ1 receptors has been shown to have neuroprotective effects, particularly in the context of neuroinflammation and oxidative stress (Maurice et al., 2019, Mavlyutov et al., 2013, Mavlyutov et al., 2015).

σ1 receptors are expressed in both neurons and glial cells, and their activation can reduce oxidative stress and modulate inflammatory responses (Gekker et al., 2006, Jia et al., 2018). Agonists of σ1 receptors, such as fluvoxamine and donepezil, have been found to rescue cognitive impairments induced by subchronic PCP treatment in rodents (Hashimoto et al., 2007, Kunitachi et al., 2009), suggesting a potential therapeutic pathway for mitigating the cognitive deficits associated with NMDA receptor hypofunction.

Additionally, σ1 receptors have been implicated in the regulation of synaptic plasticity and LTP, which are critical for learning and memory processes. By interacting with NMDA receptors and other signalling pathways, σ1 receptors may help restore normal synaptic function and reduce the cognitive deficits caused by PCP (Martina et al., 2007, Pabba et al., 2014).

The interplay between NMDA receptor hypofunction, interneuron dysfunction, and neuroinflammation highlights the complex mechanisms underlying PCP-induced cognitive deficits. PV+ interneurons, PNNs, and glial cells all play crucial roles in maintaining neuronal circuit function and synaptic plasticity. The activation of σ1 receptors presents a common mechanism and promising avenue for neuroprotection, offering potential therapeutic strategies for mitigating the cognitive and neuroinflammatory effects of NMDA receptor hypofunction.

5.2 Aims

- Investigate the role of σ1 receptor activation in modulating neuronal oscillations in the ACC and CA3 to understand how σ1 receptor activation influences KA-evoked beta and gamma oscillations in the ACC and CA3.
- Assess the impact of σ1 receptor activation on PV and SST expression following PCP exposure to determine whether σ1 receptor activation alters the PV to SST expression ratio in ACC slices exposed to PCP.
- Explore the role of σ1 receptors in modulating microglial and astrocyte reactivity after NMDA antagonism to investigate the impact of σ1 receptor activation on microglial and astrocyte responses in ACC slices exposed to PCP.
- Elucidate how σ1 receptors influence neuronal oscillations, interneuron marker expression, and glial activity in the context of NMDA receptor antagonism.

5.3 Methods

5.3.1 Animals

Acute rodent brain tissue slices were prepared from wild-type, male Lister Hooded rats (7 – 10 weeks) as described in Chapter 2.2. Animals were anaesthetised with inhaled isoflurane prior to injection (i.m.) of ketamine (100 mg/kg) and xylazine (10 mg/kg). Animals were intracardially perfused with 60 ml of sucrose-modified ACSF (Table 2.2), and the brain was removed and placed in ice-cold sucrose-modified ACSF. Animals prepared for LTP recordings were anaesthetised with inhaled isoflurane prior to cervical dislocation and decapitation. The brain was then removed and submerged in ice-cold oxygenated hippocampal ACSF (Table 2.2).

5.3.2 *In vitro* electrophysiology – high frequency oscillations

5.3.2.1 ACC and hippocampus slice recordings

Following removal of the brain, ACC and hippocampus slices were prepared as described in chapter 3.3.2 - 3.3.3.

5.3.2.2 Data analysis of beta and gamma frequency activity

Oscillations were evoked using KA. Field oscillations were recorded, and power spectral density analysis was performed as described in chapter 3.3.5. As multiple tissue slices could be obtained from each animal, two values *(n / N)* are presented below to represent slice (*n*) and animal (*N*) numbers, respectively. For statistical analysis, 60 second epochs were analysed at 10 minute intervals. Due to large variance in baseline area power measurements, percentage change from the control mean (% control) was calculated and analysed.

5.3.2.3 Pharmacological compounds

All drugs were bath applied to circulating ACSF. KA was applied 30 minutes after slices were placed in the recording chamber, to induce and maintain oscillations, and was present throughout the experiment (3 – 5 hours). The NMDA receptor antagonist, PCP (10 µM), σ1R agonists SKF-10047 (10 µM) and PRE-084 (10 and 20 µM), and σ1R antagonist NE-100 (10 µM) were applied for 1 hour once oscillations had stabilised.

5.3.3 *In vitro* electrophysiology – long-term potentiation (LTP)

5.3.3.1 LTP recordings

Following removal of the brain, the whole brain was hemi-sected along the midline and sliced in ice-cold oxygenated hippocampal ACSF parasagittally (Figure 2.3a), to elongate the CA1 region in the hippocampal slice. The two halves were mounted on a vibrating microtome stage. Horizontal tissue slices (400 µm) were cut, and slices were trimmed to isolate the hippocampus (Figure 2.3b) and transferred to a holding chamber at room temperature for approximately 1 hour before being placed in the recording interface chamber where slices were perfused with oxygenated hippocampus ACSF maintained at 32°C. After 30 minutes, the recording microelectrode and metal stimulating electrode were positioned in the CA1 of the hippocampus, along the Schaffer-collateral pathway (Figure 2.5).

5.3.3.2 Data analysis of evoked fEPSPs and high frequency stimulation

The Schaffer-collateral pathway was stimulated at approximately 20% maximal response. A single 0.02ms pulse was delivered every 20s and the amplitude of the fEPSP was measured. Following a 20 minute stable baseline, tetanic HFS (100 Hz, 1 sec) protocol was delivered to induce LTP and the peak amplitude (mV) of the response was measured.

In initial experiments, to optimise LTP induction, 2 protocols were trialled. Following a 20 minute baseline, a 2 burst HFS was delivered (100 Hz, 1 sec x 2), followed by a 20 minute recording of the fEPSP response. A 4 burst (100 Hz, 1 sec x 4) HFS was then delivered, and the proceeding 20 minutes recorded. The peak amplitude (mV) of the response was measured. For statistical analysis, the average peak amplitude was calculated from 5 minute epochs; immediately before the first HFS (baseline), 20 minutes after the 2 burst HFS protocol (2 burst) and 20 minutes after the 4 burst HFS protocol. All data were normalised to baseline (% control).

Subsequent experiments were performed in control conditions (ACSF only) and/or in the presence of bath applied pharmacological compound (DAP5, PCP or PRE-084). Once stable, a 20 minute baseline was recorded, followed by a 2 burst HFS, and a further 40 minute recording of the fEPSP response. The peak amplitude (mV) of the response was measured. For statistical analysis, the average peak

amplitude was calculated from 5 minute epochs; immediately before HFS (baseline) and 40 minutes after the 2 burst HFS protocol. As multiple tissue slices could be obtained from each animal, two values *(n / N)* are presented below to represent slice (*n*) and animal (*N*) numbers, respectively. All data were normalised to baseline (% control).

5.3.3.3 Pharmacological compounds

All drugs were bath applied to circulating ACSF, 30 minutes after slices were placed in the recording chamber and were present throughout the experiment. The pharmacological compounds include NMDA receptor antagonists DAP5 (10 µM) and PCP (10 µM), and σ1R agonist PRE-084 (10 µM).

5.3.4 Immunohistochemistry – immunofluorescence

5.3.4.1 Slice preparation

ACC tissue for immunohistochemical experiments was prepared from animals as described in Chapter 2.1 and 2.2. Slices prepared from each individual animal were divided between multiple interface chambers, perfused with oxygenated ACSF and allowed to equilibrate for 30 minutes in the bath, followed by a 4 hour incubation period in different incubation conditions (Table 5.1). Slices in the PRE-084 (KA + PCP) condition were pre-incubated with ACSF containing PRE-084 (10 µM) for the initial 30 minutes, whilst slices were allowed to equilibrate, before additionally applying KA and PCP. Slices used for immunohistochemistry were not used for electrophysiological recordings.

Following the incubation period, slices were fixed in PFA buffered solution (4%) for 12 hours, then transferred to cryoprotectant, where they were stored at -20°C until required for immunofluorescence staining. In preparation of staining, slices were transferred to a sucrose (30%) PBS solution, 24 hours before re-sectioning. Sections (40 µm) were cut at -20°C, using a freeze-stage microtome, and stored in PBS in 24-well plates until staining.

Table 5.1 The incubation conditions of slices used for immunohistochemical experiments, including the compounds and concentrations applied to circulating ACSF.

Incubation condition	Compounds applied to ACSF (compound concentration; µM)
Control	Normal recording ACSF only
KA	Kainate (800 nM)
KA + PCP	Kainate (800 nM) + PCP (10 µM)
(PRE-084) KA + PCP	PRE-084 (10 µM; + 30 minutes pre-incubation) + Kainate (800 nM) + PCP (10 µM)

5.3.4.2 Free-floating immunohistochemistry

For immunofluorescence staining, sections were stained free-floating using a combination of antibodies (Table 5.2). When staining for PNNs, SST and PV (combination 1), an initial antigen retrieval step was performed in citrate buffer solution (pH 6.0), heated to 80°C. Sections were then incubated in PBS, Triton X-100 (0.3%) and normal donkey serum (3%) to prevent non-specific binding. Primary antibodies and secondary antibodies (Table 5.2) were diluted in a solution of PBS, Triton X-100 (0.3%) and normal donkey serum (3%). Sections were incubated with primary antibodies, and biotinylated *Wisteria floribunda* lectin for combination 1, overnight (18 – 20 hours) at 4°C. Sections were incubated in secondary antibodies for 2 hours, at room temperature, whilst avoiding light exposure. Sections were mounted on glass microscope slides and cover-slipped using Fluoromount-G™ Mounting Medium, with DAPI. See figure 2.7 for an outline of the full staining protocol.

Table 5.2 List of primary and secondary antibody combinations used. Combinations of biological targets, and their primary (host species, if applicable) and secondary antibodies (wavelength), used for immunofluorescence experiments.

Target	Primary antibody (Host) / other reagent	Secondary antibody / avidin conjugate (Wavelength)
Combination 1		
Somatostatin-positive interneurons (SST+)	Anti-somatostatin (Mouse)	Donkey anti-mouse IgG (568)
Parvalbumin-positive interneurons (PV+)	Anti-parvalbumin (Rabbit)	Donkey anti-rabbit IgG (647)
Perineuronal nets (PNNs)	Biotinylated *Wisteria Floribunda* Lectin (WFA)	Streptavidin, fluorescein (488)
Nuclear DNA	DAPI	(405)
Combination 2		
Microglia (Iba1+)	Anti-Iba1 (Goat)	Donkey anti-goat IgG (488)
Reactive astrocytes (GFAP+)	Anti-GFAP (Chicken)	Donkey anti-chicken IgG (647)
Nuclear DNA	DAPI	(405)

5.3.4.3 Confocal imaging and FIJI image analysis

Imaging was performed using and an SP8 DLS confocal microscope. To image combination 1, tile scans were taken at 2x 20x (equal to 40x) magnification of the whole region of interest (ACC) to get an overview image of the section. To image combination 2, Z-stacks were taken at 40x magnification to sample across the ACC, capturing images from the superficial (layers II / III) and deep (layer V) layers (Figure 2.7).

All image analysis was performed using the image analysis software Fiji, as described in chapter 2.6.3. Briefly, average brightness and contrast values for each channel were applied across all images, background noise was removed, and appropriate filters were applied. GFAP stains astrocytic processes around blood

vessels as well as reactive astrocytes, therefore all blood vessels were drawn around in Fiji, by hand, and removed before performing any further analysis. Average threshold values were applied across all images and further noise was cleaned using the ‘remove outliers’ and the ‘despeckle’ function.

Particle analysis was performed for each channel. For statistical analysis, percentage area (%Area) and integrated density (ID) of fluorescence for GFAP, Iba1, PV, SST and WFA were calculated. At least two sections from each slice were imaged per condition, per animal. Slices from at least 4 animals were included in each condition. Section %Area and IDs were averaged for each animal (*N*) and compared across the different conditions (Table 5.1).

5.4 Results

5.4.1 Sigma-1 receptor agonist SKF-10047 mimics effects of PCP on ACC oscillations

Use of the σ1 receptor agonist SKF-10047 led to the initial identification of the σ1 receptor, because of the psychomimetic effects it produced in humans (Freeman and Bunney, 1984). These psychomimetic effects mimicked those induced by PCP (Ishikawa and Hashimoto, 2009). Further investigation revealed that the σ1 receptor is distinct from the PCP-binding site on the NMDA receptor. However, the effects of SKF-10047 initially sparked interest in the potential role of the σ1 receptor in psychosis. To explore the similarity between PCP and SKF-10047, SKF-10047 was applied to beta and gamma KA-evoked ACC oscillations.

Firstly, SKF-10047 (10 μM) was applied to slices exhibiting stable beta oscillations. SKF-10047 application resulted in a rapid, large increase in the magnitude of beta oscillations over 60 minutes (Figure 5.1a). Peak frequency analysis (Figure 5.1b) comparing control to SKF-10047 (60 minutes) application found SKF-10047 significantly decreased the peak frequency of beta oscillations from 25.5 (IQR 21.8 – 29.9) Hz to 23.1 (IQR 20.3 – 25.9) Hz (p = 0.031; Wilcoxon matched-pairs test), indicating a slowing of the oscillation. Area power analysis (Figure 5.1c) demonstrated that SKF-10047 induced an increase in beta power to 246.9 (IQR 108.4 – 332.9)% from control 100.8 (IQR 99.8 – 104.9)%, however the effect was not statistically significant (p 0.094; Wilcoxon matched-pairs test) likely due to the large variability in the response to SKF-1007. It was clear that in some slices σ1 receptor activation evoked a 200 - 300% increase, similar to the changes seen with PCP in Chapter 3. However, because some slices showed little change overall the group was not significantly different from control.

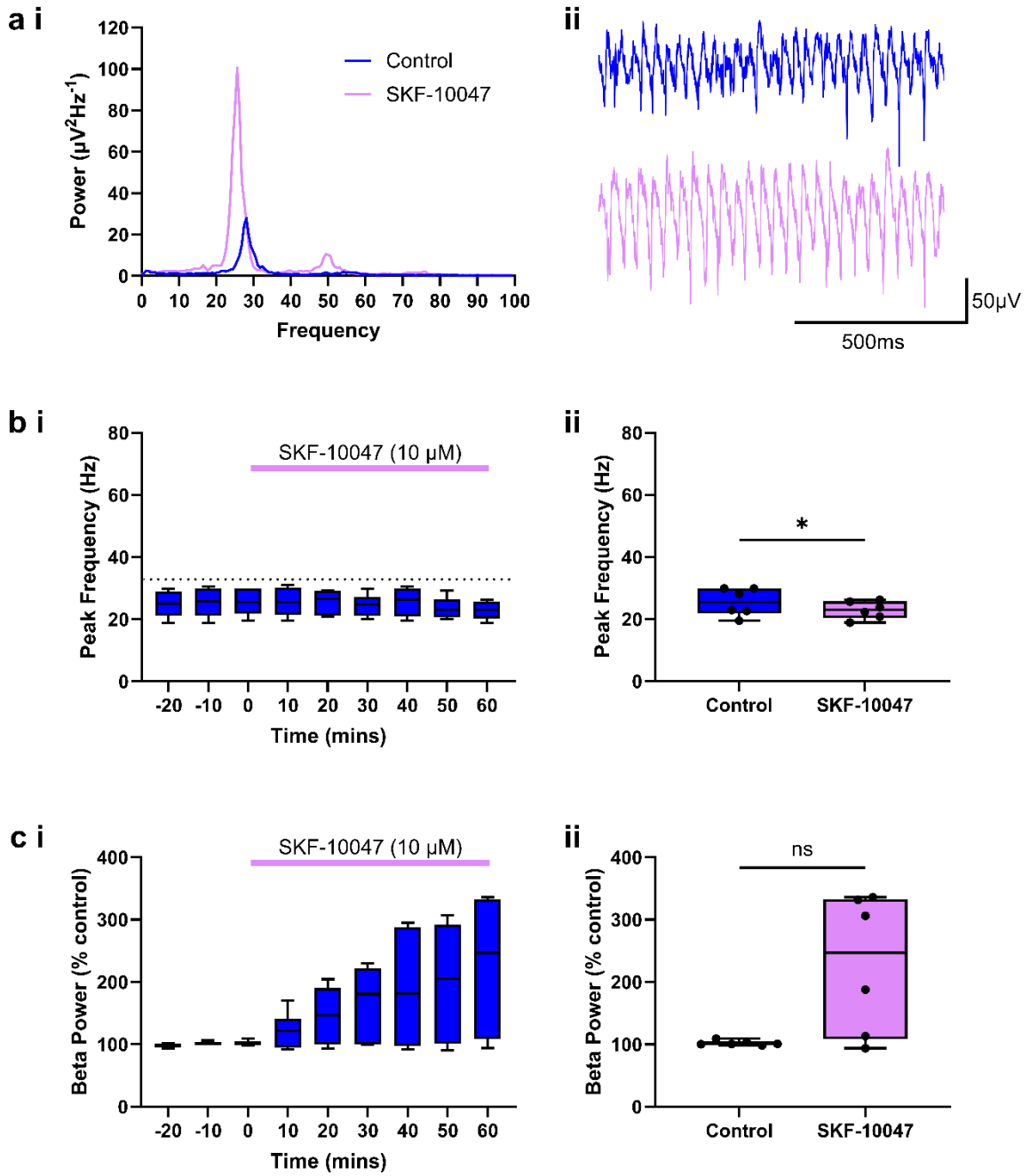

Figure 5.1 SKF-10047 induces a large increase in KA-evoked beta area power in rat ACC slices. (a) Example (i) power spectra and (ii) traces from one experiment: control prior to SKF-10047 (blue solid line), and after 60 minutes SKF-10047 (lilac solid line). (b) Time-course plot (medians with IQR) shows no effect of SKF-10047 (applied for duration of lilac bar) on median beta peak frequency and c) a significant increase in median (IQR) beta area power following SKF-10047 (applied for duration of lilac bar) application Total slices / animals (*n* / *N*) = 6 / 4.

Next, SKF-10047 was applied to slices exhibiting stable gamma oscillations. Application of SKF-10047 also lead to a large increase in the magnitude of gamma oscillations over 60 minutes (Figure 5.2a). Peak frequency analysis (Figure 5.2b) comparing control to SKF-10047 (60 minutes) application found SKF-10047 had no significant effect on the peak frequency of gamma oscillations in control 44.9 (IQR 38.3 – 46.7) Hz vs 60 minutes SKF-10047 application 43.1 (IQR 34.6 – 47.0) Hz (p > 0.078; Wilcoxon matched-pairs test). Area power analysis (Figure 5.2c) demonstrated that SKF-10047 induced a significantly large increase in gamma power from control 99.6 (IQR 98.2 – 102.6)% to 183.9 (IQR 145.10 – 220.5)% (p = 0.008; Wilcoxon matched-pairs test). Interestingly, SKF-10047 induced a large increase in gamma power, similar to PCP, but without altering the oscillations frequency.

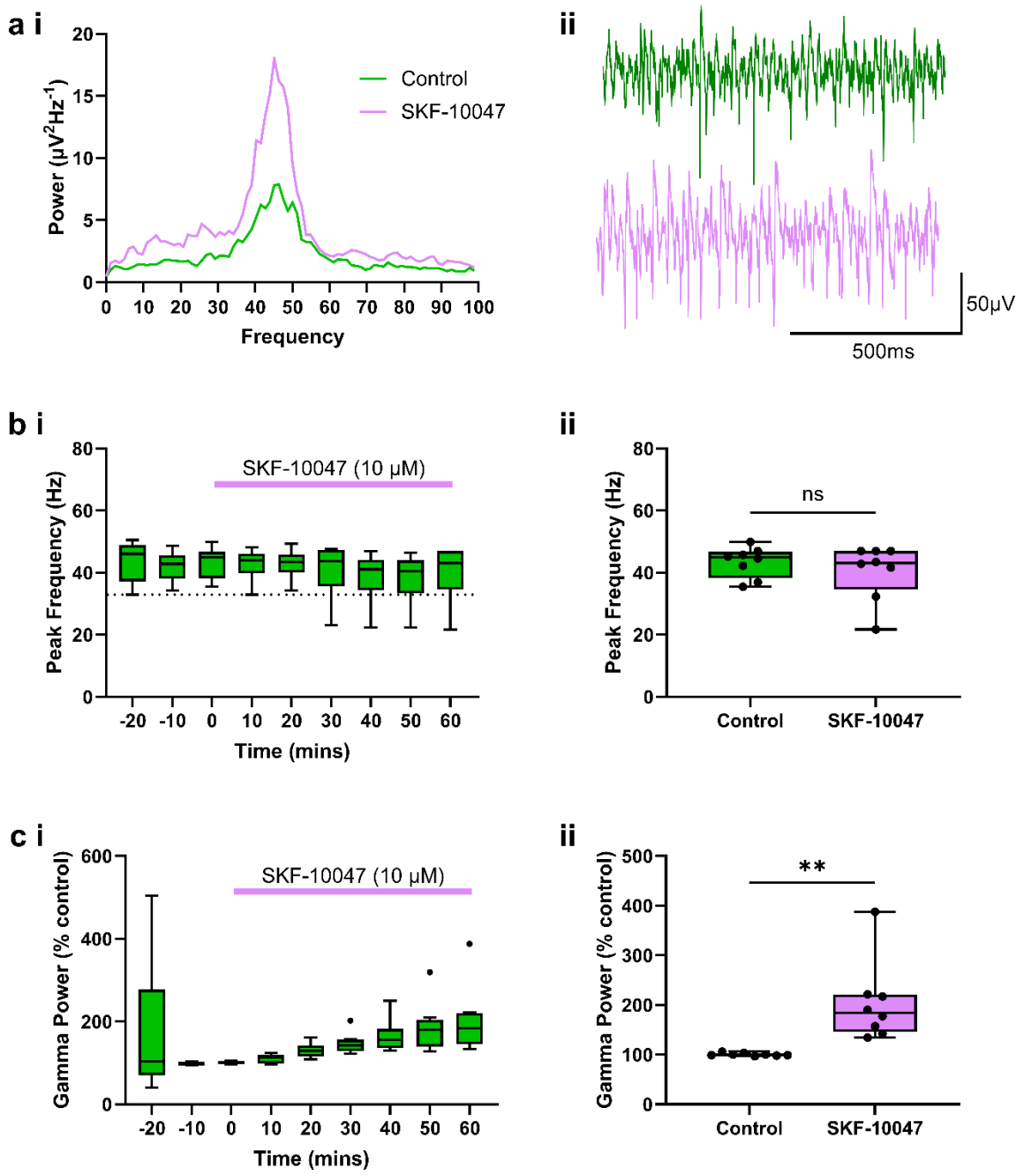

Figure 5.2 SKF-10047 induces a large increase in KA-evoked gamma area power in rat ACC slices. (a) Example (i) power spectra and (ii) traces from one experiment: control prior to SKF-10047 (green), and after 60 minutes SKF-10047 (lilac). (b) Time-course plot (medians with IQR) shows no effect of SKF-10047 (applied for duration of lilac bar) on median gamma peak frequency and c) a significant increase in median (IQR) gamma area power following SKF-10047 (applied for duration of lilac bar) application Total slices / animals (*n* / *N*) = 8 / 4.

5.4.2 PRE-084, a specific sigma-1 receptor agonist, increases ACC gamma power

Since the discovery of the σ1 receptor, more specific ligands have been developed and made available. PRE-084 is a specific σ1 receptor agonist. I therefore explored the effect of applying PRE-084 to discern the specific σ1 receptor impact seen previously with SKF-10047, on beta and gamma oscillations (Figure 5.3).

Firstly, PRE-04 (10 µM) was applied to slices exhibiting stable beta oscillations. PRE-084 had no significant effect on the peak frequency of beta oscillations, following 60 minutes application (p = 0.094; Wilcoxon matched-pairs test; Figure 5.3ai). There was also no significant effect of PRE-084 on beta power (p = 0.469; Wilcoxon matched-pairs test; Figure 5.3aii).

PRE-084 (10 µM) was also applied to slices exhibiting stable gamma oscillations. PRE-084 had no significant effect on the peak frequency of gamma oscillations, following 60 minutes application (p = 0.250; Wilcoxon matched-pairs test; Figure 5.3bi). There was also no significant effect of PRE-084 on gamma power (p = 0.250; Wilcoxon matched-pairs test; Figure 5.3bii). Although not statistically significant, there was a moderate increase in gamma power from 106.2 (IQR 103 – 109)% in control to 125.6 (IQR 109 – 138)% with PRE-084.

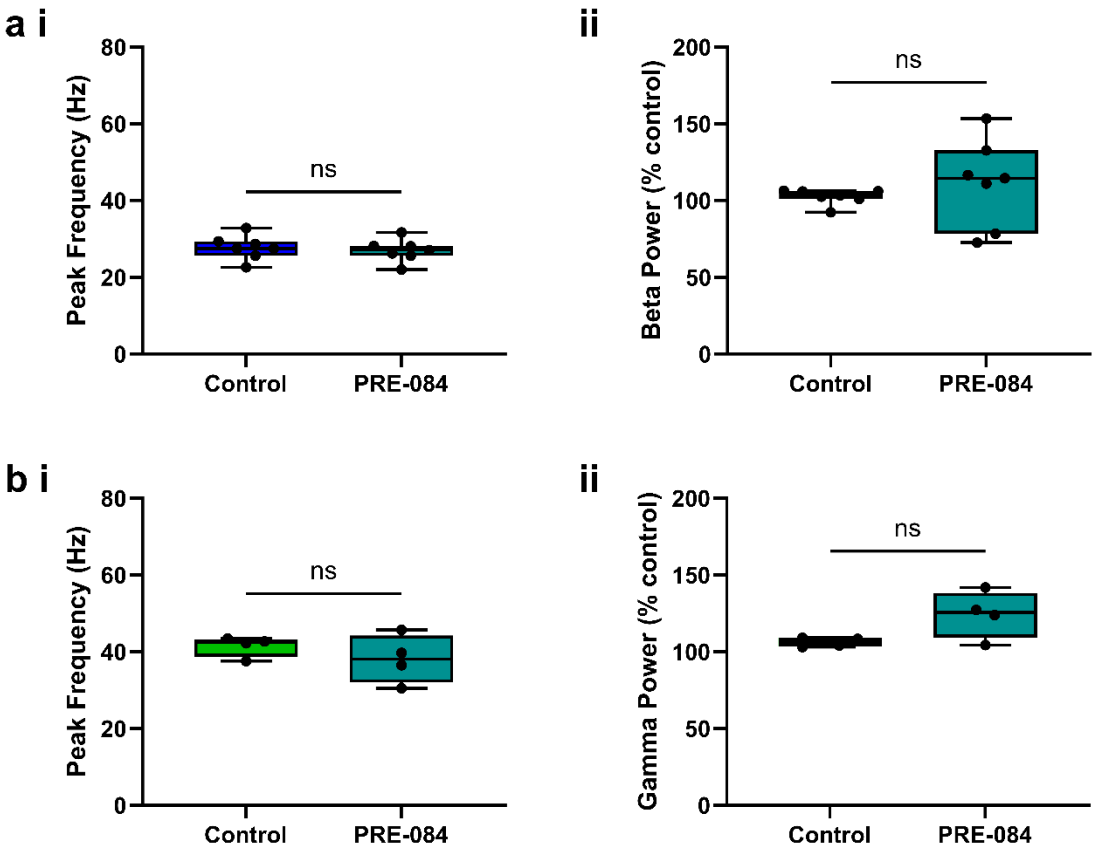

Figure 5.3 The specific σ1 receptor agonist PRE-084 moderately increases KA-evoked gamma power in rat ACC slices. (a) Effect of PRE-084 (10 µM) on beta oscillation (i) peak frequency (Hz) and (ii) power (% control), following 60 minutes application. (b) Effect of PRE-084 (10 µM) on gamma oscillation (i) peak frequency (Hz) and (ii) power (% control), following 60 minutes application. Total slices / animals (*n* / *N*) = 4 / 3.

5.4.3 Sigma-1 receptor antagonist NE-100 blocks SKF-10047 effects on ACC oscillations

Activating σ1 receptors using SKF-10047 increased beta and gamma oscillation power, however SKF-10047 is a non-specific σ1 receptor agonist and is also reported to act as a NMDA receptor antagonist. Interestingly, the σ1 receptor agonist PRE-084 had no significant effect on either beta or gamma power. Therefore, to evaluate the σ1 receptor action of SKF-10047, the effect of SKF-10047 on high frequency oscillations was assessed in the presence of a specific σ1 receptor antagonist, NE-100. NE-100 (10 µM) was applied to stable beta and gamma frequency oscillations to block σ1 receptors for 40 minutes, prior to SKF-10047 (10 µM) application (Figure 5.4a).

First, the effect of σ-receptor blockade on SKF-10047 action was assessed in stable beta oscillations. A RM One-way ANOVA test was performed to compare the effect of NE-100 and SKF-10047 application on peak frequency (Hz) and beta power (% control). There was no significant effect of either compound on the mean peak frequency (F (1.104, 4.415) = 5.997, p = 0.065; Figure 5.4bi), suggesting that neither NE-100, nor SKF-10047, effected oscillation frequency. There was also no significant effect on mean beta power (F (1.291, 5.172) = 0.6654, p = 0.490; Figure 5.4bii), demonstrating that NE-100 alone does not alter beta power, but that the increase in beta power induced by SKF-10047 (Figure 5.1cii) was occluded by σ1 receptor blockade. Notably, the beta power decreased slightly when both NE-100 and SKF-10047 were applied, an effect not seen in the absence of the antagonist.

The effect of σ-receptor blockade on stable gamma frequency oscillations was also assessed. A RM One-way ANOVA test was performed to compare the effect of NE-100 and SKF-10047 application on peak frequency (Hz) and gamma power (% control). There was a significant effect of compound application on mean peak frequency (F (1.152, 4.609) = 8.284, p = 0.036; Figure 5.4ci). Multiple comparisons analysis showed there was no significant change in mean peak frequency between control (39.9 ± 2.8 Hz) and NE-100 (37.7 ± 2.3 Hz) (p = 0.595; Tukey's multiple comparisons). However, there was a significant reduction in frequency between NE-100 and NE-100 + SKF-10047 (28.6 ± 2.9 Hz) (p = 0.040; Tukey's multiple comparisons). When assessing changes in gamma power, the application of neither

compound had any significant effect on mean gamma power (F (1.209, 4.835) = 0.1547, p = 0.756; Figure 5.4cii). This suggests that blocking σ1 receptors prevents the increase in oscillation power seen in Figure 5.2cii and reduces the oscillation to a beta frequency, an effect not observed with SKF-10047 alone.

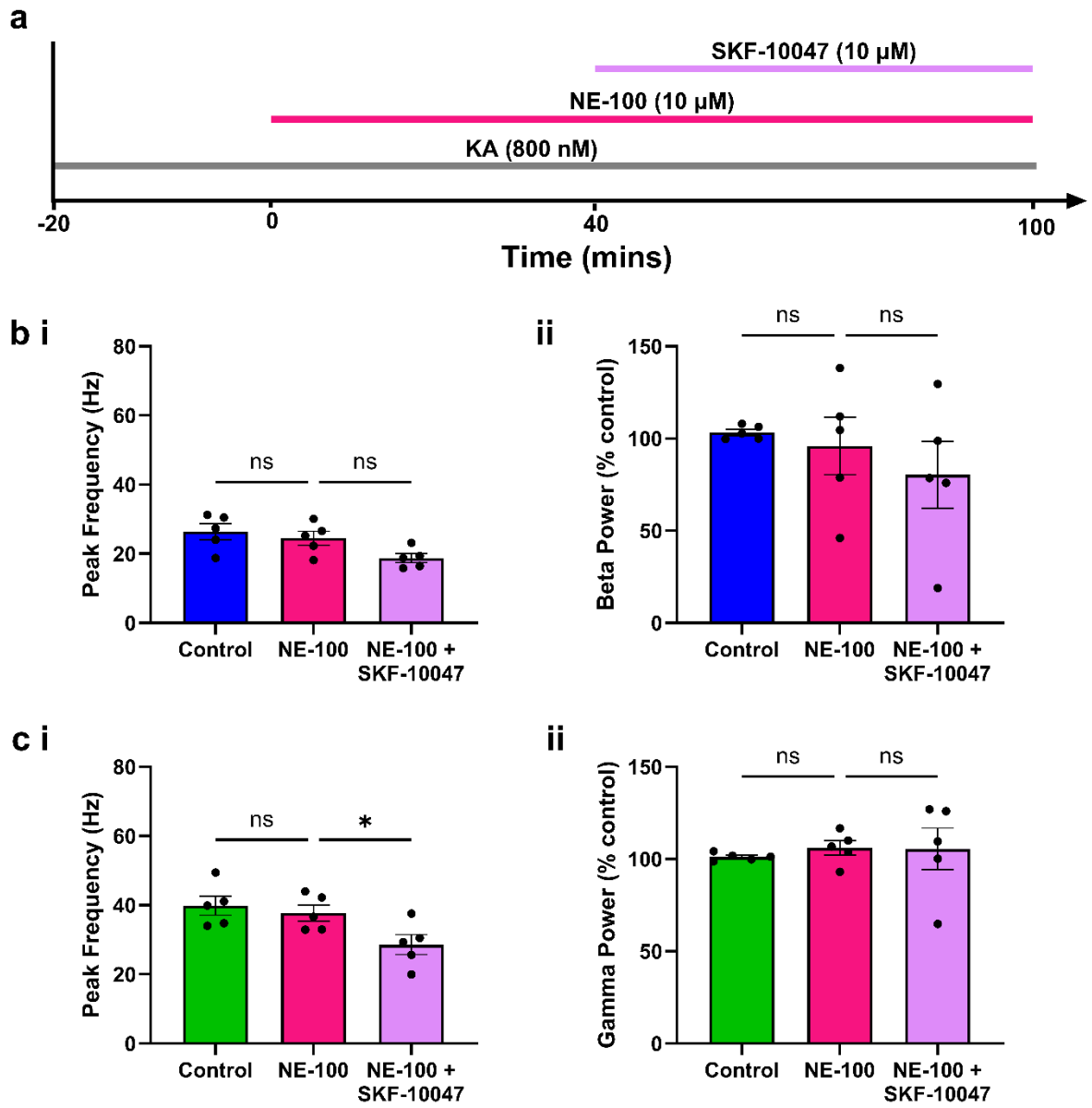

Figure 5.4 The σ1 receptor antagonist NE-100 blocks effects of SKF-10047 in KA-evoked rat ACC oscillations. (a) Schematic of experimental protocol: NE-100 (10 µM) was applied to stable KA-evoked beta / gamma oscillations for 40 minutes, and SKF-10047 (10 µM) was co-applied for a futher 60 minutes. (b) Effect of NE-100 and SKF-10047 application on ACC beta oscillation mean (± SEM) (i) peak frequency and (ii) area power. (c) Effect of NE-100 and SKF-10047 application on ACC gamma oscillation mean (± SEM) (i) peak frequency and (ii) area power. Total slices / animals (*n* / *N*) = 5 / 3.

5.4.4 Sigma-1 receptor antagonist NE-100 partially blocks PCP effects on ACC oscillations

In Chapter 3, I showed that PCP caused a very large increase in beta power when applied to KA-evoked ACC beta oscillations and gamma oscillations. Like SKF-10047, PCP has also been reported to be a σ1 receptor agonist as well as an NMDA receptor antagonist. Therefore, to evaluate the σ1 receptor action of PCP, the effect of PCP on high frequency oscillations was assessed in the presence of the σ1 receptor antagonist, NE-100. NE-100 (10 μM) was applied to stable beta and gamma frequency oscillations to block σ1 receptors for 40 minutes, prior to PCP (10 μM) application (Figure 5.5a).

First, the effect of σ-receptor blockade on the action of PCP was assessed in stable beta oscillations (Figure 5.5b). A RM One-way ANOVA test was performed to compare the effect of NE-100 and PCP application on peak frequency (Hz) and beta power (% control). There was a significant effect of compound application on mean peak frequency ($F (1.586, 14.28) = 7.338$, $p = 0.009$; Figure 5.5bi). Multiple comparisons analysis showed there was no significant change in mean peak frequency between control (21.9 ± 1.1 Hz) and NE-100 (22.2 ± 1.09 Hz) ($p = 0.889$; Tukey's multiple comparisons). However, there was a small but significant reduction in frequency between NE-100 and NE-100 + PCP (19.1 ± 1.5 Hz) ($p = 0.021$; Tukey's multiple comparisons). When assessing changes in beta power, compound application had no significant effect on mean beta power ($F (1.098, 10.98) = 3.440$, $p = 0.088$; Figure 5.5bii), demonstrating that NE-100 alone does not affect beta power, and that the increase in beta power induced by PCP (Figure 3.3c) was, at least partially, occluded by σ1 receptor blockade.

The effect of σ-receptor blockade was also assessed in stable gamma oscillations (Figure 5.5c). A RM One-way ANOVA test was performed to compare the effect of NE-100 and PCP application on peak frequency (Hz) and gamma power (% control). There was a significant effect of compound application on median peak frequency ($F (1.717, 13.73) = 10.88$, $p = 0.002$; Figure 5.5ci). Multiple comparisons analysis showed there was no significant change in mean peak frequency between control (39.9 ± 2.2 Hz) and NE-100 (35.6 ± 2.6 Hz) ($p = 0.201$; Tukey's multiple comparisons). However, there was a significant reduction in frequency between

control and NE-100 + PCP (26.5 ± 2.4 Hz) (p = 0.008; Tukey's multiple comparisons). When assessing changes in gamma power, compound application had no significant effect on median gamma power (F (1.069, 8.551) = 3.846, p = 0.082; Figure 5.5cii). This result suggests that NE-100 alone does not affect gamma power or frequency, but the addition of PCP shifts the oscillation to a beta frequency, as seen in chapter 3. It does suggest the increase in gamma power induced by PCP alone (Figure 3.3c) was, at least partially, occluded by σ1 receptor blockade. However, there is still a moderate increase in gamma power from NE-100 (111.2 ± 12.5%) to NE-100 + PCP (213.3 ± 58.8%), and high variability in the data indicates that application of PCP under σ1 receptor blockade has a mixed, potentially disruptive, effect on gamma oscillations.

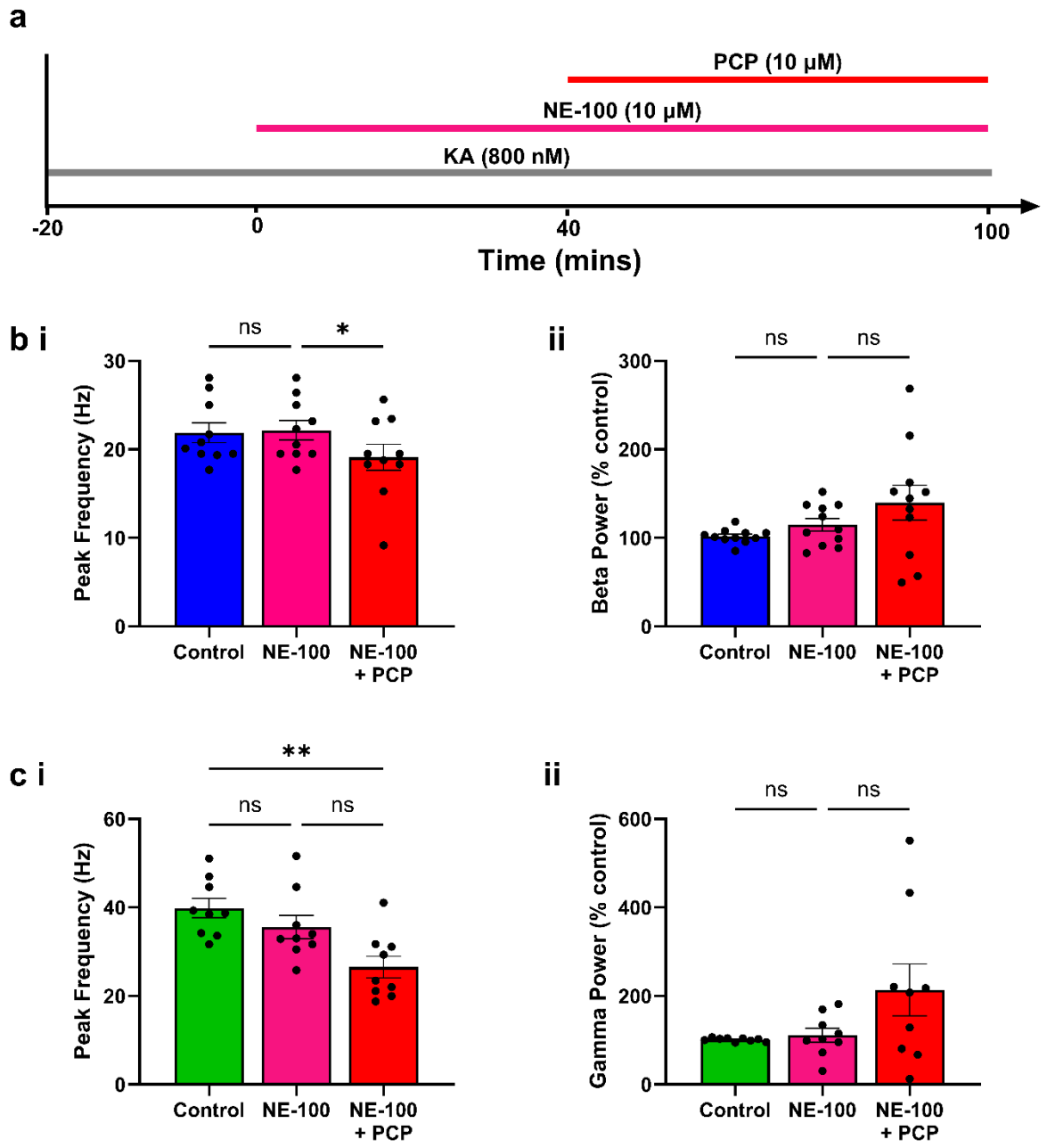

Figure 5.5 The σ1 receptor antagonist NE-100 blocks effects of PCP in KA-evoked rat ACC oscillations. (a) Schematic of experimental protocol: NE-100 (10 µM) was applied to stable KA-evoked beta / gamma oscillations for 40 minutes, and PCP (10 µM) was co-applied for a futher 60 minutes. (b) Effect of NE-100 and PCP application on ACC beta oscillation mean (± SEM) (i) peak frequency and (ii) area power. (c) Effect of NE-100 and PCP application on ACC gamma oscillation mean (± SEM) (i) peak frequency and (ii) area power. Total slices / animals (*n* / *N*) = 9 – 10 / 6 - 8

5.4.5 Sigma-1 receptor agonist PRE-084 blocks PCP effects on ACC gamma oscillations

The effect of σ-receptor agonist PRE-084 had no effect on beta and gamma peak frequency or power when applied alone. However, *in vivo* behavioural rodent studies have shown that σ1 receptor agonists can significantly attenuate NMDA receptor antagonist-induced cognitive deficits (Hashimoto et al., 2007, Kunitachi et al., 2009, Maurice et al., 1994, Maurice and Privat, 1997). Therefore, to explore whether acute σ1 receptor activation had any effect on PCP action, I used the same protocol as chapter 5.4.3 and 5.4.4 and bath-applied PRE-084 to stable beta and gamma oscillations for 40 minutes, before co-applying PCP (10 µM) for a further 60 minutes.

First, the effect of σ-receptor activation on PCP action was assessed in stable beta oscillations. A Friedman test was performed to compare the effect of PRE-084 and PCP application on peak frequency (Hz) and beta power (% control) (Figure 5.6a). There was not a significant effect of compound application on median peak frequency ($X^2 = 3.43$, $p = 0.237$; Figure 5.6ai), showing that neither PRE-084, nor subsequent PCP, application significantly affected peak frequency. When assessing changes in beta power, compound application did have a significant effect on median beta power ($X^2 = 12.3$, $p = 0.0003$; Figure 5.6aii). Multiple comparisons analysis showed there was no significant change in median beta power between control (98.7 [IQR 97.1 – 107.9]%) and PRE-084 (107.8 [IQR 94.7 – 114]%) ($p = 0.544$; Dunn's multiple comparisons). However, there was a significant increase in median beta power from control to PRE-084 + PCP (165.5 [IQR 149 – 239]%) ($p = 0.002$; Dunn's multiple comparisons). Therefore, PRE-084 does not appear to attenuate the effect of PCP on KA-evoked beta oscillations.

Next, the effect of σ1 receptor activation on PCP action was assessed in stable gamma oscillations (Figure 5.6b). A Friedman test was performed to compare the effect of PRE-084 and PCP application on peak frequency (Hz) and gamma power (% control). There was not a significant effect of compound application on median peak frequency ($X^2 = 4.33$, $p = 0.142$; Figure 5.6bi), showing that neither PRE-084, nor the subsequent PCP application, significantly affected peak frequency. Interestingly, only 2 of 6 slices (33.3%) shifted from a gamma frequency oscillation to a beta frequency oscillation, compared to 85% when PCP was applied alone (Figure 3.4). When

assessing changes in gamma power, compound application did have a significant effect on median gamma power (X^2 = 1.00, p = 0.740; Figure 5.6bii). Remarkably, PRE-084 attenuated the effect of PCP on KA-evoked gamma oscillations, blocking the shift to, and significant increase in, beta.

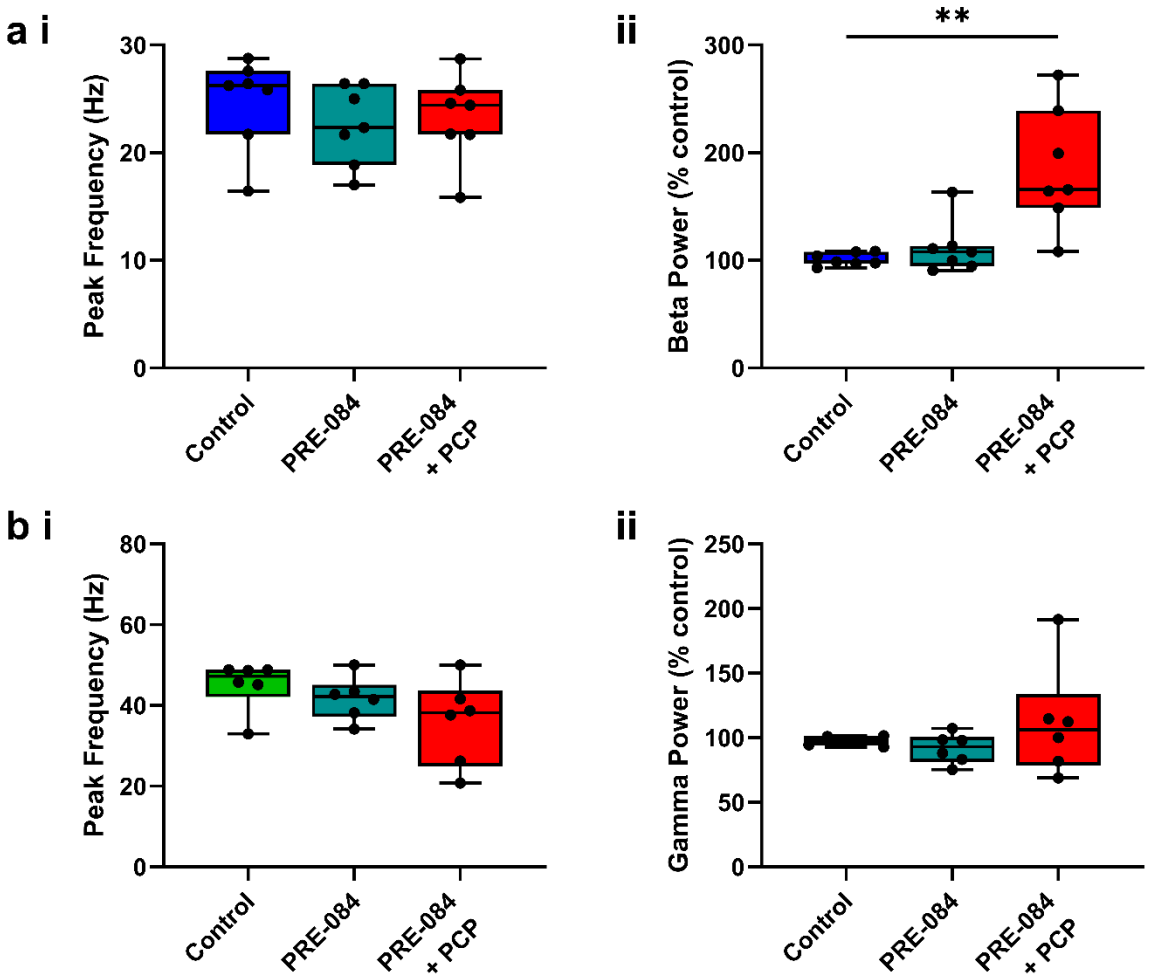

Figure 5.6 The σ1 receptor agonist PRE-084 blocks effects of PCP in KA-evoked rat ACC gamma oscillations. (a) Effect of PRE-084 and PCP application on ACC beta oscillation median (IQR) (i) peak frequency and (ii) beta power. (c) Effect of PRE-084 and PCP application on ACC gamma oscillation median (IQR) (i) peak frequency and (ii) gamma power**.** Total slices / animals (*n* / *N*) = 6 – 7 / 4.

5.4.6 σ1 receptor agonists, SKF-10047 and PRE-084, have no effect on CA3 oscillations

The effect of SKF-10047 on ACC beta and gamma oscillations is similar to the effect of PCP. Previously, I showed that PCP had no effect of CA3 hippocampal gamma oscillations (Figure 3.7), in stark contrast to ACC findings. SKF-10047 was, therefore, applied to hippocampus slices exhibiting a stable gamma frequency oscillation for 60 minutes, to explore similarities in the hippocampus (Figure. 5.7). Peak frequency and area power were measured between 15 and 80 Hz. Following 60 minutes SKF-10047 application there was no change in the peak frequency of gamma oscillations (p = 0.695; paired t test; Figure 5.7b). Gamma power was also not significantly different following 60 minutes SKF-10047 application (p = 0.697; paired t test; Figure 5.7c). These findings are similar to the effects found with PCP on CA3 oscillations, further supporting similarities between the σ1 receptor agonist SKF-10047 and NMDA receptor antagonist PCP as they exhibit similar regional differences in their actions.

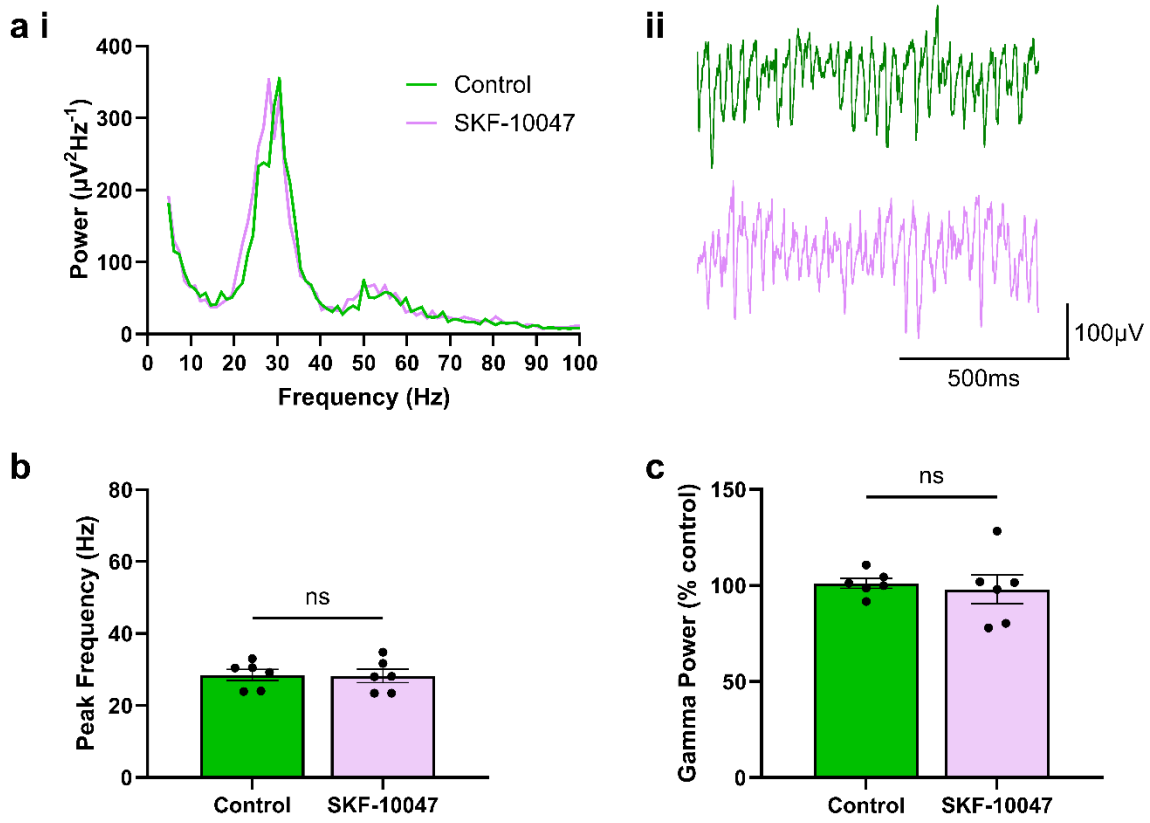

Figure 5.7 SKF-10047 does not affect KA-evoked rat CA3 gamma oscillations. (a) Example (i) power spectra and (ii) traces from one experiment: control prior to SKF-10047 (green), and after 60 minutes SKF-10047 (lilac). Effect of 60 minutes application of SKF-10047 (10 μM) on stable CA3 gamma oscillations on mean (± SEM) (b) peak frequency (Hz) and (c) gamma power (% control). Total slices / animals (*n* / *N* = 6 / 4.

PRE-084 is a selective σ1 receptor agonist, unlike SKF-10047 which also acts as an NMDA receptor antagonist. To assess the specific effect of σ1 receptor activation on KA-evoked CA3 hippocampal gamma oscillations, PRE-084 was applied for 60 minutes to stable gamma frequency oscillations (Figure 5.8). Peak frequency analysis showed PRE-084 had no effect on the peak frequency of gamma oscillations ($p = 0.173$; paired *t* test; Figure 5.8b). Gamma power was also not significantly different following 60 minutes PRE-084 application ($p = 0.849$; paired *t* test; Figure 5.8c). This data shows that σ1 receptor agonists do not increase KA-evoked CA3 gamma oscillations.

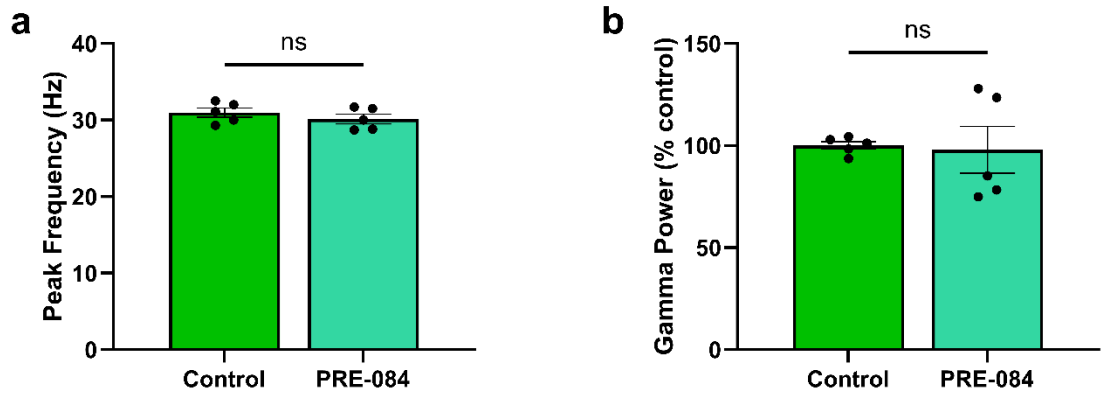

Figure 5.8 PRE-084 does not affect KA-evoked rat CA3 gamma oscillations. Effect of 60 minutes application of PRE-084 (10 µM) on stable CA3 gamma oscillations on mean (± SEM) (a) peak frequency (Hz) and (b) gamma power (% control) Total slices / animals (*n* / *N*) = 5 / 3.

5.4.7 Activating σ1 receptors using PRE-084 increases hippocampal LTP while PCP attenuated LTP

Tetanic stimulation results in persistent changes in synaptic strength thought to underlie learning and memory (Bliss and Lomo, 1973, Gardner-Medwin and Wilkie, 1976). LTP can be induced and measured *in vitro* from the CA1 of the hippocampus, following stimulation of the Schaffer collateral pathway. LTP of the Schaffer collateral pathway is highly NMDA receptor dependent and thus is likely to be affected by the NMDA hypofunction in schizophrenia. As previously mentioned, PCP impairs hippocampal LTP recorded from the CA1, *in vitro* (Stringer et al., 1984).

As PCP had no effect on hippocampal CA3 oscillations it would be interesting to explore the effect on an alternative neuronal mechanism underlying learning and memory. Studies suggest σ1 receptor agonists can also modulate LTP, enhancing it through NMDA-dependent mechanisms (Martina et al., 2007). Therefore, to understand how these two different receptors may affect LTP in this slice model, LTP was induced and recorded *in vitro* from rat hippocampal slices in the presence of PCP and PRE-084.

It is well established that HFS of 100 Hz for 1 s can induce LTP in rodent slices of the hippocampus, however, results and reliability are known to vary depending on the protocol used. Therefore, a reliable, stable technique for inducing LTP in rodent slices first needed to be establish. To optimise LTP induction, 2 protocols were trialled in preliminary experiments (Figure 5.9). Firstly, following a 20 minute baseline, a HFS was delivered twice (2 bursts; 100 Hz, 1 sec x 2), followed by a 20 minute recording of the fEPSP response. This first stimulation was then followed by a 4 burst (100 Hz, 1 sec x 4) HFS and a further 20 minutes recorded (Figure 5.9a). The peak amplitude (mV) of the response was measured and normalised to baseline (% control) to assess LTP induction (Figure 5.9b).

A RM One-way ANOVA test was performed to compare the effect of stimulation protocols on fEPSP amplitude (% control). There was a statistically significant difference in fEPSP amplitude between at least two groups ($F(1.137, 4.550) = 75.53$, $p < 0.001$; Figure 5.9c). The mean fEPSP amplitude was significantly increased from 102.6 (± 1.3)% pre-stimulation to 150.6 (± 3.7)% 20 minutes post-2 burst HFS ($p < 0.001$; Tukey's multiple comparisons). Also, 4 burst HFS significantly increased mean

fEPSP amplitude further to 182 (± 8.50)%, compared to control (p = 0.002; Tukey's multiple comparisons) and 2 burst stimulation (p = 0.012; Tukey's multiple comparisons).

LTP was reliably induced in all slices (n = 5), using both the 2 and 4 burst protocol, suggesting that the chosen HFS protocol was robust and reliable. The aim was to induce a response which could be either amplified or depressed by pharmacological manipulation, therefore, the 2 burst protocol was used for further LTP experiments.

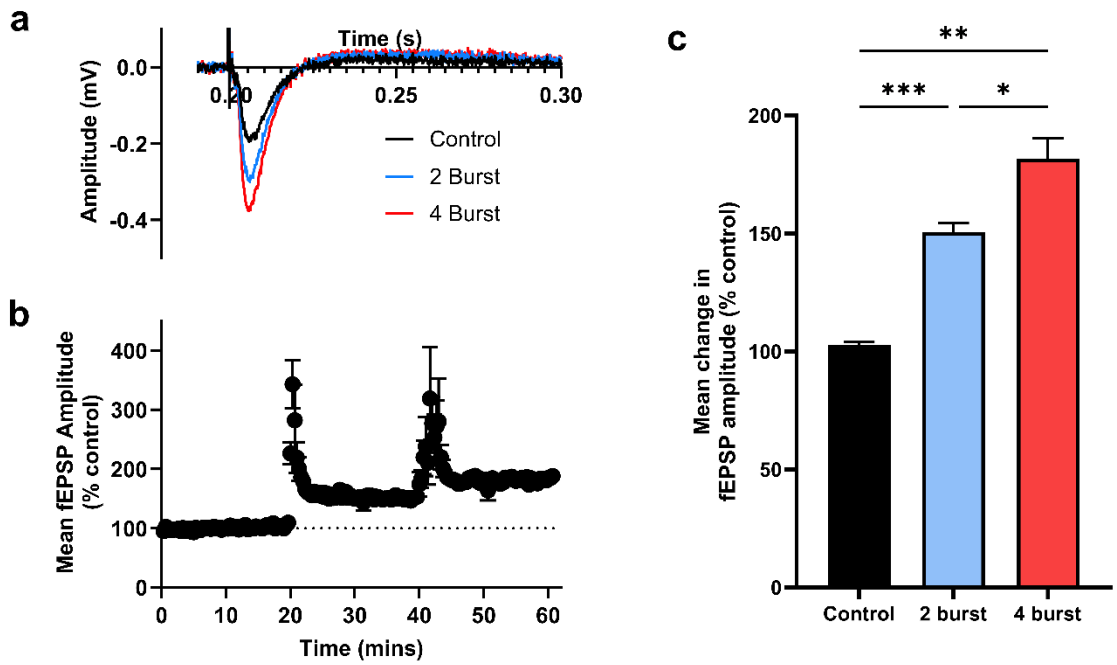

Figure 5.9 LTP induced in rat hippocampal slices, using HFS. (a) Mean fEPSP responses before 100Hz, 1s HFS stimualtion (control; black), 20 minutes afer 2 burst HFS stimualtion (blue) and 20 minutes after 4 burst HFS (red). (b) Time-course showing mean (± SEM) fEPSP amplitude from control (0 – 20 mins), 2 burst HFS (20 – 40 mins) and 4 burst HFS (40 - 60 mins), normalised to control. (c) Mean (± SEM) fEPSP amplitude following 2 burst and 4 burst HFS, normalised to control. Total slices / animals (*n* / *N*) = 5 / 3.

Using the 2 burst HFS protocol, the fEPSP amplitude was recorded for 20 minutes of stable baseline, followed by the 2 burst HFS and then a further 40 minutes post-stimulation was recorded (Figure 5.10). Control recordings were performed in ACSF only (black data points). To confirm previous findings that LTP in the Schaffer collateral pathway is NMDA-dependent (Collingridge et al., 1983), and further validate the protocol, DAP5 (100 µM) was applied at the beginning of the recording to the circulating bath solution (Figure 5.10a). To assess the effect of NMDA receptor blockade and σ1 receptor activation, the same protocol was performed in the presence of PCP (10 µM; Figure 5.10b) and PRE-084 (10 µM; Figure 5.10c), respectively.

A two-way ANOVA was performed to analyse the effect of HFS and compound application on mean fEPSP amplitude. A two-way ANOVA revealed that there was a statistically significant interaction between the effects of HFS and compound application ($F(3, 64) = 66.74$, $p < 0.001$). Simple main effects analysis showed that HFS did have a statistically significant effect on mean fEPSP amplitude ($p < 0.001$). In all conditions, the mean fEPSP amplitude increased significantly 40 minutes post 2 burst HFS: control (97.2 ± 2.27% to 155.4 ± 2.24%; $p < 0.001$); DAP5 (93.2 ± 0.93% to 133.0 ± 1.43%; $p < 0.001$); PCP (98.9 ± 1.08% to 121.6 ± 0.95%; $p < 0.001$); PRE-084 (104.1 ± 0.89% to 164.3 ± 1.6)%; $p < 0.001$) (Tukey's multiple comparisons; Figure 5.10d), indicating successful induction of LTP regardless of NMDA receptor blockade or σ1 receptor activation.

Compound effects on 'normal' LTP was also assessed using simple main effects analysis. Compound also had a significant effect on mean fEPSP amplitude ($p < 0.001$). In control slices, the mean fEPSP amplitude increased to 155.4 (± 2.24)% following HFS. In comparison, mean fEPSP amplitude was significantly smaller post-HFS in the presence of DAP5 (133.0 ± 1.43; $p < 0.0001$; Tukey's multiple comparisons) and PCP (121.6 ± 0.95%; $p < 0.0001$; Tukey's multiple comparisons; Figure 5.10d). These results repeat previous findings that DAP5 and PCP reduce LTP (Stringer et al., 1984, Collingridge et al., 1983), confirming CA1 LTP is NMDA-dependent. However, DAP5 did not attenuate LTP as entirely as expected. When the σ1 receptor agonist PRE-084 was applied, the mean fEPSP amplitude 40 minutes post-HFS was significantly increased (164.3 ± 1.61%), compared to control ($p = 0.0026$; Tukey's multiple comparisons). This data demonstrated activating σ1 receptors increases LTP in the CA1 of the rat hippocampus.

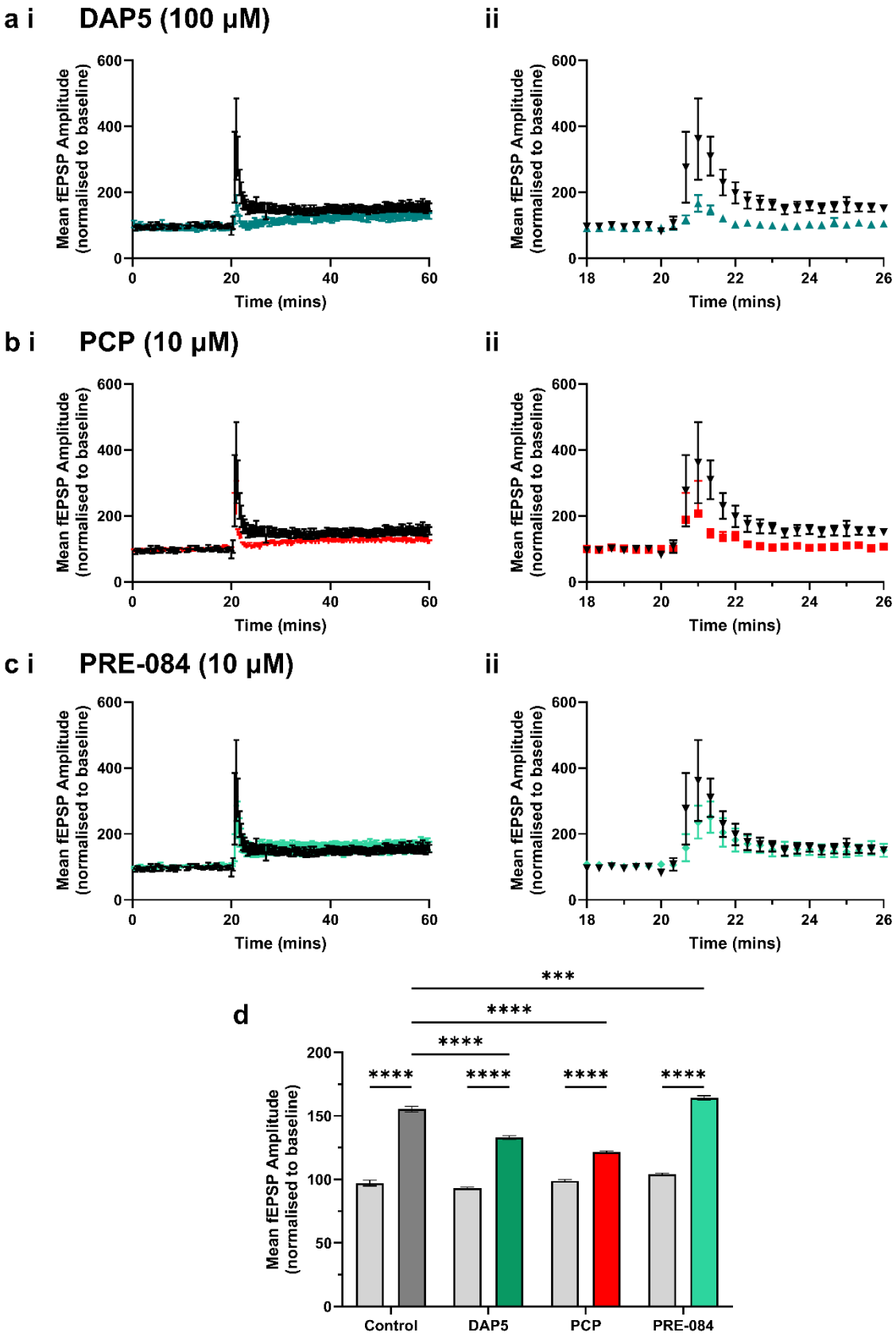
a i
DAP5 (100 µM)
ii
b i
PCP (10 µM)
ii
c i
PRE-084 (10 µM)
ii
Mean fEPSP Amplitude (normalised to baseline)
Time (mins)
d
***
****
****
****
****
****
****
Control
DAP5
PCP
PRE-084

Figure 5.10 LTP is attenuated by NMDA receptor antagonists DAP5 and PCP, and increased by σ1 receptor agonist PRE-084, in rat hippocampal slices. The effect of compound application on fEPSP amplitude before (baseline; *t* = 0 – 20 mins) and after (*t* = 20 - 40 mins) HFS (2 x 1s 100Hz), delivered at *t* = 20 minutes, compared to control slices where no compound was present (black). (a) Mean fEPSP peak amplitude (% control) in the presence of DAP5 (100 µM; green), showing (i) entire 60 minute time course, and (ii) expanded at point of HFS (*t* = 20 mins). (b) Mean fEPSP peak amplitude (% control) in the presence of PCP (10 µM; red), showing (i) entire 60 minute time course, and (ii) expanded at point of HFS (*t* = 20 mins). (c) Mean fEPSP peak amplitude (% control) in the presence of PRE-084 (10 µM; blue), showing (i) entire 60 minute time course, and (ii) expanded at point of HFS (*t* = 20 mins). (d) Mean fEPSP amplitude (% control) comparing baseline (pre-HFS; *t* = 15 – 20 mins) to 40 minutes post-HFS, in control slices (grey), DAP5, PCP, and PRE-04 conditions. All data is normalised to baseline (% control). Total slices / animals (*n* / *N*) = 5 – 6 / 4 - 5

Here, I have shown that LTP can be induced and sustained for 40 minutes post stimulation demonstrating so called early-LTP. Also, LTP is still induced in the presence of NMDA receptor antagonists DAP5 and PCP, however the fEPSP amplitude is reduced. As an aside, there is also a marked decrease in fEPSP amplitude after the initial post-tetanic potentiation (PTP), 0 – 2 minutes post stimulation, in the presence of DAP5 and PCP, however this has not been quantified (Figure 5.10aii-bii). Interestingly, this data also shows that PRE-084 increases LTP above control levels, suggesting σ1 receptor activation enhances *in vitro* CA1 LTP.

5.4.8 Modelling the acute impact of NMDA receptor hypofunction and neuroprotective effects of σ1 receptor activation on PV+ and SST+ interneurons, and PNNs, in rat ACC

The mechanisms underlying learning and memory are thought to be orchestrated by inhibitory interneurons, including PV+ and SST+ interneurons. PV+ interneurons are fast-spiking in nature, and are supported by PNNs, an extracellular structure that regulates interneuron excitability and supports neuronal plasticity. Human studies have found a loss of PV expression (Beasley and Reynolds, 1997, Chung et al., 2016, Hashimoto et al., 2003, Lewis et al., 2005, Sakai et al., 2008) and SST expression (Fung et al., 2010, Hashimoto et al., 2008) in the PFC of patients with schizophrenia. Post-mortem studies also found decreased PNN density in the dlPFC of patients with schizophrenia (Alcaide et al., 2019, Lisboa et al., 2024, Mauney et al., 2013).

Therefore, I used an acute slice model to explore the effects of NMDA receptor hypofunction, using PCP, on interneuron and PNN populations. In chapter 3, I showed that PCP drives abberantly large beta oscillations in the ACC. In this chapter, I have shown that ACC beta and gamma oscillations can be modulated by σ1 receptor activation. As KA-evoked CA3 gamma oscillations were not modulated by NMDA receptor antagonist PCP or σ1 receptor agonists, the rest of this thesis focuses on the ACC slice model.

ACC slices were placed in an interface electrophysiology recording chamber for 30 minutes and exposed to control or “pathological” conditions, via circulating bath solution, for 4 hours. Control slices were bathed in ACSF only. PV is a small, mostly cytosolic Ca^{2+}-binding protein expressed in GABAergic cortical interneurons (Hof et al., 1999, Jinno and Kosaka, 2004). Here, I found clear expression of PV in neuronal somas and processes across the ACC (Figure 5.11). PV was expressed in cell bodies that were and were not surrounded by PNNs. PV expression appeared in two bands, one in the superficial ACC (L2) and one in deep ACC (L5/6). SST is a neuropeptide also expressed by interneurons and acts as both a neurotransmitter and neuromodulator (Pittaluga et al., 2021). SST+ cells are the second largest population of GABAergic neurons in the cortex (Riedemann, 2019), however SST+ cells also include some long range projection neurons, the axons of which extend across

different cortical regions (Fisher et al., 2024). I also found clear SST immunoreactivity in neuronal somas and processes across the ACC in a similar pattern to PV. SST immunoreactivity was more punctated than PV, and the number of SST+ cells appeared far fewer than PV+ cells (Figure 5.11). No PNNs were seen surrounding SST+ cell bodies. WFA+ PNNs were present in the ACC with a clear net-like structure, specifically in L4/5, with few PNNs seen in L2/3 (Figure 5.11).

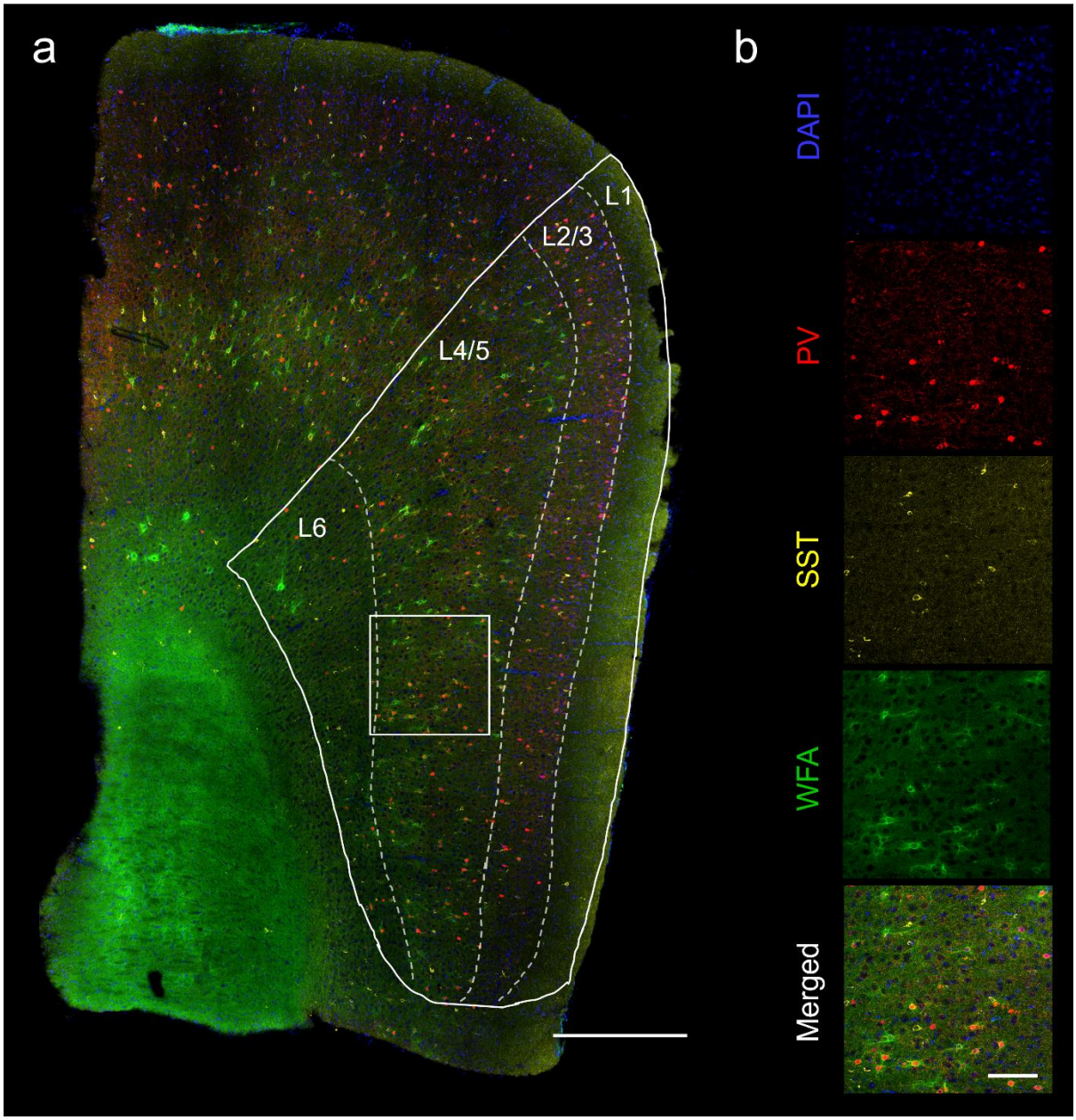

Figure 5.11 Expression of PV+ and SST+ interneurons, and PNNs in control ACC slices prepared from WT Lister hooded rat. Example (a) whole slice and (b) magnified x40 images showing PV+ neuronal somas and processes stained in red, SST+ neuronal somas and processes stained in yellow, and PNNs stained with WFA in green. All nuclei were stained with DAPI in blue. The ACC region is outlined in white, with L1-6 indicated with dashed lines. Scale bars = (a) 500 µm and (b) 100 µm.

To model ‘normal’ KA-evoked oscillations, slices were incubated in KA (800nM) for 4 hours. To model NMDA receptor hypofunction and subsequent ‘pathological’ oscillations, slices were incubated in KA (800 nM) and PCP (10 µM) for 4 hours. To assess the effect of σ1 receptor activation, slices were pre-incubated with PRE-084 (10 µM) during the initial 30 minute period, before also being incubated with KA (800 nM) and PCP (10 µM) for 4 hours. Slices were then PFA-fixed, re-sectioned and stained for WFA for PNNs (green), SST (yellow), and PV (red) (Figure 5.11). Sections were imaged on a confocal microscope (described in 5.3.3.3) and the %Area and ID of WFA, SST and PV immunofluorescence across the whole ACC region were measured and analysed (Figures 5.11 & 5.12).

σ1 receptors play a role in many of the identified pathological mechanisms of schizophrenia, including cognitive impairment, NMDA receptor modulation and oxidative stress, so I also explored whether activating σ1 receptors prior to PCP exposure alters the effect of PCP on interneuron or PNN density. PV functions as a calcium buffer, and calcium modulation activates σ1 receptors, which translocate to the plasma membrane to interact with NMDA receptors, enhancing NMDA currents (Martina et al., 2007, Rousseaux and Greene, 2016). Exposing slices to KA and PCP was expected to reduce PV expression compared to KA-only slices. Therefore, activating σ1 receptors with PRE-084 pre-incubation was expected to protect PV expression, compared to KA and PCP slices.

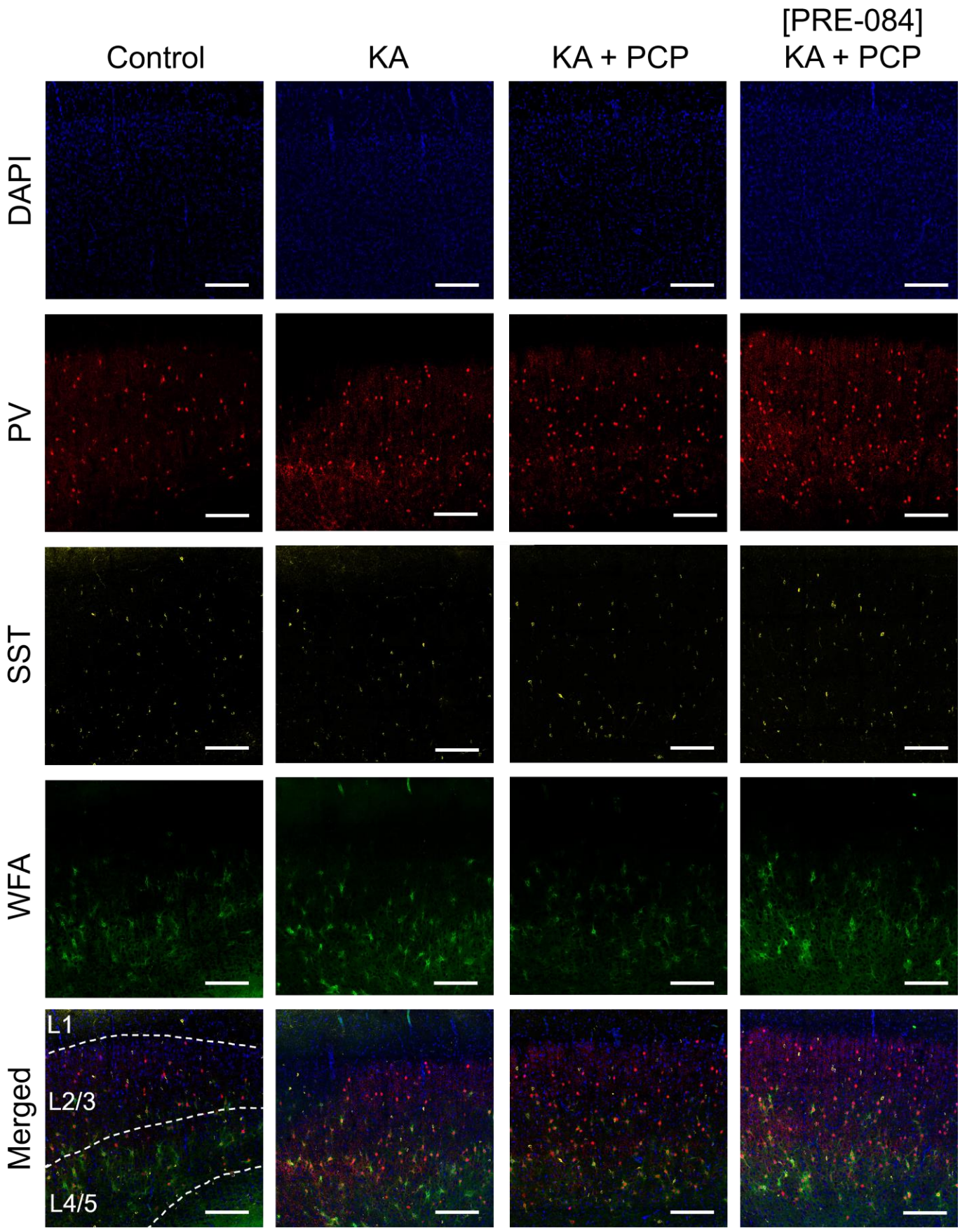
Control
KA
KA + PCP
[PRE-084]
KA + PCP
DAPI
PV
SST
WFA
Merged
L1
L2/3
L4/5

Figure 5.12 Expression of PV+ and SST+ interneurons, and PNNs in WT Lister hooded rat ACC slices exposed to NMDA receptor blockade and σ1 receptor activation. An example area taken across layers I – VI of the ACC showing expression of PV+ interneurons stained with PV (red), SST+ interneurons stained with SST (yellow), PNNs stained with WFA (green) and all nuclei stained with DAPI (blue), in slices exposed to control conditions (ACSF only); KA (800 nM) only; KA + PCP (10 µM), and pre-incubated with PRE-084 (10 µM) and then exposed to KA + PCP. Scale bar = 200 µm.

To quantify the amount of immunoreactivity, %Area was used to measure the amount of PV in cell bodies, axons, and dendrites. When comparing the PV+ %Area of the different conditions, there was no significant differences between any slice condition (Kruskal-Wallis X^2 = 1.78, p = 0.618; Figure 5.13a). Looking at the distribution of the data, a trend could be observed: those slices exposed to KA (0.239 [IQR 0.10 – 0.66]%) and KA + PCP 0.283 (IQR [0.14 – 1.04]) had a lower median PV+ %Area than control (0.283 [IQR 0.14 – 1.04]%). When pre-incubated with PRE-084, the median PV+ %Area of [PRE-084] KA + PCP slices (0.674 [IQR 0.25 – 0.88]%) was larger than that of KA and KA + PCP and the distribution was similar to that of control slices.

When comparing PV+ ID across conditions, again there were no significant differences between any conditions (Kruskal-Wallis X^2 = 4.91, p = 0.178; Figure 5.13b), however a trend could be observed. In all conditions exposed to KA, the median PV+ ID was less than the median PV+ ID of control slices (1030 [IQR 750 – 1293] AU) vs KA (602 [IQR 514 – 1005] AU); vs KA + PCP (671 [IQR 575 – 903] AU); vs [PRE-084] KA + PCP (747 [IQR 683 – 865] AU), however the median PV+ ID of slices pre-incubated with PRE-084 was slightly higher than KA and KA + PCP.

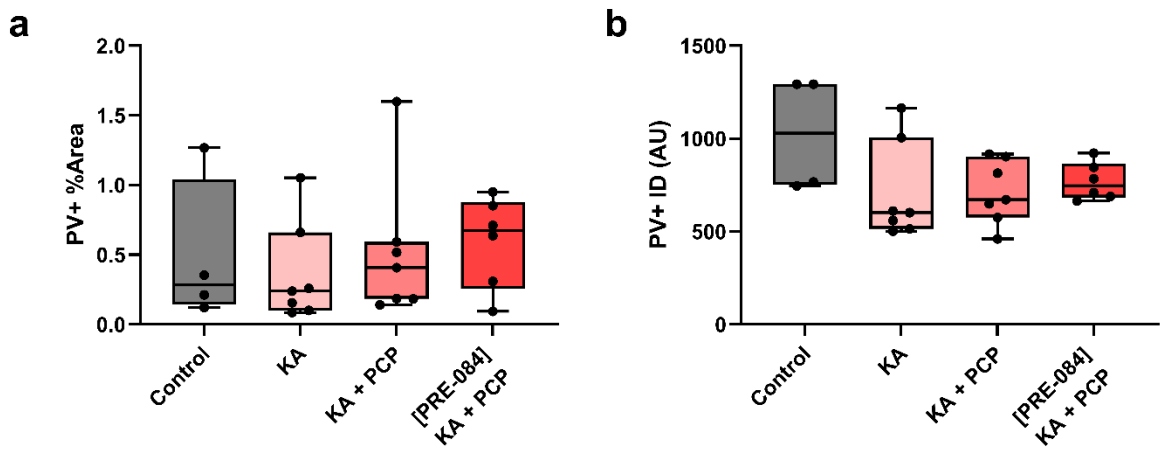

Figure 5.13 PV+ interneuron expression in WT Lister hooded rat ACC slices exposed to NMDA receptor blockade and σ1 receptor activation. The median (a) %Area and (b) ID (AU) of PV expression across the ACC in control (grey), KA (800 nM) only (light red), KA + PCP (10 µM; red), and pre-incubated with PRE-084 (10 µM) and then exposed to KA + PCP (dark red) slices. Animals (*N*) = 4 – 7 (represented by black data points).

When comparing the SST+ %Area of the different conditions, there was no significant differences between any slice condition (Kruskal-Wallis X^2 = 1.13, p = 0.770; Figure 5.14a). Looking at the distribution of the data, a trend could be observed: in all conditions exposed to KA, the median SST+ %Area was higher than the median SST+ %Area of control slices (control 0.1914 (IQR 0.08 – 0.30)% vs KA 0.403 (IQR 0.14 – 0.47)%; vs KA + PCP (0.202 (IQR 0.11 – 0.38)%; vs ([PRE-084] KA + PCP 0.259 (IQR 0.10 – 0.71)%).

However, interestingly, when comparing SST+ ID across conditions, there as a significant difference between at least two slice conditions (Kruskal-Wallis X^2 = 9.32, p = 0.025; Figure 5.14b). Post-hoc analysis showed the median SST+ ID of KA slices (313.4 [IQR 288 – 346] AU) was significantly higher than control (230.2 [IQR 184 – 235] AU) (Dunn's multiple comparisons; p = 0.037). Although not statistically significant, the median SST+ ID of KA + PCP (671 [IQR 575 – 903] AU) and [PRE-084] KA + PCP (747 [IQR 683 – 865] AU), were also higher than that of control (Figure 5.14b). Where the median SST+ ID of KA + PCP slices was similar to KA slices, slices pre-incubated with PRE-084 were slightly decreased from the KA and KA + PCP groups.

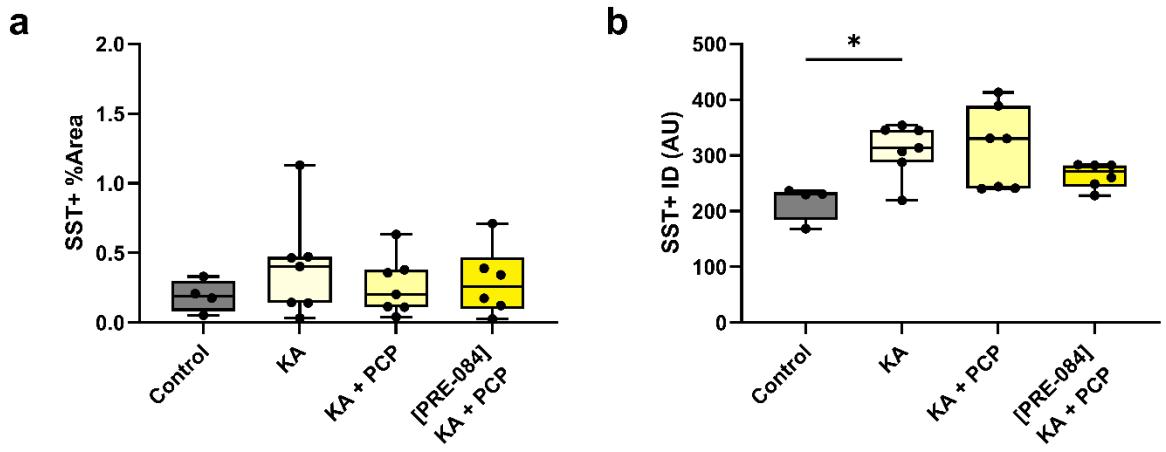

Figure 5.14 SST interneuron expression in WT Lister hooded rat ACC slices exposed to NMDA receptor blockade and σ1 receptor activation. The median (a) %Area and (b) ID (AU) SST expression across the ACC in control (grey), KA (800 nM) only (light yellow), KA + PCP (10 µM; yellow), and pre-incubated with PRE-084 (10 µM) and then exposed to KA + PCP (dark yellow) slices. Animals (*N*) = 4 – 7 (represented by black data points).

Although lacking statistical significance, the observed trends suggest that exposure to the different conditions has opposing effects on PV+ and SST+ expression (Figures 5.13 & 5.14). Where PV+ ID decreased following exposure to KA and KA + PCP, SST+ ID increased. Furthermore, where pre-incubation with PRE-084 slightly increased PV+ ID compared to KA + PCP, it reduced SST+ ID. Therefore, to see if there was a relationship between the two interneuron markers, I calculated the PV+ to SST+ ratio (PV+:SST+) of both %Area and ID across the 4 groups (Figure 5.15).

When comparing the ratio of PV+:SST+ %Area, there was no significant differences between any slice condition (Kruskal-Wallis $X^2 = 5.55$, $p = 0.136$; Figure 5.15a). However, there was a small decrease in the median PV+:SST+ %Area of the KA (1.40 [IQR 0.39 – 1.81]%) and KA + PCP (1.64 [IQR 1.45 – 2.02]%) slices, compared to control (2.18 [IQR 0.99 – 5.19]%). The median PV+:SST+ %Area of the PRE-084 slices was more comparable to control ([PRE-084] KA + PCP 2.35 [IQR 1.89 – 3.60]%).

When comparing the ratio of PV+:SST+ ID, there as a significant difference between at least two slice conditions (Kruskal-Wallis $X^2 = 8.33$, $p = 0.040$; Figure 5.15b). Post-hoc analysis showed the median SST+ ID of KA slices (1.92 [IQR 1.45 – 3.50] AU) was significantly less than control (4.95 [IQR 3.60 – 5.59] AU) (Dunn's multiple comparisons; $p = 0.038$). Although not statistically significant, the median PV+:SST+ ID of KA + PCP (2.66 [IQR 1.48 – 3.38] AU) and [PRE-084] KA + PCP (3.00 [IQR 2.48 – 3.19] AU), were also less than that of control (Figure 5.15b). Where the median SST+ ID of KA + PCP slices was similar to KA slices, slices pre-incubated with PRE-084 were slightly increased compared to the KA and KA + PCP groups.

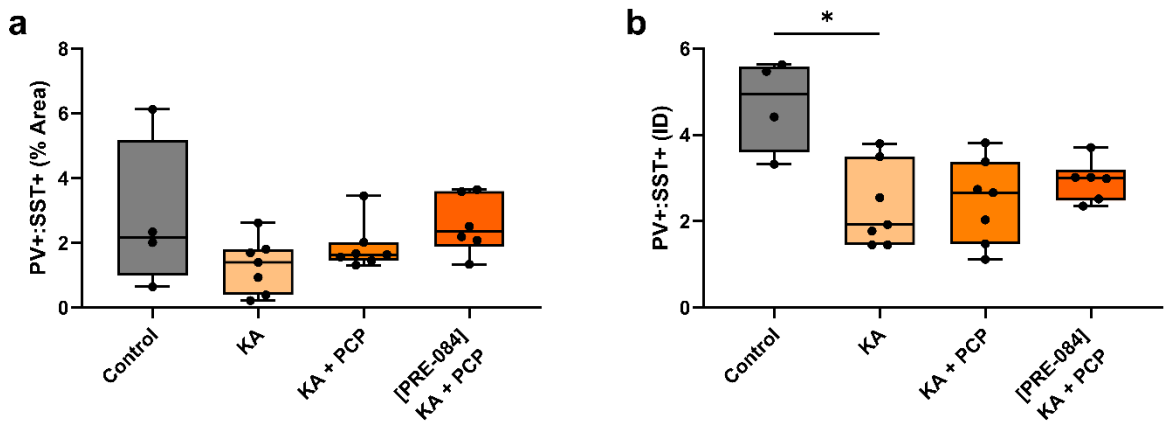

Figure 5.15 Ratio of PV to SST (PV+:SST+) expression in WT Lister hooded rat ACC slices exposed to NMDA receptor blockade and σ1 receptor activation. The median (a) %Area and (b) ID (AU) ratio of PV to SST expression across the ACC in control (grey), KA (800 nM) only (light orange), KA + PCP (10 µM; orange), and pre-incubated with PRE-084 (10 µM) and then exposed to KA + PCP (dark orange) slices. Following PCP exposure, the ratio of PV+:SST+ ID is significantly reduced compared to control. Animals (*N*) = 4 – 7 (represented by black data points).

The lectin *Wisteria floribunda* agglutinin (WFA) binds to the terminal N-acetylgalactosamine residues of CSPGs of PNNs (Young and Williams, 1985). Like PV, PNNs are also decreased in in post-mortem studies, specifically in the PFC (Alcaide et al., 2019, Lisboa et al., 2024, Mauney et al., 2013), vHPC (Shah and Lodge, 2013), and amygdala (Lisboa et al., 2024, Pantazopoulos et al., 2015) of patients with schizophrenia. PV expression is directly affected by the presence or absence of PNNs (Yamada and Jinno, 2014), therefore I would expect that WFA+ expression would follow a similar pattern to PV+ expression.

There was clear expression of WFA in the ACC in control slices (Figure 5.11), where a high density of PNNs could be seen in the deep layers, and with lower expression levels in the superficial layers. When comparing WFA %Area of the different conditions, there was no significant differences between any slice condition (Kruskal-Wallis $X^2 = 1.06$, $p = 0.788$; Figure 5.16a). When comparing WFA ID of the different conditions, there was also no significant differences between any slice condition (Kruskal-Wallis $X^2 = 1.06$, $p = 0.788$; Figure 5.16b). Although not statistically significant, a trend across the groups could be seen. The median ID of KA + PCP slices (371.5 [IQR 265 – 470] AU) was decreased compared to control (493.4 [IQR 298 – 1650] AU) and KA (512.6 [IQR 382 – 774] AU) slices. Furthermore, when pre-incubated with PRE-084, the median WFA ID was higher than KA+ PCP ID and more comparable to control values ([PRE-084] KA + PCP 442 [IQR 404 – 535] AU).

This data shows that acute exposure to PCP may reduce WFA-PNN binding in ACC slices, suggesting a decrease in PNNs. Due to high variability between sections and animals this conclusion is tentative, however, it does suggest that NMDA receptor hypofunction may reduce PNN size or integrity in rat ACC.

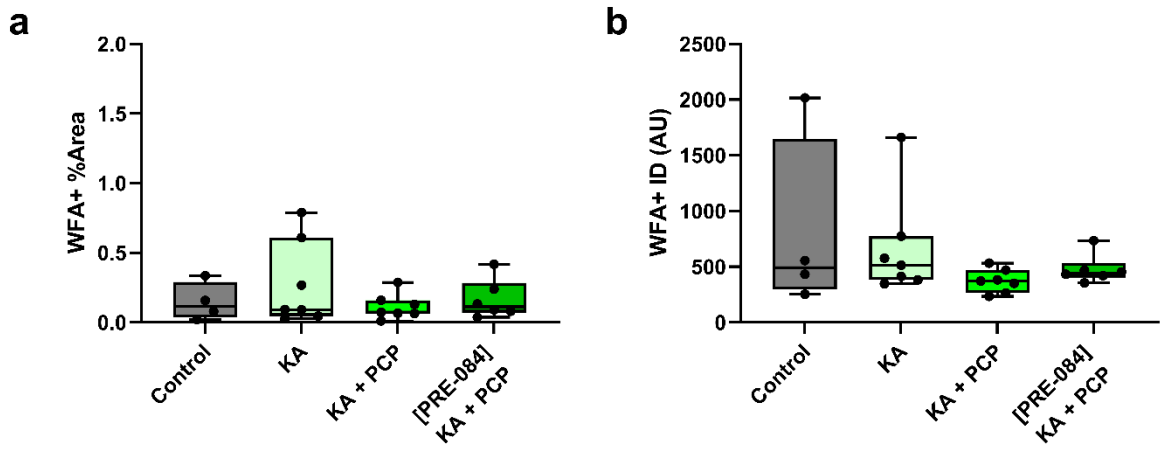

Figure 5.16 PNN expression in WT Lister hooded rat ACC slices exposed to NMDA receptor blockade and σ1 receptor activation. The median (a) %Area and (b) ID (AU) of WFA expression across the ACC in control (grey), KA (800 nM) only (light green), KA + PCP (10 µM; green), and pre-incubated with PRE-084 (10 µM) and then exposed to KA + PCP (dark green) slices. Animals (*N*) = 4 – 7 (represented by black data points).

5.4.9 Modelling the acute impact of NMDA receptor hypofunction and neuroprotective effects of σ1 receptor activation on astrocytes and microglia, in rat ACC

Neuroinflammation is a feature of psychosis in patients with schizophrenia, and not necessarily present in stable patients (Doorduin et al., 2009). Region specific neuroinflammation may evolve into chronic neuroinflammation which has been linked to schizophrenia pathology and reported in a number of post-mortem studies (Bayer et al., 1999, Radewicz et al., 2000, Wierzba-Bobrowicz et al., 2005). Glial changes have also been associated with the cognitive deficits (Anderson et al., 2013, de Oliveira Figueiredo et al., 2022, Zhuo et al., 2023). Therefore, I wanted to explore whether acute PCP exposure could drive early, acute neuroinflammation in my acute slice model of NMDA receptor hypofunction.

To assess the impact of PCP on neuroinflammation, I used the same acute slice model described in 5.4.7 to assess changes in reactive astrocytes (GFAP immunoreactivy) and microglia (Iba1 immunoreactivity). Activated σ1 receptors play a role in neuroprotection (Maurice et al., 2019, Mavlyutov et al., 2013, Mavlyutov et al., 2015). Therefore, I also assessed whether activating σ1 receptors using PRE-084 prior to PCP exposure may affect GFAP and Iba1 expression.

Slices were exposed to control, KA, KA + PCP, and [PRE-084] KA + PCP conditions, as described above (5.4.7), then PFA-fixed, re-sectioned and stained for GFAP for reactive astrocytes (red), and Iba1 for microglia (green) (Figure 5.17). Sections were imaged on a confocal microscope, using a random sampling approach (described in 5.3.3.3). The %Area and ID of GFAP and Iba1 were measured within each sample area and analysed (Figures 5.17 & 5.18).

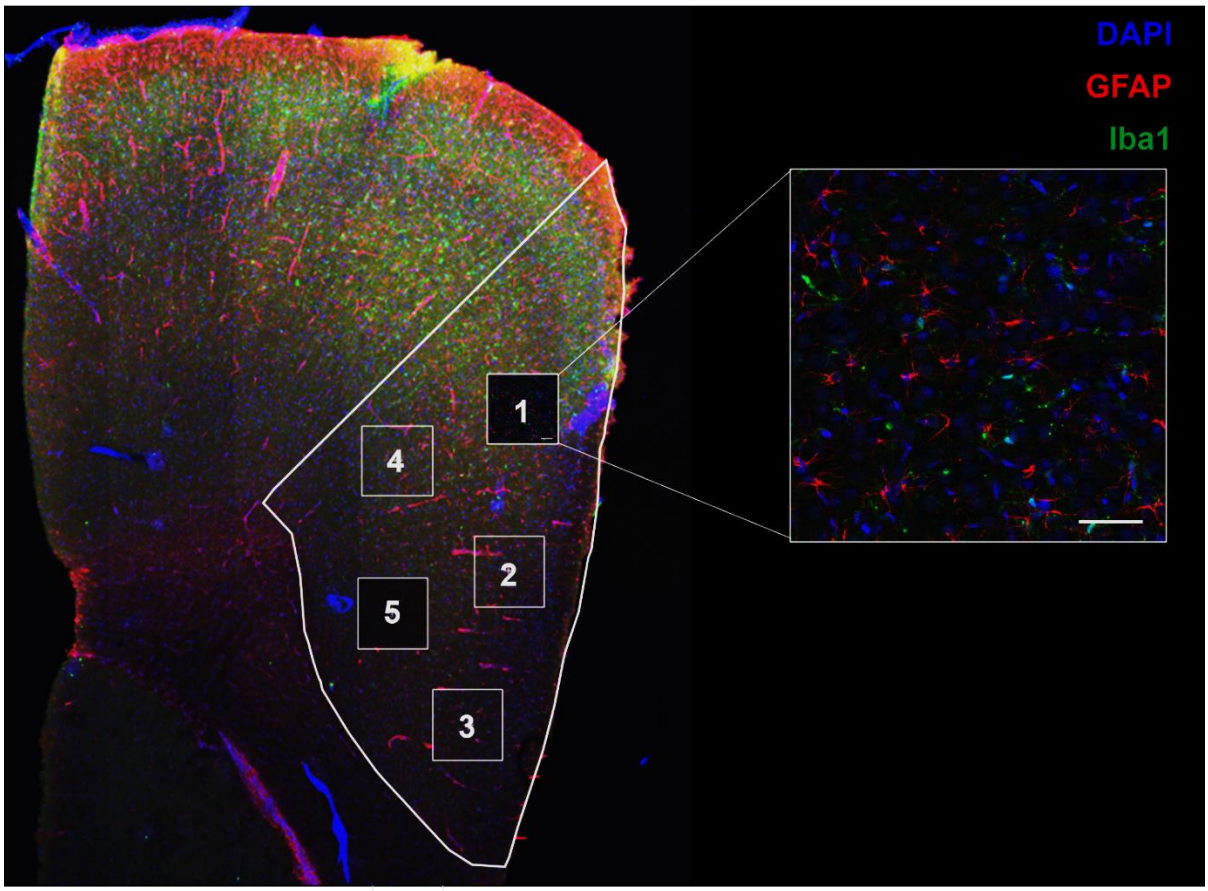

Figure 5.17 Microglia and reactive astrocytes in the ACC of control WT Lister hooded rat slices. Example whole slice and magnified x40 images showing reactive astrocytes stained with GFAP in red, microglia stained with Iba1 in green, and all nuclei stained with DAPI in blue. Z-stacks were taken from sample areas in the superficial (boxes 1 – 3) and deep (4 – 5) layers. Scale bar = 50 µm.

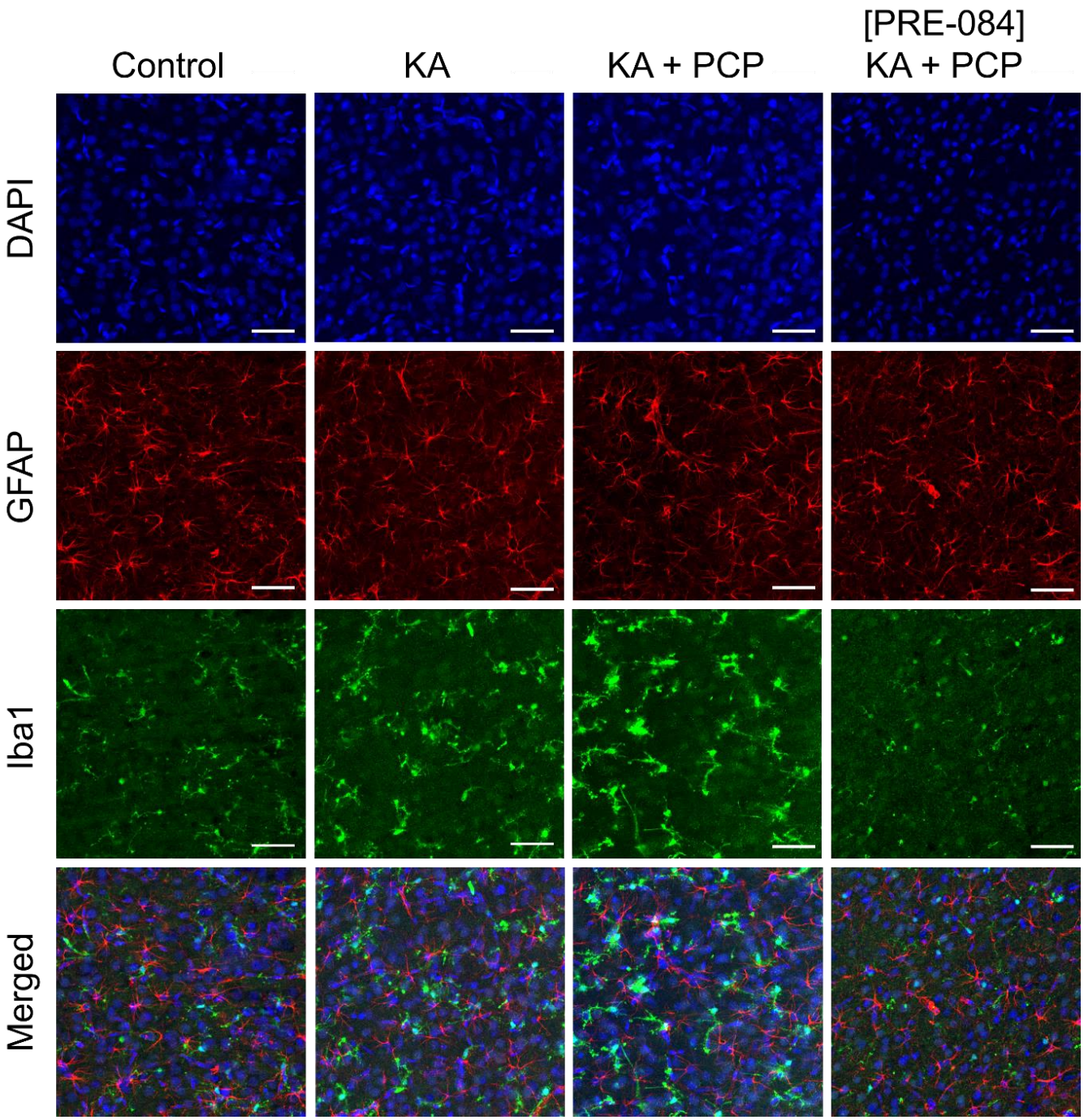

Figure 5.18 Microglia and reactive astrocytes in WT Lister hooded rat ACC slices exposed to NMDA receptor blockade and σ1 receptor activation. Expression of reactive astrocytes stained with GFAP (red), microglia stained with Iba1 (green), and all nuclei stained with DAPI (blue), in slices exposed to control conditions (ACSF only); KA (800 nM) only; KA + PCP (10 µM), and pre-incubated with PRE-084 (10 µM) and then exposed to KA + PCP. Scale bar = 50 µm.

I first compared GFAP+ expression across the whole ACC but found that when comparing GFAP+ %Area immunofluorescence of the different conditions, there was no significant differences between any slice condition (One-way ANOVA F (3, 21) = 0.4724, p = 0.705; Figure 5.19ai). When comparing the GFAP+ ID of the different conditions, there was also no significant differences between any slice condition (One-way ANOVA F (3, 21) = 0.09602, p = 0.961; Figure 5.19aii). This data suggests that there are no changes in GFAP %Area or ID across the ACC *in vitro*, when acutely exposed to PCP. There are also no further changes when activating σ1 receptors, using PRE-084.

Laminar distribution of reactive astrocytes can vary, as reported by Al-Musawi et al. (2024) in the hippocampus. As there was no change in mean GFAP+ expression across the whole ACC, I next divided my sample areas into superficial and deep layers to assess whether there were any laminar changes (Figure 5.19b).

A two-way ANOVA was performed to analyse the effect of slice condition and cortical layer on mean GFAP+ %Area (Figure 5.19bi). A two-way ANOVA revealed that there was not a statistically significant interaction between the effects of slice condition and layer (F (3, 21) = 0.1539, p = 0.926). Simple main effects analysis showed that slice condition did not have a statistically significant effect on GFAP+ %Area (p = 0.686). However, simple main effects analysis showed that layer did have a statistically significant effect on GFAP+ %Area (p = 0.001), where the mean GFAP+ %Area was higher in superficial layers (8.387 ± 0.74%) compared to deep layers (6.161 ± 0.81%), of the ACC.

A two-way ANOVA was also performed to analyse the effect of slice condition and cortical layer on mean GFAP+ ID (Figure 5.19bii). A two-way ANOVA revealed that there was not a statistically significant interaction between the effects of slice condition and layer (F (3, 21) = 0.1968, p = 0.897). Simple main effects analysis showed that slice condition did not have a statistically significant effect on GFAP+ ID (p = 0.695). Again, simple main effects analysis did show that layer had a statistically significant effect on GFAP+ ID (p < 0.001), where the mean GFAP+ ID was higher in superficial layers (1609 ± 123 AU) compared to deep layers (1170 ± 81.5 AU), of the ACC.

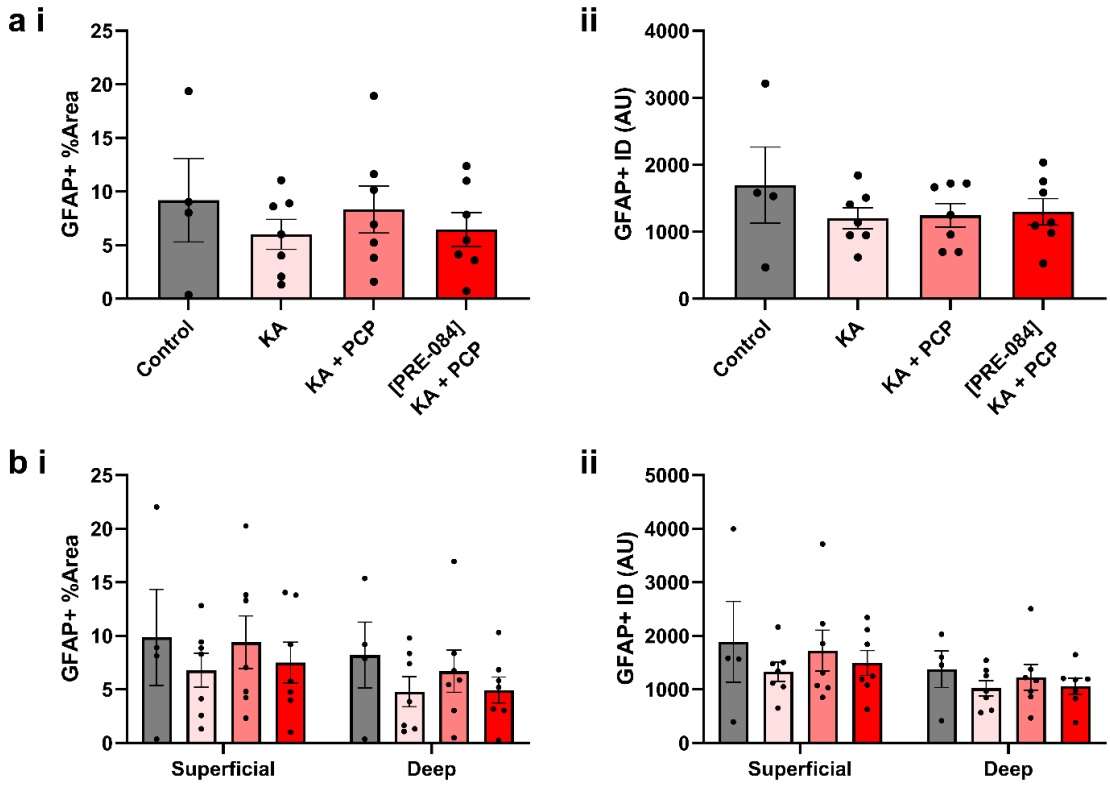

Figure 5.19 GFAP immunofluorescence in WT Lister hooded rat ACC slices exposed to NMDA receptor blockade and σ1 receptor activation. (a) The mean (i) %Area and (aii) ID (AU) of GFAP expression across the ACC in control (grey), KA (800 nM) only (light red), KA + PCP (10 µM; red), and pre-incubated with PRE-084 (10 µM) and then exposed to KA + PCP (dark red) slices. (b) The mean (i) %Area and (bii) ID (AU) of GFAP expression seperated into superficial and deep layers of the ACC in control (grey), KA (800 nM) only (light red); KA + PCP (10 µM; red), and pre-incubated with PRE-084 (10 µM) and then exposed to KA + PCP (dark red). Animals (*N*) = 4 – 7 (represented by black data points).

Next, I compared Iba1+ expression across the whole ACC, but found that when comparing Iba1+ %Area of the different conditions, there was no significant differences between any slice condition (One-way ANOVA F (3, 21) = 0.988, $p = 0.418$; Figure 5.20ai). When comparing the Iba1+ ID of the different conditions, there was no significant differences between any slice condition (One-way ANOVA F (3, 21) = 1.732, $p = 0.191$; Figure 5.20aii). This data suggests that there are no changes in Iba1 %Area or ID across the ACC *in vitro*, when acutely exposed to PCP. There are also no further changes when activating σ1 receptors, using PRE-084.

However, when looking at the distribution of the data, a trend could be observed: following incubation with KA, mean Iba1+ %Area was higher (2.029 ± 0.59%) compared to control (1.90 ± 0.50%). When incubated with KA + PCP, mean Iba1+ %Area was 2.43 (± 0.69)%, higher compared to KA alone. When pre-incubated with the σ1 receptor agonist, mean Iba1+ %Area was lower (1.55 ± 0.33%), than KA + PCP and control slices. A similar trend was seen when looking at the distribution of GFAP+ ID: control 982.2 ± 123 AU; KA 1139 ± 211 AU; KA + PCP 1154 ± 186 AU; [PRE-084] KA + PCP 709 ± 53.7 AU.

As there were no significant differences in Iba1+ expression between groups across the whole ACC, I again divided my sample areas into superficial and deep layers to assess whether there were any significant laminar differences (Figure 5.20b).

A two-way ANOVA was performed to analyse the effect of slice condition and cortical layer on mean Iba1+ %Area (Figure 5.20bi). A two-way ANOVA revealed that there was not a statistically significant interaction between the effects of slice condition and layer F (3, 21) = 0.6338, $p = 0.602$). Simple main effects analysis showed that slice condition did not have a statistically significant effect on Iba1+ %Area ($p = 0.401$). Simple main effects analysis showed that layer also did not have a statistically significant effect on Iba1+ %Area ($p = 0.058$).

A two-way ANOVA was also performed to analyse the effect of slice condition and cortical layer on mean Iba1+ ID (Figure 5.20bii). A two-way ANOVA revealed that there was not a statistically significant interaction between the effects of slice condition and layer (F (3, 21) = 0.2613, $p = 0.853$). Simple main effects analysis showed that slice condition did not have a statistically significant effect on Iba1+ ID ($p = 0.326$). Simple main effects analysis showed that layer also did not have a statistically

significant effect on Iba1+ ID (p = 0.060). Again, looking at the distribution, the laminar data demonstrated the same trend described above, and was consistent across the superficial and deep layers. This data also suggests that microglia cells are evenly distributed across the layers of the ACC, similar to findings in the hippocampus (Al-Musawi et al., 2024, Jinno et al., 2007).

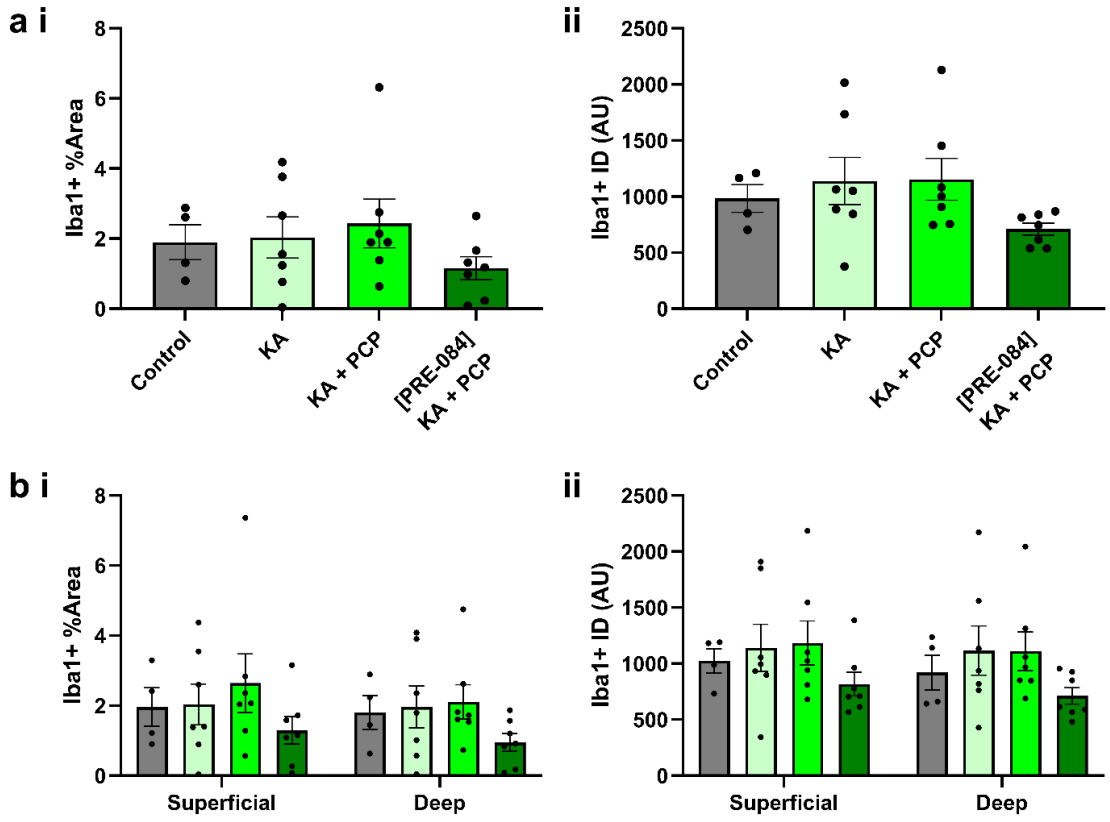

Figure 5.20 Iba1 immunofluorescence in WT Lister hooded rat ACC slices exposed to NMDA receptor blockade and σ1 receptor activation. (a) The mean (i) %Area and (ii) ID (AU) of Iba1 expression across the ACC in control (grey), KA (800 nM) only (light green), KA + PCP (10 µM; green), and pre-incubated with PRE-084 (10 µM) and then exposed to KA + PCP (dark green) slices. (b) The mean (i) %Area and (ii) ID (AU) of Iba1 expression seperated into superficial and deep layers of the ACC in control (grey), KA (800 nM) only (light green); KA + PCP (10 µM; green), and pre-incubated with PRE-084 (10 µM) and then exposed to KA + PCP (dark green). Animals (*N*) = 4 – 7 (represented by black data points).

5.5 Discussion

Summary of the main findings in Chapter 5:

- SKF-10047, a mixed σ1 receptor agonist and NMDA receptor antagonist, increased KA-evoked ACC beta and gamma oscillation power, similar to PCP. Unlike PCP, SKF-10047 did not cause gamma oscillations to shift to a beta frequency.
- σ1 receptor agonists SKF-10047 and PRE-084 had no effect on KA-evoked CA3 gamma oscillations.
- The σ1 receptor antagonist NE-100 blocked the action of SKF-10047 action in the ACC, and attenuated PCP effect, on beta and gamma oscillations. The σ1 receptor agonist PRE-084 also partially blocked the effects of PCP KA-evoked ACC gamma oscillations.
- When applied alone, PRE-084 induced a small increase in ACC gamma oscillation power, but not beta.
- Acute exposure of ACC slices to KA decreased PV expression, whilst increasing SST expression. Addition of PCP or PRE-084 had little effect on levels of expression.
- Acute exposure of ACC slices to KA + PCP marginally increased expression of the microglial marker Iba1 and may be normalised by activating σ1 receptors. No effect of PCP or PRE-084 was found in reactive astrocytes.

Early behavioural observations found SKF-10047 caused a psychosis-like state and a new sub-type of opioid receptor, the “sigma / opioid receptor”, was proposed (Martin et al., 1976). It was later discovered through binding assays that the identified SKF-10047 binding protein was not a type of opioid receptor (Su, 1982), and the receptor was renamed the “sigma receptor”. SKF-10047 caused further confusion as it reportedly had high affinity for the PCP-binding site on the NMDA receptor (Vaupel, 1983), as an NMDA receptor antagonist (Nishikawa et al., 2000). PCP is also non-specific and has a considerable affinity for σ receptors, where it also acts as a σ1 receptor agonist (Vaupel, 1983). Later binding studies using specific ligands for both

the PCP-binding site (tenocyclidine) and σ receptors (pentazocine), clearly distinguished the two receptors (Gundlach et al., 1986, Largent et al., 1986, Tam, 1985). The affinity of SKF-10047 for the PCP-binding site on NMDA receptors likely accounts for its psychosis-like effects and the behavioural similarities observed with PCP. In this chapter, I have demonstrated that when applied to KA-evoked ACC beta and gamma oscillations, SKF-10047 has a very similar effect on oscillation power to that seen with PCP, likely due to the NMDA receptor antagonist effect of SKF-10047. Interestingly, when applied to KA-evoked ACC gamma oscillations, SKF-10047 did not cause a shift to a beta frequency oscillation, as was seen with PCP. This could suggest that SKF-10047 has a greater effect on PV+ interneuron NMDA receptors, than those on SST+ interneurons, driving gamma oscillations and not beta oscillations, however this needs further investigation.

The acute actions of σ1 receptors include modulation of ion channels, namely NMDA receptors, and K^+ channels and IP3 receptors. A number of current antipsychotics are σ1 receptor agonists, and may have pro-cognitive effects by activating σ1 receptors (Hayashi and Su, 2004). Using a selective σ1 receptor agonist, PRE-084, only a modest increase in KA-evoked ACC gamma power was induced, whilst having no effect on beta oscillation power. A reduced effect on oscillations with a specific σ1 receptor agonist suggests that the PCP exerts its effects through NMDA receptors. However, this increase in gamma does suggest that activating σ1 receptors modulates PV+ interneurons to some degree.

PCP blocks NMDA channels at sub-micromolar ranges, suggesting that the remarkably large increases in KA-evoked beta and gamma power in the ACC are due to modulation by NMDA receptor antagonism. Early *in vivo* experiments found that both PCP and SKF-10047 increased cortical EEG spectral power between 20 and 50 Hz, in female rats, but was not changed by MK-801 (Marquis et al., 1989). Unlike PCP, MK-801 is not considered a σ1 receptor ligand (Rousseaux and Greene, 2016). This would suggest that it is, in part, the σ1 receptor agonist component of PCP, and not NMDA receptor antagonism, that drives an increase in oscillatory power. This idea is supported by my findings in chapter 3.4.4 where PCP increased KA-evoked beta power, but other NMDA receptor antagonists MK-801 and DAP5 did not.

The mechanisms underlying σ1 receptor and NMDA receptor interactions are not fully understood. Daily administration of PCP (10 mg/kg), over 10 days followed by a three day washout period, reduces levels of σ1 receptors in the frontal cortex and hippocampus of mice, as determined by western blot (Ishima et al., 2009). These associations between σ1 receptors and NMDA receptors suggest σ1 receptors could play a significant role in modulating PCP effects on beta and gamma oscillations. Yet, it has been reported that σ1 receptor activation increases NMDA receptor subunit GluN2 expression at the plasma membrane of hippocampal cells of mice exposed to PRE-084 *in vivo*, possibly by σ1 receptors associating with newly synthesized NMDA receptors and trafficking them to the membrane (Pabba et al., 2014). σ1 receptor agonists enhance the affinity of the σ1 receptor for GluN1 binding (Balasuriya et al., 2013, Rodríguez-Muñoz et al., 2015), and potentiate NMDA currents (Martina et al., 2007), thus enhancing NMDA receptor function. This appears to be supported by *in vivo* behavioural data that found PRE-084 and SA4503, another selective σ1 receptor agonist, attenuated MK-801-induced behavioural cognitive deficits in mice (Maurice et al., 1994, Maurice and Privat, 1997). Subchronic administration of the antidepressant fluvoxamine, a selective serotonin reuptake inhibitor (SSRI) and σ1 receptor agonist, had a similar effect and significantly improved PCP-induced cognitive impairment in mice (Hashimoto et al., 2007). The cognitive improvement was also reversed by treatment with the σ1 receptor antagonist NE-100 (Hashimoto et al., 2007). This effect was also seen with the cognitive enhancer donepezil and was again reversed by NE-100 (Kunitachi et al., 2009), suggesting σ1 receptor activation has a therapeutic effect on NMDA receptor hypofunction.

Here, I have modelled previous *in vivo* findings in my ACC slice model of NMDA receptor hypofunction, using gamma oscillations as a biomarker for cognitive dysfunction. Remarkably, PRE-084 blocked the effect of PCP on KA-evoked gamma oscillations. Not only was the increase in oscillation power attenuated, the shift from gamma to beta was also reduced. Interestingly, PRE-084 did not attenuate PCP's effect on beta power. Gamma oscillations are orchestrated by PV+ interneurons whereas SST+ interneurons are proposed to orchestrate beta oscillations (Chen et al., 2017, Fuchs et al., 2007, Kuki et al., 2015, Tamás et al., 2000, Whittington et al., 1995). σ1 receptors are widely expressed in principal neurons and interneurons, including PV+ and SST+ interneurons (Liu et al., 2023). σ1 receptors may have less modulatory

interactions with NMDA receptors on SST+ interneurons, compared to PV+ interneurons.

The pharmacology of σ1 receptors is complex and reconciling all the different reported NMDA-σ receptor interactions with my data is not straightforward. σ1 receptor antagonists, such as NE-100, reduce the affinity of σ1 receptors for GluN1 binding, reducing NMDA receptor function (Rodríguez-Muñoz et al., 2015). This is contradictory to my findings where, in the presence of NE-100, a σ1 receptor antagonist, the PCP-induced increase in beta power was somewhat attenuated, compared to PCP alone. However, literature regarding the direct effect of σ1 receptor antagonism on PCP oscillation action is lacking. It would be interesting in future studies to look at the effect of NE-100 on oscillations in animals treated with PCP, *in vivo*.

The small reduction in PCP enhanced oscillatory power I observed with NE-100 could be due to NE-100 blocking the σ1 receptor component of PCPs action. Confusingly, similar effects were seen with both the σ1 receptor agonist PRE-084 and antagonist NE-100. σ1 receptor agonists show a bell-shaped dose-response curve characterized by low-dose stimulation and high-dose inhibition (Cobos et al., 2008). As PCP is also a σ1 receptor agonist, it may be that when PRE-084 and PCP were co-applied, the activation of σ1 receptors tipped from stimulation to inhibition, impairing the PCP effect, like seen with NE-100 + PCP.

There is convincing evidence that treatment with selective σ1 receptor agonists, such as PRE-084, is beneficial in attenuating the NMDA receptor hypofunction induced by PCP. Whilst some of my findings support this, the intricacies of σ1 receptor pharmacology and its effects on NMDA receptor activity complicate the interpretation of the interactions between σ1 receptors and NMDA receptors. These findings imply that the attenuation of PCP-induced effects by both NE-100 and PRE-084 could result from different mechanisms converging on σ1 receptor regulation, which in turn alters NMDA receptor function. Further research is needed to clarify the dose-dependent and receptor-specific factors that underlie these complex pharmacological interactions.

In contrast to its effects in the ACC, PCP did not modulate KA-evoked gamma oscillations in the CA3 region, nor did SKF-10047 or PRE-084. Surprisingly, given the

interest in the role of σ1 receptors and learning and memory, no studies have been conducted assessing the effect of a σ1 receptor agonist on hippocampal gamma oscillations. This regional specificity may relate to differences in σ1 receptor expression. Notably, there is a higher level of σ1 receptor mRNA in the frontal lobe of the adult male rat compared to the hippocampus, as determined by northern blot and *in situ* hybridization (Zamanillo et al., 2000). Despite this, σ1 receptor expression is frequently reported to be particularly high in the hippocampus (Sałaciak and Pytka, 2022). Additionally, Mishina et al. (2008) have shown that σ1 receptors exhibit a greater binding potential in the hippocampus compared to the frontal lobe. Within the hippocampus, σ1 receptor expression is higher in the pyramidal cell layer of CA3 higher than CA1 and CA2 (Kitaichi et al., 2000), suggesting functional variability. Interestingly, *in vivo* studies report that high doses of PCP and other NMDA receptor antagonists enhance hippocampal gamma oscillations (Ehrlichman et al., 2009; Saunders et al., 2012). This discrepancy between *in vivo* and *in vitro* findings underscores the need for further investigation into compensatory mechanisms in hippocampal networks. Regarding the PFC, specific σ1 receptor distribution studies are lacking, however it is known that there is higher σ1 receptor expression in the deeper laminae than superficial (Kitaichi et al., 2000). Better understanding of σ1 receptor distribution could help understand specific regional differences.

Stable KA-evoked CA3 gamma oscillations are not modulated by NMDA receptor antagonist PCP or σ1 receptor agonists. Given the integral role of the hippocampus in learning and memory (Eichenbaum, 1999, Kandel and Spencer, 1968), these findings are surprising. Leung (1985) showed that a high dose of PCP increased hippocampal gamma oscillations, *in vivo.* A number of other *in vivo* studies have found that NMDA receptor antagonists, ketamine and MK-801, also enhance gamma power *in vivo* (Ehrlichman et al., 2009, Kittelberger et al., 2012, Lazarewicz et al., 2010, Saunders et al., 2012). The hippocampus is a densely packed, highly organised laminar structure of neurons, that may be able to compensate for acute NMDA receptor blockade *in vitro*. *In vivo,* the hippocampus receives inputs from other brain regions, including the ACC and amygdala, via the EC (Rolls, 2019). Slice preparation and hippocampal isolation severs inputs to the EC, therefore *in vitro* preparations may restrict the effect of PCP in the CA3 by reducing NMDA receptor-mediated inputs. Further investigations should be performed to confirm this.

Beyond oscillations, I found that σ1 receptor activation enhanced LTP in the CA1 region. While beta and gamma oscillations are known to be critical for learning and memory the cellular correlate of learning has been proposed to be LTP. LTP induction requires postsynaptic activation of NMDA receptors and an increase in postsynaptic Ca^{2+} (Collingridge et al., 1983, Lynch et al., 1983).

LTP can be reliably induced using a 2 burst HFS along the Schaffer collateral pathway of CA1 in the rat hippocampus, as previously reported (Harris et al., 1984, Mosleh et al., 2023). Although not entirely inhibited, LTP was significantly attenuated in the presence of NMDA receptor antagonists DAP5 and PCP. Early LTP studies in rat CA1 found that DAP5 (50 μM) (Harris et al., 1984) and PCP (10 μM) (Stringer et al., 1984), completely blocked LTP, however, this could be due to slight variations in stimulation protocols or slice preparation techniques.

While NMDA receptor antagonists attenuated LTP, I found PRE-084 significantly enhanced LTP following HFS. Martina et al. (2007) reported that pentazocine, another high-affinity and high-specificity σ1 receptor agonist, activates σ1 receptors and potentiates NMDA receptor responses and LTP, preventing a small conductance Ca^{2+}-activated K^+ current (SK channels). These results align with reports of σ1 receptor agonists potentiating NMDA receptor responses and improving cognitive deficits in rodent models of NMDA receptor hypofunction (Hashimoto et al., 2007). Whether σ1 receptor activation can rescue PCP-induced impairments in LTP remains an important area for future research.

KA exposure increased SST expression while reducing PV expression and PNNs in the ACC, suggesting differential activation of interneuron subtypes. PV+ and SST+ interneurons play distinct roles in neuronal oscillations, with PV+ interneurons driving gamma oscillations and SST+ interneurons driving beta oscillations. PV acts as a calcium buffer, protecting neurons from calcium overload (Heizmann, 1993, Lee et al., 2000), while SST+ is a neuromodulator involved in synaptic transmission (Pittaluga et al., 2021).

Both SST and PV expression are activity-dependent (Hou and Yu, 2013, Patz et al., 2004), this suggests that SST+ interneurons were more active in KA-treated slices, compared to control, leading to increased SST expression. SST+ interneurons receive strong intracortical excitation and some inhibit PV+ interneurons (Tremblay et

al., 2016). A subpopulation of non-Martinotti SST+ interneurons, named X94-neurons, mediate inhibition on PV-interneurons in both layers 2/3 and 5 (Pfeffer et al., 2013) and could establish a shift from somatic PV+ interneuron-driven inhibition to dendritic SST+ interneuron-driven inhibition (Scheyltjens and Arckens, 2016). This implies that PV expression was reduced by increased SST+ interneuron activity. The presumed increase in SST interneuron activity may also explain the shift to lower beta frequency activity I observed with PCP application.

Many studies to-date have investigated the subchronic effect of NMDA receptor antagonist on the levels of PV expression, rather than assess the acute effects of PCP. One subchronic study found that PV expression was unaffected by subchronic PCP or ketamine treatment in adult mice and rats (Benneyworth et al., 2011). A subchronic PCP study, looking specifically at the adult rat PFC, found reduced PV+ cell density compared to control (McKibben et al., 2010). Particularly, there was a greater reduction in the infralimbic and prelimbic PV+ cell density, compared to the ACC (McKibben et al., 2010). More recently, PV protein was also found to be reduced in mouse frontal cortex and hippocampus following subchronic PCP treatment, compared to vehicle treated controls (Gigg et al., 2020). Romón et al. (2011) investigated acute effects of NMDA receptor antagonists, sacrificing rats 4- and 24 hours following injection (1 mg/kg; i.p.) with MK-801. They reported no change in PV mRNA in the PFC after 4 hours, but a decrease 24 hours post-injection. Hervig et al. (2016) conducted an acute study that sacrificed rats 1 hour after PCP injection (10 mg/kg; s.c.), and measured PV and c-Fos immunoreactivity. c-Fos is an immediate early gene whose expression indicates increased neuronal activity in response to stimuli (Bullitt, 1990). They found that there was no increase in ACC or PFC of PV labelled cells co-labelled with c-Fos in the PCP treated group, compared to vehicle treated controls. These results, paired with my own findings suggest that an acute 4 hour PCP exposure may not be sufficient to change PV expression in the ACC.

Most PV+ and SST+ interneurons express σ1 receptors, with around 80-90% of PV+ interneurons and ~90% of SST+ interneurons immunoreactive for the σ1 receptor, in the mouse ACC (Liu et al., 2023), however, there is, to my knowledge no other studies exploring the effect of σ1 receptor activation on PV and SST expression. PV functions as a calcium buffer, and calcium modulation activates σ1 receptors, which translocate to the plasma membrane to interact with NMDA receptors,

enhancing NMDA currents (Martina et al., 2007, Rousseaux and Greene, 2016). Therefore, PRE-084 was expected to buffer PCP-induced NMDA receptor hypofunction, and cause less of a reduction in PV expression, compared to KA + PCP slices. My electrophysiological data showed that PRE-084 attenuated PCP's effect on KA-evoked gamma oscillations in the ACC but immunofluorescence staining found it had little impact on PV expression.

When applied to KA-evoked beta oscillations, PCP caused a significant increase in beta power, which PRE-084 did not attenuate. I anticipated PCP would increase SST expression, with no change under PRE-084 pre-incubation. However, no changes in SST expression were observed with either PCP or PRE+084 and PCP. SST expression depends on BDNF signalling (Glorioso et al., 2006, Guilloux et al., 2012, Martinowich et al., 2011), and NMDA receptor inhibition decreases BDNF (Hansen et al., 2004), which likely reduces SST expression. σ1 receptor activation increases BDNF release, suggesting PRE-084 should enhance SST expression (Lin and Sibille, 2015), yet my results showed no effect of either PCP or PRE-084 beyond KA application. Like PV, 4 hours of PCP exposure may not be sufficient to change SST expression in the ACC and a subchronic treatment regimen could be a better method for assessing the effects of σ1 receptor activation on interneuron changes.

The GluN2A and GluN2C NMDA receptor subunits are highly expressed in PV interneurons, compared to neighbouring pyramidal cells (Picard et al., 2019). Specific knockout of the GluN2A subunit in mice ($GluN2A^{-/-}$) disrupts sensorimotor gating, and impairs cognitive function and spatial working memory, compared to WT. These $GluN2A^{-/-}$ mice also showed a significant increase in neuropeptide Y (NPY) and SST expression (Lu et al., 2024). NPY alterations have also been associated with schizophrenia (Stålberg et al., 2014) and NPY promotes dopamine release by activating σ1 receptors (Ault and Werling, 1997). Furthermore, immunofluorescence staining showed a significant increase in NPY-positive cell density in mPFC of $GluN2A^{-/-}$ mice (Lu et al., 2024).

A trend similar to PV expression was observed when comparing WFA ID across groups. This suggests that application of KA + PCP reduced PNNs, compared to KA slices. Memory consolidation within the ACC is dependent on PNN formation (Shi et al., 2019). A key role of PNNs is to protect neurons from oxidative stress. PNN density

can decrease rapidly in response to specific stimuli (Fawcett et al., 2022). Acute stress or neuronal activity can also trigger rapid PNN remodeling, partly through the release of metalloproteinases, which alter the extracellular matrix structure (Fawcett et al., 2022). Increased levels of oxidative stress are associated with schziophrenia (Murray et al., 2021) and is a known pathological mechanism causing PV+ interneuron impairment. Here we found that PNN density decreased with PV decrease. Evidence sugests that PNNs are themselves susceptible to oxidative stress when oxidative burden is high, causing both PV+ interneuron and PNN impairment (Steullet et al., 2017). This would suggest that overactivation of SST+ interneurons imparied PV+ interneurons, and PNNs, by increasing oxidative stress.

Finally, acute PCP exposure in ACC slices increased neuroinflammatory markers, with trends indicating elevated microglial activation. Neuroinflammation, driven by interactions between neurons and glial cells like astrocytes and microglia, can harm the CNS when it becomes acute or chronic (Minogue, 2017). Chronic neuroinflammation is linked to schizophrenia pathology, with changes in microglia and astrocytes contributing to cognitive deficits in the disorder (Anderson et al., 2013, de Oliveira Figueiredo et al., 2022, Zhuo et al., 2023). Changes in expression of interneuron markers have been linked with increased neuroinflammation and oxidative stress, caused by NMDA receptor hypofunction. In this chapter, I aimed to link decreased PV expression, caused by NMDA receptor hypofunction, and increased neuroinflammation, in my ACC slices.

Increased levels of ROS and oxidative stress damage are reported in studies of patients with schizophrenia, microglia produce ROS and microglial ROS likely contributes to increased oxidative stress (Simpson and Oliver, 2020). In this chapter, I found a trend that showed KA increased Iba1 %Area and ID compared to control slices, with further increases following KA + PCP treatment. These findings suggest that acute PCP exposure may increase microglia expression in ACC slices *in vitro*. In a review of schizophrenia animal models, Steullet et al. (2017) reported that PV+ interneuron deficits in the ACC were in all cases accompanied by oxidative stress. Paired with my findings, this suggests that microglial activation occurs first, and PV changes occur following a more prolonged period of NMDA receptor hypofunction. To explore this further, more sensitive markers could be used in combination with Iba1, such as inducible nitric oxide synthase (iNOS), a marker for oxidative stress.

Activation of σ1 receptors reportedly has neuroprotective effects, including the reduction of oxidative stress and neuroinflammation (Jia et al., 2018). It is hypothesised that activating σ1 receptors has therapeutic potential in cognitive disorders (Gekker et al., 2006, Hashimoto et al., 2007). Pre-incubation with PRE-084 prior to KA + PCP exposure reduced Iba1 %Area and ID compared to untreated slices, suggesting σ1 receptor activation decreases microglial reactivity. Microglia express high levels of σ1 receptors, and *in vitro* studies show that σ1 receptor activation suppresses microglial migration, cytokine release, and actin cytoskeleton rearrangement by modulating intracellular calcium (Hall et al., 2009). Similarly, in a mouse model of ALS, PRE-084 reduced microglial reactivity by modulating NMDA receptor calcium influx (Mancuso et al., 2012). These findings suggest that targeting σ1 receptors may mitigate cognitive deficits associated with microglial activation and NMDA receptor hypofunction in schizophrenia.

Astrocytes contribute to maintaining homeostasis through ion transportation (Lia et al., 2023), neurotransmitter uptake and release of neurotransmitter precursors (Sofroniew, 2020) and ROS degradation (Chen et al., 2020). Evidence for astrocytic changes in schizophrenia is conflicting; some studies report increased GFAP mRNA and altered morphology (Tarasov et al., 2020, Webster et al., 2005) , while others find no change in GFAP expression in the ACC of patients (Radewicz et al., 2000). In this chapter, I found no changes in the %Area or ID of GFAP expression across any of my ACC slice conditions. In a mouse model of epilepsy, Sano et al. (2021) showed that there was microglial activation and proinflammatory cytokine release following status epilepticus in the mouse hippocampus. Critically, activating microglia induced reactive astrocyte activation (Sano et al., 2021). This may suggest that 4 hours of exposure to PCP was sufficient to start inducing microglial changes but may have been insufficient to evoke a change in GFAP expression. Alternatively, the morphology and pathological responses of astrocytes to stimuli are highly heterogenous (Sofroniew, 2020). Assessing changes in astrocyte morphology may give greater insights into the effects of PCP application, and subsequent NMDA receptor hypofunction.

Although σ1 receptors are expressed in astrocytes (Choi et al., 2022, Tagashira et al., 2023), PRE-084 pre-treatment did not affect GFAP expression, compared to any other condition. Studies exploring the effects of σ1 receptor activation on astrocytes are lacking. Regardless, one study did find that GFAP expression and

astrogliosis was induced in primary neuron-glia cultures, prepared from a σ1 receptor KO mouse model (Weng et al., 2017), while chronic PRE-084 treatment reduced reactive astrocytosis in an MND mouse model (Peviani et al., 2014). Although no change in GFAP was observed here, there is mounting evidence that σ1 receptors may modulate reactive astrocytes. Greater understanding of astrocytic changes in schizophrenia are needed, to understand whether σ1 receptor activation may be a beneficial target for future treatment.

5.6 Conclusions

This chapter has highlighted the complex interactions between PCP, σ1 receptors, and NMDA receptor function in a rat model of NMDA receptor hypofunction. My findings suggest that while σ1 receptor activation may attenuate some of the cognitive deficits associated with NMDA receptor hypofunction, the pharmacological effects are nuanced and context-dependent. The role of σ1 receptors in modulating ACC oscillations was apparent, as evidenced by the differential effects of σ1 agonists like PRE-084 and antagonists such as NE-100 on PCP-induced beta and gamma oscillations. These findings support the hypothesis that σ1 receptors play a modulatory role, likely interacting with NMDA receptors in a manner that affects neuronal oscillatory activity and interneuron dynamics.

Importantly, the selective activation of σ1 receptors appeared to counteract PCP-induced effects in specific neuronal populations, particularly PV+ interneurons. However, the lack of significant changes in SST and PV expression following acute treatment indicates that longer-term, or subchronic exposure, may be required to observe the full impact of σ1 receptor modulation on interneuron activity. Moreover, σ1 receptor activation also demonstrated potential neuroprotective effects, particularly in reducing microglial activation, suggesting its relevance in mitigating neuroinflammation and oxidative stress, which are implicated in schizophrenia pathology.

Overall, this study emphasised the therapeutic potential of σ1 receptor agonists in addressing cognitive dysfunctions associated with NMDA receptor hypofunction, yet also revealed the need for further exploration of dose- and time-dependent factors in σ1 receptor pharmacology. The differential effects on GABAergic interneuron marker expression, oscillatory dynamics, and neuroinflammation point to the complexity of σ1 receptor modulation and warrant deeper investigation into its mechanisms of action.

Chapter 6. General discussion

6.1 Discussion

High frequency oscillations, such as beta and gamma, are used as biomarkers for cognitive function. Changes in gamma oscillations have been linked specifically with deficits in working memory in patients with schizophrenia. Beta and gamma oscillations can be evoked by different neurotransmitter agonists, such as the glutamatergic agonist KA, and recorded *in vitro* from rodent and human brain tissue, as shown in this thesis.

The development of gamma oscillations in the CA3 is closely linked to the maturation of GABAergic interneurons, particularly PV+ and SST+ interneurons, which play critical roles in modulating network activity (Jinno and Kosaka, 2002, Luhmann and Khazipov, 2018). Notably, only single-peak oscillations were recorded, indicating a tendency toward low-gamma activity in the CA3, in contrast to distinct beta and gamma oscillations observed in other brain regions, such as the ACC (Roopun et al., 2008). Studies suggest that gamma oscillations emerge in the hippocampus around P15, correlating with behavioural observations that show gamma activity *in vivo* does not manifest in rats until the second postnatal week (Lahtinen et al., 2002, Tsintsadze et al., 2015). The oscillatory patterns of the CA3 are not only a function of intrinsic neuronal properties but also modulate the development of mature inhibitory circuits.

Interestingly, when examining the impact of PCP, I found that it did not significantly alter the power of CA3 gamma oscillations. This stability contrasts with the findings in the ACC, where PCP application had notable effects on oscillatory power. This disparity underscores the functional differences between these two regions, with the ACC exhibiting more diverse and flexible excitatory-inhibitory network necessary for its broader range of cognitive functions (Bush et al., 2000, Kilavik et al., 2013). Previous *in vivo* studies have suggested that NMDA receptor blockade can enhance gamma activity (Hakami et al., 2009, Kittelberger et al., 2012). A lack of PCP effect is surprising given the established roles of NMDA receptors in modulating hippocampal oscillatory dynamics (Eichenbaum, 1999, Kandel and Spencer, 1968). However, isolating the hippocampus, and severing the inputs received from other brain regions, necessary for dynamic oscillatory activity could cause this lack of effect. The direct effects of σ1 receptor activation in the CA3 has not been explored previously. In this study, the application of the selective σ1 receptor agonist PRE-084 also did not

affect gamma oscillations, a novel and significant finding given the supposed role of σ1 receptors in learning and memory mechanisms. However, PRE-084 did increase LTP in the CA1 suggesting there is still a role for σ1 receptors in learning and memory. A compelling future study could involve treating animals with PRE-084 *in vivo*, followed by recording LTP responses from slices prepared from those animals in the presence of PCP.

In the neocortex, gamma frequency oscillations have been repeatedly observed following KA application (Adams et al., 2017, Middleton et al., 2008, Roopun et al., 2008). Beta (20 – 32.9 Hz) and gamma (33 – 80 Hz) frequency oscillations were defined based on the bimodal frequency distribution found in this study, revealing that the ACC predominantly exhibited beta oscillations (65%) compared to gamma (35%) after KA application, a higher gamma to beta ratio than previously reported (Adams et al., 2017). Acute PCP exposure to stable KA-evoked oscillations in the ACC led to a dramatic increase in beta power and a shift from gamma to beta oscillations when gamma activity was initially present. While previous studies have shown NMDA receptor blockade typically increases gamma power in both *in vivo* and *in vitro* models (Hakami et al., 2009, Lemercier et al., 2017, Rebollo et al., 2018), this study's findings suggest a distinct frequency shift in the ACC, aligning with other research showing slower beta oscillations emerging in similar conditions (Middleton et al., 2008, Roopun et al., 2006).

The shift from gamma to beta activity observed here may be explained by a compensatory increase in SST+ interneuron activity, as these cells have slower intrinsic properties and weaker inhibitory influence, driving beta oscillations while suppressing gamma activity (Jang et al., 2020, Xu and Callaway, 2009). The density and distribution of these interneurons in ACC slices may influence the predominance of beta or gamma oscillations. The proportion of PV+ and SST+ interneurons in the rat ACC is unreported, however in mouse PV+ interneurons make up between 40 and 50% of GABAergic interneurons in the neocortex, whilst SST+ constitute around 30% (Riedemann, 2019). Although the proportions of GABAergic interneurons in the rat ACC were not quantified in this thesis, the %Area of PV was higher than that of SST indicating that the population of PV+ interneurons was higher than that of SST+ interneurons. In this study, 4 hour KA incubation revealed increased SST expression and decreased PV expression, which are both activity-dependent (Hou and Yu, 2013;

Patz et al., 2004). This suggests enhanced SST+ interneuron activity, which inhibits PV+ interneurons, likely underlies the dominance of beta oscillations in the ACC. Interestingly, while PRE-084 attenuated the increase in KA-evoked gamma oscillation power caused by PCP, it had no effect on beta power. Since gamma oscillations are primarily driven by PV+ interneurons, while beta oscillations are associated with SST+ interneurons, it appears that σ1 receptor activation exerts differential effects on these interneuron populations (Liu et al., 2023). The lack of effect on beta oscillations suggests that σ1 receptors may have more limited control over SST+ interneurons compared to PV+ interneurons.

Loss of both PV+ and SST+ interneurons have been reported in post-mortem studies of patients with schizophrenia (Fung et al., 2010, Hashimoto et al., 2008, Konradi et al., 2011). While many animal studies focus on subchronic effects of NMDA receptor antagonists on PV expression, this study provides insights into the acute effects of both PV and SST. *In vivo,* PCP induces schizophrenia-like behaviours in animals, including cognitive deficits and reduced PV expression in brain regions such as the prelimbic cortex (McKibben et al., 2010), cingulate cortex, and hippocampus (Abdul-Monim et al., 2007). Similarly, the MAM model shows decreased PV+ density in the DG, mPFC, ACC, and ventral subiculum (Du and Grace, 2016, Lodge et al., 2009). However, one study did find that subchronic PCP or ketamine treatment does not affect PV expression in adult rodents (Benneyworth et al., 2011). In contrast, acute studies suggest there is a delayed reduction in PV expression following NMDA receptor antagonist administration (Hervig et al., 2016, Romón et al., 2011). These findings, paired with the present study, suggest that a 4-hour exposure to PCP may not be sufficient to cause sustained loss of PV or SST in the ACC, though longer exposures may reveal changes. Longer exposures *in vitro* would need to be balanced with maintaining the health of the tissue, which could become a confounding factor in and of itself. Alternatively, future studies could assess changes in PV and SST expression following an acute PCP injection *in vivo,* as well as quantifying other markers such as c-Fos, a marker of cellular activity.

By activating Group II mGlu receptors, the mGlu2/3 agonist LY354740 and the specific mGlu2 agonist LY541850 reduced the power of the aberrant beta activity induced by PCP. However, the frequency shift from gamma to beta was not reversed, likely due to persistent network plasticity changes caused by PCP. This suggests that

mGlu2 activation may help modulate abnormal oscillations linked to NMDA receptor dysfunction, a key feature in schizophrenia models. Previous studies have shown that mGlu2 receptor activation can mitigate PCP-induced glutamate efflux and symptoms like cognitive and motor impairments (Moghaddam and Adams, 1998). It would be interesting in a future study to explore the impact of mGlu2 activation on SST and PV expression and assess whether suppressing oscillations via metabotropic glutamate receptors has a significant impact on specific interneuron activity.

Increased oxidative stress and ROS are commonly reported in schizophrenia studies, with microglia being a primary source of ROS (Simpson and Oliver, 2020). In this study, Iba1 expression, a marker of microglial activation, increased following 4 hours of KA application and further increased with KA + PCP treatment. This supports the hypothesis that even acute PCP exposure may activate microglia, potentially contributing to the pathology of NMDA receptor hypofunction. Notably, microglial activation has been linked to subsequent PV+ interneuron deficits in schizophrenia (Steullet et al., 2017), suggesting a pathological cascade where microglial activation precedes PV changes. The neuroprotective effects of σ1 receptors, particularly in reducing oxidative stress and neuroinflammation, are well-documented (Jia et al., 2018). In this study, pre-incubation with PRE-084 reduced microglial activation in KA + PCP slices, as indicated by decreased Iba1 expression. Microglia express high levels of σ1 receptors, and their activation can be suppressed by σ1 receptor activation, which inhibits calcium influx and cytokine release (Hall et al., 2009). This suggests that σ1 receptor activation could counteract the neuroinflammatory processes that exacerbate cognitive dysfunction in schizophrenia models.

In contrast, no changes in GFAP expression were observed across any conditions, suggesting that astrocyte activation may not be as responsive to σ1 receptor modulation in this acute model. Previous studies have shown conflicting results regarding σ1 receptor effects on astrocytes, with some models demonstrating reductions in astrogliosis following σ1 receptor activation (Peviani et al., 2014), while others show increased GFAP expression in σ1 receptor knockout models (Weng et al., 2017). These findings highlight the need for further investigation into σ1 receptor effects on astrocytes and their role in maintaining neuronal homeostasis. The role of astrocytes in schizophrenia remains debated. While some studies report altered astrocyte morphology and increased GFAP expression in schizophrenia patients

(Tarasov et al., 2020, Webster et al., 2005), others find no changes in GFAP levels (Radewicz et al., 2000). In this study, the absence of GFAP changes across conditions suggests that astrocytes might not exhibit overt activation in this acute setting. However, the heterogeneity of astrocyte responses to stimuli (Sofroniew, 2020) suggests that further investigation into astrocyte morphology could provide deeper insights into the effects of PCP and NMDA receptor hypofunction on glial function.

Microglia activation precedes and induces cytokine release, which can cause increased ROS and oxidative stress, which in turn can lead to increased astrocyte activation, high ATP production and further microglial activation reactive astrocyte activation (Gehrmann et al., 1995, Neumann et al., 2009, Sano et al., 2021). This acute slice model has found that NMDA receptor hypofunction drives SST activity, whilst dampening PV, inducing an increase in microglia. If sustained, this may cause loss of both PV+ and SST+ interneurons due to harmful levels of ROS and oxidative stress. Future studies could quantify markers of ROS and oxidative stress in this slice model following 4 hours of PCP exposure, to assess whether there are any early signs of ROS or oxidative stress. Extending the duration of PCP incubation in the slices could also provide valuable insights into whether more pronounced changes in glial activity and neuroinflammatory markers emerge at later time points.

PCP is classically categorised as an NMDA receptor antagonist. In addition to NMDA receptors, PCP also acts as an agonist on σ1 receptors (Vaupel, 1983) which may explain the differences found in this thesis between PCP and other NMDA receptor antagonists on ACC oscillations. SKF-10047 is a prototypic σ1 receptor agonist that also acts on NMDA receptors as an antagonist (Nishikawa et al., 2000, Vaupel, 1983). In this study, we demonstrated that SKF-10047 has a significant impact on KA-evoked oscillations in the ACC, similar to PCP, likely due to its dual function as a σ1 receptor agonist and NMDA receptor antagonist. Interestingly, although SKF-10047 increased oscillatory power, it did not induce the shift from gamma to beta oscillations observed with PCP, suggesting that these frequency shifts are not solely mediated by σ1 receptor activation.

The binding profile of σ1 receptors is very diverse and includes many antipsychotics (Hayashi and Su, 2004), which makes σ1 receptors particularly interesting in the treatment of schizophrenia symptoms. The acute actions of σ1

receptor activation include modulation of ion channels, such as NMDA receptors and K^+ channels. While selective σ1 receptor agonists like PRE-084 had a modest effect on gamma power, SKF-10047 greatly increased ACC oscillation power in both beta and gamma ranges. This likely reflects the compound's NMDA receptor antagonist properties, as PCP blocks NMDA receptors at sub-micromolar concentrations, driving significant increases in oscillatory power (Marquis et al., 1989).

σ1 receptors also play an important role in regulating NMDA receptor activity. Repeated PCP administration has been shown to reduce σ1 receptor expression in the PFC (Ishima et al., 2009), indicating an intricate relationship between these receptors. While σ1 receptor activation enhances NMDA receptor trafficking to the membrane and potentiates NMDA currents (Balasuriya et al., 2013, Pabba et al., 2014), σ1 receptor agonists like PRE-084 have been shown to attenuate cognitive deficits induced by NMDA receptor hypofunction in mice (Hashimoto et al., 2007, Maurice and Privat, 1997). This aligns with our findings, where PRE-084 blocked the effects of PCP on gamma oscillations in the ACC.

σ1 receptor agonists and antagonists also demonstrated complex interactions. PRE-084 and the σ1 receptor antagonist NE-100 both attenuated PCP's effect on gamma oscillations, yet NE-100 slightly reduced the increase in beta power. This could be due to the bell-shaped dose-response curve of σ1 receptor agonists, where low doses stimulate and high doses inhibit σ1 receptor activity (Cobos et al., 2008). Therefore, when PRE-084 and PCP were co-applied, σ1 receptor activation may have shifted from stimulation to inhibition, producing effects like those seen with NE-100.

In conclusion, the interactions between σ1 and NMDA receptors are complex and multifaceted, with σ1 receptor activation offering potential therapeutic benefits in addressing NMDA receptor hypofunction and related cognitive deficits. However, the differential effects of σ1 receptor agonists and antagonists, as well as their impact on various interneuron populations, suggest that further research is needed to unravel these intricate pharmacological interactions. Understanding the dose-dependent effects of σ1 receptor modulation could pave the way for new therapeutic approaches for disorders such as schizophrenia.

6.2 Limitations and future work

In this thesis, I found that the novel selective orthosteric mGlu2 agonist / mGlu3 antagonist LY541850 modulates PCP-induced changes in beta oscillation. This showed that activating mGlu2 receptors could be a useful future therapeutic target. To validate my acute slice model, future studies could explore the effects of current medications known to have positive effects on both the positive and cognitive symptoms of schizophrenia, such as SGAs (eg. clozapine and risperidone) and TGAs (eg. aripiprazole and brexpiprazole). Comparing the effects of current medications to the effect of LY541850 could give a better understanding of the mechanisms of current medications, as well as improved assessment of novel interventions.

The lack of effect on interneurons and glia following 4 hours of PCP incubation indicated that 4 hours of exposure may not be sufficient to trigger the more permanent and pathological hallmarks of NDMA receptor hypofunction. Initial experiments suggested there were increases in both Iba1 and GFAP expression, however increasing the group data reduced the significance due to large inter-animal variability. This is the limiting factor of the acute slice model presented in this thesis. Unpublished data from our lab shows that oscillations can be evoked and recorded many hours after slice preparation. However, we have also found that KA-evoked oscillations can continually build in power for 6-8 hours and subsequently “crash”. This lack of stability may be indicative of slice health, suggesting that the results of any longer applications may be biologically confounded. Recording the oscillatory behaviour of the slices prior to staining could allow us to account for such variability.

As previously highlighted, the distribution of PV+ and SST+ interneurons vary throughout the rodent ACC. When analysing PV and SST expression throughout the ACC, the caudal-rostral position of the ACC sections was not considered. Furthermore, although all electrophysiology experiments were recorded from layer V of the ACC, again the caudal-rostral position of the ACC sections was not considered. If both factors had been accounted for and analysed, a greater examination of the specific regions of the ACC could have been conducted. This would have allowed me to explore the relationship between interneuron population and oscillation frequency more explicitly.

Furthermore, a lack of statistical significance was found throughout my immunohistochemistry results. This is likely due to the high variability in my staining, even though standard procedures were taken to minimise section to section staining variability. With hindsight, a more rigours criteria for the ACC sections used for incubation, staining and analysis could have minimised variability. Ideally, slices from the same rostral-caudal position of the ACC would have been used across all experimental conditions, however the number of conditions and too few slices from one animal make this difficult. Slight variations in animal preparations and electrophysiology rig conditions may have impacted tissue health, which would particularly impact markers for glia, including GFAP and Iba1. Although measures are taken, brain slice preparation is a traumatic process, which may have limited the ability to modulate GFAP and/or Iba1 expression. This highlights the limitations of using prepared brain slices *in vitro* to model pathology known to affect glia. In future, more control steps could be implemented to assess the level of glial activation caused solely by 4 hours of rig incubation. This could include taking slices immediately post-slicing, or following holding chamber recovery, as well as comparing to sections from PFA-fixed whole brains.

Schizophrenia presents differently in male and female patients (Leger and Neill, 2016, Mendrek and Mancini-Marïe, 2016) and sex differences in schizophrenia animal models are becoming increasingly apparent (Gogos and van den Buuse, 2023). Males show poorer performance in measures of executive function and verbal memory, whereas females showed greater deficits in visual memory and attention (Mendrek and Mancini-Marïe, 2016). This study only used adolescent / young adult male rats therefore it would also be important to look at the same NMDA receptor hypofunction model in slices taken from female rats to identify any sex differences. The differences in cognitive impairment may manifest in different regional changes, however this would need to be properly explored.

In summary, the acute slice model presented in this thesis offers a valuable tool for investigating the immediate effects of pharmacological interventions and their impact on neuronal and glial cell markers. However, further research is required to determine the full potential and limitations of this *in vitro* system for broader applications.

References

ABDUL-MONIM, Z., NEILL, J. C. & REYNOLDS, G. P. 2007. Sub-chronic psychotomimetic phencyclidine induces deficits in reversal learning and alterations in parvalbumin-immunoreactive expression in the rat. *J Psychopharmacol,* 21**,** 198-205.

ABRAHAM, W. C. & BEAR, M. F. 1996. Metaplasticity: the plasticity of synaptic plasticity. *Trends Neurosci,* 19**,** 126-30.

ABRAHAM, W. C. & MASON, S. E. 1988. Effects of the NMDA receptor/channel antagonists CPP and MK801 on hippocampal field potentials and long-term potentiation in anesthetized rats. *Brain Res,* 462**,** 40-6.

ADAMS, N. E., SHERFEY, J. S., KOPELL, N. J., WHITTINGTON, M. A. & LEBEAU, F. E. 2017. Hetereogeneity in neuronal intrinsic properties: a possible mechanism for hub-like properties of the rat anterior cingulate cortex during network activity. *Eneuro,* 4.

ADAMS, R. & DAVID, A. S. 2007. Patterns of anterior cingulate activation in schizophrenia: a selective review. *Neuropsychiatr Dis Treat,* 3**,** 87-101.

AERY JONES, E. A., RAO, A., ZILBERTER, M., DJUKIC, B., BANT, J. S., GILLESPIE, A. K., KOUTSODENDRIS, N., NELSON, M., YOON, S. Y., HUANG, K., YUAN, H., GILL, T. M., HUANG, Y. & FRANK, L. M. 2021. Dentate gyrus and CA3 GABAergic interneurons bidirectionally modulate signatures of internal and external drive to CA1. *Cell Rep,* 37**,** 110159.

AGUILAR, D. D., GIUFFRIDA, A. & LODGE, D. J. 2016. THC and endocannabinoids differentially regulate neuronal activity in the prefrontal cortex and hippocampus in the subchronic PCP model of schizophrenia. *Journal of Psychopharmacology,* 30**,** 169-181.

AL-MUSAWI, I., DENNIS, B. H., CLOWRY, G. J. & LEBEAU, F. E. N. 2024. Evidence for prodromal changes in neuronal excitability and neuroinflammation in the hippocampus in young alpha-synuclein (A30P) transgenic mice. *Frontiers in Dementia,* 3.

ALCAIDE, J., GUIRADO, R., CRESPO, C., BLASCO-IBÁÑEZ, J. M., VAREA, E., SANJUAN, J. & NACHER, J. 2019. Alterations of perineuronal nets in the dorsolateral prefrontal cortex of neuropsychiatric patients. *International Journal of Bipolar Disorders,* 7**,** 24.

ALEMAN, A. & KAHN, R. S. 2005. Strange feelings: Do amygdala abnormalities dysregulate the emotional brain in schizophrenia? *Progress in Neurobiology,* 77**,** 283-298.

ALHERZ, F., ALHERZ, M. & ALMUSAWI, H. 2017. NMDAR hypofunction and somatostatin-expressing GABAergic interneurons and receptors: A newly identified correlation and its effects in schizophrenia. *Schizophrenia Research: Cognition,* 8**,** 1-6.

ALI, F., GERHARD, D. M., SWEASY, K., POTHULA, S., PITTENGER, C., DUMAN, R. S. & KWAN, A. C. 2020. Ketamine disinhibits dendrites and enhances calcium signals in prefrontal dendritic spines. *Nature Communications,* 11**,** 72.

AMITAI, N., KUCZENSKI, R., BEHRENS, M. M. & MARKOU, A. 2012. Repeated phencyclidine administration alters glutamate release and decreases GABA markers in the prefrontal cortex of rats. *Neuropharmacology,* 62**,** 1422-31.

ANASTASIADES, P. G. & CARTER, A. G. 2021. Circuit organization of the rodent medial prefrontal cortex. *Trends in Neurosciences,* 44**,** 550-563.

ANDERSEN, J. V., MARKUSSEN, K. H., JAKOBSEN, E., SCHOUSBOE, A., WAAGEPETERSEN, H. S., ROSENBERG, P. A. & ALDANA, B. I. 2021. Glutamate metabolism and recycling at the excitatory synapse in health and neurodegeneration. *Neuropharmacology,* 196**,** 108719.

ANDERSEN, J. V., SCHOUSBOE, A. & VERKHRATSKY, A. 2022. Astrocyte energy and neurotransmitter metabolism in Alzheimer's disease: Integration of the glutamate/GABA-glutamine cycle. *Progress in Neurobiology,* 217**,** 102331.

ANDERSON, G., MAES, M. & BERK, M. 2013. Schizophrenia is primed for an increased expression of depression through activation of immuno-inflammatory, oxidative and nitrosative stress, and tryptophan catabolite pathways. *Prog Neuropsychopharmacol Biol Psychiatry,* 42**,** 101-14.

ANDRÁSFALVY, B. K. & MAGEE, J. C. 2004. Changes in AMPA receptor currents following LTP induction on rat CA1 pyramidal neurones. *J Physiol,* 559**,** 543-54.

ANTONOUDIOU, P., TAN, Y. L., KONTOU, G., UPTON, A. L. & MANN, E. O. 2020. Parvalbumin and Somatostatin Interneurons Contribute to the Generation of Hippocampal Gamma Oscillations. *J Neurosci,* 40**,** 7668-7687.

ANVER, H., WARD, P. D., MAGONY, A. & VREUGDENHIL, M. 2011. NMDA receptor hypofunction phase couples independent γ-oscillations in the rat visual cortex. *Neuropsychopharmacology,* 36**,** 519-28.

ARIME, Y. & AKIYAMA, K. 2017. Abnormal neural activation patterns underlying working memory impairment in chronic phencyclidine-treated mice. *PLOS ONE,* 12**,** e0189287.

ARNOLD, S. E., FRANZ, B. R., TROJANOWSKI, J. Q., MOBERG, P. J. & GUR, R. E. 1996. Glial fibrillary acidic protein-immunoreactive astrocytosis in elderly patients with schizophrenia and dementia. *Acta neuropathologica,* 91**,** 269-277.

ASCOLI, G., ALONSO-NANCLARES, L., ANDERSON, S., BARRIONUEVO, G., BENAVIDES-PICCIONE, R., BURKHALTER, A., BUZSÁKI, G., CAULI, B., DEFELIPE, J. & FAIRÉN, A. 2008. Yuste The Petilla Interneuron Nomenclature Group (PING) R. Petilla terminology: Nomenclature of features of GABAergic interneurons of the cerebral cortex. *Nat. Rev. Neurosci,* 9**,** 557-568.

ATALLAH, B. V. & SCANZIANI, M. 2009. Instantaneous modulation of gamma oscillation frequency by balancing excitation with inhibition. *Neuron,* 62**,** 566-577.

AULT, D. T. & WERLING, L. L. 1997. Differential modulation of NMDA-stimulated [3H]dopamine release from rat striatum by neuropeptide Y and σ receptor ligands. *Brain Research,* 760**,** 210-217.

BADIMON, A., STRASBURGER, H. J., AYATA, P., CHEN, X., NAIR, A., IKEGAMI, A., HWANG, P., CHAN, A. T., GRAVES, S. M. & UWERU, J. O. 2020. Negative feedback control of neuronal activity by microglia. *Nature,* 586**,** 417-423.

BALASURIYA, D., STEWART, A. P. & EDWARDSON, J. M. 2013. The σ-1 receptor interacts directly with GluN1 but not GluN2A in the GluN1/GluN2A NMDA receptor. *J Neurosci,* 33**,** 18219-24.

BALMER, T. S. 2016. Perineuronal nets enhance the excitability of fast-spiking neurons. *ENeuro,* 3.

BARADITS, M., KAKUSZI, B., BÁLINT, S., FULLAJTÁR, M., MÓD, L., BITTER, I. & CZOBOR, P. 2019. Alterations in resting-state gamma activity in patients with schizophrenia: a high-density EEG study. *European Archives of Psychiatry and Clinical Neuroscience,* 269**,** 429-437.

BARTOS, M., VIDA, I. & JONAS, P. 2007. Synaptic mechanisms of synchronized gamma oscillations in inhibitory interneuron networks. *Nature reviews neuroscience,* 8**,** 45-56.

BASAR-EROGLU, C., BRAND, A., HILDEBRANDT, H., KAROLINA KEDZIOR, K., MATHES, B. & SCHMIEDT, C. 2007. Working memory related gamma oscillations in schizophrenia patients. *Int J Psychophysiol,* 64**,** 39-45.

BAŞAR, E. 2013. Brain oscillations in neuropsychiatric disease. *Dialogues Clin Neurosci,* 15**,** 291-300.

BAŞAR, E., BAŞAR-EROGLU, C., KARAKAŞ, S. & SCHÜRMANN, M. 2001. Gamma, alpha, delta, and theta oscillations govern cognitive processes. *International journal of psychophysiology,* 39**,** 241-248.

BAYER, T. A., BUSLEI, R., HAVAS, L. & FALKAI, P. 1999. Evidence for activation of microglia in patients with psychiatric illnesses. *Neuroscience letters,* 271**,** 126-128.

BEASLEY, C. L. & REYNOLDS, G. P. 1997. Parvalbumin-immunoreactive neurons are reduced in the prefrontal cortex of schizophrenics. *Schizophr Res,* 24**,** 349-55.

BEASLEY, C. L., ZHANG, Z. J., PATTEN, I. & REYNOLDS, G. P. 2002. Selective deficits in prefrontal cortical GABAergic neurons in schizophrenia defined by the presence of calcium-binding proteins. *Biol Psychiatry,* 52**,** 708-15.

BEKER, S., GOLDIN, M., MENKES-CASPI, N., KELLNER, V., CHECHIK, G. & STERN, E. A. 2016. Amyloid-β disrupts ongoing spontaneous activity in sensory cortex. *Brain Struct Funct,* 221**,** 1173-88.

BENES, F. M., DAVIDSON, J. & BIRD, E. D. 1986. Quantitative Cytoarchitectural Studies of the Cerebral Cortex of Schizophrenics. *Archives of General Psychiatry,* 43**,** 31-35.

BENEYTO, M., ABBOTT, A., HASHIMOTO, T. & LEWIS, D. A. 2011. Lamina-specific alterations in cortical GABAA receptor subunit expression in schizophrenia. *Cerebral cortex,* 21**,** 999-1011.

BENNETT, M. L. & VIAENE, A. N. 2021. What are activated and reactive glia and what is their role in neurodegeneration? *Neurobiol Dis,* 148**,** 105172.

BENNEYWORTH, M. A., ROSEMAN, A. S., BASU, A. C. & COYLE, J. T. 2011. Failure of NMDA receptor hypofunction to induce a pathological reduction in PV-positive GABAergic cell markers. *Neuroscience Letters,* 488**,** 267-271.

BIAŁOŃ, M. & WĄSIK, A. 2022. Advantages and Limitations of Animal Schizophrenia Models. *International Journal of Molecular Sciences,* 23**,** 5968.

BIDERMAN, N., BAKKOUR, A. & SHOHAMY, D. 2020. What Are Memories For? The Hippocampus Bridges Past Experience with Future Decisions. *Trends in Cognitive Sciences,* 24**,** 542-556.

BLEULER, E. 1911. *Dementia praecox: oder Gruppe der Schizophrenien*, F. Deuticke.

BLISS, T. & COLLINGRIDGE, G. L. 2019. Persistent memories of long-term potentiation and the N-methyl-d-aspartate receptor. *Brain Neurosci Adv,* 3**,** 2398212819848213.

BLISS, T. V. & GARDNER-MEDWIN, A. R. 1973. Long-lasting potentiation of synaptic transmission in the dentate area of the unanaestetized rabbit following stimulation of the perforant path. *J Physiol,* 232**,** 357-74.

BLISS, T. V. & LOMO, T. 1973. Long-lasting potentiation of synaptic transmission in the dentate area of the anaesthetized rabbit following stimulation of the perforant path. *J Physiol,* 232**,** 331-56.

BOBES, J., GARCIA-PORTILLA, M. P., BASCARAN, M. T., SAIZ, P. A. & BOUZOÑO, M. 2007. Quality of life in schizophrenic patients. *Dialogues in clinical neuroscience,* 9**,** 215-226.

BONANNI, E., DI COSCIO, E., MAESTRI, M., CARNICELLI, L., TSEKOU, H., ECONOMOU, N. T., PAPARRIGOPOULOS, T., BONAKIS, A., PAPAGEORGIOU, S. G., VASSILOPOULOS, D., SOLDATOS, C. R., MURRI, L. & KTONAS, P. Y. 2012. Differences in EEG delta frequency characteristics and patterns in slow-wave sleep between dementia patients and controls: a pilot study. *J Clin Neurophysiol,* 29**,** 50-4.

BORDEN, L. A., SMITH, K. E., HARTIG, P. R., BRANCHEK, T. A. & WEINSHANK, R. L. 1992. Molecular heterogeneity of the gamma-aminobutyric acid (GABA) transport system. Cloning of two novel high affinity GABA transporters from rat brain. *Journal of Biological Chemistry,* 267**,** 21098-21104.

BOURAS, C., KÖVARI, E., HOF, P. R., RIEDERER, B. M. & GIANNAKOPOULOS, P. 2001. Anterior cingulate cortex pathology in schizophrenia and bipolar disorder. *Acta Neuropathologica,* 102**,** 373-379.

BOWIE, C. R. & HARVEY, P. D. 2006. Cognitive deficits and functional outcome in schizophrenia. *Neuropsychiatr Dis Treat,* 2**,** 531-6.

BREIER, A., MALHOTRA, A. K., PINALS, D. A., WEISENFELD, N. I. & PICKAR, D. 1997. Association of ketamine-induced psychosis with focal activation of the prefrontal cortex in healthy volunteers. *Am J Psychiatry,* 154**,** 805-11.

BROCA, P. 1878. Le grand lobe limbique et la scissure limbique dans la série des mammifères. *Revue d´ Anthropologie, 2e série***,** 385-598.

BRÜCKNER, G., BRAUER, K., HÄRTIG, W., WOLFF, J. R., RICKMANN, M. J., DEROUICHE, A., DELPECH, B., GIRARD, N., OERTEL, W. H. & REICHENBACH, A. 1993. Perineuronal nets provide a polyanionic, glia-associated form of microenvironment around certain neurons in many parts of the rat brain. *Glia,* 8**,** 183-200.

BUCKLEY, N. A. & SANDERS, P. 2000. Cardiovascular adverse effects of antipsychotic drugs. *Drug Saf,* 23**,** 215-28.

BUHL, E. H., TAMÁS, G. & FISAHN, A. 1998. Cholinergic activation and tonic excitation induce persistent gamma oscillations in mouse somatosensory cortex in vitro. *The Journal of physiology,* 513**,** 117-126.

BULLITT, E. 1990. Expression of c-fos-like protein as a marker for neuronal activity following noxious stimulation in the rat. *J Comp Neurol,* 296**,** 517-30.

BURBAEVA, G. S., BOKSHA, I. S., TURISHCHEVA, M. S., VOROBYEVA, E. A., SAVUSHKINA, O. K. & TERESHKINA, E. B. 2003. Glutamine synthetase and glutamate dehydrogenase in the prefrontal cortex of patients with schizophrenia. *Progress in Neuro-Psychopharmacology and Biological Psychiatry,* 27**,** 675-680.

BURDA, J. E. & SOFRONIEW, M. V. 2014. Reactive gliosis and the multicellular response to CNS damage and disease. *Neuron,* 81**,** 229-248.

BUSH, G., LUU, P. & POSNER, M. I. 2000. Cognitive and emotional influences in anterior cingulate cortex. *Trends Cogn Sci,* 4**,** 215-222.

BUSH, G., VOGT, B., HOLMES, J., DALE, A., GREVE, D., JENIKE, M. & ROSEN, B. 2002. Dorsal anterior cingulate cortex: A role in reward-based decision making. *Proceedings of the National Academy of Sciences of the United States of America,* 99**,** 523-8.

BUSKILA, Y., BREEN, P. P., TAPSON, J., VAN SCHAIK, A., BARTON, M. & MORLEY, J. W. 2014. Extending the viability of acute brain slices. *Scientific Reports,* 4**,** 5309.

BUZSÁKI, G. 2005. Theta rhythm of navigation: link between path integration and landmark navigation, episodic and semantic memory. *Hippocampus,* 15**,** 827-40.

BUZSÁKI, G. & MOSER, E. I. 2013. Memory, navigation and theta rhythm in the hippocampal-entorhinal system. *Nature neuroscience,* 16**,** 130-138.

CADINU, D., GRAYSON, B., PODDA, G., HARTE, M. K., DOOSTDAR, N. & NEILL, J. C. 2018. NMDA receptor antagonist rodent models for cognition in schizophrenia and identification of novel drug treatments, an update. *Neuropharmacology,* 142**,** 41-62.

CALVER, A. R., MEDHURST, A. D., ROBBINS, M. J., CHARLES, K. J., EVANS, M. L., HARRISON, D. C., STAMMERS, M., HUGHES, S. A., HERVIEU, G., COUVE, A., MOSS, S. J., MIDDLEMISS, D. N. & PANGALOS, M. N. 2000. The expression of GABA(B1) and GABA(B2) receptor subunits in the cNS differs from that in peripheral tissues. *Neuroscience,* 100**,** 155-70.

CARBON, M. & CORRELL, C. U. 2014. Thinking and acting beyond the positive: the role of the cognitive and negative symptoms in schizophrenia. *CNS Spectr,* 19 Suppl 1**,** 38-52; quiz 35-7, 53.

CARCELLER, H., GUIRADO, R., RIPOLLES-CAMPOS, E., TERUEL-MARTI, V. & NACHER, J. 2020. Perineuronal Nets Regulate the Inhibitory Perisomatic Input onto Parvalbumin Interneurons and γ Activity in the Prefrontal Cortex. *J Neurosci,* 40**,** 5008-5018.

CARDIN, J. A., CARLÉN, M., MELETIS, K., KNOBLICH, U., ZHANG, F., DEISSEROTH, K., TSAI, L.-H. & MOORE, C. I. 2009. Driving fast-spiking cells induces gamma rhythm and controls sensory responses. *Nature,* 459**,** 663-667.

CARLÉN, M. 2017. What constitutes the prefrontal cortex? *Science,* 358**,** 478-482.

CARTMELL, J. & SCHOEPP, D. D. 2000. Regulation of neurotransmitter release by metabotropic glutamate receptors. *Journal of neurochemistry,* 75**,** 889-907.

CARULLI, D., PIZZORUSSO, T., KWOK, J. C., PUTIGNANO, E., POLI, A., FOROSTYAK, S., ANDREWS, M. R., DEEPA, S. S., GLANT, T. T. & FAWCETT, J. W. 2010. Animals lacking link protein have attenuated perineuronal nets and persistent plasticity. *Brain,* 133**,** 2331-47.

CEMBROWSKI, M. S. & SPRUSTON, N. 2019. Heterogeneity within classical cell types is the rule: lessons from hippocampal pyramidal neurons. *Nature Reviews Neuroscience,* 20**,** 193-204.

CHALKIADAKI, K., VELLI, A., KYRIAZIDIS, E., STAVROULAKI, V., VOUVOUTSIS, V., CHATZAKI, E., AIVALIOTIS, M. & SIDIROPOULOU, K. 2019. Development of the MAM model of schizophrenia in mice: Sex similarities and differences of hippocampal and prefrontal cortical function. *Neuropharmacology,* 144**,** 193-207.

CHEN, G., ZHANG, Y., LI, X., ZHAO, X., YE, Q., LIN, Y., TAO, H. W., RASCH, M. J. & ZHANG, X. 2017. Distinct Inhibitory Circuits Orchestrate Cortical beta and gamma Band Oscillations. *Neuron,* 96**,** 1403-1418.e6.

CHEN, T.-S., HUANG, T.-H., LAI, M.-C. & HUANG, C.-W. 2023. The Role of Glutamate Receptors in Epilepsy. *Biomedicines,* 11**,** 783.

CHEN, Y., QIN, C., HUANG, J., TANG, X., LIU, C., HUANG, K., XU, J., GUO, G., TONG, A. & ZHOU, L. 2020. The role of astrocytes in oxidative stress of central nervous system: A mixed blessing. *Cell Prolif,* 53**,** e12781.

CHERUBINI, E. & CONTI, F. 2001. Generating diversity at GAB Aergic synapses. *Trends in Neurosciences,* 24**,** 155-162.
CHO, R. Y., KONECKY, R. O. & CARTER, C. S. 2006. Impairments in frontal cortical gamma synchrony and cognitive control in schizophrenia. *Proc Natl Acad Sci U S A,* 103**,** 19878-83.
CHODIRKER, B. N., CHUDLEY, A. E., RAY, M., WICKSTROM, D. E. & RIORDAN, D. L. 1987. Fragile 19p13 in a family with mental illness. *Clin Genet,* 31**,** 1-6.
CHOI, J.-G., CHOI, S.-R., KANG, D.-W., KIM, J., PARK, J. B., LEE, J.-H. & KIM, H.-W. 2022. Sigma-1 receptor increases intracellular calcium in cultured astrocytes and contributes to mechanical allodynia in a model of neuropathic pain. *Brain Research Bulletin,* 178**,** 69-81.
CHUNG, D. W., FISH, K. N. & LEWIS, D. A. 2016. Pathological basis for deficient excitatory drive to cortical parvalbumin interneurons in schizophrenia. *American Journal of Psychiatry,* 173**,** 1131-1139.
COAN, E. J., SAYWOOD, W. & COLLINGRIDGE, G. L. 1987. MK-801 blocks NMDA receptor-mediated synaptic transmission and long term potentiation in rat hippocampal slices. *Neurosci Lett,* 80**,** 111-4.
COBOS, E. J., ENTRENA, J. M., NIETO, F. R., CENDÁN, C. M. & DEL POZO, E. 2008. Pharmacology and therapeutic potential of sigma(1) receptor ligands. *Curr Neuropharmacol,* 6**,** 344-66.
COHEN, S. M., TSIEN, R. W., GOFF, D. C. & HALASSA, M. M. 2015. The impact of NMDA receptor hypofunction on GABAergic neurons in the pathophysiology of schizophrenia. *Schizophr Res,* 167**,** 98-107.
COLGIN, L. L., DENNINGER, T., FYHN, M., HAFTING, T., BONNEVIE, T., JENSEN, O., MOSER, M.-B. & MOSER, E. I. 2009. Frequency of gamma oscillations routes flow of information in the hippocampus. *Nature,* 462**,** 353-357.
COLLINGRIDGE, G. L., KEHL, S. J. & MCLENNAN, H. 1983. Excitatory amino acids in synaptic transmission in the Schaffer collateral-commissural pathway of the rat hippocampus. *J Physiol,* 334**,** 33-46.
CONTI, F., ZUCCARELLO, L. V., BARBARESI, P., MINELLI, A., BRECHA, N. C. & MELONE, M. 1999. Neuronal, glial, and epithelial localization of gamma-aminobutyric acid transporter 2, a high-affinity gamma-aminobutyric acid plasma membrane transporter, in the cerebral cortex and neighboring structures. *J Comp Neurol,* 409**,** 482-94.
COPELAND, C. S., NEALE, S. A., NISENBAUM, E. S. & SALT, T. E. 2022. Group II metabotropic glutamate receptor (mGlu(2) and mGlu(3)) roles in thalamic processing. *Br J Pharmacol,* 179**,** 1607-1619.
COPELAND, C. S., WALL, T. M., SIMS, R. E., NEALE, S. A., NISENBAUM, E., PARRI, H. R. & SALT, T. E. 2017. Astrocytes modulate thalamic sensory processing via mGlu2 receptor activation. *Neuropharmacology,* 121**,** 100-110.
CORRELL, C. U. & SCHOOLER, N. R. 2020. Negative symptoms in schizophrenia: a review and clinical guide for recognition, assessment, and treatment. *Neuropsychiatric disease and treatment***,** 519-534.
COYLE, J. T. 1996. The Glutamatergic Dysfunction Hypothesis for Schizophrenia. *Harvard Review of Psychiatry,* 3**,** 241-253.
COYLE, J. T. 2006. Glutamate and schizophrenia: beyond the dopamine hypothesis. *Cellular and molecular neurobiology,* 26**,** 363-382.
CULLEN, A. E., DICKSON, H., DOWNS, J., HEDGES, E. P., KEMPTON, M. J., LAURENS, K. R., MA, S. Y. & MACCABE, J. H. 2020. Academic achievement

and schizophrenia: a systematic meta-analysis. *Psychological Medicine,* 50**,** 1949-1965.
CUNNINGHAM, M. O., DAVIES, C. H., BUHL, E. H., KOPELL, N. & WHITTINGTON, M. A. 2003. Gamma oscillations induced by kainate receptor activation in the entorhinal cortex in vitro. *J Neurosci,* 23**,** 9761-9.
DAVALOS, D., GRUTZENDLER, J., YANG, G., KIM, J. V., ZUO, Y., JUNG, S., LITTMAN, D. R., DUSTIN, M. L. & GAN, W.-B. 2005. ATP mediates rapid microglial response to local brain injury in vivo. *Nature neuroscience,* 8**,** 752-758.
DE LA PRIDA, L. M. & HUBERFELD, G. 2019. Inhibition and oscillations in the human brain tissue in vitro. *Neurobiology of Disease,* 125**,** 198-210.
DE NÓ, R. L. 1934. *Studies on the Structure of the Cerebral Cortex: Continuation of the study of the ammonic system. II*, Johann Ambrosius Barth.
DE OLIVEIRA FIGUEIREDO, E. C., CALÌ, C., PETRELLI, F. & BEZZI, P. 2022. Emerging evidence for astrocyte dysfunction in schizophrenia. *Glia,* 70**,** 1585-1604.
DEFELIPE, J., LÓPEZ-CRUZ, P. L., BENAVIDES-PICCIONE, R., BIELZA, C., LARRAÑAGA, P., ANDERSON, S., BURKHALTER, A., CAULI, B., FAIRÉN, A. & FELDMEYER, D. 2013. New insights into the classification and nomenclature of cortical GABAergic interneurons. *Nature Reviews Neuroscience,* 14**,** 202-216.
DIENEL, S. J. & LEWIS, D. A. 2019. Alterations in cortical interneurons and cognitive function in schizophrenia. *Neurobiology of Disease,* 131**,** 104208.
DINGLEDINE, R., BORGES, K., BOWIE, D. & TRAYNELIS, S. F. 1999. The Glutamate Receptor Ion Channels. *Pharmacological Reviews,* 51**,** 7-62.
DOISCHER, D., HOSP, J. A., YANAGAWA, Y., OBATA, K., JONAS, P., VIDA, I. & BARTOS, M. 2008. Postnatal differentiation of basket cells from slow to fast signaling devices. *Journal of Neuroscience,* 28**,** 12956-12968.
DOMINGUEZ, C., PRIETO, L., VALLI, M. J., MASSEY, S. M., BURES, M., WRIGHT, R. A., JOHNSON, B. G., ANDIS, S. L., KINGSTON, A., SCHOEPP, D. D. & MONN, J. A. 2005. Methyl Substitution of 2-Aminobicyclo[3.1.0]hexane 2,6-Dicarboxylate (LY354740) Determines Functional Activity at Metabotropic Glutamate Receptors: Identification of a Subtype Selective mGlu2 Receptor Agonist. *Journal of Medicinal Chemistry,* 48**,** 3605-3612.
DONG, M., LU, L., ZHANG, L., ZHANG, Y.-S., NG, C. H., UNGVARI, G. S., LI, G., MENG, X., WANG, G. & XIANG, Y.-T. 2019. Quality of Life in Schizophrenia: A Meta-Analysis of Comparative Studies. *Psychiatric Quarterly,* 90**,** 519-532.
DOORDUIN, J., DE VRIES, E. F., WILLEMSEN, A. T., DE GROOT, J. C., DIERCKX, R. A. & KLEIN, H. C. 2009. Neuroinflammation in schizophrenia-related psychosis: a PET study. *Journal of Nuclear Medicine,* 50**,** 1801-1807.
DOSTROVSKY, J. & O'KEEFE, J. 1971. The hippocampus as a spatial map. Preliminary evidence from unit activity in the freely moving rat. *Brain research,* 34**,** 171-175.
DU, Y. & GRACE, A. A. 2016. Loss of Parvalbumin in the Hippocampus of MAM Schizophrenia Model Rats Is Attenuated by Peripubertal Diazepam. *International Journal of Neuropsychopharmacology,* 19.
DUGLADZE, T., SCHMITZ, D., WHITTINGTON, M. A., VIDA, I. & GLOVELI, T. 2012. Segregation of axonal and somatic activity during fast network oscillations. *Science,* 336**,** 1458-1461.

DUNCAN, C. E., WEBSTER, M. J., ROTHMOND, D. A., BAHN, S., ELASHOFF, M. & WEICKERT, C. S. 2010. Prefrontal GABAA receptor α-subunit expression in normal postnatal human development and schizophrenia. *Journal of psychiatric research,* 44**,** 673-681.

EGERTON, A., CHADDOCK, C. A., WINTON-BROWN, T. T., BLOOMFIELD, M. A. P., BHATTACHARYYA, S., ALLEN, P., MCGUIRE, P. K. & HOWES, O. D. 2013. Presynaptic Striatal Dopamine Dysfunction in People at Ultra-high Risk for Psychosis: Findings in a Second Cohort. *Biological Psychiatry,* 74**,** 106-112.

EHRLICHMAN, R., GANDAL, M., MAXWELL, C., LAZAREWICZ, M., FINKEL, L., CONTRERAS, D., TURETSKY, B. & SIEGEL, S. 2009. N-methyl-d-aspartic acid receptor antagonist–induced frequency oscillations in mice recreate pattern of electrophysiological deficits in schizophrenia. *Neuroscience,* 158**,** 705-712.

EICHENBAUM, H. 1999. The hippocampus and mechanisms of declarative memory. *Behavioural brain research,* 103**,** 123-133.

ENGEL, M., SNIKERIS, P., MATOSIN, N., NEWELL, K. A., HUANG, X.-F. & FRANK, E. 2016. mGluR2/3 agonist LY379268 rescues NMDA and GABAA receptor level deficits induced in a two-hit mouse model of schizophrenia. *Psychopharmacology,* 233**,** 1349-1359.

ERLANDER, M. G., TILLAKARATNE, N. J., FELDBLUM, S., PATEL, N. & TOBIN, A. J. 1991. Two genes encode distinct glutamate decarboxylases. *Neuron,* 7**,** 91-100.

EYO, U. B., PENG, J., MURUGAN, M., MO, M., LALANI, A., XIE, P., XU, P., MARGOLIS, D. J. & WU, L.-J. 2016. Regulation of physical microglia–neuron interactions by fractalkine signaling after status epilepticus. *Eneuro,* 3.

EYO, U. B., PENG, J., SWIATKOWSKI, P., MUKHERJEE, A., BISPO, A. & WU, L.-J. 2014. Neuronal hyperactivity recruits microglial processes via neuronal NMDA receptors and microglial P2Y12 receptors after status epilepticus. *Journal of Neuroscience,* 34**,** 10528-10540.

FAVUZZI, E., MARQUES-SMITH, A., DEOGRACIAS, R., WINTERFLOOD, C. M., SÁNCHEZ-AGUILERA, A., MANTOAN, L., MAESO, P., FERNANDES, C., EWERS, H. & RICO, B. 2017. Activity-dependent gating of parvalbumin interneuron function by the perineuronal net protein brevican. *Neuron,* 95**,** 639-655. e10.

FAWCETT, J. W., FYHN, M., JENDELOVA, P., KWOK, J. C. F., RUZICKA, J. & SORG, B. A. 2022. The extracellular matrix and perineuronal nets in memory. *Molecular Psychiatry,* 27**,** 3192-3203.

FAWCETT, J. W., OOHASHI, T. & PIZZORUSSO, T. 2019. The roles of perineuronal nets and the perinodal extracellular matrix in neuronal function. *Nature Reviews Neuroscience,* 20**,** 451-465.

FEATHERSTONE, R. E., RIZOS, Z., NOBREGA, J. N., KAPUR, S. & FLETCHER, P. J. 2007. Gestational methylazoxymethanol acetate treatment impairs select cognitive functions: parallels to schizophrenia. *Neuropsychopharmacology,* 32**,** 483-492.

FELL, M. J., MCKINZIE, D. L., MONN, J. A. & SVENSSON, K. A. 2012. Group II metabotropic glutamate receptor agonists and positive allosteric modulators as novel treatments for schizophrenia. *Neuropharmacology,* 62**,** 1473-1483.

FERGUSON, B. R. & GAO, W. J. 2018. PV Interneurons: Critical Regulators of E/I Balance for Prefrontal Cortex-Dependent Behavior and Psychiatric Disorders. *Front Neural Circuits,* 12**,** 37.

FINO, E. & YUSTE, R. 2011. Dense inhibitory connectivity in neocortex. *Neuron,* 69**,** 1188-1203.

FISAHN, A., CONTRACTOR, A., TRAUB, R. D., BUHL, E. H., HEINEMANN, S. F. & MCBAIN, C. J. 2004. Distinct Roles for the Kainate Receptor Subunits GluR5 and GluR6 in Kainate-Induced Hippocampal Gamma Oscillations. *The Journal of Neuroscience,* 24**,** 9658-9668.

FISAHN, A., PIKE, F. G., BUHL, E. H. & PAULSEN, O. 1998. Cholinergic induction of network oscillations at 40 Hz in the hippocampus in vitro. *Nature,* 394**,** 186-9.

FISCHER, F. P., KASTURE, A. S., HUMMEL, T. & SUCIC, S. 2022. Molecular and Clinical Repercussions of GABA Transporter 1 Variants Gone Amiss: Links to Epilepsy and Developmental Spectrum Disorders. *Frontiers in Molecular Biosciences,* 9.

FISH, K. N., SWEET, R. A. & LEWIS, D. A. 2011. Differential Distribution of Proteins Regulating GABA Synthesis and Reuptake in Axon Boutons of Subpopulations of Cortical Interneurons. *Cerebral Cortex,* 21**,** 2450-2460.

FISHER, J., VERHAGEN, M., LONG, Z., MOISSIDIS, M., YAN, Y., HE, C., WANG, J., MICOLI, E., ALASTRUEY, C. M., MOORS, R., MARÍN, O., MI, D. & LIM, L. 2024. Cortical somatostatin long-range projection neurons and interneurons exhibit divergent developmental trajectories. *Neuron,* 112**,** 558-573.e8.

FITZGERALD, P. J. & WATSON, B. O. 2018. Gamma oscillations as a biomarker for major depression: an emerging topic. *Transl Psychiatry,* 8**,** 177.

FLAGSTAD, P., MØRK, A., GLENTHØJ, B. Y., VAN BEEK, J., MICHAEL-TITUS, A. T. & DIDRIKSEN, M. 2004. Disruption of neurogenesis on gestational day 17 in the rat causes behavioral changes relevant to positive and negative schizophrenia symptoms and alters amphetamine-induced dopamine release in nucleus accumbens. *Neuropsychopharmacology,* 29**,** 2052-2064.

FLOREZ, C. M., MCGINN, R. J., LUKANKIN, V., MARWA, I., SUGUMAR, S., DIAN, J., HAZRATI, L. N., CARLEN, P. L., ZHANG, L. & VALIANTE, T. A. 2015. In vitro recordings of human neocortical oscillations. *Cereb Cortex,* 25**,** 578-97.

FORNITO, A., YÜCEL, M., DEAN, B., WOOD, S. J. & PANTELIS, C. 2009. Anatomical abnormalities of the anterior cingulate cortex in schizophrenia: bridging the gap between neuroimaging and neuropathology. *Schizophr Bull,* 35**,** 973-93.

FRANKLE, W. G., CHO, R. Y., PRASAD, K. M., MASON, N. S., PARIS, J., HIMES, M. L., WALKER, C., LEWIS, D. A. & NARENDRAN, R. 2015. In vivo measurement of GABA transmission in healthy subjects and schizophrenia patients. *Am J Psychiatry,* 172**,** 1148-59.

FRASSONI, C., BENTIVOGLIO, M., SPREAFICO, R., SÁNCHEZ, M. P., PUELLES, L. & FAIREN, A. 1991. Postnatal development of calbindin and parvalbumin immunoreactivity in the thalamus of the rat. *Brain Res Dev Brain Res,* 58**,** 243-9.

FREEMAN, A. S. & BUNNEY, B. S. 1984. The effects of phencyclidine and N-allylnormetazocine on midbrain dopamine neuronal activity. *Eur J Pharmacol,* 104**,** 287-93.

FREUND, T. F. 2003. Interneuron diversity series: rhythm and mood in perisomatic inhibition. *Trends in neurosciences,* 26**,** 489-495.

FUCHS, E. C., ZIVKOVIC, A. R., CUNNINGHAM, M. O., MIDDLETON, S., LEBEAU, F. E., BANNERMAN, D. M., ROZOV, A., WHITTINGTON, M. A., TRAUB, R. D., RAWLINS, J. N. & MONYER, H. 2007. Recruitment of parvalbumin-positive interneurons determines hippocampal function and associated behavior. *Neuron,* 53**,** 591-604.

FUNG, S. J., WEBSTER, M. J., SIVAGNANASUNDARAM, S., DUNCAN, C., ELASHOFF, M. & WEICKERT, C. S. 2010. Expression of interneuron markers in the dorsolateral prefrontal cortex of the developing human and in schizophrenia. *Am J Psychiatry,* 167**,** 1479-88.

FURTH, K. E., MCCOY, A. J., DODGE, C., WALTERS, J. R., BUONANNO, A. & DELAVILLE, C. 2017. Neuronal correlates of ketamine and walking induced gamma oscillations in the medial prefrontal cortex and mediodorsal thalamus. *PLoS One,* 12**,** e0186732.

GAEBEL, W. & KERST, A. 2019. The debate about renaming schizophrenia: a new name would not resolve the stigma. *Epidemiol Psychiatr Sci,* 28**,** 258-261.

GAO, C., JIANG, J., TAN, Y. & CHEN, S. 2023. Microglia in neurodegenerative diseases: mechanism and potential therapeutic targets. *Signal Transduction and Targeted Therapy,* 8**,** 359.

GAO, X. M., SAKAI, K., ROBERTS, R. C., CONLEY, R. R., DEAN, B. & TAMMINGA, C. A. 2000. Ionotropic glutamate receptors and expression of N-methyl-D-aspartate receptor subunits in subregions of human hippocampus: effects of schizophrenia. *Am J Psychiatry,* 157**,** 1141-9.

GARDNER-MEDWIN, A. R. & WILKIE, D. R. 1976. The recall of events through the learning of associations between their parts. *Proceedings of the Royal Society of London. Series B. Biological Sciences,* 194**,** 375-402.

GEHRMANN, J., MATSUMOTO, Y. & KREUTZBERG, G. W. 1995. Microglia: intrinsic immuneffector cell of the brain. *Brain research reviews,* 20**,** 269-287.

GEKKER, G., HU, S., SHENG, W. S., ROCK, R. B., LOKENSGARD, J. R. & PETERSON, P. K. 2006. Cocaine-induced HIV-1 expression in microglia involves sigma-1 receptors and transforming growth factor-beta1. *Int Immunopharmacol,* 6**,** 1029-33.

GHOSE, S., CROOK, J. M., BARTUS, C. L., SHERMAN, T. G., HERMAN, M. M., HYDE, T. M., KLEINMAN, J. E. & AKIL, M. 2008. Metabotropic glutamate receptor 2 and 3 gene expression in the human prefrontal cortex and mesencephalon in schizophrenia. *Int J Neurosci,* 118**,** 1609-27.

GIGG, J., MCEWAN, F., SMAUSZ, R., NEILL, J. & HARTE, M. K. 2020. Synaptic biomarker reduction and impaired cognition in the sub-chronic PCP mouse model for schizophrenia. *Journal of Psychopharmacology,* 34**,** 115-124.

GILL, K. M. & GRACE, A. A. 2014. Corresponding decrease in neuronal markers signals progressive parvalbumin neuron loss in MAM schizophrenia model. *International Journal of Neuropsychopharmacology,* 17**,** 1609-1619.

GIULIANO, A. J., LI, H., MESHOLAM-GATELY, R. I., SORENSON, S. M., WOODBERRY, K. A. & SEIDMAN, L. J. 2012. Neurocognition in the psychosis risk syndrome: a quantitative and qualitative review. *Curr Pharm Des,* 18**,** 399-415.

GLORIOSO, C., SABATINI, M., UNGER, T., HASHIMOTO, T., MONTEGGIA, L. M., LEWIS, D. A. & MIRNICS, K. 2006. Specificity and timing of neocortical transcriptome changes in response to BDNF gene ablation during embryogenesis or adulthood. *Mol Psychiatry,* 11**,** 633-48.

GLUCK, M. R., THOMAS, R. G., DAVIS, K. L. & HAROUTUNIAN, V. 2002. Implications for altered glutamate and GABA metabolism in the dorsolateral prefrontal cortex of aged schizophrenic patients. *American Journal of Psychiatry,* 159**,** 1165-1173.

GLYKOS, V., WHITTINGTON, M. A. & LEBEAU, F. E. N. 2015. Subregional differences in the generation of fast network oscillations in the rat medial prefrontal cortex (mPFC) in vitro. *The Journal of Physiology,* 593**,** 3597-3615.
GOETZ, T., ARSLAN, A., WISDEN, W. & WULFF, P. 2007. GABA(A) receptors: structure and function in the basal ganglia. *Prog Brain Res,* 160**,** 21-41.
GOGOS, A., KUSLJIC, S., THWAITES, S. J. & VAN DEN BUUSE, M. 2017. Sex differences in psychotomimetic-induced behaviours in rats. *Behavioural Brain Research,* 322**,** 157-166.
GOGOS, A. & VAN DEN BUUSE, M. 2023. Sex Differences in Psychosis: Focus on Animal Models. *Curr Top Behav Neurosci,* 62**,** 133-163.
GOLDSMITH, D. R., RAPAPORT, M. H. & MILLER, B. J. 2016. A meta-analysis of blood cytokine network alterations in psychiatric patients: comparisons between schizophrenia, bipolar disorder and depression. *Mol Psychiatry,* 21**,** 1696-1709.
GONZALEZ-BURGOS, G. & LEWIS, D. A. 2008. GABA neurons and the mechanisms of network oscillations: implications for understanding cortical dysfunction in schizophrenia. *Schizophr Bull,* 34**,** 944-61.
GONZALEZ-MAESO, J., ANG, R. L., YUEN, T., CHAN, P., WEISSTAUB, N. V., LOPEZ-GIMENEZ, J. F., ZHOU, M. M., OKAWA, Y., CALLADO, L. F., MILLIGAN, G., GINGRICH, J. A., FILIZOLA, M., MEANA, J. J. & SEALFON, S. C. 2008. Identification of a serotonin/glutamate receptor complex implicated in psychosis. *Nature,* 452**,** 93-U9.
GORDON, J. A. 2010. Testing the glutamate hypothesis of schizophrenia. *Nature Neuroscience,* 13**,** 2-4.
GOTO, A. 2022. Synaptic plasticity during systems memory consolidation. *Neuroscience Research,* 183**,** 1-6.
GRAY, C. M., KONIG, P., ENGEL, A. K. & SINGER, W. 1989. Oscillatory responses in cat visual cortex exhibit inter-columnar synchronization which reflects global stimulus properties. *Nature,* 338**,** 334-7.
GRENT-'T-JONG, T., GROSS, J., GOENSE, J., WIBRAL, M., GAJWANI, R., GUMLEY, A. I., LAWRIE, S. M., SCHWANNAUER, M., SCHULTZE-LUTTER, F., NAVARRO SCHRÖDER, T., KOETHE, D., LEWEKE, F. M., SINGER, W. & UHLHAAS, P. J. 2018. Resting-state gamma-band power alterations in schizophrenia reveal E/I-balance abnormalities across illness-stages. *Elife,* 7.
GRETENKORD, S., REES, A., WHITTINGTON, M. A., GARTSIDE, S. E. & LEBEAU, F. E. N. 2016. Dorsal vs. ventral differences in fast Up-state-associated oscillations in the medial prefrontal cortex of the urethane-anesthetized rat. *Journal of Neurophysiology,* 117**,** 1126-1142.
GRIEBEL, G., PICHAT, P., BOULAY, D., NAIMOLI, V., POTESTIO, L., FEATHERSTONE, R., SAHNI, S., DEFEX, H., DESVIGNES, C., SLOWINSKI, F., VIGÉ, X., BERGIS, O. E., SHER, R., KOSLEY, R., KONGSAMUT, S., BLACK, M. D. & VARTY, G. B. 2016. The mGluR2 positive allosteric modulator, SAR218645, improves memory and attention deficits in translational models of cognitive symptoms associated with schizophrenia. *Scientific Reports,* 6**,** 35320.
GROSMARK, ANDRES D., MIZUSEKI, K., PASTALKOVA, E., DIBA, K. & BUZSÁKI, G. 2012. REM Sleep Reorganizes Hippocampal Excitability. *Neuron,* 75**,** 1001-1007.
GROUSELLE, D., WINSKY-SOMMERER, R., DAVID, J. P., DELACOURTE, A., DOURNAUD, P. & EPELBAUM, J. 1998. Loss of somatostatin-like

immunoreactivity in the frontal cortex of Alzheimer patients carrying the apolipoprotein epsilon 4 allele. *Neurosci Lett,* 255**,** 21-4.

GU, G., LORRAIN, D. S., WEI, H., COLE, R. L., ZHANG, X., DAGGETT, L. P., SCHAFFHAUSER, H. J., BRISTOW, L. J. & LECHNER, S. M. 2008. Distribution of metabotropic glutamate 2 and 3 receptors in the rat forebrain: Implication in emotional responses and central disinhibition. *Brain Research,* 1197**,** 47-62.

GUAN, A., WANG, S., HUANG, A., QIU, C., LI, Y., LI, X., WANG, J., WANG, Q. & DENG, B. 2022. The role of gamma oscillations in central nervous system diseases: Mechanism and treatment. *Front Cell Neurosci,* 16**,** 962957.

GUERRA, A., FEURRA, M., PELLEGRINO, G. & BRITTAIN, J. S. 2019. Investigating and Modulating Physiological and Pathological Brain Oscillations: The Role of Oscillatory Activity in Neural Plasticity. *Neural Plast,* 2019**,** 9403195.

GUILLOUX, J. P., DOUILLARD-GUILLOUX, G., KOTA, R., WANG, X., GARDIER, A. M., MARTINOWICH, K., TSENG, G. C., LEWIS, D. A. & SIBILLE, E. 2012. Molecular evidence for BDNF- and GABA-related dysfunctions in the amygdala of female subjects with major depression. *Mol Psychiatry,* 17**,** 1130-42.

GUNDLACH, A. L., LARGENT, B. L. & SNYDER, S. H. 1986. Autoradiographic localization of sigma receptor binding sites in guinea pig and rat central nervous system with (+)3H-3-(3-hydroxyphenyl)-N-(1-propyl)piperidine. *J Neurosci,* 6**,** 1757-70.

GUO, J. Y., RAGLAND, J. D. & CARTER, C. S. 2019. Memory and cognition in schizophrenia. *Mol Psychiatry,* 24**,** 633-642.

HABER, S. N., LIU, H., SEIDLITZ, J. & BULLMORE, E. 2022. Prefrontal connectomics: from anatomy to human imaging. *Neuropsychopharmacology,* 47**,** 20-40.

HAENSCHEL, C., BITTNER, R. A., WALTZ, J., HAERTLING, F., WIBRAL, M., SINGER, W., LINDEN, D. E. & RODRIGUEZ, E. 2009. Cortical oscillatory activity is critical for working memory as revealed by deficits in early-onset schizophrenia. *J Neurosci,* 29**,** 9481-9.

HÄFNER, H., MAURER, K., LÖFFLER, W., FÄTKENHEUER, B., AN DER HEIDEN, W., RIECHER-RÖSSLER, A., BEHRENS, S. & GATTAZ, W. F. 1994. The epidemiology of early schizophrenia. Influence of age and gender on onset and early course. *Br J Psychiatry Suppl***,** 29-38.

HAKAMI, T., JONES, N. C., TOLMACHEVA, E. A., GAUDIAS, J., CHAUMONT, J., SALZBERG, M., O'BRIEN, T. J. & PINAULT, D. 2009. NMDA receptor hypofunction leads to generalized and persistent aberrant gamma oscillations independent of hyperlocomotion and the state of consciousness. *PLoS One,* 4**,** e6755.

HALBERSTADT, A. L. 1995. The phencyclidine-glutamate model of schizophrenia. *Clin Neuropharmacol,* 18**,** 237-49.

HALL, A. A., HERRERA, Y., AJMO, C. T., JR., CUEVAS, J. & PENNYPACKER, K. R. 2009. Sigma receptors suppress multiple aspects of microglial activation. *Glia,* 57**,** 744-54.

HANNA, L., CEOLIN, L., LUCAS, S., MONN, J., JOHNSON, B., COLLINGRIDGE, G., BORTOLOTTO, Z. & LODGE, D. 2013. Differentiating the roles of mGlu2 and mGlu3 receptors using LY541850, an mGlu2 agonist/mGlu3 antagonist. *Neuropharmacology,* 66**,** 114-121.

HANSEN, H. H., BRIEM, T., DZIETKO, M., SIFRINGER, M., VOSS, A., RZESKI, W., ZDZISINSKA, B., THOR, F., HEUMANN, R., STEPULAK, A., BITTIGAU, P. &

IKONOMIDOU, C. 2004. Mechanisms leading to disseminated apoptosis following NMDA receptor blockade in the developing rat brain. *Neurobiology of Disease,* 16**,** 440-453.
HANSEN, K. B., YI, F., PERSZYK, R. E., FURUKAWA, H., WOLLMUTH, L. P., GIBB, A. J. & TRAYNELIS, S. F. 2018. Structure, function, and allosteric modulation of NMDA receptors. *Journal of General Physiology,* 150**,** 1081-1105.
HARRIS, E. W., GANONG, A. H. & COTMAN, C. W. 1984. Long-term potentiation in the hippocampus involves activation of N-methyl-D-aspartate receptors. *Brain Research,* 323**,** 132-137.
HÄRTIG, W., BRAUER, K. & BRÜCKNER, G. 1992. Wisteria floribunda agglutinin-labelled nets surround parvalbumin-containing neurons. *Neuroreport,* 3**,** 869-72.
HASHIMOTO, K., FUJITA, Y. & IYO, M. 2007. Phencyclidine-induced cognitive deficits in mice are improved by subsequent subchronic administration of fluvoxamine: role of sigma-1 receptors. *Neuropsychopharmacology,* 32**,** 514-21.
HASHIMOTO, T., BAZMI, H. H., MIRNICS, K., WU, Q., SAMPSON, A. R. & LEWIS, D. A. 2008. Conserved regional patterns of GABA-related transcript expression in the neocortex of subjects with schizophrenia. *Am J Psychiatry,* 165**,** 479-89.
HASHIMOTO, T., VOLK, D. W., EGGAN, S. M., MIRNICS, K., PIERRI, J. N., SUN, Z., SAMPSON, A. R. & LEWIS, D. A. 2003. Gene expression deficits in a subclass of GABA neurons in the prefrontal cortex of subjects with schizophrenia. *J Neurosci,* 23**,** 6315-26.
HAYASHI, T. 2019. The Sigma-1 Receptor in Cellular Stress Signaling. *Frontiers in Neuroscience,* 13.
HAYASHI, T. & SU, T. P. 2004. Sigma-1 receptor ligands: potential in the treatment of neuropsychiatric disorders. *CNS Drugs,* 18**,** 269-84.
HEBB, D. O. 1949. *The organization of behavior; a neuropsychological theory,* Oxford, England, Wiley.
HEIZMANN, C. W. 1993. Calcium signaling in the brain. *Acta neurobiologiae experimentalis,* 53**,** 15-23.
HELLEWELL, S. B., BRUCE, A., FEINSTEIN, G., ORRINGER, J., WILLIAMS, W. & BOWEN, W. D. 1994. Rat liver and kidney contain high densities of sigma 1 and sigma 2 receptors: characterization by ligand binding and photoaffinity labeling. *Eur J Pharmacol,* 268**,** 9-18.
HERVIG, M. E., THOMSEN, M. S., KALLÓ, I. & MIKKELSEN, J. D. 2016. Acute phencyclidine administration induces c-Fos-immunoreactivity in interneurons in cortical and subcortical regions. *Neuroscience,* 334**,** 13-25.
HILL, S. L., SHAO, L. & BEASLEY, C. L. 2021. Diminished levels of the chemokine fractalkine in post-mortem prefrontal cortex in schizophrenia but not bipolar disorder. *The World Journal of Biological Psychiatry,* 22**,** 94-103.
HIYOSHI, T., HIKICHI, H., KARASAWA, J.-I. & CHAKI, S. 2014a. Metabotropic glutamate receptors regulate cortical gamma hyperactivities elicited by ketamine in rats. *Neuroscience Letters,* 567**,** 30-34.
HIYOSHI, T., KAMBE, D., KARASAWA, J. & CHAKI, S. 2014b. Differential effects of NMDA receptor antagonists at lower and higher doses on basal gamma band oscillation power in rat cortical electroencephalograms. *Neuropharmacology,* 85**,** 384-96.
HIYOSHI, T., KAMBE, D., KARASAWA, J. & CHAKI, S. 2014c. Involvement of glutamatergic and GABAergic transmission in MK-801-increased gamma band

oscillation power in rat cortical electroencephalograms. *Neuroscience,* 280**,** 262-274.
HJORTHØJ, C., STÜRUP, A. E., MCGRATH, J. J. & NORDENTOFT, M. 2017. Years of potential life lost and life expectancy in schizophrenia: a systematic review and meta-analysis. *The Lancet Psychiatry,* 4**,** 295-301.
HOF, P. R., GLEZER, I. I., CONDÉ, F., FLAGG, R. A., RUBIN, M. B., NIMCHINSKY, E. A. & VOGT WEISENHORN, D. M. 1999. Cellular distribution of the calcium-binding proteins parvalbumin, calbindin, and calretinin in the neocortex of mammals: phylogenetic and developmental patterns. *Journal of Chemical Neuroanatomy,* 16**,** 77-116.
HOLCOMB, H. H., LAHTI, A. C., MEDOFF, D. R., CULLEN, T. & TAMMINGA, C. A. 2005. Effects of Noncompetitive NMDA Receptor Blockade on Anterior Cingulate Cerebral Blood Flow in Volunteers with Schizophrenia. *Neuropsychopharmacology,* 30**,** 2275-2282.
HOLLMANN, M. 1999. Structure of ionotropic glutamate receptors. *Ionotropic glutamate receptors in the CNS.* Springer.
HOMAYOUN, H. & MOGHADDAM, B. 2007. NMDA receptor hypofunction produces opposite effects on prefrontal cortex interneurons and pyramidal neurons. *Journal of Neuroscience,* 27**,** 11496-11500.
HOU, Z. H. & YU, X. 2013. Activity-regulated somatostatin expression reduces dendritic spine density and lowers excitatory synaptic transmission via postsynaptic somatostatin receptor 4. *J Biol Chem,* 288**,** 2501-9.
HOWARD, M. W., RIZZUTO, D. S., CAPLAN, J. B., MADSEN, J. R., LISMAN, J., ASCHENBRENNER-SCHEIBE, R., SCHULZE-BONHAGE, A. & KAHANA, M. J. 2003. Gamma oscillations correlate with working memory load in humans. *Cereb Cortex,* 13**,** 1369-74.
HRADETZKY, E., SANDERSON, T. M., TSANG, T. M., SHERWOOD, J. L., FITZJOHN, S. M., LAKICS, V., MALIK, N., SCHOEFFMANN, S., O'NEILL, M. J. & CHENG, T. M. 2012. The methylazoxymethanol acetate (MAM-E17) rat model: molecular and functional effects in the hippocampus. *Neuropsychopharmacology,* 37**,** 364-377.
HU, H., GAN, J. & JONAS, P. 2014. Fast-spiking, parvalbumin+ GABAergic interneurons: From cellular design to microcircuit function. *Science,* 345**,** 1255263.
HUANG, X., LI, Y., LIU, H., XU, J., TAN, Z., DONG, H., TIAN, B., WU, S. & WANG, W. 2022. Activation of basolateral amygdala to anterior cingulate cortex circuit alleviates MK-801 induced social and cognitive deficits of schizophrenia. *Frontiers in Cellular Neuroscience,* 16.
HUANG, Z. J. & PAUL, A. 2019. The diversity of GABAergic neurons and neural communication elements. *Nature Reviews Neuroscience,* 20**,** 563-572.
HUGHES, H., BRADY, L. J. & SCHOONOVER, K. E. 2024. GABAergic dysfunction in postmortem dorsolateral prefrontal cortex: implications for cognitive deficits in schizophrenia and affective disorders. *Front Cell Neurosci,* 18**,** 1440834.
HYLIN, M. J., ORSI, S. A., MOORE, A. N. & DASH, P. K. 2013. Disruption of the perineuronal net in the hippocampus or medial prefrontal cortex impairs fear conditioning. *Learn Mem,* 20**,** 267-73.
ISHIKAWA, M. & HASHIMOTO, K. 2009. *The role of sigma-1 receptors in the pathophysiology of neuropsychiatric diseases*.
ISHIMA, T., FUJITA, Y., KOHNO, M., KUNITACHI, S., HORIO, M., TAKATSU, Y., MINASE, T., TANIBUCHI, Y., HAGIWARA, H., IYO, M. & HASHIMOTO, K.

2009. *Improvement of Phencyclidine-Induced Cognitive Deficits in Mice by Subsequent Subchronic Administration of Fluvoxamine, but not Sertraline*.
ISHIZUKA, N., WEBER, J. & AMARAL, D. G. 1990. Organization of intrahippocampal projections originating from CA3 pyramidal cells in the rat. *Journal of comparative neurology,* 295**,** 580-623.
ITZHAK, Y., HILLER, J. M. & SIMON, E. J. 1985. Characterization of specific binding sites for [3H](d)-N-allylnormetazocine in rat brain membranes. *Molecular pharmacology,* 27**,** 46-52.
IVERSEN, L. L., IVERSEN, S. D., BLOOM, F., DOUGLAS, C., BROWN, M. & VALE, W. 1978. Calcium-dependent release of somatostatin and neurotensin from rat brain in vitro. *Nature,* 273**,** 161-3.
IZQUIERDO, P., ATTWELL, D. & MADRY, C. 2019. Ion Channels and Receptors as Determinants of Microglial Function. *Trends Neurosci,* 42**,** 278-292.
JACKSON, M. E., HOMAYOUN, H. & MOGHADDAM, B. 2004. NMDA receptor hypofunction produces concomitant firing rate potentiation and burst activity reduction in the prefrontal cortex. *Proc Natl Acad Sci U S A,* 101**,** 8467-72.
JACOB, T. C. 2019. Neurobiology and Therapeutic Potential of α5-GABA Type A Receptors. *Frontiers in Molecular Neuroscience,* 12.
JAFARI, Z., KOLB, B. E. & MOHAJERANI, M. H. 2020. Neural oscillations and brain stimulation in Alzheimer's disease. *Prog Neurobiol,* 194**,** 101878.
JANG, H. J., CHUNG, H., ROWLAND, J. M., RICHARDS, B. A., KOHL, M. M. & KWAG, J. 2020. Distinct roles of parvalbumin and somatostatin interneurons in gating the synchronization of spike times in the neocortex. *Sci Adv,* 6**,** eaay5333.
JANHUNEN, S. K., SVÄRD, H., TALPOS, J., KUMAR, G., STECKLER, T., PLATH, N., LERDRUP, L., RUBY, T., HAMAN, M., WYLER, R. & BALLARD, T. M. 2015. The subchronic phencyclidine rat model: relevance for the assessment of novel therapeutics for cognitive impairment associated with schizophrenia. *Psychopharmacology,* 232**,** 4059-4083.
JAVITT, D. 1987. Negative schizophrenic symptomatology and the PCP (phencyclidine) model of schizophrenia. *The Hillside journal of clinical psychiatry,* 9**,** 12-35.
JAVITT, D. C. & ZUKIN, S. R. 1991. Recent advances in the phencyclidine model of schizophrenia. *Am J Psychiatry,* 148**,** 1301-8.
JIA, J., CHENG, J., WANG, C. & ZHEN, X. 2018. Sigma-1 Receptor-Modulated Neuroinflammation in Neurological Diseases. *Frontiers in Cellular Neuroscience,* 12.
JINNO, S., FLEISCHER, F., ECKEL, S., SCHMIDT, V. & KOSAKA, T. 2007. Spatial arrangement of microglia in the mouse hippocampus: a stereological study in comparison with astrocytes. *Glia,* 55**,** 1334-47.
JINNO, S. & KOSAKA, T. 2002. Patterns of expression of calcium binding proteins and neuronal nitric oxide synthase in different populations of hippocampal GABAergic neurons in mice. *Journal of Comparative Neurology,* 449**,** 1-25.
JINNO, S. & KOSAKA, T. 2003. Patterns of expression of neuropeptides in GABAergic nonprincipal neurons in the mouse hippocampus: Quantitative analysis with optical disector. *Journal of Comparative Neurology,* 461**,** 333-349.
JINNO, S. & KOSAKA, T. 2004. Parvalbumin is expressed in glutamatergic and GABAergic corticostriatal pathway in mice. *Journal of Comparative Neurology,* 477**,** 188-201.

JOBSON, D. D., HASE, Y., CLARKSON, A. N. & KALARIA, R. N. 2021. The role of the medial prefrontal cortex in cognition, ageing and dementia. *Brain Commun,* 3**,** fcab125.

JOHNSON, J., CHEN, T. K., RICKMAN, D. W., EVANS, C. & BRECHA, N. C. 1996. Multiple γ-aminobutyric acid plasma membrane transporters GAT-1, GAT-2, GAT-3 in the rat retina. *Journal of Comparative Neurology,* 375**,** 212-224.

JOHNSON, K. & JONES, S. 1990. Neuropharmacology of phencyclidine: basic mechanisms and therapeutic potential. *Annual review of pharmacology and toxicology,* 30**,** 707-750.

JORDAN, J. T. 2019. The rodent hippocampus as a bilateral structure: A review of hemispheric lateralization. *bioRxiv***,** 150193.

JUMAH, F. & DOSSANI, R. 2019. Neuroanatomy, Cingulate Cortex.

KAALUND, S. S., RIISE, J., BROBERG, B. V., FABRICIUS, K., KARLSEN, A. S., SECHER, T., PLATH, N. & PAKKENBERG, B. 2013. Differential expression of parvalbumin in neonatal phencyclidine-treated rats and socially isolated rats. *Journal of Neurochemistry,* 124**,** 548-557.

KAAR, S. J., ANGELESCU, I., MARQUES, T. R. & HOWES, O. D. 2019. Pre-frontal parvalbumin interneurons in schizophrenia: a meta-analysis of post-mortem studies. *Journal of Neural Transmission,* 126**,** 1637-1651.

KALKMAN, H. O. & LOETSCHER, E. 2003. GAD67: the link between the GABA-deficit hypothesis and the dopaminergic- and glutamatergic theories of psychosis. *Journal of Neural Transmission,* 110**,** 803-812.

KÁLLAI, V., LÉNÁRD, L., PÉCZELY, L., GÁLOSI, R., DUSA, D., TÓTH, A., LÁSZLÓ, K., KERTES, E., KOVÁCS, A., ZAGORACZ, O., BERTA, B., KARÁDI, Z. & OLLMANN, T. 2020. Cognitive performance of the MAM-E17 schizophrenia model rats in different age-periods. *Behavioural Brain Research,* 379**,** 112345.

KALUS, P., SENITZ, D. & BECKMANN, H. 1997. Altered distribution of parvalbumin-immunoreactive local circuit neurons in the anterior cingulate cortex of schizophrenic patients. *Psychiatry Res,* 75**,** 49-59.

KANAANI, J., KOLIBACHUK, J., MARTINEZ, H. & BAEKKESKOV, S. 2010. Two distinct mechanisms target GAD67 to vesicular pathways and presynaptic clusters. *J Cell Biol,* 190**,** 911-25.

KANDEL, E. R. & SPENCER, W. A. 1968. Cellular neurophysiological approaches in the study of learning. *Physiological reviews,* 48**,** 65-134.

KANE, J. M., MARDER, S. R., SCHOOLER, N. R., WIRSHING, W. C., UMBRICHT, D., BAKER, R. W., WIRSHING, D. A., SAFFERMAN, A., GANGULI, R. & MCMENIMAN, M. 2001. Clozapine and haloperidol in moderately refractory schizophrenia: a 6-month randomized and double-blind comparison. *Archives of General Psychiatry,* 58**,** 965-972.

KANEDA, M. & OSAKA, N. 2008. Role of anterior cingulate cortex during semantic coding in verbal working memory. *Neuroscience letters,* 436**,** 57-61.

KANIGOWSKI, D., BOGAJ, K., BARTH, A. L. & URBAN-CIECKO, J. 2023. Somatostatin-expressing interneurons modulate neocortical network through GABAb receptors in a synapse-specific manner. *Sci Rep,* 13**,** 8780.

KAPUR, S. & SEEMAN, P. 2002. NMDA receptor antagonists ketamine and PCP have direct effects on the dopamine D(2) and serotonin 5-HT(2)receptors-implications for models of schizophrenia. *Mol Psychiatry,* 7**,** 837-44.

KARGIEMAN, L., SANTANA, N., MENGOD, G., CELADA, P. & ARTIGAS, F. 2007. Antipsychotic drugs reverse the disruption in prefrontal cortex function

produced by NMDA receptor blockade with phencyclidine. *Proc Natl Acad Sci U S A,* 104**,** 14843-8.
KATO, G., INADA, H., WAKE, H., AKIYOSHI, R., MIYAMOTO, A., ETO, K., ISHIKAWA, T., MOORHOUSE, A. J., STRASSMAN, A. M. & NABEKURA, J. 2016. Microglial contact prevents excess depolarization and rescues neurons from excitotoxicity. *eneuro,* 3.
KESNER, R. P. & DAKIS, M. 1993. Phencyclidine disrupts acquisition and retention performance within a spatial continuous recognition memory task. *Pharmacol Biochem Behav,* 44**,** 419-24.
KESNER, R. P. & HOPKINS, R. O. 2006. Mnemonic functions of the hippocampus: a comparison between animals and humans. *Biol Psychol,* 73**,** 3-18.
KESNER, R. P. & ROLLS, E. T. 2015. A computational theory of hippocampal function, and tests of the theory: new developments. *Neuroscience & Biobehavioral Reviews,* 48**,** 92-147.
KILAVIK, B. E., ZAEPFFEL, M., BROVELLI, A., MACKAY, W. A. & RIEHLE, A. 2013. The ups and downs of beta oscillations in sensorimotor cortex. *Experimental neurology,* 245**,** 15-26.
KINGSTON, A. E., ORNSTEIN, P. L., WRIGHT, R. A., JOHNSON, B. G., MAYNE, N. G., BURNETT, J. P., BELAGAJE, R., WU, S. & SCHOEPP, D. D. 1998. LY341495 is a nanomolar potent and selective antagonist of group II metabotropic glutamate receptors. *Neuropharmacology,* 37**,** 1-12.
KITAICHI, K., CHABOT, J.-G., MOEBIUS, F. F., FLANDORFER, A., GLOSSMANN, H. & QUIRION, R. 2000. Expression of the purported sigma1 (σ1) receptor in the mammalian brain and its possible relevance in deficits induced by antagonism of the NMDA receptor complex as revealed using an antisense strategy. *Journal of Chemical Neuroanatomy,* 20**,** 375-387.
KITTELBERGER, K., HUR, E. E., SAZEGAR, S., KESHAVAN, V. & KOCSIS, B. 2012. Comparison of the effects of acute and chronic administration of ketamine on hippocampal oscillations: relevance for the NMDA receptor hypofunction model of schizophrenia. *Brain Structure and Function,* 217**,** 395-409.
KLAUSBERGER, T. & SOMOGYI, P. 2008. Neuronal diversity and temporal dynamics: the unity of hippocampal circuit operations. *Science,* 321**,** 53-57.
KLUR, S., MULLER, C., PEREIRA DE VASCONCELOS, A., BALLARD, T., LOPEZ, J., GALANI, R., CERTA, U. & CASSEL, J. C. 2009. Hippocampal-dependent spatial memory functions might be lateralized in rats: An approach combining gene expression profiling and reversible inactivation. *Hippocampus,* 19**,** 800-816.
KOH, W., KWAK, H., CHEONG, E. & LEE, C. J. 2023. GABA tone regulation and its cognitive functions in the brain. *Nature Reviews Neuroscience,* 24**,** 523-539.
KONRADI, C., YANG, C. K., ZIMMERMAN, E. I., LOHMANN, K. M., GRESCH, P., PANTAZOPOULOS, H., BERRETTA, S. & HECKERS, S. 2011. Hippocampal interneurons are abnormal in schizophrenia. *Schizophr Res,* 131**,** 165-73.
KRIEGSTEIN, A. & ALVAREZ-BUYLLA, A. 2009. The glial nature of embryonic and adult neural stem cells. *Annu Rev Neurosci,* 32**,** 149-84.
KRUSE, A. O. & BUSTILLO, J. R. 2022. Glutamatergic dysfunction in Schizophrenia. *Transl Psychiatry,* 12**,** 500.
KRYSTAL, J. H., ABI-SAAB, W., PERRY, E., D'SOUZA, D. C., LIU, N., GUEORGUIEVA, R., MCDOUGALL, L., HUNSBERGER, T., BELGER, A., LEVINE, L. & BREIER, A. 2005. Preliminary evidence of attenuation of the disruptive effects of the NMDA glutamate receptor antagonist, ketamine, on

working memory by pretreatment with the group II metabotropic glutamate receptor agonist, LY354740, in healthy human subjects. *Psychopharmacology,* 179**,** 303-309.

KRYSTAL, J. H., KARPER, L. P., SEIBYL, J. P., FREEMAN, G. K., DELANEY, R., BREMNER, J. D., HENINGER, G. R., BOWERS, M. B., JR. & CHARNEY, D. S. 1994. Subanesthetic effects of the noncompetitive NMDA antagonist, ketamine, in humans. Psychotomimetic, perceptual, cognitive, and neuroendocrine responses. *Arch Gen Psychiatry,* 51**,** 199-214.

KUKI, T., FUJIHARA, K., MIWA, H., TAMAMAKI, N., YANAGAWA, Y. & MUSHIAKE, H. 2015. Contribution of parvalbumin and somatostatin-expressing GABAergic neurons to slow oscillations and the balance in beta-gamma oscillations across cortical layers. *Front Neural Circuits,* 9**,** 6.

KUNITACHI, S., FUJITA, Y., ISHIMA, T., KOHNO, M., HORIO, M., TANIBUCHI, Y., SHIRAYAMA, Y., IYO, M. & HASHIMOTO, K. 2009. Phencyclidine-induced cognitive deficits in mice are ameliorated by subsequent subchronic administration of donepezil: role of sigma-1 receptors. *Brain Res,* 1279**,** 189-96.

KWOK, J. C. F., DICK, G., WANG, D. & FAWCETT, J. W. 2011. Extracellular matrix and perineuronal nets in CNS repair. *Developmental Neurobiology,* 71**,** 1073-1089.

KWON, J. S., O'DONNELL, B. F., WALLENSTEIN, G. V., GREENE, R. W., HIRAYASU, Y., NESTOR, P. G., HASSELMO, M. E., POTTS, G. F., SHENTON, M. E. & MCCARLEY, R. W. 1999. Gamma frequency-range abnormalities to auditory stimulation in schizophrenia. *Archives of general psychiatry,* 56**,** 1001-1005.

LAHTI, A. C., KOFFEL, B., LAPORTE, D. & TAMMINGA, C. A. 1995. Subanesthetic doses of ketamine stimulate psychosis in schizophrenia. *Neuropsychopharmacology,* 13**,** 9-19.

LAHTINEN, H., PALVA, J. M., SUMANEN, S., VOIPIO, J., KAILA, K. & TAIRA, T. 2002. Postnatal development of rat hippocampal gamma rhythm in vivo. *Journal of neurophysiology,* 88**,** 1469-1474.

LANGE, M. D., JÜNGLING, K., PAULUKAT, L., VIELER, M., GABURRO, S., SOSULINA, L., BLAESSE, P., SREEPATHI, H. K., FERRAGUTI, F. & PAPE, H.-C. 2014. Glutamic Acid Decarboxylase 65: A Link Between GABAergic Synaptic Plasticity in the Lateral Amygdala and Conditioned Fear Generalization. *Neuropsychopharmacology,* 39**,** 2211-2220.

LARGENT, B. L., GUNDLACH, A. L. & SNYDER, S. H. 1986. Pharmacological and autoradiographic discrimination of sigma and phencyclidine receptor binding sites in brain with (+)-[3H]SKF 10,047, (+)-[3H]-3-[3-hydroxyphenyl]-N-(1-propyl)piperidine and [3H]-1-[1-(2-thienyl)cyclohexyl]piperidine. *J Pharmacol Exp Ther,* 238**,** 739-48.

LARUELLE, M. 2013. The Second Revision of the Dopamine Theory of Schizophrenia: Implications for Treatment and Drug Development. *Biological Psychiatry,* 74**,** 80-81.

LAU, A. & TYMIANSKI, M. 2010. Glutamate receptors, neurotoxicity and neurodegeneration. *Pflügers Archiv - European Journal of Physiology,* 460**,** 525-542.

LAU, C. G., TAKEUCHI, K., RODENAS-RUANO, A., TAKAYASU, Y., MURPHY, J., BENNETT, M. V. & ZUKIN, R. S. 2009. Regulation of NMDA receptor Ca2+ signalling and synaptic plasticity. *Biochem Soc Trans,* 37**,** 1369-74.

LAURBERG, S. & SØRENSEN, K. 1981. Associational and commissural collaterals of neurons in the hippocampal formation (hilus fasciae dentatae and subfield CA3). *Brain research,* 212**,** 287-300.
LAZAREWICZ, M. T., EHRLICHMAN, R. S., MAXWELL, C. R., GANDAL, M. J., FINKEL, L. H. & SIEGEL, S. J. 2010. Ketamine modulates theta and gamma oscillations. *Journal of cognitive neuroscience,* 22**,** 1452-1464.
LE DUIGOU, C., SIMONNET, J., TELEÑCZUK, M. T., FRICKER, D. & MILES, R. 2014. Recurrent synapses and circuits in the CA3 region of the hippocampus: an associative network. *Frontiers in cellular neuroscience,* 7**,** 262.
LE PEN, G., GOUREVITCH, R., HAZANE, F., HOAREAU, C., JAY, T. & KREBS, M.-O. 2006. Peri-pubertal maturation after developmental disturbance: a model for psychosis onset in the rat. *Neuroscience,* 143**,** 395-405.
LEBEAU, F. E. N., TOWERS, S. K., TRAUB, R. D., WHITTINGTON, M. A. & BUHL, E. H. 2002. Fast network oscillations induced by potassium transients in the rat hippocampus in vitro. *The Journal of Physiology,* 542**,** 167-179.
LEE, G. & ZHOU, Y. 2019. NMDAR Hypofunction Animal Models of Schizophrenia. *Front Mol Neurosci,* 12**,** 185.
LEE, J., HUDSON, M. R., O'BRIEN, T. J., NITHIANANTHARAJAH, J. & JONES, N. C. 2017. Local NMDA receptor hypofunction evokes generalized effects on gamma and high-frequency oscillations and behavior. *Neuroscience,* 358**,** 124-136.
LEE, S. H., ROSENMUND, C., SCHWALLER, B. & NEHER, E. 2000. Differences in Ca2+ buffering properties between excitatory and inhibitory hippocampal neurons from the rat. *The Journal of Physiology,* 525**,** 405-418.
LEGER, M. & NEILL, J. C. 2016. A systematic review comparing sex differences in cognitive function in schizophrenia and in rodent models for schizophrenia, implications for improved therapeutic strategies. *Neurosci Biobehav Rev,* 68**,** 979-1000.
LEMERCIER, C. E., HOLMAN, C. & GEREVICH, Z. 2017. Aberrant alpha and gamma oscillations ex vivo after single application of the NMDA receptor antagonist MK-801. *Schizophrenia Research,* 188**,** 118-124.
LESH, T. A., NIENDAM, T. A., MINZENBERG, M. J. & CARTER, C. S. 2011. Cognitive control deficits in schizophrenia: mechanisms and meaning. *Neuropsychopharmacology,* 36**,** 316-38.
LEUNG, L. W. 1985. Spectral analysis of hippocampal EEG in the freely moving rat: effects of centrally active drugs and relations to evoked potentials. *Electroencephalogr Clin Neurophysiol,* 60**,** 65-77.
LEWIS, D. A. 2014. Inhibitory neurons in human cortical circuits: substrate for cognitive dysfunction in schizophrenia. *Current opinion in neurobiology,* 26**,** 22-26.
LEWIS, D. A., HASHIMOTO, T. & VOLK, D. W. 2005. Cortical inhibitory neurons and schizophrenia. *Nature Reviews Neuroscience,* 6**,** 312-324.
LI, D., PAN, Q., XIAO, Y. & HU, K. 2024a. Advances in the study of phencyclidine-induced schizophrenia-like animal models and the underlying neural mechanisms. *Schizophrenia (Heidelb),* 10**,** 65.
LI, M. L., GULCHINA, Y., MONACO, S. A., XING, B., FERGUSON, B. R., LI, Y. C., LI, F., HU, X. Q. & GAO, W. J. 2017. Juvenile treatment with a novel mGluR2 agonist/mGluR3 antagonist compound, LY395756, reverses learning deficits and cognitive flexibility impairments in adults in a neurodevelopmental model of schizophrenia. *Neurobiol Learn Mem,* 140**,** 52-61.

LI, R., MA, X., WANG, G., YANG, J. & WANG, C. 2016. Why sex differences in schizophrenia? *J Transl Neurosci (Beijing),* 1**,** 37-42.
LI, X., WU, X., LU, T., KUANG, C., SI, Y., ZHENG, W., LI, Z. & XUE, Y. 2024b. Perineuronal Nets in the CNS: Architects of Memory and Potential Therapeutic Target in Neuropsychiatric Disorders. *Int J Mol Sci,* 25.
LIA, A., DI SPIEZIO, A., VITALINI, L., TORE, M., PUJA, G. & LOSI, G. 2023. Ion Channels and Ionotropic Receptors in Astrocytes: Physiological Functions and Alterations in Alzheimer's Disease and Glioblastoma. *Life,* 13**,** 2038.
LIDDLE, P. F. 1987. The symptoms of chronic schizophrenia. A re-examination of the positive-negative dichotomy. *Br J Psychiatry,* 151**,** 145-51.
LIN, L. C. & SIBILLE, E. 2015. Somatostatin, neuronal vulnerability and behavioral emotionality. *Molecular Psychiatry,* 20**,** 377-387.
LISBOA, J. R. F., COSTA, O., PAKES, G. H., COLODETE, D. A. E. & GOMES, F. V. 2024. Perineuronal net density in schizophrenia: A systematic review of postmortem brain studies. *Schizophrenia Research,* 271**,** 100-109.
LISMAN, J. 2010. Working Memory: The Importance of Theta and Gamma Oscillations. *Current Biology,* 20**,** R490-R492.
LISMAN, J. E., COYLE, J. T., GREEN, R. W., JAVITT, D. C., BENES, F. M., HECKERS, S. & GRACE, A. A. 2008. Circuit-based framework for understanding neurotransmitter and risk gene interactions in schizophrenia. *Trends in neurosciences,* 31**,** 234-242.
LIU, C.-M., LIU, Y.-L., HWU, H.-G., FANN, C. S.-J., YANG, U.-C., HSU, P.-C., CHANG, C.-C., CHEN, W. J., HWANG, T.-J. & HSIEH, M. H. 2019a. Genetic associations and expression of extra-short isoforms of disrupted-in-schizophrenia 1 in a neurocognitive subgroup of schizophrenia. *Journal of human genetics,* 64**,** 653-663.
LIU, Q., GUO, Q., FANG, L.-P., YAO, H., SCHELLER, A., KIRCHHOFF, F. & HUANG, W. 2023. Specific detection and deletion of the sigma-1 receptor widely expressed in neurons and glial cells in vivo. *Journal of Neurochemistry,* 164**,** 764-785.
LIU, Y. U., YING, Y., LI, Y., EYO, U. B., CHEN, T., ZHENG, J., UMPIERRE, A. D., ZHU, J., BOSCO, D. B. & DONG, H. 2019b. Neuronal network activity controls microglial process surveillance in awake mice via norepinephrine signaling. *Nature neuroscience,* 22**,** 1771-1781.
LODGE, D. J., BEHRENS, M. M. & GRACE, A. A. 2009. A loss of parvalbumin-containing interneurons is associated with diminished oscillatory activity in an animal model of schizophrenia. *Journal of Neuroscience,* 29**,** 2344-2354.
LORANGER, A. W. 1984. Sex difference in age at onset of schizophrenia. *Arch Gen Psychiatry,* 41**,** 157-61.
LU, Y., MU, L., ELSTROTT, J., FU, C., SUN, C., SU, T., MA, X., YAN, J., JIANG, H., HANSON, J. E., GENG, Y. & CHEN, Y. 2024. Differential depletion of GluN2A induces heterogeneous schizophrenia-related phenotypes in mice. *eBioMedicine,* 102.
LUBY, E. D., COHEN, B. D., ROSENBAUM, G., GOTTLIEB, J. S. & KELLEY, R. 1959. Study of a new schizophrenomimetic drug; sernyl. *AMA Arch Neurol Psychiatry,* 81**,** 363-9.
LUHMANN, H. J. & KHAZIPOV, R. 2018. Neuronal activity patterns in the developing barrel cortex. *Neuroscience,* 368**,** 256-267.

LUNDQVIST, M., ROSE, J., HERMAN, P., BRINCAT, S. L., BUSCHMAN, T. J. & MILLER, E. K. 2016. Gamma and beta bursts underlie working memory. *Neuron,* 90**,** 152-164.

LYNCH, G., LARSON, J., KELSO, S., BARRIONUEVO, G. & SCHOTTLER, F. 1983. Intracellular injections of EGTA block induction of hippocampal long-term potentiation. *Nature,* 305**,** 719-721.

MAĆKOWIAK, M., BATOR, E., LATUSZ, J., MORDALSKA, P. & WĘDZONY, K. 2014. Prenatal MAM administration affects histone H3 methylation in postnatal life in the rat medial prefrontal cortex. *European Neuropsychopharmacology,* 24**,** 271-289.

MAILMAN, R. B. & MURTHY, V. 2010. Third generation antipsychotic drugs: partial agonism or receptor functional selectivity? *Curr Pharm Des,* 16**,** 488-501.

MALHOTRA, A. K., PINALS, D. A., ADLER, C. M., ELMAN, I., CLIFTON, A., PICKAR, D. & BREIER, A. 1997. Ketamine-induced exacerbation of psychotic symptoms and cognitive impairment in neuroleptic-free schizophrenics. *Neuropsychopharmacology,* 17**,** 141-50.

MANAHAN-VAUGHAN, D., VON HAEBLER, D., WINTER, C., JUCKEL, G. & HEINEMANN, U. 2008a. A single application of MK801 causes symptoms of acute psychosis, deficits in spatial memory, and impairment of synaptic plasticity in rats. *Hippocampus,* 18**,** 125-134.

MANAHAN-VAUGHAN, D., WILDFÖRSTER, V. & THOMSEN, C. 2008b. Rescue of hippocampal LTP and learning deficits in a rat model of psychosis by inhibition of glycine transporter-1 (GlyT1). *European Journal of Neuroscience,* 28**,** 1342-1350.

MANN, E. O. & MODY, I. 2010. Control of hippocampal gamma oscillation frequency by tonic inhibition and excitation of interneurons. *Nat Neurosci,* 13**,** 205-12.

MANN, E. O., SUCKLING, J. M., HAJOS, N., GREENFIELD, S. A. & PAULSEN, O. 2005. Perisomatic feedback inhibition underlies cholinergically induced fast network oscillations in the rat hippocampus in vitro. *Neuron,* 45**,** 105-117.

MAREK, G. J., WRIGHT, R. A., SCHOEPP, D. D., MONN, J. A. & AGHAJANIAN, G. K. 2000. Physiological antagonism between 5-hydroxytryptamine(2A) and group II metabotropic glutamate receptors in prefrontal cortex. *J Pharmacol Exp Ther,* 292**,** 76-87.

MARIC, N. P., JOVICIC, M. J., MIHALJEVIC, M. & MILJEVIC, C. 2016. Improving Current Treatments for Schizophrenia. *Drug Dev Res,* 77**,** 357-367.

MARÍN, O. 2024. Parvalbumin interneuron deficits in schizophrenia. *European Neuropsychopharmacology,* 82**,** 44-52.

MARINO, M. & CONN, P. 2002. Direct and indirect modulation of the N-methyl D-aspartate receptor: potential for the development of novel antipsychotic therapies. *Current Drug Targets-CNS & Neurological Disorders,* 1**,** 1-16.

MARKS, W., YOKOSE, J., KITAMURA, T. & OGAWA, S. 2022. Neuronal Ensembles Organize Activity to Generate Contextual Memory. *Frontiers in Behavioral Neuroscience,* 16**,** 805132.

MARONEY, M. 2022. Management of cognitive and negative symptoms in schizophrenia. *Ment Health Clin,* 12**,** 282-299.

MARQUES, T. R., ASHOK, A. H., ANGELESCU, I., BORGAN, F., MYERS, J., LINGFORD-HUGHES, A., NUTT, D. J., VERONESE, M., TURKHEIMER, F. E. & HOWES, O. D. 2021. GABA-A receptor differences in schizophrenia: a positron emission tomography study using [11C]Ro154513. *Molecular Psychiatry,* 26**,** 2616-2625.

MARQUIS, K. L., PAQUETTE, N. C., GUSSIO, R. P. & MORETON, J. E. 1989. Comparative electroencephalographic and behavioral effects of phencyclidine, (+)-SKF-10,047 and MK-801 in rats. *Journal of Pharmacology and Experimental Therapeutics,* 251**,** 1104.

MARTIN, W. R., EADES, C. G., THOMPSON, J. A., HUPPLER, R. E. & GILBERT, P. E. 1976. The effects of morphine- and nalorphine- like drugs in the nondependent and morphine-dependent chronic spinal dog. *J Pharmacol Exp Ther,* 197**,** 517-32.

MARTINA, M., TURCOTTE, M.-E. B., HALMAN, S. & BERGERON, R. 2007. The sigma-1 receptor modulates NMDA receptor synaptic transmission and plasticity via SK channels in rat hippocampus. *The Journal of Physiology,* 578**,** 143-157.

MARTINOWICH, K., SCHLOESSER, R. J., JIMENEZ, D. V., WEINBERGER, D. R. & LU, B. 2011. Activity-dependent brain-derived neurotrophic factor expression regulates cortistatin-interneurons and sleep behavior. *Molecular Brain,* 4**,** 11.

MAUNEY, S. A., ATHANAS, K. M., PANTAZOPOULOS, H., SHASKAN, N., PASSERI, E., BERRETTA, S. & WOO, T.-U. W. 2013. Developmental Pattern of Perineuronal Nets in the Human Prefrontal Cortex and Their Deficit in Schizophrenia. *Biological Psychiatry,* 74**,** 427-435.

MAURICE, T. & PRIVAT, A. 1997. SA4503, a novel cognitive enhancer with σ1 receptor agonist properties, facilitates NMDA receptor-dependent learning in mice. *European Journal of Pharmacology,* 328**,** 9-18.

MAURICE, T., SU, T. P., PARISH, D. W., NABESHIMA, T. & PRIVAT, A. 1994. PRE-084, a sigma selective PCP derivative, attenuates MK-801-induced impairment of learning in mice. *Pharmacol Biochem Behav,* 49**,** 859-69.

MAURICE, T., VOLLE, J. N., STREHAIANO, M., CROUZIER, L., PEREIRA, C., KALOYANOV, N., VIRIEUX, D. & PIRAT, J. L. 2019. Neuroprotection in non-transgenic and transgenic mouse models of Alzheimer's disease by positive modulation of σ(1) receptors. *Pharmacol Res,* 144**,** 315-330.

MAVLYUTOV, T. A., EPSTEIN, M. L., VERBNY, Y. I., HUERTA, M. S., ZAITOUN, I., ZISKIND-CONHAIM, L. & RUOHO, A. E. 2013. Lack of sigma-1 receptor exacerbates ALS progression in mice. *Neuroscience,* 240**,** 129-34.

MAVLYUTOV, T. A., GUO, L. W., EPSTEIN, M. L. & RUOHO, A. E. 2015. Role of the Sigma-1 receptor in Amyotrophic Lateral Sclerosis (ALS). *J Pharmacol Sci,* 127**,** 10-6.

MAYER, M. L., WESTBROOK, G. L. & GUTHRIE, P. B. 1984. Voltage-dependent block by Mg2+ of NMDA responses in spinal cord neurones. *Nature,* 309**,** 261-263.

MCCARLEY, R. W., WIBLE, C. G., FRUMIN, M., HIRAYASU, Y., LEVITT, J. J., FISCHER, I. A. & SHENTON, M. E. 1999. MRI anatomy of schizophrenia. *Biological psychiatry,* 45**,** 1099-1119.

MCGARRY, L. M. & CARTER, A. G. 2016. Inhibitory Gating of Basolateral Amygdala Inputs to the Prefrontal Cortex. *J Neurosci,* 36**,** 9391-406.

MCKIBBEN, C. E., JENKINS, T. A., ADAMS, H. N., HARTE, M. K. & REYNOLDS, G. P. 2010. Effect of pretreatment with risperidone on phencyclidine-induced disruptions in object recognition memory and prefrontal cortex parvalbumin immunoreactivity in the rat. *Behavioural Brain Research,* 208**,** 132-136.

MCNALLY, J. M., MCCARLEY, R. W., MCKENNA, J. T., YANAGAWA, Y. & BROWN, R. E. 2011. Complex receptor mediation of acute ketamine application on in

vitro gamma oscillations in mouse prefrontal cortex: modeling gamma band oscillation abnormalities in schizophrenia. *Neuroscience,* 199**,** 51-63.
MECONI, F., ANDERL-STRAUB, S., RAUM, H., LANDGREBE, M., LANGGUTH, B., BÄUML, K. T. & HANSLMAYR, S. 2016. Aberrant prefrontal beta oscillations predict episodic memory encoding deficits in schizophrenia. *Neuroimage Clin,* 12**,** 499-505.
MENDELSOHN, L. G., KALRA, V., JOHNSON, B. G. & KERCHNER, G. A. 1985. Sigma opioid receptor: characterization and co-identity with the phencyclidine receptor. *Journal of Pharmacology and Experimental Therapeutics,* 233**,** 597-602.
MENDREK, A. & MANCINI-MARÏE, A. 2016. Sex/gender differences in the brain and cognition in schizophrenia. *Neurosci Biobehav Rev,* 67**,** 57-78.
MENEZES, M. M., SANTINI, M. A., BENVENGA, M. J., MAREK, G. J., MERCHANT, K. M., MIKKELSEN, J. D. & SVENSSON, K. A. 2013. The mGlu2/3 Receptor Agonists LY354740 and LY379268 Differentially Regulate Restraint-Stress-Induced Expression of c-Fos in Rat Cerebral Cortex. *Neuroscience journal,* 2013**,** 736439-736439.
MERRITT, K., EGERTON, A., KEMPTON, M. J., TAYLOR, M. J. & MCGUIRE, P. K. 2016. Nature of glutamate alterations in schizophrenia: a meta-analysis of proton magnetic resonance spectroscopy studies. *JAMA psychiatry,* 73**,** 665-674.
MIDDLETON, S., JALICS, J., KISPERSKY, T., LEBEAU, F. E. N., ROOPUN, A. K., KOPELL, N. J., WHITTINGTON, M. A. & CUNNINGHAM, M. O. 2008. NMDA receptor-dependent switching between different gamma rhythm-generating microcircuits in entorhinal cortex. *Proceedings of the National Academy of Sciences,* 105**,** 18572-18577.
MILLER, E. K., LUNDQVIST, M. & BASTOS, A. M. 2018. Working Memory 2.0. *Neuron,* 100**,** 463-475.
MINOGUE, A. M. 2017. Role of infiltrating monocytes/macrophages in acute and chronic neuroinflammation: Effects on cognition, learning and affective behaviour. *Progress in Neuro-Psychopharmacology and Biological Psychiatry,* 79**,** 15-18.
MISHINA, M., OHYAMA, M., ISHII, K., KITAMURA, S., KIMURA, Y., ODA, K.-I., KAWAMURA, K., SASAKI, T., KOBAYASHI, S., KATAYAMA, Y. & ISHIWATA, K. 2008. Low density of sigma1 receptors in early Alzheimer's disease. *Annals of Nuclear Medicine,* 22**,** 151-156.
MITCHELL, E. J., BRETT, R. R., ARMSTRONG, J. D., SILLITO, R. R. & PRATT, J. A. 2020. Temporal dissociation of phencyclidine: Induced locomotor and social alterations in rats using an automated homecage monitoring system - implications for the 3Rs and preclinical drug discovery. *J Psychopharmacol,* 34**,** 709-715.
MODY, I. & PEARCE, R. A. 2004. Diversity of inhibitory neurotransmission through GABAA receptors. *Trends in neurosciences,* 27**,** 569-575.
MOGHADDAM, B. & ADAMS, B. 1998. Reversal of phencyclidine effects by a group II metabotropic glutamate receptor agonist in rats. *Science,* 281**,** 1349 - 1352.
MOGHADDAM, B., ADAMS, B., VERMA, A. & DALY, D. 1997. Activation of glutamatergic neurotransmission by ketamine: a novel step in the pathway from NMDA receptor blockade to dopaminergic and cognitive disruptions associated with the prefrontal cortex. *J Neurosci,* 17**,** 2921-7.

MOGHADDAM, B. & JAVITT, D. 2012. From revolution to evolution: the glutamate hypothesis of schizophrenia and its implication for treatment. *Neuropsychopharmacology,* 37**,** 4-15.

MOHNS, E. J. & BLUMBERG, M. S. 2008. Synchronous bursts of neuronal activity in the developing hippocampus: modulation by active sleep and association with emerging gamma and theta rhythms. *Journal of Neuroscience,* 28**,** 10134-10144.

MOORE, H., JENTSCH, J. D., GHAJARNIA, M., GEYER, M. A. & GRACE, A. A. 2006. A neurobehavioral systems analysis of adult rats exposed to methylazoxymethanol acetate on E17: implications for the neuropathology of schizophrenia. *Biological psychiatry,* 60**,** 253-264.

MORAN, L. V. & HONG, L. E. 2011. High vs low frequency neural oscillations in schizophrenia. *Schizophr Bull,* 37**,** 659-63.

MORI, T., HAYASHI, T., HAYASHI, E. & SU, T.-P. 2013. Sigma-1 Receptor Chaperone at the ER-Mitochondrion Interface Mediates the Mitochondrion-ER-Nucleus Signaling for Cellular Survival. *PLOS ONE,* 8**,** e76941.

MORIYOSHI, K., MASU, M., ISHII, T., SHIGEMOTO, R., MIZUNO, N. & NAKANISHI, S. 1991. Molecular cloning and characterization of the rat NMDA receptor. *Nature,* 354**,** 31-37.

MORROW, J. A., GILFILLAN, R. & NEALE, S. A. 2012. CHAPTER 4 Glutamatergic Approaches for the Treatment of Schizophrenia. *Drug Discovery for Psychiatric Disorders.* The Royal Society of Chemistry.

MOSLEH, M., JAVAN, M. & FATHOLLAHI, Y. 2023. The properties of long-term potentiation at SC-CA1/ TA-CA1 hippocampal synaptic pathways depends upon their input pathway activation patterns. *IBRO Neurosci Rep,* 14**,** 358-365.

MULLIN, A. P., SADANANDAPPA, M. K., MA, W., DICKMAN, D. K., VIJAYRAGHAVAN, K., RAMASWAMI, M., SANYAL, S. & FAUNDEZ, V. 2015. Gene dosage in the dysbindin schizophrenia susceptibility network differentially affect synaptic function and plasticity. *Journal of Neuroscience,* 35**,** 325-338.

MURRAY, A. J., ROGERS, J. C., KATSHU, M. Z. U. H., LIDDLE, P. F. & UPTHEGROVE, R. 2021. Oxidative Stress and the Pathophysiology and Symptom Profile of Schizophrenia Spectrum Disorders. *Frontiers in Psychiatry,* 12.

MURUETA-GOYENA, A., ORTUZAR, N., LAFUENTE, J. V. & BENGOETXEA, H. 2020. Enriched Environment Reverts Somatostatin Interneuron Loss in MK-801 Model of Schizophrenia. *Molecular Neurobiology,* 57**,** 125-134.

NAKAZAWA, K. & SAPKOTA, K. 2020. The origin of NMDA receptor hypofunction in schizophrenia. *Pharmacol Ther,* 205**,** 107426.

NĂSTASE, M. G., VLAICU, I. & TRIFU, S. C. 2022. Genetic polymorphism and neuroanatomical changes in schizophrenia. *Rom J Morphol Embryol,* 63**,** 307-322.

NEILL, J. C., BARNES, S., COOK, S., GRAYSON, B., IDRIS, N. F., MCLEAN, S. L., SNIGDHA, S., RAJAGOPAL, L. & HARTE, M. K. 2010. Animal models of cognitive dysfunction and negative symptoms of schizophrenia: Focus on NMDA receptor antagonism. *Pharmacology & Therapeutics,* 128**,** 419-432.

NELSON, M. D., SAYKIN, A. J., FLASHMAN, L. A. & RIORDAN, H. J. 1998. Hippocampal volume reduction in schizophrenia as assessed by magnetic resonance imaging: a meta-analytic study. *Archives of general psychiatry,* 55**,** 433-440.

NEUHÄUSEL, T. S. & GEREVICH, Z. 2024. Sex-specific effects of subchronic NMDA receptor antagonist MK-801 treatment on hippocampal gamma oscillations. *Frontiers in Neuroscience,* 18.

NEUMANN, H., KOTTER, M. R. & FRANKLIN, R. J. 2009. Debris clearance by microglia: an essential link between degeneration and regeneration. *Brain,* 132**,** 288-295.

NEWSON, J. & THIAGARAJAN, T. 2018. EEG frequency bands in psychiatric disorders: a review of resting state studies. Front Hum Neurosci 12: 521.

NICOLL, R. A. 2017. A Brief History of Long-Term Potentiation. *Neuron,* 93**,** 281-290.

NIEDERMEYER, E. 1997. Alpha rhythms as physiological and abnormal phenomena. *Int J Psychophysiol,* 26**,** 31-49.

NIMMERJAHN, A., KIRCHHOFF, F. & HELMCHEN, F. 2005. Resting microglial cells are highly dynamic surveillants of brain parenchyma in vivo. *Science,* 308**,** 1314-1318.

NISHIKAWA, H., HASHINO, A., KUME, T., KATSUKI, H., KANEKO, S. & AKAIKE, A. 2000. Involvement of direct inhibition of NMDA receptors in the effects of sigma-receptor ligands on glutamate neurotoxicity in vitro. *Eur J Pharmacol,* 404**,** 41-8.

NISWENDER, C. M. & CONN, P. J. 2010. Metabotropic Glutamate Receptors: Physiology, Pharmacology, and Disease. *Annual Review of Pharmacology and Toxicology,* 50**,** 295-322.

NOLI, B., SANNA, F., BRANCIA, C., D'AMATO, F., MANCONI, B., VINCENZONI, F., MESSANA, I., MELIS, M., ARGIOLAS, A., FERRI, G.-L. & COCCO, C. 2017. Profiles of VGF Peptides in the Rat Brain and Their Modulations after Phencyclidine Treatment. *Frontiers in Cellular Neuroscience,* 11.

NUECHTERLEIN, K. H., BARCH, D. M., GOLD, J. M., GOLDBERG, T. E., GREEN, M. F. & HEATON, R. K. 2004. Identification of separable cognitive factors in schizophrenia. *Schizophrenia research,* 72**,** 29-39.

OHI, K., HASHIMOTO, R., YASUDA, Y., FUKUMOTO, M., YAMAMORI, H., UMEDA-YANO, S., KAMINO, K., IKEZAWA, K., AZECHI, M., IWASE, M., KAZUI, H., KASAI, K. & TAKEDA, M. 2011. The SIGMAR1 gene is associated with a risk of schizophrenia and activation of the prefrontal cortex. *Prog Neuropsychopharmacol Biol Psychiatry,* 35**,** 1309-15.

OHMORI, O., SHINKAI, T., SUZUKI, T., OKANO, C., KOJIMA, H., TERAO, T. & NAKAMURA, J. 2000. Polymorphisms of the σ1 receptor gene in schizophrenia: An association study. *American Journal of Medical Genetics,* 96**,** 118-122.

OLAJIDE, O. A. & SARKER, S. D. 2020. Chapter Five - Anti-inflammatory natural products. *In:* SARKER, S. D. & NAHAR, L. (eds.) *Annual Reports in Medicinal Chemistry.* Academic Press.

OSWALD, R. E., BAMBERGER, M. J. & MCLAUGHLIN, J. T. 1984. Mechanism of phencyclidine binding to the acetylcholine receptor from Torpedo electroplaque. *Mol Pharmacol,* 25**,** 360-8.

OTA, Y., ZANETTI, A. T. & HALLOCK, R. M. 2013. The role of astrocytes in the regulation of synaptic plasticity and memory formation. *Neural Plast,* 2013**,** 185463.

OU, Y., NI, X., GAO, X., YU, Y., ZHANG, Y., WANG, Y., LIU, J., YIN, Z., RONG, J., SUN, M., CHEN, J., TANG, Z., XIAO, W. & ZHAO, L. 2024. Structural and functional changes of anterior cingulate cortex subregions in migraine without

aura: relationships with pain sensation and pain emotion. *Cerebral Cortex,* 34**,** bhae040.

PABBA, M., WONG, A. Y. C., AHLSKOG, N., HRISTOVA, E., BISCARO, D., NASSRALLAH, W., NGSEE, J. K., SNYDER, M., BEIQUE, J.-C. & BERGERON, R. 2014. NMDA Receptors Are Upregulated and Trafficked to the Plasma Membrane after Sigma-1 Receptor Activation in the Rat Hippocampus. *The Journal of Neuroscience,* 34**,** 11325-11338.

PALMISANO, A., PANDIT, S., SMERALDA, C. L., DEMCHENKO, I., ROSSI, S., BATTELLI, L., RIVOLTA, D., BHAT, V. & SANTARNECCHI, E. 2024. The Pathophysiological Underpinnings of Gamma-Band Alterations in Psychiatric Disorders. *Life (Basel),* 14.

PALOMERO-GALLAGHER, N., HOFFSTAEDTER, F., MOHLBERG, H., EICKHOFF, S. B., AMUNTS, K. & ZILLES, K. 2019. Human Pregenual Anterior Cingulate Cortex: Structural, Functional, and Connectional Heterogeneity. *Cereb Cortex,* 29**,** 2552-2574.

PANTAZOPOULOS, H., MARKOTA, M., JAQUET, F., GHOSH, D., WALLIN, A., SANTOS, A., CATERSON, B. & BERRETTA, S. 2015. Aggrecan and chondroitin-6-sulfate abnormalities in schizophrenia and bipolar disorder: a postmortem study on the amygdala. *Translational Psychiatry,* 5**,** e496-e496.

PAOLICELLI, R. C., BOLASCO, G., PAGANI, F., MAGGI, L., SCIANNI, M., PANZANELLI, P., GIUSTETTO, M., FERREIRA, T. A., GUIDUCCI, E. & DUMAS, L. 2011. Synaptic pruning by microglia is necessary for normal brain development. *science,* 333**,** 1456-1458.

PAOLICELLI, R. C., SIERRA, A., STEVENS, B., TREMBLAY, M.-E., AGUZZI, A., AJAMI, B., AMIT, I., AUDINAT, E., BECHMANN, I., BENNETT, M., BENNETT, F., BESSIS, A., BIBER, K., BILBO, S., BLURTON-JONES, M., BODDEKE, E., BRITES, D., BRÔNE, B., BROWN, G. C., BUTOVSKY, O., CARSON, M. J., CASTELLANO, B., COLONNA, M., COWLEY, S. A., CUNNINGHAM, C., DAVALOS, D., DE JAGER, P. L., DE STROOPER, B., DENES, A., EGGEN, B. J. L., EYO, U., GALEA, E., GAREL, S., GINHOUX, F., GLASS, C. K., GOKCE, O., GOMEZ-NICOLA, D., GONZÁLEZ, B., GORDON, S., GRAEBER, M. B., GREENHALGH, A. D., GRESSENS, P., GRETER, M., GUTMANN, D. H., HAASS, C., HENEKA, M. T., HEPPNER, F. L., HONG, S., HUME, D. A., JUNG, S., KETTENMANN, H., KIPNIS, J., KOYAMA, R., LEMKE, G., LYNCH, M., MAJEWSKA, A., MALCANGIO, M., MALM, T., MANCUSO, R., MASUDA, T., MATTEOLI, M., MCCOLL, B. W., MIRON, V. E., MOLOFSKY, A. V., MONJE, M., MRACSKO, E., NADJAR, A., NEHER, J. J., NENISKYTE, U., NEUMANN, H., NODA, M., PENG, B., PERI, F., PERRY, V. H., POPOVICH, P. G., PRIDANS, C., PRILLER, J., PRINZ, M., RAGOZZINO, D., RANSOHOFF, R. M., SALTER, M. W., SCHAEFER, A., SCHAFER, D. P., SCHWARTZ, M., SIMONS, M., SMITH, C. J., STREIT, W. J., TAY, T. L., TSAI, L.-H., VERKHRATSKY, A., VON BERNHARDI, R., WAKE, H., WITTAMER, V., WOLF, S. A., WU, L.-J. & WYSS-CORAY, T. 2022. Microglia states and nomenclature: A field at its crossroads. *Neuron,* 110**,** 3458-3483.

PAPP, G., WITTER, M. P. & TREVES, A. 2007. The CA3 network as a memory store for spatial representations. *Learning & memory,* 14**,** 732-744.

PATIL, S., ZHANG, L., MARTENYI, F., LOWE, S., JACKSON, K., ANDREEV, B., AVEDISOVA, A., BARDENSTEIN, L., GUROVICH, I. & MOROZOVA, M. 2007. Activation of mGlu2/3 receptors as a new approach to treat schizophrenia: a randomized Phase 2 clinical trial. *Nat Med,* 13**,** 1102 - 1107.

PATZ, S., GRABERT, J., GORBA, T., WIRTH, M. J. & WAHLE, P. 2004. Parvalbumin expression in visual cortical interneurons depends on neuronal activity and TrkB ligands during an Early period of postnatal development. *Cereb Cortex,* 14**,** 342-51.

PEI, J. C., LUO, D. Z., GAU, S. S., CHANG, C. Y. & LAI, W. S. 2021. Directly and Indirectly Targeting the Glycine Modulatory Site to Modulate NMDA Receptor Function to Address Unmet Medical Needs of Patients With Schizophrenia. *Front Psychiatry,* 12**,** 742058.

PELVIG, D. P., PAKKENBERG, H., STARK, A. K. & PAKKENBERG, B. 2008. Neocortical glial cell numbers in human brains. *Neurobiology of Aging,* 29**,** 1754-1762.

PEREZ, S. M., BOLEY, A. & LODGE, D. J. 2019. Region specific knockdown of Parvalbumin or Somatostatin produces neuronal and behavioral deficits consistent with those observed in schizophrenia. *Transl Psychiatry,* 9**,** 264.

PETRASCH-PARWEZ, E., SCHÖBEL, A., BENALI, A., MOINFAR, Z., FÖRSTER, E., BRÜNE, M. & JUCKEL, G. 2020. Lateralization of increased density of Iba1-immunopositive microglial cells in the anterior midcingulate cortex of schizophrenia and bipolar disorder. *European Archives of Psychiatry and Clinical Neuroscience,* 270**,** 819-828.

PEVIANI, M., SALVANESCHI, E., BONTEMPI, L., PETESE, A., MANZO, A., ROSSI, D., SALMONA, M., COLLINA, S., BIGINI, P. & CURTI, D. 2014. Neuroprotective effects of the Sigma-1 receptor (S1R) agonist PRE-084, in a mouse model of motor neuron disease not linked to SOD1 mutation. *Neurobiology of disease,* 62**,** 218-232.

PFEFFER, C. K., XUE, M., HE, M., HUANG, Z. J. & SCANZIANI, M. 2013. Inhibition of inhibition in visual cortex: the logic of connections between molecularly distinct interneurons. *Nat Neurosci,* 16**,** 1068-76.

PICARD, N., TAKESIAN, A. E., FAGIOLINI, M. & HENSCH, T. K. 2019. NMDA 2A receptors in parvalbumin cells mediate sex-specific rapid ketamine response on cortical activity. *Molecular Psychiatry,* 24**,** 828-838.

PIETERSEN, A. N. J., PATEL, N., JEFFERYS, J. G. R. & VREUGDENHIL, M. 2009. Comparison between spontaneous and kainate-induced gamma oscillations in the mouse hippocampus in vitro. *European Journal of Neuroscience,* 29**,** 2145-2156.

PITTALUGA, A., ROGGERI, A., VALLARINO, G. & OLIVERO, G. 2021. Somatostatin, a Presynaptic Modulator of Glutamatergic Signal in the Central Nervous System. *Int J Mol Sci,* 22.

PLATT, S. R. 2007. The role of glutamate in central nervous system health and disease – A review. *The Veterinary Journal,* 173**,** 278-286.

POELS, E. M., KEGELES, L. S., KANTROWITZ, J. T., JAVITT, D. C., LIEBERMAN, J. A., ABI-DARGHAM, A. & GIRGIS, R. R. 2014. Glutamatergic abnormalities in schizophrenia: a review of proton MRS findings. *Schizophrenia research,* 152**,** 325-332.

PÓSFAI, B., CSERÉP, C., ORSOLITS, B. & DÉNES, Á. 2019. New Insights into Microglia–Neuron Interactions: A Neuron's Perspective. *Neuroscience,* 405**,** 103-117.

PRASAD, P. D., LI, H. W., FEI, Y. J., GANAPATHY, M. E., FUJITA, T., PLUMLEY, L. H., YANG-FENG, T. L., LEIBACH, F. H. & GANAPATHY, V. 1998. Exon-intron structure, analysis of promoter region, and chromosomal localization of the human type 1 sigma receptor gene. *J Neurochem,* 70**,** 443-51.

PRICE, R., SALAVATI, B., GRAFF-GUERRERO, A., BLUMBERGER, D. M., MULSANT, B. H., DASKALAKIS, Z. J. & RAJJI, T. K. 2014. Effects of antipsychotic D2 antagonists on long-term potentiation in animals and implications for human studies. *Prog Neuropsychopharmacol Biol Psychiatry,* 54**,** 83-91.

PROVENCHER, H. L. & MUESER, K. T. 1997. Positive and negative symptom behaviors and caregiver burden in the relatives of persons with schizophrenia. *Schizophrenia Research,* 26**,** 71-80.

RADEWICZ, K., GAREY, L. J., GENTLEMAN, S. M. & REYNOLDS, R. 2000. Increase in HLA-DR immunoreactive microglia in frontal and temporal cortex of chronic schizophrenics. *Journal of Neuropathology & Experimental Neurology,* 59**,** 137-150.

RAJMOHAN, V. & MOHANDAS, E. 2007. The limbic system. *Indian J Psychiatry,* 49**,** 132-9.

RAY, M. T., WEICKERT, C. S., WYATT, E. & WEBSTER, M. J. 2011. Decreased BDNF, trkB-TK+ and GAD67 mRNA expression in the hippocampus of individuals with schizophrenia and mood disorders. *Journal of Psychiatry and Neuroscience,* 36**,** 195-203.

REBOLLO, B., PEREZ-ZABALZA, M., RUIZ-MEJIAS, M., PEREZ-MENDEZ, L. & SANCHEZ-VIVES, M. V. 2018. Beta and Gamma Oscillations in Prefrontal Cortex During NMDA Hypofunction: An In Vitro Model of Schizophrenia Features. *Neuroscience,* 383**,** 138-149.

RÉUS, G. Z., FRIES, G. R., STERTZ, L., BADAWY, M., PASSOS, I., BARICHELLO, T., KAPCZINSKI, F. & QUEVEDO, J. 2015. The role of inflammation and microglial activation in the pathophysiology of psychiatric disorders. *Neuroscience,* 300**,** 141-154.

REYNOLDS, G. P. & NEILL, J. C. 2016. Modelling the cognitive and neuropathological features of schizophrenia with phencyclidine. *J Psychopharmacol,* 30**,** 1141-1144.

RIEDEMANN, T. 2019. Diversity and Function of Somatostatin-Expressing Interneurons in the Cerebral Cortex. *Int J Mol Sci,* 20.

RIPKE, S., NEALE, B. M., CORVIN, A., WALTERS, J. T. R., FARH, K.-H., HOLMANS, P. A., LEE, P., BULIK-SULLIVAN, B., COLLIER, D. A., HUANG, H., PERS, T. H., AGARTZ, I., AGERBO, E., ALBUS, M., ALEXANDER, M., AMIN, F., BACANU, S. A., BEGEMANN, M., BELLIVEAU JR, R. A., BENE, J., BERGEN, S. E., BEVILACQUA, E., BIGDELI, T. B., BLACK, D. W., BRUGGEMAN, R., BUCCOLA, N. G., BUCKNER, R. L., BYERLEY, W., CAHN, W., CAI, G., CAMPION, D., CANTOR, R. M., CARR, V. J., CARRERA, N., CATTS, S. V., CHAMBERT, K. D., CHAN, R. C. K., CHEN, R. Y. L., CHEN, E. Y. H., CHENG, W., CHEUNG, E. F. C., ANN CHONG, S., ROBERT CLONINGER, C., COHEN, D., COHEN, N., CORMICAN, P., CRADDOCK, N., CROWLEY, J. J., CURTIS, D., DAVIDSON, M., DAVIS, K. L., DEGENHARDT, F., DEL FAVERO, J., DEMONTIS, D., DIKEOS, D., DINAN, T., DJUROVIC, S., DONOHOE, G., DRAPEAU, E., DUAN, J., DUDBRIDGE, F., DURMISHI, N., EICHHAMMER, P., ERIKSSON, J., ESCOTT-PRICE, V., ESSIOUX, L., FANOUS, A. H., FARRELL, M. S., FRANK, J., FRANKE, L., FREEDMAN, R., FREIMER, N. B., FRIEDL, M., FRIEDMAN, J. I., FROMER, M., GENOVESE, G., GEORGIEVA, L., GIEGLING, I., GIUSTI-RODRÍGUEZ, P., GODARD, S., GOLDSTEIN, J. I., GOLIMBET, V., GOPAL, S., GRATTEN, J., DE HAAN, L., HAMMER, C., HAMSHERE, M. L., HANSEN, M., HANSEN, T., HAROUTUNIAN, V.,

HARTMANN, A. M., HENSKENS, F. A., HERMS, S., HIRSCHHORN, J. N., HOFFMANN, P., HOFMAN, A., HOLLEGAARD, M. V., HOUGAARD, D. M., IKEDA, M., JOA, I., et al. 2014. Biological insights from 108 schizophrenia-associated genetic loci. *Nature,* 511**,** 421-427.

RODRÍGUEZ-MUÑOZ, M., SÁNCHEZ-BLÁZQUEZ, P., HERRERO-LABRADOR, R., MARTÍNEZ-MURILLO, R., MERLOS, M., VELA, J. M. & GARZÓN, J. 2015. The σ1 receptor engages the redox-regulated HINT1 protein to bring opioid analgesia under NMDA receptor negative control. *Antioxid Redox Signal,* 22**,** 799-818.

ROLLS, E. T. 2019. The cingulate cortex and limbic systems for emotion, action, and memory. *Brain Struct Funct,* 224**,** 3001-3018.

ROMÓN, T., MENGOD, G. & ADELL, A. 2011. Expression of parvalbumin and glutamic acid decarboxylase-67 after acute administration of MK-801. Implications for the NMDA hypofunction model of schizophrenia. *Psychopharmacology,* 217**,** 231-238.

ROOPUN, A. K., CUNNINGHAM, M. O., RACCA, C., ALTER, K., TRAUB, R. D. & WHITTINGTON, M. A. 2008. Region-Specific Changes in Gamma and Beta2 Rhythms in NMDA Receptor Dysfunction Models of Schizophrenia. *Schizophrenia Bulletin,* 34**,** 962-973.

ROOPUN, A. K., MIDDLETON, S. J., CUNNINGHAM, M. O., LEBEAU, F. E., BIBBIG, A., WHITTINGTON, M. A. & TRAUB, R. D. 2006. A beta2-frequency (20-30 Hz) oscillation in nonsynaptic networks of somatosensory cortex. *Proc Natl Acad Sci U S A,* 103**,** 15646-50.

ROTARU, D. C., YOSHINO, H., LEWIS, D. A., ERMENTROUT, G. B. & GONZALEZ-BURGOS, G. 2011. Glutamate receptor subtypes mediating synaptic activation of prefrontal cortex neurons: relevance for schizophrenia. *Journal of Neuroscience,* 31**,** 142-156.

ROTHMAN, S. M. & OLNEY, J. W. 1987. Excitotoxity and the NMDA receptor. *Trends in Neurosciences,* 10**,** 299-302.

ROUSSEAUX, C. G. & GREENE, S. F. 2016. Sigma receptors [σRs]: biology in normal and diseased states. *Journal of receptor and signal transduction research,* 36**,** 327-388.

RUDY, B., FISHELL, G., LEE, S. & HJERLING-LEFFLER, J. 2011. Three groups of interneurons account for nearly 100% of neocortical GABAergic neurons. *Dev Neurobiol,* 71**,** 45-61.

RYSKAMP, D. A., KORBAN, S., ZHEMKOV, V., KRASKOVSKAYA, N. & BEZPROZVANNY, I. 2019. Neuronal Sigma-1 Receptors: Signaling Functions and Protective Roles in Neurodegenerative Diseases. *Frontiers in Neuroscience,* 13.

SAKAI, T., OSHIMA, A., NOZAKI, Y., IDA, I., HAGA, C., AKIYAMA, H., NAKAZATO, Y. & MIKUNI, M. 2008. Changes in density of calcium-binding-protein-immunoreactive GABAergic neurons in prefrontal cortex in schizophrenia and bipolar disorder. *Neuropathology,* 28**,** 143-50.

SAKURAI, T., GAMO, N. J., HIKIDA, T., KIM, S.-H., MURAI, T., TOMODA, T. & SAWA, A. 2015. Converging models of schizophrenia – Network alterations of prefrontal cortex underlying cognitive impairments. *Progress in Neurobiology,* 134**,** 178-201.

SAŁACIAK, K. & PYTKA, K. 2022. Revisiting the sigma-1 receptor as a biological target to treat affective and cognitive disorders. *Neuroscience & Biobehavioral Reviews,* 132**,** 1114-1136.

SAMMONS, R. P., VEZIR, M., MORENO-VELASQUEZ, L., CANO, G., ORLANDO, M., SIEVERS, M., GRASSO, E., METODIEVA, V. D., KEMPTER, R., SCHMIDT, H. & SCHMITZ, D. 2024. Structure and function of the hippocampal CA3 module. *Proceedings of the National Academy of Sciences,* 121**,** e2312281120.

SANO, F., SHIGETOMI, E., SHINOZAKI, Y., TSUZUKIYAMA, H., SAITO, K., MIKOSHIBA, K., HORIUCHI, H., CHEUNG, D. L., NABEKURA, J., SUGITA, K., AIHARA, M. & KOIZUMI, S. 2021. Reactive astrocyte-driven epileptogenesis is induced by microglia initially activated following status epilepticus. *JCI Insight,* 6.

SANTOS-SILVA, T., DOS SANTOS FABRIS, D., DE OLIVEIRA, C. L., GUIMARÃES, F. S. & GOMES, F. V. 2023. Prefrontal and Hippocampal Parvalbumin Interneurons in Animal Models for Schizophrenia: A Systematic Review and Meta-analysis. *Schizophrenia Bulletin,* 50**,** 210-223.

SAUNDERS, J. A., GANDAL, M. J. & SIEGEL, S. J. 2012. NMDA antagonists recreate signal-to-noise ratio and timing perturbations present in schizophrenia. *Neurobiology of disease,* 46**,** 93-100.

SAVOLAINEN, K., IHALAINEN, J., HÄMÄLÄINEN, E., TANILA, H. & FORSBERG, M. M. 2021. Phencyclidine-induced cognitive impairments in repeated touchscreen visual reversal learning tests in rats. *Behavioural Brain Research,* 404**,** 113057.

SCHAFER, D. P., LEHRMAN, E. K., KAUTZMAN, A. G., KOYAMA, R., MARDINLY, A. R., YAMASAKI, R., RANSOHOFF, R. M., GREENBERG, M. E., BARRES, B. A. & STEVENS, B. 2012. Microglia sculpt postnatal neural circuits in an activity and complement-dependent manner. *Neuron,* 74**,** 691-705.

SCHARNOWSKI, F., NICHOLSON, A. A., PICHON, S., ROSA, M. J., REY, G., EICKHOFF, S. B., VAN DE VILLE, D., VUILLEUMIER, P. & KOUSH, Y. 2020. The role of the subgenual anterior cingulate cortex in dorsomedial prefrontal-amygdala neural circuitry during positive-social emotion regulation. *Hum Brain Mapp,* 41**,** 3100-3118.

SCHEYLTJENS, I. & ARCKENS, L. 2016. The Current Status of Somatostatin-Interneurons in Inhibitory Control of Brain Function and Plasticity. *Neural Plast,* 2016**,** 8723623.

SCHMIDT, R., HERROJO RUIZ, M., KILAVIK, B. E., LUNDQVIST, M., STARR, P. A. & ARON, A. R. 2019. Beta Oscillations in Working Memory, Executive Control of Movement and Thought, and Sensorimotor Function. *The Journal of Neuroscience,* 39**,** 8231.

SCHOEPP, D. D. 2001. Unveiling the functions of presynaptic metabotropic glutamate receptors in the central nervous system. *Journal of Pharmacology and Experimental Therapeutics,* 299**,** 12-20.

SCHOEPP, D. D., JANE, D. E. & MONN, J. A. 1999. Pharmacological agents acting at subtypes of metabotropic glutamate receptors. *Neuropharmacology,* 38**,** 1431-1476.

SCOVILLE, W. B. & MILNER, B. 1957. Loss of recent memory after bilateral hippocampal lesions. *J Neurol Neurosurg Psychiatry,* 20**,** 11-21.

SEEMAN, M. V. 2021. History of the dopamine hypothesis of antipsychotic action. *World J Psychiatry,* 11**,** 355-364.

SENKOWSKI, D. & GALLINAT, J. 2015. Dysfunctional prefrontal gamma-band oscillations reflect working memory and other cognitive deficits in schizophrenia. *Biological psychiatry,* 77**,** 1010-1019.

SEYMOUR, B. & DOLAN, R. 2008. Emotion, Decision Making, and the Amygdala. *Neuron,* 58**,** 662-671.
SHAH, A. & LODGE, D. J. 2013. A loss of hippocampal perineuronal nets produces deficits in dopamine system function: relevance to the positive symptoms of schizophrenia. *Translational Psychiatry,* 3**,** e215-e215.
SHEN, H. H. 2018. Core Concept: Perineuronal nets gain prominence for their role in learning, memory, and plasticity. *Proc Natl Acad Sci U S A,* 115**,** 9813-9815.
SHI, W., WEI, X., WANG, X., DU, S., LIU, W., SONG, J. & WANG, Y. 2019. Perineuronal nets protect long-term memory by limiting activity-dependent inhibition from parvalbumin interneurons. *Proceedings of the National Academy of Sciences,* 116**,** 27063-27073.
SHINOZAKI, R., HOJO, Y., MUKAI, H., HASHIZUME, M. & MURAKOSHI, T. 2016. Kainate-induced network activity in the anterior cingulate cortex. *Neuroscience,* 325**,** 20-29.
SIMPSON, D. S. A. & OLIVER, P. L. 2020. ROS Generation in Microglia: Understanding Oxidative Stress and Inflammation in Neurodegenerative Disease. *Antioxidants (Basel),* 9.
SOCHOCKA, M., DINIZ, B. S. & LESZEK, J. 2017. Inflammatory Response in the CNS: Friend or Foe? *Molecular Neurobiology,* 54**,** 8071-8089.
SOFRONIEW, M. V. 2015. Astrocyte barriers to neurotoxic inflammation. *Nature Reviews Neuroscience,* 16**,** 249-263.
SOFRONIEW, M. V. 2020. Astrocyte Reactivity: Subtypes, States, and Functions in CNS Innate Immunity. *Trends Immunol,* 41**,** 758-770.
SOFRONIEW, M. V. & VINTERS, H. V. 2010. Astrocytes: biology and pathology. *Acta Neuropathologica,* 119**,** 7-35.
SOHAL, V. S., ZHANG, F., YIZHAR, O. & DEISSEROTH, K. 2009. Parvalbumin neurons and gamma rhythms enhance cortical circuit performance. *Nature,* 459**,** 698-702.
SOMOGYI, P. 1977. A specific 'axo-axonal'interneuron in the visual cortex of the rat. *Brain Res,* 136**,** 345-350.
SORG, B. A., BERRETTA, S., BLACKTOP, J. M., FAWCETT, J. W., KITAGAWA, H., KWOK, J. C. & MIQUEL, M. 2016. Casting a Wide Net: Role of Perineuronal Nets in Neural Plasticity. *J Neurosci,* 36**,** 11459-11468.
SPELLMAN, T., RIGOTTI, M., AHMARI, S. E., FUSI, S., GOGOS, J. A. & GORDON, J. A. 2015. Hippocampal–prefrontal input supports spatial encoding in working memory. *Nature,* 522**,** 309-314.
SPENCER, K. M., NESTOR, P. G., PERLMUTTER, R., NIZNIKIEWICZ, M. A., KLUMP, M. C., FRUMIN, M., SHENTON, M. E. & MCCARLEY, R. W. 2004. Neural synchrony indexes disordered perception and cognition in schizophrenia. *Proc Natl Acad Sci U S A,* 101**,** 17288-93.
SPIERS, H. J., BURGESS, N., MAGUIRE, E. A., BAXENDALE, S. A., HARTLEY, T., THOMPSON, P. J. & O'KEEFE, J. 2001. Unilateral temporal lobectomy patients show lateralized topographical and episodic memory deficits in a virtual town. *Brain,* 124**,** 2476-2489.
STAFFORD, I., TOMIE, A. & WAGNER, G. C. 1983. Effects of SKF-10047 in the phencyclidine-dependent rat: Evidence for common receptor mechanisms. *Drug and Alcohol Dependence,* 12**,** 151-156.
STÅLBERG, G., EKSELIUS, L., LINDSTRÖM, L. H., LARHAMMAR, D. & BODÉN, R. 2014. Neuropeptide Y, social function and long-term outcome in schizophrenia. *Schizophrenia research,* 156**,** 223-227.

STEULLET, P., CABUNGCAL, J. H., COYLE, J., DIDRIKSEN, M., GILL, K., GRACE, A. A., HENSCH, T. K., LAMANTIA, A. S., LINDEMANN, L., MAYNARD, T. M., MEYER, U., MORISHITA, H., O'DONNELL, P., PUHL, M., CUENOD, M. & DO, K. Q. 2017. Oxidative stress-driven parvalbumin interneuron impairment as a common mechanism in models of schizophrenia. *Mol Psychiatry,* 22**,** 936-943.

STEULLET, P., CABUNGCAL, J. H., CUÉNOD, M. & DO, K. Q. 2014. Fast oscillatory activity in the anterior cingulate cortex: dopaminergic modulation and effect of perineuronal net loss. *Front Cell Neurosci,* 8**,** 244.

STRANGE, B. A., WITTER, M. P., LEIN, E. S. & MOSER, E. I. 2014. Functional organization of the hippocampal longitudinal axis. *Nature Reviews Neuroscience,* 15**,** 655-669.

STRINGER, J. L., GREENFIELD, L. J., HACKETT, J. T. & GUYENET, P. G. 1983. Blockade of long-term potentiation by phencyclidine and sigma opiates in the hippocampus in vivo and in vitro. *Brain Res,* 280**,** 127-38.

STRINGER, J. L., HACKETT, J. T. & GUYENET, P. G. 1984. Long-term potentiation blocked by phencyclidine and cyclazocine in vitro. *European Journal of Pharmacology,* 98**,** 381-388.

SU, T. P. 1982. Evidence for sigma opioid receptor: binding of [3H]SKF-10047 to etorphine-inaccessible sites in guinea-pig brain. *J Pharmacol Exp Ther,* 223**,** 284-90.

SULLIVAN, P. F. 2013. Questions about DISC1 as a genetic risk factor for schizophrenia. *Molecular psychiatry,* 18**,** 1050-1052.

SWANSON, L., WYSS, J. & COWAN, W. 1978. An autoradiographic study of the organization of intrahippocampal association pathways in the rat. *Journal of comparative neurology,* 181**,** 681-715.

SZALAY, G., MARTINECZ, B., LÉNÁRT, N., KÖRNYEI, Z., ORSOLITS, B., JUDÁK, L., CSÁSZÁR, E., FEKETE, R., WEST, B. L. & KATONA, G. 2016. Microglia protect against brain injury and their selective elimination dysregulates neuronal network activity after stroke. *Nature communications,* 7**,** 11499.

TAGASHIRA, H., BHUIYAN, M. S., SHINODA, Y., KAWAHATA, I., NUMATA, T. & FUKUNAGA, K. 2023. Sigma-1 receptor is involved in modification of ER-mitochondria proximity and Ca2+ homeostasis in cardiomyocytes. *Journal of Pharmacological Sciences,* 151**,** 128-133.

TAKAHASHI, M., SHIRAKAWA, O., TOYOOKA, K., KITAMURA, N., HASHIMOTO, T., MAEDA, K., KOIZUMI, S., WAKABAYASHI, K., TAKAHASHI, H. & SOMEYA, T. 2000. Abnormal expression of brain-derived neurotrophic factor and its receptor in the corticolimbic system of schizophrenic patients. *Molecular psychiatry,* 5**,** 293-300.

TAM, S. W. 1985. (+)-[3H]SKF 10,047, (+)-[3H]ethylketocyclazocine, mu, kappa, delta and phencyclidine binding sites in guinea pig brain membranes. *Eur J Pharmacol,* 109**,** 33-41.

TAMÁS, G., BUHL, E. H., LÖRINCZ, A. & SOMOGYI, P. 2000. Proximally targeted GABAergic synapses and gap junctions synchronize cortical interneurons. *Nat Neurosci,* 3**,** 366-71.

TANAKA-KOSHIYAMA, K., KOSHIYAMA, D., MIYAKOSHI, M., JOSHI, Y. B., MOLINA, J. L., SPROCK, J., BRAFF, D. L. & LIGHT, G. A. 2020. Abnormal Spontaneous Gamma Power Is Associated With Verbal Learning and Memory Dysfunction in Schizophrenia. *Front Psychiatry,* 11**,** 832.

TANDON, R., GAEBEL, W., BARCH, D. M., BUSTILLO, J., GUR, R. E., HECKERS, S., MALASPINA, D., OWEN, M. J., SCHULTZ, S. & TSUANG, M. 2013.

Definition and description of schizophrenia in the DSM-5. *Schizophrenia research,* 150**,** 3-10.
TANQUEIRO, S. R., MOURO, F. M., FERREIRA, C. B., FREITAS, C. F., FONSECA-GOMES, J., SIMÕES DO COUTO, F., SEBASTIÃO, A. M., DAWSON, N. & DIÓGENES, M. J. 2021. Sustained NMDA receptor hypofunction impairs brain-derived neurotropic factor signalling in the PFC, but not in the hippocampus, and disturbs PFC-dependent cognition in mice. *J Psychopharmacol,* 35**,** 730-743.
TARASOV, V. V., SVISTUNOV, A. A., CHUBAREV, V. N., SOLOGOVA, S. S., MUKHORTOVA, P., LEVUSHKIN, D., SOMASUNDARAM, S. G., KIRKLAND, C. E., BACHURIN, S. O. & ALIEV, G. 2020. Alterations of Astrocytes in the Context of Schizophrenic Dementia. *Frontiers in Pharmacology,* 10.
TAVARES, L. C. S. & TORT, A. B. L. 2022. Hippocampal-prefrontal interactions during spatial decision-making. *Hippocampus,* 32**,** 38-54.
TEIXEIRA, C. M., POMEDLI, S. R., MAEI, H. R., KEE, N. & FRANKLAND, P. W. 2006. Involvement of the anterior cingulate cortex in the expression of remote spatial memory. *Journal of Neuroscience,* 26**,** 7555-7564.
TER WAL, M. & TIESINGA, P. H. E. 2021. Comprehensive characterization of oscillatory signatures in a model circuit with PV- and SOM-expressing interneurons. *Biol Cybern,* 115**,** 487-517.
THOMPSON, L., KHUC, J., SACCANI, M. S., ZOKAEI, N. & CAPPELLETTI, M. 2021. Gamma oscillations modulate working memory recall precision. *Experimental Brain Research,* 239**,** 2711-2724.
TIKKA, S. K., YADAV, S., NIZAMIE, S. H., DAS, B., TIKKA, D. L. & GOYAL, N. 2014. Schneiderian first rank symptoms and gamma oscillatory activity in neuroleptic naïve first episode schizophrenia: a 192 channel EEG study. *Psychiatry Investig,* 11**,** 467-75.
TOONEY, P. A. & CHAHL, L. A. 2004. Neurons expressing calcium-binding proteins in the prefrontal cortex in schizophrenia. *Prog Neuropsychopharmacol Biol Psychiatry,* 28**,** 273-8.
TRANTHAM-DAVIDSON, H. & LAVIN, A. 2019. Loss of dysbindin-1 affects GABAergic transmission in the PFC. *Psychopharmacology,* 236**,** 3291-3300.
TRAUB, R., WHITTINGTON, M., COLLING, S., BUZSAKI, G. & JEFFERYS, J. 1996. Analysis of gamma rhythms in the rat hippocampus in vitro and in vivo. *The Journal of physiology,* 493**,** 471-484.
TRAYNELIS, S. F., WOLLMUTH, L. P., MCBAIN, C. J., MENNITI, F. S., VANCE, K. M., OGDEN, K. K., HANSEN, K. B., YUAN, H., MYERS, S. J. & DINGLEDINE, R. 2010. Glutamate receptor ion channels: structure, regulation, and function. *Pharmacol Rev,* 62**,** 405-96.
TREMBLAY, R., LEE, S. & RUDY, B. 2016. GABAergic interneurons in the neocortex: from cellular properties to circuits. *Neuron,* 91**,** 260-292.
TRÉPANIER, M., HOPPERTON, K., MIZRAHI, R., MECHAWAR, N. & BAZINET, R. 2016. Postmortem evidence of cerebral inflammation in schizophrenia: a systematic review. *Molecular psychiatry,* 21**,** 1009-1026.
TSINTSADZE, V., MINLEBAEV, M., SUCHKOV, D., CUNNINGHAM, M. O. & KHAZIPOV, R. 2015. Ontogeny of kainate-induced gamma oscillations in the rat CA3 hippocampus in vitro. *Front Cell Neurosci,* 9**,** 195.
TSIRIGOTIS, K. 2018. Indirect self-destructiveness in individuals with schizophrenia. *Braz J Psychiatry,* 40**,** 41-47.

TURNER, J. P. & SALT, T. E. 2003. Group II and III metabotropic glutamate receptors and the control of the TRN input to rat thalamocortical neurones *in vitro*. *Neuroscience,* 122**,** 459-469.
TYSZKIEWICZ, J. P., GU, Z., WANG, X., CAI, X. & YAN, Z. 2004. Group II metabotropic glutamate receptors enhance NMDA receptor currents via a protein kinase C-dependent mechanism in pyramidal neurones of rat prefrontal cortex. *The Journal of physiology,* 554**,** 765-777.
UHLHAAS, P. J. 2011. High-frequency oscillations in schizophrenia. *Clin EEG Neurosci,* 42**,** 77-82.
UHLHAAS, P. J. & SINGER, W. 2010. Abnormal neural oscillations and synchrony in schizophrenia. *Nature Reviews Neuroscience,* 11**,** 100-113.
UMPIERRE, A. D. & WU, L. J. 2021. How microglia sense and regulate neuronal activity. *Glia,* 69**,** 1637-1653.
URBAN-CIECKO, J. & BARTH, A. L. 2016. Somatostatin-expressing neurons in cortical networks. *Nat Rev Neurosci,* 17**,** 401-9.
VAN HEUKELUM, S., MARS, R. B., GUTHRIE, M., BUITELAAR, J. K., BECKMANN, C. F., TIESINGA, P. H. E., VOGT, B. A., GLENNON, J. C. & HAVENITH, M. N. 2020. Where is Cingulate Cortex? A Cross-Species View. *Trends in Neurosciences,* 43**,** 285-299.
VAN HEUKELUM, S., MOGAVERO, F., VAN DE WAL, M. A. E., GEERS, F. E., FRANÇA, A. S. C., BUITELAAR, J. K., BECKMANN, C. F., GLENNON, J. C. & HAVENITH, M. N. 2019. Gradient of Parvalbumin- and Somatostatin-Expressing Interneurons Across Cingulate Cortex Is Differentially Linked to Aggression and Sociability in BALB/cJ Mice. *Front Psychiatry,* 10**,** 809.
VAN ROSSUM, J. M. 1966. The significance of dopamine-receptor blockade for the mechanism of action of neuroleptic drugs. *Arch Int Pharmacodyn Ther,* 160**,** 492-4.
VAN STRIEN, N., CAPPAERT, N. & WITTER, M. 2009. The anatomy of memory: an interactive overview of the parahippocampal–hippocampal network. *Nature reviews neuroscience,* 10**,** 272-282.
VAN VUGT, M. K., SCHULZE-BONHAGE, A., LITT, B., BRANDT, A. & KAHANA, M. J. 2010. Hippocampal gamma oscillations increase with memory load. *J Neurosci,* 30**,** 2694-9.
VAUPEL, D. B. 1983. Naltrexone fails to antagonize the sigma effects of PCP and SKF 10,047 in the dog. *Eur J Pharmacol,* 92**,** 269-74.
VEIT, J., HAKIM, R., JADI, M. P., SEJNOWSKI, T. J. & ADESNIK, H. 2017. Cortical gamma band synchronization through somatostatin interneurons. *Nature Neuroscience,* 20**,** 951-959.
VEIT, J., HANDY, G., MOSSING, D. P., DOIRON, B. & ADESNIK, H. 2023. Cortical VIP neurons locally control the gain but globally control the coherence of gamma band rhythms. *Neuron,* 111**,** 405-417.e5.
VERKHRATSKY, A. & NEDERGAARD, M. 2018. Physiology of Astroglia. *Physiol Rev,* 98**,** 239-389.
VICKERS, C. A., DICKSON, K. S. & WYLLIE, D. J. 2005. Induction and maintenance of late-phase long-term potentiation in isolated dendrites of rat hippocampal CA1 pyramidal neurones. *J Physiol,* 568**,** 803-13.
VIDAL-ITRIAGO, A., RADFORD, R. A. W., ARAMIDEH, J. A., MAUREL, C., SCHERER, N. M., DON, E. K., LEE, A., CHUNG, R. S., GRAEBER, M. B. & MORSCH, M. 2022. Microglia morphophysiological diversity and its implications for the CNS. *Frontiers in Immunology,* 13.

VINSON, P. N. & CONN, P. J. 2012. Metabotropic glutamate receptors as therapeutic targets for schizophrenia. *Neuropharmacology,* 62**,** 1461-1472.

VIVIEN, J., EL AZRAOUI, A., LHERAUX, C., LANORE, F., AOUIZERATE, B., HERRY, C., HUMEAU, Y. & BIENVENU, T. C. M. 2023. Axo-axonic cells in neuropsychiatric disorders: a systematic review. *Front Cell Neurosci,* 17**,** 1212202.

VOGT, B. A. 2016. Midcingulate cortex: Structure, connections, homologies, functions and diseases. *J Chem Neuroanat,* 74**,** 28-46.

VOLK, D. W., AUSTIN, M. C., PIERRI, J. N., SAMPSON, A. R. & LEWIS, D. A. 2001. GABA transporter-1 mRNA in the prefrontal cortex in schizophrenia: decreased expression in a subset of neurons. *American Journal of Psychiatry,* 158**,** 256-265.

WALLER, R., MANDEYA, M., VINEY, E., SIMPSON, J. E. & WHARTON, S. B. 2020. Histological characterization of interneurons in Alzheimer's disease reveals a loss of somatostatin interneurons in the temporal cortex. *Neuropathology,* 40**,** 336-346.

WALLS, A. B., NILSEN, L. H., EYJOLFSSON, E. M., VESTERGAARD, H. T., HANSEN, S. L., SCHOUSBOE, A., SONNEWALD, U. & WAAGEPETERSEN, H. S. 2010. GAD65 is essential for synthesis of GABA destined for tonic inhibition regulating epileptiform activity. *J Neurochem,* 115**,** 1398-408.

WANG, A. K. & MILLER, B. J. 2018. Meta-analysis of Cerebrospinal Fluid Cytokine and Tryptophan Catabolite Alterations in Psychiatric Patients: Comparisons Between Schizophrenia, Bipolar Disorder, and Depression. *Schizophr Bull,* 44**,** 75-83.

WANG, A. Y., LOHMANN, K. M., YANG, C. K., ZIMMERMAN, E. I., PANTAZOPOULOS, H., HERRING, N., BERRETTA, S., HECKERS, S. & KONRADI, C. 2011. Bipolar disorder type 1 and schizophrenia are accompanied by decreased density of parvalbumin- and somatostatin-positive interneurons in the parahippocampal region. *Acta Neuropathol,* 122**,** 615-26.

WANG, B., KE, W., GUANG, J., CHEN, G., YIN, L., DENG, S., HE, Q., LIU, Y., HE, T., ZHENG, R., JIANG, Y., ZHANG, X., LI, T., LUAN, G., LU, H. D., ZHANG, M., ZHANG, X. & SHU, Y. 2016. Firing Frequency Maxima of Fast-Spiking Neurons in Human, Monkey, and Mouse Neocortex. *Frontiers in Cellular Neuroscience,* 10.

WANG, D.-S., JU, L., PINGUELO, A. G., KANESHWARAN, K., HAFFEY, S. C., LECKER, I., GOHIL, H., WHEELER, M. B., KAUSTOV, L., ARIZA, A., YU, M., VOLCHUK, A., STEINBERG, B. E., GOLDENBERG, N. M. & ORSER, B. A. 2024. Crosstalk between GABAA receptors in astrocytes and neurons triggered by general anesthetic drugs. *Translational Research,* 267**,** 39-53.

WANG, H., LIU, F., CHEN, W., SUN, X., CUI, W., DONG, Z., ZHAO, K., ZHANG, H., LI, H. & XING, G. 2018. Genetic recovery of ErbB4 in adulthood partially restores brain functions in null mice. *Proceedings of the National Academy of Sciences,* 115**,** 13105-13110.

WANG, L., ZHAO, D., WANG, M., WANG, Y., VREUGDENHIL, M., LIN, J. & LU, C. 2020. Modulation of Hippocampal Gamma Oscillations by Dopamine in Heterozygous Reeler Mice in vitro. *Frontiers in Cellular Neuroscience,* 13.

WEBSTER, M. J., O'GRADY, J., KLEINMAN, J. E. & WEICKERT, C. S. 2005. Glial fibrillary acidic protein mRNA levels in the cingulate cortex of individuals with depression, bipolar disorder and schizophrenia. *Neuroscience,* 133**,** 453-461.

WEICKERT, C., HYDE, T., LIPSKA, B., HERMAN, M., WEINBERGER, D. & KLEINMAN, J. 2003. Reduced brain-derived neurotrophic factor in prefrontal cortex of patients with schizophrenia. *Molecular psychiatry,* 8**,** 592-610.

WEISS, A. P., SCHACTER, D. L., GOFF, D. C., RAUCH, S. L., ALPERT, N. M., FISCHMAN, A. J. & HECKERS, S. 2003. Impaired hippocampal recruitment during normal modulation of memory performance in schizophrenia. *Biological psychiatry,* 53**,** 48-55.

WEISS, A. P., ZALESAK, M., DEWITT, I., GOFF, D., KUNKEL, L. & HECKERS, S. 2004. Impaired hippocampal function during the detection of novel words in schizophrenia. *Biological Psychiatry,* 55**,** 668-675.

WEISSMAN, A. D., CASANOVA, M. F., KLEINMAN, J. E., LONDON, E. D. & DE SOUZA, E. B. 1991. Selective loss of cerebral cortical sigma, but not PCP binding sites in schizophrenia. *Biol Psychiatry,* 29**,** 41-54.

WEISSMAN, A. D., SU, T. P., HEDREEN, J. C. & LONDON, E. D. 1988. Sigma receptors in post-mortem human brains. *Journal of Pharmacology and Experimental Therapeutics,* 247**,** 29.

WENG, T. Y., HUNG, D. T., SU, T. P. & TSAI, S. A. 2017. Loss of Sigma-1 Receptor Chaperone Promotes Astrocytosis and Enhances the Nrf2 Antioxidant Defense. *Oxid Med Cell Longev,* 2017**,** 4582135.

WHITELAW, B. S., STOESSEL, M. B. & MAJEWSKA, A. K. 2023. Movers and shakers: Microglial dynamics and modulation of neural networks. *Glia,* 71**,** 1575-1591.

WHITTINGTON, M. A., STANFORD, I. M., COLLING, S. B., JEFFERYS, J. G. & TRAUB, R. D. 1997. Spatiotemporal patterns of γ frequency oscillations tetanically induced in the rat hippocampal slice. *The Journal of physiology,* 502**,** 591-607.

WHITTINGTON, M. A., TRAUB, R. D. & JEFFERYS, J. G. 1995. Synchronized oscillations in interneuron networks driven by metabotropic glutamate receptor activation. *Nature,* 373**,** 612-5.

WIERZBA-BOBROWICZ, T., LEWANDOWSKA, E., LECHOWICZ, W., STĘPIEŃ, T. & PASENNIK, E. 2005. Quantitative analysis of activated microglia, ramified and damage of processes in the frontal and temporal lobes of chronic schizophrenics. *Folia Neuropathologica,* 43**,** 81-89.

WIESCHOLLECK, V. & MANAHAN-VAUGHAN, D. 2013. Long-lasting changes in hippocampal synaptic plasticity and cognition in an animal model of NMDA receptor dysfunction in psychosis. *Neuropharmacology,* 74**,** 48-58.

WINGERT, J. C. & SORG, B. A. 2021. Impact of Perineuronal Nets on Electrophysiology of Parvalbumin Interneurons, Principal Neurons, and Brain Oscillations: A Review. *Front Synaptic Neurosci,* 13**,** 673210.

WINTERER, G. 2010. Why do patients with schizophrenia smoke? *Current Opinion in Psychiatry,* 23**,** 112-119.

WITKIN, J. M., PANDEY, K. P. & SMITH, J. L. 2022. Clinical investigations of compounds targeting metabotropic glutamate receptors. *Pharmacology Biochemistry and Behavior,* 219**,** 173446.

WOLF, C., JACKSON, M. C., KISSLING, C., THOME, J. & LINDEN, D. E. 2011. Dysbindin-1 genotype effects on emotional working memory. *Molecular psychiatry,* 16**,** 145-155.

WOMELSDORF, T., SCHOFFELEN, J. M., OOSTENVELD, R., SINGER, W., DESIMONE, R., ENGEL, A. K. & FRIES, P. 2007. Modulation of neuronal interactions through neuronal synchronization. *Science,* 316**,** 1609-12.

WOO, T. U., WALSH, J. P. & BENES, F. M. 2004. Density of glutamic acid decarboxylase 67 messenger RNA-containing neurons that express the N-methyl-D-aspartate receptor subunit NR2A in the anterior cingulate cortex in schizophrenia and bipolar disorder. *Arch Gen Psychiatry,* 61**,** 649-57.

WU, S. J., SEVIER, E., DWIVEDI, D., SALDI, G.-A., HAIRSTON, A., YU, S., ABBOTT, L., CHOI, D. H., SHERER, M., QIU, Y., SHINDE, A., LENAHAN, M., RIZZO, D., XU, Q., BARRERA, I., KUMAR, V., MARRERO, G., PRÖNNEKE, A., HUANG, S., KULLANDER, K., STAFFORD, D. A., MACOSKO, E., CHEN, F., RUDY, B. & FISHELL, G. 2023. Cortical somatostatin interneuron subtypes form cell-type-specific circuits. *Neuron,* 111**,** 2675-2692.e9.

WULFF, P., PONOMARENKO, A. A., BARTOS, M., KOROTKOVA, T. M., FUCHS, E. C., BÄHNER, F., BOTH, M., TORT, A. B., KOPELL, N. J. & WISDEN, W. 2009. Hippocampal theta rhythm and its coupling with gamma oscillations require fast inhibition onto parvalbumin-positive interneurons. *Proceedings of the National Academy of Sciences,* 106**,** 3561-3566.

XING, B., HAN, G., WANG, M. J., SNYDER, M. A. & GAO, W. J. 2018. Juvenile treatment with mGluR2/3 agonist prevents schizophrenia-like phenotypes in adult by acting through GSK3β. *Neuropharmacology,* 137**,** 359-371.

XU, P., CHEN, A., LI, Y., XING, X. & LU, H. 2019. Medial prefrontal cortex in neurological diseases. *Physiol Genomics,* 51**,** 432-442.

XU, X. & CALLAWAY, E. M. 2009. Laminar Specificity of Functional Input to Distinct Types of Inhibitory Cortical Neurons. *The Journal of Neuroscience,* 29**,** 70-85.

YAMADA, J. & JINNO, S. 2014. Age-related differences in oligodendrogenesis across the dorsal-ventral axis of the mouse hippocampus. *Hippocampus,* 24**,** 1017-1029.

YAMAGUCHI, Y. 2000. Lecticans: organizers of the brain extracellular matrix. *Cell Mol Life Sci,* 57**,** 276-89.

YAMAMOTO, J., SUH, J., TAKEUCHI, D. & TONEGAWA, S. 2014. Successful Execution of Working Memory Linked to Synchronized High-Frequency Gamma Oscillations. *Cell,* 157**,** 845-857.

YOON, B.-E. & LEE, C. J. 2014. GABA as a rising gliotransmitter. *Frontiers in neural circuits,* 8**,** 141.

YU, W., ZHU, H., WANG, Y., LI, G., WANG, L. & LI, H. 2015. Reactive Transformation and Increased BDNF Signaling by Hippocampal Astrocytes in Response to MK-801. *PLOS ONE,* 10**,** e0145651.

ZAMANILLO, D., ANDREU, F., OVALLE, S., PÉREZ, M. P., ROMERO, G., FARRÉ, A. J. & GUITART, X. 2000. Up-regulation of sigma1 receptor mRNA in rat brain by a putative atypical antipsychotic and sigma receptor ligand. *Neuroscience Letters,* 282**,** 169-172.

ZANELLI, J., MOLLON, J., SANDIN, S., MORGAN, C., DAZZAN, P., PILECKA, I., MARQUES, T. R., DAVID, A. S., MORGAN, K., FEARON, P., DOODY, G. A., JONES, P. B., MURRAY, R. M. & REICHENBERG, A. 2019. Cognitive Change in Schizophrenia and Other Psychoses in the Decade Following the First Episode. *American Journal of Psychiatry,* 176**,** 811-819.

ZEMLA, R. & BASU, J. 2017. Hippocampal function in rodents. *Curr Opin Neurobiol,* 43**,** 187-197.

ZENG, C., LU, Y., WEI, X., SUN, L., WEI, L., OU, S., HUANG, Q. & WU, Y. 2024. Parvalbumin Regulates GAD Expression through Calcium Ion Concentration to Affect the Balance of Glu-GABA and Improve KA-Induced Status Epilepticus in PV-Cre Transgenic Mice. *ACS Chemical Neuroscience,* 15**,** 1951-1966.

ZENG, H. & SANES, J. R. 2017. Neuronal cell-type classification: challenges, opportunities and the path forward. *Nature Reviews Neuroscience,* 18**,** 530-546.

ZHANG, C., DENG, Y., DAI, H., ZHOU, W., TIAN, J., BING, G. & ZHAO, L. 2017. Effects of dimethyl sulfoxide on the morphology and viability of primary cultured neurons and astrocytes. *Brain Research Bulletin,* 128**,** 34-39.

ZHANG, H., WATROUS, A. J., PATEL, A. & JACOBS, J. 2018. Theta and alpha oscillations are traveling waves in the human neocortex. *Neuron,* 98**,** 1269-1281. e4.

ZHANG, J., ZHANG, X., CHEN, G., HUANG, L. & SUN, Y. 2022. EEG emotion recognition based on cross-frequency granger causality feature extraction and fusion in the left and right hemispheres. *Frontiers in Neuroscience,* 16.

ZHANG, L., GAO, Y.-Z., ZHAO, C.-J., XIA, J.-Y., YANG, J.-J. & JI, M.-H. 2023. Reduced inhibitory and excitatory input onto parvalbumin interneurons mediated by perineuronal net might contribute to cognitive impairments in a mouse model of sepsis-associated encephalopathy. *Neuropharmacology,* 225**,** 109382.

ZHANG, Y., CHEN, Y., BRESSLER, S. L. & DING, M. 2008. Response preparation and inhibition: the role of the cortical sensorimotor beta rhythm. *Neuroscience,* 156**,** 238-46.

ZHANG, Z. & REYNOLDS, G. A selective deficit in the relative density of parvalbumin-immunoreactive neurons in the hippocampus in schizophrenia. Schizophrenia Research, 2001. ELSEVIER SCIENCE BV PO BOX 211, 1000 AE AMSTERDAM, NETHERLANDS, 65-65.

ZHENG, C., XU, Y., CHEN, G., TAN, Y., ZENG, W., WANG, J., CHENG, C., YANG, X., NIE, S., ZHANG, Z. & CAO, X. 2020. Distinct anti-dyskinetic effects of amantadine and group II metabotropic glutamate receptor agonist LY354740 in a rodent model: An electrophysiological perspective. *Neurobiology of Disease,* 139**,** 104807.

ZHU, S., WANG, H., SHI, R., ZHANG, R., WANG, J., KONG, L., SUN, Y., HE, J., KONG, J., WANG, J.-F. & LI, X.-M. 2014. Chronic Phencyclidine Induces Inflammatory Responses and Activates GSK3β in Mice. *Neurochemical Research,* 39**,** 2385-2393.

ZHUO, C., TIAN, H., SONG, X., JIANG, D., CHEN, G., CAI, Z., PING, J., CHENG, L., ZHOU, C. & CHEN, C. 2023. Microglia and cognitive impairment in schizophrenia: translating scientific progress into novel therapeutic interventions. *Schizophrenia,* 9**,** 42.

ZUKIN, S. R. & ZUKIN, S. R. 1981. Demonstration of [3H] Cyclazocine Binding to Mutiple Opiate Receptor Sites. *Molecular Pharmacology,* 20**,** 246-254.